

TECHNISCHE UNIVERSITÄT MÜNCHEN



Dissecting brain-specific functions of
histone deacetylases 1 and 3 by using
genetic mouse models

Michaela Katja Stangl

TECHNISCHE UNIVERSITÄT MÜNCHEN



Dissecting brain-specific functions of histone deacetylases 1 and 3 by using genetic mouse models

Michaela Katja Stangl

Vollständiger Abdruck der von der Fakultät Wissenschaftszentrum Weihenstephan für Ernährung, Landnutzung und Umwelt der Technischen Universität München zur Erlangung des akademischen Grades eines

Doktors der Naturwissenschaften

genehmigten Dissertation.

Vorsitzender: Univ.-Prof. Dr. R. Torres Ruiz

Prüfer der Dissertation: 1. Univ.-Prof. Dr. W. Wurst

2. Univ.-Prof. Dr. K. H. Schneitz

Die Dissertation wurde am 31.05.2016 bei der Technischen Universität München eingereicht und durch die Fakultät Wissenschaftszentrum Weihenstephan für Ernährung, Landnutzung und Umwelt am 29.09.2016 angenommen.

1.5.2	The contribution of epigenetic mechanisms related to HDACs to memory formation and learning	44
1.5.3	Neuropsychiatric diseases triggered by epigenetic mechanisms involve HDACs	46
2	AIM OF THE THESIS.....	48
3	MATERIAL AND METHODS.....	51
3.1	Material.....	51
3.1.1	Buffers and Solutions	51
3.1.1.1	Buffers for agarose gel electrophoresis	51
3.1.1.2	Buffers and solutions for <i>in situ</i> hybridization (<i>ISH</i>).....	51
3.1.1.3	Buffers and solutions for Western blotting.....	54
3.1.1.4	Buffers and solutions for lacZ staining	56
3.1.1.5	Other buffers and solutions	56
3.1.2	Media for bacterial cultures.....	57
3.1.3	Oligonucleotides.....	58
3.1.3.1	Primers used for <i>ISH</i> probe cloning procedures	58
3.1.3.2	Primers used for genotyping	59
3.1.4	Riboprobes for <i>in situ</i> hybridization (<i>ISH</i>)	60
3.1.5	Antibodies	60
3.1.6	<i>Escherichia coli</i> (<i>E. coli</i>) strains.....	61
3.1.7	Animals.....	61
3.2	Methods	62
3.2.1	Microbiological methods.....	62
3.2.1.1	Preparation of electrocompetent bacteria	62
3.2.1.2	Transformation of electrocompetent bacteria	62
3.2.1.3	Glycerol stocks.....	63
3.2.2	Preparation and analysis of nucleic acids	63
3.2.2.1	RNA isolation	63
3.2.2.2	Preparation of plasmid DNA from bacteria.....	63

3.2.2.3	DNA preparation from mouse tail tissue	64
3.2.2.4	Agarose gel electrophoresis	64
3.2.2.5	Photometric measurement of DNA and RNA concentrations	64
3.2.2.6	Restriction digest of plasmid DNA and PCR products for analytical purposes	64
3.2.2.7	Sequencing	65
3.2.3	Polymerase Chain Reaction (PCR)	65
3.2.4	Cloning techniques	66
3.2.4.1	Restriction digest of plasmid DNA and PCR products for preparative purposes .	66
3.2.4.2	DNA gel extraction	66
3.2.4.3	Ligation of DNA fragments	67
3.2.4.4	TOPO TA cloning.....	67
3.2.5	<i>In situ</i> hybridization (ISH)	67
3.2.5.1	Tissue preparation.....	68
3.2.5.2	Preparation of radioactive riboprobes.....	68
3.2.5.3	Pre-treatment of brain slices.....	70
3.2.5.4	Hybridization of riboprobes	70
3.2.5.5	Washing of brain slices.....	71
3.2.5.6	Autoradiography	71
3.2.5.7	Dipping radiolabeled brain slices in silver staining solution	71
3.2.5.8	Nissl staining.....	72
3.2.5.9	Figure preparation.....	72
3.2.6	Western blot analysis.....	72
3.2.7	Animal housing.....	73
3.2.8	Behavioral testing.....	73
3.2.8.1	Open field (OF) test	74
3.2.8.2	Elevated plus maze (EPM) test.....	74
3.2.8.3	Dark/light box (DaLi) test	75
3.2.8.4	Forced swim test (FST)	75

3.2.8.5	Social approach/avoidance (SA) test.....	76
3.2.8.6	Female urine sniffing test (FUST)	76
3.2.8.7	Chronic social defeat stress (CSDS) paradigm	77
3.2.8.8	Acute stress response and sampling during CSDS paradigm	77
3.2.8.9	Water Cross Maze (WCM) test.....	77
3.2.9	Statistics	79
4	RESULTS.....	80
4.1	Distribution of the classical HDACs throughout the adult murine brain	80
4.2	Establishing the oral application of tamoxifen via chow to activate the Cre/loxP system in conditional transgenic mouse models	91
4.2.1	Oral tamoxifen administration via food pellets in CRH overexpressing mice.....	93
4.2.1.1	Tamoxifen administration via food pellets results in efficient CreER ^{T2} -mediated recombination in the CNS.....	94
4.2.1.2	Tamoxifen administration via food pellets changes feeding behavior of CRH overexpressing mice	98
4.3	Genetically dissecting brain-specific functions of histone deacetylase 1 (HDAC1)	107
4.3.1	Generation of conditional Hdac1 knockout mice	107
4.3.1.1	Analysis of <i>Hdac1</i> -expression using lacZ reporter mice.....	107
4.3.1.2	Establishment of conditional Hdac1 knockout mice	111
4.3.2	Behavioral characterization of conditional Hdac1 knockout mice lacking HDAC1 in principal forebrain neurons	116
4.3.2.1	Basal behavioral screening of conditional Hdac1 knockout mice.....	116
4.3.2.2	Effects of chronic social defeat stress (CSDS) on conditional Hdac1 knockout mice.....	122
4.3.2.3	Cognitive performance of conditional Hdac1 knockout mice.....	133
4.4	Genetically dissecting brain-specific functions of histone deacetylase 3 (HDAC3)	136
4.4.1	Generation of conditional Hdac3 knockout mice	136
4.4.1.1	Analysis of <i>Hdac3</i> -expression using lacZ reporter mice.....	136

4.4.1.2	Establishment of conditional Hdac3 knockout mice	140
4.4.2	Behavioral characterization of conditional Hdac3 knockout mice lacking HDAC3 in principal forebrain neurons	145
4.4.2.1	Basal behavioral screening of conditional Hdac3 knockout mice	145
4.4.2.2	Effects of chronic social defeat stress (CSDS) on conditional Hdac3 knockout mice	151
4.4.2.3	Cognitive performance of Hdac3 conditional knockout mice	162
5	DISCUSSION	164
5.1	Distribution of the classical HDACs throughout the adult murine brain	164
5.2	Establishing the oral application of tamoxifen via chow to activate the Cre/loxP system in conditional transgenic mouse models	172
5.3	Genetically dissecting brain-specific functions of histone deacetylase 1 (HDAC1) and histone deacetylase 3 (HDAC3)	175
6	GENERAL CONCLUSION AND OUTLOOK.....	186
7	SUPPLEMENTS.....	189
7.1	Control experiment to rule out influences of Cre recombinase on mice behavior	189
8	REFERENCES.....	191
9	CURRICULUM VITAE	220
10	ACKNOWLEDGMENTS.....	224
11	ERKLÄRUNG	225

LIST OF FIGURES AND TABLES

- Figure 1.** Chromatin formation and structure.
- Figure 2.** Epigenetic mechanisms.
- Figure 3.** Predestined lysine side chains of histone molecules.
- Figure 4.** Evolutionary relationship between classical HDACs.
- Figure 5.** Characterization of the classical HDAC proteins.
- Figure 6.** HDAC1 and HDAC2 containing multi-protein complexes.
- Figure 7.** Localization of antisense nucleotide probes designed for ISH of *Mus musculus Hdac1-11*.
- Figure 8.** Distribution of *Hdac1-11* mRNA within the adult murine brain.
- Figure 9.** Detailed representation of the expression pattern of class I *Hdacs*.
- Figure 10.** Detailed representation of the expression pattern of class II *Hdacs*.
- Figure 11.** Detailed representation of the expression pattern of *Hdac11* as the only class IV member.
- Figure 12.** Activation of the Cre/loxP system using tamoxifen administration.
- Figure 13.** Description of the CRH-COE^{IFB} mouse line.
- Figure 14.** Analysis of *lacZ* expression upon tamoxifen treatment (first approach).
- Figure 15.** Analysis of *lacZ* expression upon tamoxifen treatment (second approach).
- Figure 16.** Determination of food intake of CRH-COE^{IFB} mice treated with TCS chow.
- Figure 17.** Excluding effects of CRH overexpression on food intake.
- Figure 18.** Determination of water intake of CRH-COE^{IFB} mice treated with TCS chow.
- Figure 19.** Excluding effects of CRH overexpression on water intake.
- Figure 20.** Body weight change of CRH-COE^{IFB} mice treated with TCS chow.
- Figure 21.** Schematic representation of the *Hdac1* wild-type locus and the *lacZ* reporter allele generated by targeted trapping.
- Figure 22.** *Hdac1* expression revealed by *Hdac1-lacZ* reporter mice.
- Figure 23.** Breeding scheme to generate conditional *Hdac1* knockout mice.
- Figure 24.** Schematic representation of the *Hdac1* wild-type locus, *lacZ* allele, floxed allele and knockout allele generated by targeted trapping and subsequent excision via Flp and Cre.
- Figure 25.** Verification of HDAC1 disruption in conditional *Hdac1* knockout mice upon tamoxifen treatment.
- Figure 26.** Testing schedule for basal emotionality screen of conditional *Hdac1* knockout mice.
- Figure 27.** Analysis of conditional *Hdac1* knockout mice in the open field (OF).
- Figure 28.** Analysis of conditional *Hdac1* knockout mice in the elevated plus maze (EPM) test.
- Figure 29.** Analysis of conditional *Hdac1* knockout mice in the dark/light box (DaLi).
- Figure 30.** Analysis of conditional *Hdac1* knockout mice in the forced swim test (FST).
- Figure 31.** Schematic representation of the chronic social defeat stress (CSDS) paradigm and behavioral phenotyping of conditional *Hdac1* knockout mice.
- Figure 32.** Analysis of physiological parameters of conditional *Hdac1* knockout mice during and after the chronic social defeat stress (CSDS) paradigm.
- Figure 33.** Analysis of corticosterone levels of conditional *Hdac1* knockout mice subjected the chronic social defeat stress (CSDS) paradigm.

- Figure 34.** Analysis of the behavior of conditional Hdac1 knockout mice in the open field (OF) during the chronic social defeat (CSDS) paradigm.
- Figure 35.** Analysis of conditional Hdac1 knockout mice in the social approach/avoidance (SA) test during the chronic social defeat stress (CSDS) paradigm.
- Figure 36.** Analysis of conditional Hdac1 knockout mice in the female urine sniffing test (FUST) during the chronic social defeat stress (CSDS) paradigm.
- Figure 37.** Analysis of conditional Hdac1 knockout mice in the elevated plus maze (EPM) during the chronic social defeat stress (CSDS) paradigm.
- Figure 38.** Analysis of conditional Hdac1 knockout mice in the forced swim test (FST) during the chronic social defeat stress (CSDS) paradigm.
- Figure 39.** Analysis of conditional Hdac1 knockout mice in the water cross maze (WCM).
- Figure 40.** Schematic representation of the *Hdac3* wild-type locus and the *lacZ* reporter allele generated by targeted trapping.
- Figure 41.** *Hdac3* expression revealed by Hdac3-lacZ reporter mice.
- Figure 42.** Breeding scheme to generate conditional Hdac3 knockout mice.
- Figure 43.** Schematic representation of the Hdac3 wild-type locus, lacZ allele, floxed allele and knockout allele generated by targeted trapping and subsequent excision via Flp and Cre.
- Figure 44.** Verification of HDAC3 disruption in conditional Hdac3 knockout mice upon tamoxifen treatment.
- Figure 45.** Testing schedule for basal emotionality screen of Hdac3 conditional knockout mice.
- Figure 46.** Analysis of conditional Hdac3 knockout mice in the open field (OF).
- Figure 47.** Analysis of conditional Hdac3 knockout mice in the elevated plus maze (EPM) test.
- Figure 48.** Analysis of conditional Hdac3 knockout mice in the dark/light box (DaLi).
- Figure 49.** Analysis of conditional Hdac3 knockout mice in the forced swim test (FST).
- Figure 50.** Schematic representation of the chronic social defeat stress (CSDS) paradigm and behavioral phenotyping of conditional Hdac3 knockout mice.
- Figure 51.** Analysis of physiological parameters of conditional Hdac3 knockout mice during and after the chronic social defeat stress (CSDS) paradigm.
- Figure 52.** Analysis of corticosterone levels of conditional Hdac3 knockout mice subjected to the chronic social defeat stress (CSDS) paradigm.
- Figure 53.** Analysis of the behavior of conditional Hdac3 knockout mice in the open field (OF) during the chronic social defeat stress (CSDS) paradigm.
- Figure 54.** Analysis of conditional Hdac3 knockout mice in the social approach/avoidance (SA) test during the chronic social defeat stress (CSDS) paradigm.
- Figure 55.** Analysis of conditional Hdac3 knockout mice in the female urine sniffing test (FUST) during the chronic social defeat stress (CSDS) paradigm.
- Figure 56.** Analysis of conditional Hdac3 knockout mice in the elevated plus maze (EPM) during the chronic social defeat stress (CSDS) paradigm (analysis of first five minutes).
- Figure 57.** Analysis of conditional Hdac3 knockout mice in the elevated plus maze (EPM) during the chronic social defeat stress (CSDS) paradigm (analysis of first ten minutes).

- Figure 58.** Analysis of conditional Hdac3 knockout mice in the forced swim test (FST) during the chronic social defeat stress (CSDS) paradigm.
- Figure 59.** Analysis of conditional Hdac3 knockout mice in the water cross maze (WCM).
- Figure 60.** Analysis of transgenic mice of the line Camk2a-CreERT2.
-
- Table 1.** HDAC inhibitors (HDACi).
- Table 2.** Training protocol for spatial learning using the water cross maze (WCM).
- Table 3.** Classical *Hdacs* show high degree of sequence homology.
- Table 4.** Determination of expression levels of *Hdac1-11* within the adult murine brain.
- Table 5.** First approach of tamoxifen administration via food pellets.
- Table 6.** Second approach of tamoxifen administration via food pellets.

ABBREVIATIONS

4-OHT	4-hydroxytamoxifen
A	adenine
aa	amino acid
ADP	adenosine diphosphate
ALS	amyotrophic lateral sclerosis
bdnf	brain derived neurotrophic factor
BNST	bed nucleus of stria terminalis
bp	base pair
BUZ	binding-of-ubiquitin zinc
C	cytosine
CA	cornu ammonis
CamK	Ca ²⁺ /calmodulin-dependent protein kinase
cDNA	complementary DNA
CHD	chromodomain-helicase-DNA-binding protein
cKO	conditional knock-out
CNS	central nervous system
CoA	coenzyme A
COE	<i>Csfvgrh</i> conditional overexpressing
Cor26	<i>Crh</i> overexpression ROSA26
CoREST	co-repressor for elemt-1-silencing transcription factor
CpG	cytosine-phosphate-guanine
Cre	causes recombination
CREB	cAMP response element-binding protein
CSDS	chronic social defeat stress
CtBP	C-terminal binding protein
ctrl	control
Da	Dalton
DAD	deacetylase-activating domain
DaLi	dark/light
Del	deletion
DG	dentate gyrus
DMS-5	diagnostic and statistical manual of mental disorders, fifth edition
DNA	deoxyribonucleic acid
DNMT	DNA methyltransferase
E	exon
EPM	elevated plus maze
EX	embryonic day X
En	engrailed
ER	estrogen receptor
ERK	extracellular signal-regulated kinase
EUCOMM	European Conditional Mouse Mutagenesis Program
F	forward

frt	flippase recognition target
Flp	flippase
FUST	female urine sniffing test
FST	forced swim test
G	guanine
gal	galactosidase
H	histone
HAD	HDAC association domain
HAT	histone acetyltransferase
HD	histone deacetylase
HDA	histone deacetylase
HDAC	histone deacetylase
HDACi	HDAC inhibitor
HMT	histone methyltransferase zinc
HSP	heat shock protein
HUB	HDAC6- USP3, and Brap2-related
i-Cre	inducible Cre
i.p.	intraperitoneal
IRES	internal ribosomal entry site
ISH	<i>in situ</i> hybridization
K	lysine
kDa	kilo Dalton
kb	kilo base pairs
KO	knockout
lox	floxed
loxP	locus of X-over P1
LSD	lysine-specific histone demethylase
MBD	methyl-CpG-binding domain protein
MEF	myocyte enhancer factor
Mi2 α	CHD3
Mi2 β	CHD4
mRNA	messenger RNA
miRNA	microRNA
mSIN3A	paired amphipathic helix protein A
MTA	metastasis-associated protein
nAChR	nicotinic acetylcholine receptor
NAD ⁺	nicotinamide adenine dinucleotide
NCoR	nuclear receptor corepressor
neo	neomycin
NH ⁺	amino
NES	nuclear export signal
NF-Y	nuclear transcription factor Y
NLS	nuclear localization signal
NRSE	neuron-restrictive silencer element
NSC	neural stem cell

NuRD	nucleosome remodeling and deacetylating
OD	optical density
OF	open field
pA	poly-adenylation
piRNA	piwi-interacting RNA
p107	retinoblastom-like protein 1
p130	nucleolar phosphoprotein 130
PCR	polymerase chain reaction
PGK	phosphoglycerate kinase
pRb	protein retinoblastoma
PTSD	posttraumatic stress disorder
R	reverse
RbAP	retinoblastoma-associated protein
REST	RE1-silencing transcription factor
RNA	ribonucleic acid
RPD3	reduced potassium dependency protein 3
SAHA	suberoylanilide hydroxamic acid
SA	splice acceptor
SA test	social approach/avoidance test
SAP	HDAC complex subunit
siRNA	short interfering RNA
Sirt	sirtuin
SMRT	silencing mediator for retinoid and thyroid hormone receptors
SNP	single nucleotide polymorphism
SP	specificity protein
SUMO	small ubiquitin-like modifier
SV	simian virus
T	thymine
T2	type two
Tam	tamoxifen
TCS	tamoxifen citrate salt
TPX	trapoxin
TSA	trichostatin A
UTR	untranslated region
WB	Western Blot
wt	wild-type
Zn	zinc

ABSTRACT

It has been suggested that regulatory acetylation and deacetylation is considerably more widespread than presently appreciated, acting in a manner similar to phosphorylation and dephosphorylation. However, a change in acetylation has not only been recognized to be important for signaling molecules being a key means of signal transduction, but it is also important as epigenetic mark when the acetylation state of core histones is changed which strongly influences the architecture of the chromatin, thus, modulating gene activity. The balance between histone acetylation and deacetylation is mediated by opposing activities of two large protein families, the histone acetyltransferases (HATs) and the histone deacetylases (HDACs). Though HATs and HDACs have also non-histone proteins among their targets including transcription factors, cytoskeletal proteins and numerous metabolic enzymes, they received their name from their first identified targets, the histones which turns acetylation/deacetylation into an epigenetic mark. The following work focused on the studies of HDACs as epigenetic modulators. Epigenetic mechanisms seem to serve a potential role in many biological processes and pathologies and also play a pivotal role in the emerging field of neuroepigenetics. Thus, epigenetic mechanisms in the central nervous system (CNS) are just beginning to be understood and represent an exciting area of contemporary molecular and behavioral neuroscience. Therefore, we conducted comprehensive gene expression mapping of all 11 classical HDACs (class I, II and IV) throughout the murine brain in adulthood using *in situ* hybridization (ISH) analysis and imaging technologies. Our established atlas of *Hdac* mRNA expression reveals that all classical HDACs are expressed throughout the adult murine brain, each member having a unique and distinct expression pattern suggesting crucial and non-redundant roles for distinct HDAC members.

Especially in neurobiology the generation of mouse mutants harboring targeted inactivation of a desired gene or overexpression of a distinct gene in specific brain regions is used as a powerful tool to analyze a gene's role in complex brain functions such as learning and emotional behavior. However, to induce a conditional knockout or overexpression within genetic mouse models via the Cre/loxP system, no stress-free tamoxifen application was known at the beginning of the thesis and therefore, we established a tamoxifen administration in mice via food pellets. We determined as the best compromise between recombination efficacy and aversive effects of tamoxifen food (i.e. on body weight) for the spatio-temporal control of either overexpression or knockout studies in principal forebrain neurons by the use of the Camk2a-CreER^{T2} mouse line the following treatment scheme: mice are fed seven days with tamoxifen chow followed by a seven day wash-out phase with standard diet prior phenotypical analysis or behavioral testing.

Furthermore, we were interested in revealing brain-specific functions of two class I HDACs, namely HDAC1 and HDAC3. We established respective conditional mouse models and induced the knockouts in principal forebrain neurons in adulthood via the previously described tamoxifen food strategy. We could show that both enzymes are ubiquitously expressed throughout various murine tissues including the central nervous system. *Hdac1* mRNA expression throughout the adult murine brain is more general and weak with higher and specific expression only in the dentate gyrus (DG), whereas *Hdac3* mRNA is higher expressed all over the brain and ranks as the HDAC with the third highest expression level. Both conditional mouse models were subjected to several tests and comprehensively phenotyped under basal and chronically stressed conditions. Our results revealed for conditional *Hdac1* knockout mice a phenotype which is decreased in anxiety-related behavior under basal conditions and which is missing under chronically stressed conditions suggesting a role for HDAC1 in shaping of anxiety-related behavior. Furthermore, HDAC1 seems not to be involved in learning and memory processes. In contrast, conditional *Hdac3* knockout mice showed no overt phenotype in regard to emotional behaviors, but were strongly impaired in memory formation indicating that HDAC3 is important for learning and memory formation processes. Thus, our data indicates that HDAC1 and HDAC3 are not complementary to each other and are involved in totally different physiological and pathophysiological processes.

ZUSAMMENFASSUNG

Die Acetylierung und Deacetylierung spielt eine größere Rolle als ihr bisher zugetragen wurde, in Funktion und Tragweite ähnlich der der Phosphorylierung und Dephosphorylierung. Hierbei ist zum einen die Änderung des Acetylierungsmusters von Signalmolekülen als Schlüsselfunktion in vielen Signaltransduktionswegen wichtig, zum anderen aber auch die Änderung des Acetylierungsgehalts von Histonen, welcher wiederum starken Einfluss auf die Architektur des Chromatins ausübt und somit die Transkriptionsrate vieler Gene verändert. Die Balance zwischen Acetylierung und Deacetylierung wird durch zwei sich entgegenspielende große Proteinfamilien, den Histon Acetyltransferasen (HATs) und den Histon Deacetylasen (HDACs), reguliert. Der Name beider Proteinfamilien hat seinen Ursprung in deren Hauptsubstraten, den Histonen, welche die Acetylierung/Deacetylierung zu einer epigenetischen Markierung machen, obwohl natürlich auch andere Moleküle wie Transkriptionsfaktoren, Proteine des Zytoskeletts oder zahlreiche metabolische Enzyme zu ihren Zielstrukturen zählen. Die folgende Arbeit konzentriert sich auf die HDACs als epigenetische Modulatoren. Hierbei ist zu erwähnen, dass epigenetische Mechanismen eine ganze Reihe von Funktionen innehaben, sowohl in biologischen und pathologischen Prozessen als auch im aufstrebenden Feld der Neuroepigenetik. Die Forschung ist gerade erst dabei, epigenetische Mechanismen im Bereich des zentralen Nervensystems aufzudecken und zu verstehen, was ein sehr spannendes Thema auf dem Gebiet der molekularen Neurowissenschaften und Verhaltensforschung darstellt. Deshalb haben wir eine ausführliche Expressionsstudie aller elf klassischen HDACs (Klasse I, II und IV) im adulten Gehirn der Maus mit Hilfe von *in situ* Hybridisierungsanalysen durchgeführt. Der von uns entwickelte Atlas, der die Expression der *Hdac* mRNA Transkripte darstellt, zeigt, dass alle HDACs im adulten murinen Gehirn exprimiert sind und zwar jeweils mit einem einzigartigen und ganz spezifischen Expressionsmuster, was darauf hindeutet, dass die einzelnen HDAC Proteine kritische und nicht-redundante Funktionen im Gehirn zu übernehmen scheinen.

Gerade in der Neurobiologie ist die Verwendung genetischer Mausmutanten, die eine gezielte Inaktivierung bzw. Überexpression eines gewünschten Gens ermöglichen von extremer Wichtigkeit und wird oft als sehr machtvolles Werkzeug zur Analyse komplexer Genfunktionen wie Lernprozessen oder Verhaltensanalysen eingesetzt. Zu Beginn der Thesis gab es jedoch keine stressfreie Methode, um die konditionale Geninaktivierungen/Genüberexpression in Mäusen mittels des Cre/loxP Systems durch die Gabe von Tamoxifen zu induzieren. Deshalb haben wir die Tamoxifenzufuhr bei Mäusen durch die Gabe von tamoxifenhaltigem Futter etabliert und als besten Kompromiss zwischen der Effizienz der Rekombination und den aversiven Effekten des

tamoxifenhaltigen Futters (z.B. auf das Körpergewicht) konnten wir für die zeitlich und räumlich kontrollierte Inaktivierung/Überexpression eines Gens in den Prinzipalneuronen des Vorderhirns mit Hilfe der Mauslinie Camk2a-CreER^{T2} folgende Strategie bestimmen: Die Mäuse werden sieben Tage mit dem tamoxifenhaltigen Futter versorgt, gefolgt von einer siebentägigen Phase mit normalem Futter, in der das Tamoxifenfutter aus dem Körper der Mäuse ausgespült werden kann.

Des Weiteren hatten wir großes Interesse an den Gehirn-spezifischen Funktionen zweier Klasse I HDACs, den Enzymen HDAC1 und HDAC3. Unter Verwendung konditionaler Mausmodelle, in denen durch die zuvor etablierte und beschriebene Strategie mittels des tamoxifenhaltigen Futters die Geninaktivierung in allen Prinzipalneuronen des Vorderhirns im adulten Tier induziert wurde, konnten wir zeigen, dass beide Enzyme ubiquitär exprimiert sind. HDAC1 und HDAC3 sind sowohl in diversen Organen als auch im zentralen Nervensystem exprimiert. Die Expression der mRNA von *Hdac1* jedoch ist im Gehirn eher schwach und nur in ganz bestimmten Regionen stärker vorhanden, wie zum Beispiel im *gyrus dentatus* (DG) des Hippocampus. Verglichen mit HDAC1, zeigt HDAC3 hingegen gehirnweit eine generell höhere Expression und gilt unter allen klassischen HDACs als das mit der dritt höchsten Expressionsrate im murinen Gehirn. Beide konditionalen Mausmodelle wurden anhand diverser Verhaltensanalysen phänotypisiert und auch unter verschiedenen Bedingungen (stressfrei und chronischer Stress) getestet. Unsere Studien ergaben für Mäuse mit konditionaler *Hdac1* Inaktivierung einen prägnanten Phänotyp, der eine Reduktion des Angstverhaltens unter basalen Bedingungen aufweist, welche aber unter chronisch gestressten Bedingungen ausbleibt und somit für HDAC1 eine Rolle in der Angstkontrolle vorschlägt. HDAC1 scheint jedoch nicht involviert in Lernprozessen und Erinnerungen. Im Gegensatz dazu konnten wir in den Mäusen mit konditionaler *Hdac3* Inaktivierung keinen Phänotyp oder Änderung des emotionalen Verhaltens beobachten. Aber die Mäuse hatten große Defizite in Bezug auf Lernprozesse bzw. das Erinnerungsvermögen. Somit weisen unsere Ergebnisse darauf hin, dass die Enzyme HDAC1 und HDAC3 nicht komplementär zueinander agieren und mit komplett unterschiedlichen physiologischen und pathophysiologischen Prozessen assoziiert werden.

1 INTRODUCTION

1.1 Epigenetics – a brief glance at the history and definitions

Epigenetics as one of the most exciting contemporary and rapidly expanding research fields is portrayed in the press as a young and revolutionary new science. There are thousands of scientific articles arising since the beginning of the twenty-first century focusing on epigenetics, its mechanisms and relevance. But what does epigenetics mean?

Today's scientists working in the field of epigenetics, describe the term as follows: *"Epigenetics has always been all the weird and wonderful things that can't be explained by genetics."* (Denise Barlow, Vienna, Austria); *"DNA is just a tape carrying information, and a tape is no good without a player. Epigenetics is about the tape player."* (Bryan Turner, Birmingham, UK); *"Information management in the nucleus means that some of the genetic information is very very tightly packaged in the genome. Then there is genetic information that has to be on and active all the time, house-keeping genes for example. So epigenetics is a bit like information management at home, something that you need all the time you will not store away, but your old school records you keep packed in boxes in the attics."* (Peter Becker, Munich, Germany).

In biology there have always been words that have different meanings for different people. However, epigenetics is an extreme case. For a long time, each author had his own idea for defining epigenetics, because it has several meanings with independent roots. A brief look at the history demonstrates that human beings were concerned with the idea of epigenetics already more than 2000 years ago. Thus, the Greek philosopher Aristotle described in his book *'On The Origins of Animals'* (written ca. 350 BC) the notion of epigenetics by telling that the adult form of an embryo develops through gradual stages (Hurd, 2010; Rall, 1997). This debate prevailed into the nineteenth century, when Gregor Mendel realized that inheritance and development can be studied separately. However, his opinion was widely ignored as the leading biologists of his days considered inheritance and development to be the same problem (Robin Holliday, 2006; Sandler & Sandler, 1985). Whilst the field of genetics flourished in the first half of the twentieth century, the field of embryology and development was sidelined. Hence, it is remarkable that the first one who took the problem of development into account again, was one of the great pioneers in genetics. So Thomas Hunt Morgan described in 1910 *"We have two factors determining characters: heredity and the modification during development."* (Robin Holliday, 2006; Hurd, 2010; Morgan, 1910). This modification during development is referred to as epigenetics. Nevertheless, the strict separation

between genetics and developmental biology remained until the middle of the twentieth century, when a few leading biologists like Conrad Hal Waddington and Ernst Hadorn realized that the two fields were indeed related and should come together in a common discipline (Robin Holliday, 2006; Hurd, 2010). Waddington remarked in the late 1930s *“It is, surely, obvious that the fertilized egg contains constituents which have definite properties which allow only a certain limited number of reactions to occur; in so far as this is true, one may say that development proceeds on a basis of the ‘preformed’ qualities of the fertilized egg. But equally it is clear that the interaction of these constituents gives rise to new types of tissue and organ which were not present originally, and in so far development must be considered as ‘epigenetic’.”* (Hurd, 2010; Waddington, 1939). He further pronounced that *“One might say that the set of organizers and organizing relations to which a certain piece of tissue will be subject during development make up its ‘epigenetic constitution’ or ‘epigenotype’; then the appearance of a particular organ is the product of the genotype and the epigenotype, reacting with the external environment.”* (Waddington, 1939). In 1942, Waddington introduced the term epigenetics as a portmanteau of the word epigenesis and genetics (Waddington, 1939, 1942). He defined it as *“The branch of biology which studies the causal interactions between genes and their products which bring the phenotype into being”* (Dupont, Armant, & Brenner, 2009; Waddington, 1968). However, when Waddington coined the term, the physical nature of genes and their role in heredity was not known. He used it as a conceptual model of how genes might interact with their surroundings to produce a phenotype and proposed the concept of an *‘epigenetic landscape’* used as a metaphor for biological development to represent the process of cellular decision making (Hurd, 2010; Waddington, 1957). As mentioned before, there was another influential and leading developmental biologist in the middle of the twentieth century who realized as well that sooner or later the two disciplines, genetics and embryology, would coalesce. This was Ernst Hadorn in Zurich who was very successful in studying lethal factors and the development of imaginal disks in *Drosophila*. However, he was all his career long concerned about one question: *“What are the mechanisms that govern development and what are the roles of the nucleus with its genes on the one hand and the surrounding cytoplasm on the other?”* (Robin Holliday, 2002, 2006; Nöthiger, 2002). Another notable biologist during the mid-twentieth century who wanted to make connections between genetics and development was Richard Goldschmidt who hypothesized epigenetic theories for evolution, but his views were quite controversial which have earned him a reputation as a *‘scientific heretic’* (Dietrich, 2003; Goldschmidt, 1940; Robin Holliday, 2006). Besides Goldschmidt, two other great general biologists and evolutionists, Julian Huxley and John Haldane, contributed to develop the triad of *‘genetics-development-evolution’* (Robin Holliday, 2006; Huxley, 1956). In the second half of the twentieth century the field of

epigenetics gained several proponents like David Nanney, Martha Berry, Gideon Daniel Searle, Boris Ephrussi and Joshua Lederberg. Nonetheless, each of them had his own idea of the meaning of epigenetics, thus, definitions depend on the author and the year they were put forward (Haig, 2004; Robin Holliday, 2006; Nanney, 1958).

Nevertheless, there has been an explosive revolution in the field of epigenetic research in the 1990s. A renewed interest in genetic assimilation elucidating the molecular basis of Waddington's observations, and discoveries like involvement of epigenetic alterations in pathological processes paved the way for epigenetics to become not a new but exciting and extremely promising research branch. In line with this notable break-through much effort has been put into unraveling epigenetic mechanisms and further definitions of the term epigenetics arose which are contemporarily in use. Therefore, Robin Holliday proposed in 1990 to define epigenetics as *"The study of the mechanisms of temporal and spatial control of gene activity during the development of complex organisms"*. Thus, the term 'epigenetic' can be used to describe anything other than DNA sequence that influences the development of an organism (Robin Holliday, 1990, 2002, 2006). Functional morphologists are probably more familiar with Susan Herring's definition of epigenetics as *"The entire series of interactions among cells and cell products which lead to morphogenesis and differentiation"* (Haig, 2004; Herring, 1993), whereas molecular biologists rather use the definition of Arthur Riggs (1996): *"The study of mitotically and/or meiotically heritable changes in gene function that cannot be explained by changes in DNA sequence"* (Haig, 2004; Robin Holliday, 2006; Arthur D Riggs, 1996). The more discoveries and involvements of epigenetic mechanisms are made, the more definitions or redefinitions are required. Thus, in 2007 Adrian Bird described epigenetics in regard to heritable changes: *"The structural adaptation of chromosomal regions so as to register, signal or perpetuate altered activity states"* (Bird, 2007). Whereas one of the latest definitions is expressed by Danny Reinberg in 2010: *"Those processes that ensure the inheritance of variations (-genetics) above and beyond (epi-) changes in the DNA sequence"* (Bonasio, Tu, & Reinberg, 2010; Hurd, 2010). Although there are so many definitions with several different connotations for the term epigenetics we finally can combine all to a minimum fundamental description of 'epigenetics' as a type of molecular and cellular 'memory' that results in stable changes in gene expression without alterations to the DNA sequence itself.

1.2 The importance of epigenetic mechanisms

When Waddington coined the word '*epigenetics*' he related genes and gene action to development without knowing the underlying mechanisms. For a long time, scientists have sought to explain fundamental questions regarding phenomena such as cellular differentiation during embryonic development, X-chromosomal inactivation, genomic imprinting and transcriptional silencing of transposons. As time went on also the pivotal role of epigenetic mechanisms was well-characterized in pathological processes involved in cancer. Taking all the findings in epigenetic research during the last decades into account, it is nonetheless apparent that there are certain discoveries that still demand an epigenetic explanation. Thus, epigenetic mechanisms have been implicated to be the mediators of several functions also within the central nervous system which raises questions such as: What is the impact of epigenetic mechanisms on neural development and behavior, and what is the potential role of these mechanisms in neurological and psychiatric disorders? All these findings and questions highlight the need for epigenetic mechanisms.

However, in order to understand and deal with epigenetic mechanisms, it is important to first characterize chromatin and its structure. Chromatin is the reason why two meters of genomic DNA can be packed and stored within a 6 μm thin cell nucleus (Alberts et al., 2002; Kornberg, 1974). It is the higher structured order of DNA and associated proteins (Figure 1.A). At the heart of chromatin structure there are highly conserved histone proteins that function as building blocks to package the eukaryotic DNA into the most fundamental subunit of the chromatin, the nucleosome core particles. These are made up of 147 base pairs of genomic DNA wrapped around a disc-shaped core histone protein octamer that contains a histone 2xH3/2xH4 heterotetramer flanked by two H2A/H2B heterodimers. This highly conserved nucleoprotein complex occurs essentially every 200 \pm 40 base pairs throughout all eukaryotic genomes and they are linked with one another due to some base pairs of linker DNA and the histone protein H1 (Arents, Burlingame, Wang, Love, & Moudrianakis, 1991; Cosgrove & Wolberger, 2005; Hurd, 2010; Jenuwein & Allis, 2001; Kornberg & Lorch, 1999; Kornberg, 1974; Luger, Mäder, Richmond, Sargent, & Richmond, 1997; McGhee, Felsenfeld, & Eisenberg, 1980; Strahl & Allis, 2000). Nucleosome core particles and linker DNA plus H1 form a nucleosome which assemble themselves into higher-order structures and bundle together with non-histone proteins to form chromatin fibers which further condense to build up the chromosome. Chromatin fibers are highly dynamic structures and exist in several transient states of compaction to regulate the accessibility of the DNA which is important for cellular processes such as transcription/gene expression, replication, repair and recombination. The two

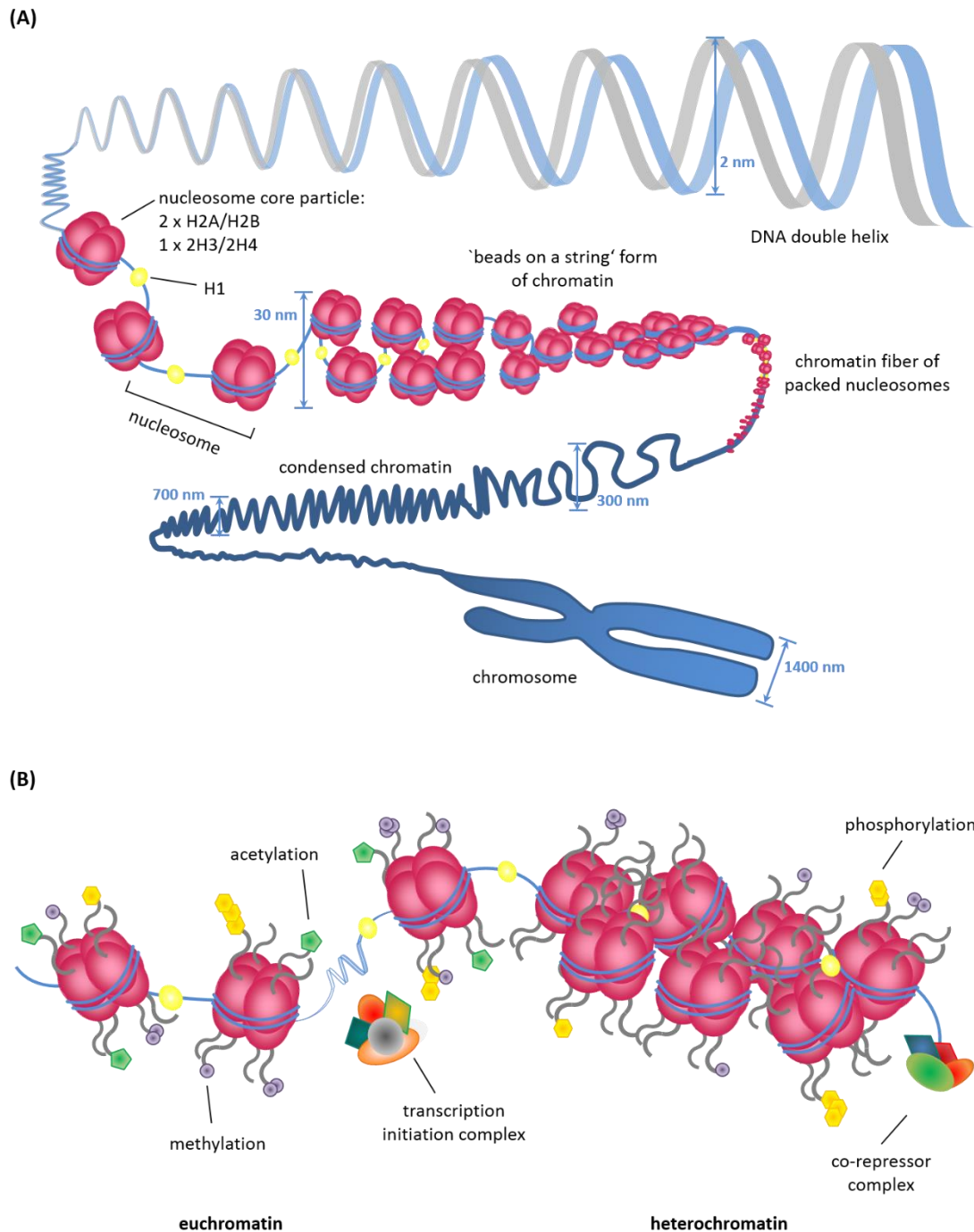


Figure 1. Chromatin formation and structure. (A) Chromatin is the complex of DNA and proteins that makes up chromosomes. The nucleic acids form a double helix consisting of double-stranded DNA. The major proteins involved in chromatin are histone proteins. The DNA is wrapped around a histone octamer consisting of two H2A/H2B heterodimers and one 2xH3/2xH4 heterotetramer making up a nucleosome core particle which in turn forms together with the linker DNA and the histone H1 a nucleosome. These assemble themselves to higher-ordered structures to form chromatin fibers and further condense to build up the chromosomes. (B) The chromatin structure is highly dynamic and exists in several interstages with two extrema, namely euchromatin (transcriptionally active) and heterochromatin (transcriptionally inactive), which are strongly influenced by various modifications.

extreme states chromatin inhabits are heterochromatin and euchromatin, but the transition is highly dynamic through transient interstages (Figure 1.B). Heterochromatin corresponds, in general, to genome regions that are highly condensed and possess inactive and transcriptionally silent genes.

Within heterochromatin, the DNA renders itself inaccessible to regulatory components of the transcription-promoting machinery. It is usually methylated in the dinucleotide CpG islands and histones are markedly hypoacetylated. By contrast, euchromatin refers to the transcriptionally active and decondensed regions of the genome and is highly accessible to nucleases. The CpG islands exist more in an unmethylated manner and histones, especially H3 and H4, are hyperacetylated (Arney & Fisher, 2004; Cosgrove & Wolberger, 2005; André Fischer, Sananbenesi, Mungenast, & Tsai, 2010; Kosak & Groudine, 2004; Owen-Hughes & Bruno, 2004; Quina, Buschbeck, & Di Croce, 2006).

It has long been appreciated that gene expression requires the orchestrated effort of not only transcription factors, but also the protein complexes that modify chromatin structure. Alterations in chromatin structure are exerted through epigenetic mechanisms which mainly rely on DNA modification on the one hand and histone modification on the other. The first epigenetic mechanism described was DNA methylation, a covalent modification that triggers heritable gene silencing (Griffith & Mahler, 1969; R Holliday & Pugh, 1975; Robin Holliday, 2006; Kiefer, 2007; Levenson & Sweatt, 2005; A D Riggs, 1975). Within a biochemical reaction catalyzed by DNA methyltransferases (DNMTs) a methyl group is attached to a cytosine DNA nucleotide (Figure 2). DNA-methylation typically occurs in the context of paired symmetrical methylation of a CpG site, in which a cytosine nucleotide is located next to a guanidine nucleotide. In the bulk of genomic DNA most single CpG sites are heavily methylated while clusters of CpG sites the so-called CpG islands remain unmethylated. Cytosine methylation triggers gene silencing in two ways, first, the methylated DNA itself may physically impede the binding of transcription factors, and second, methylated DNA attracts proteins like the methyl-CpG-binding domain proteins (MBDs) which in turn recruit co-repressor complexes harboring other chromatin remodeling proteins such as histone deacetylases (HDACs) and histone methyltransferases (HMTs). Thereby a positive feedback loop between DNA methylation and histone methylation, another fundamental epigenetic silencing mark, is fueled (Choy et al., 2010; Fujita et al., 2003; Fuks et al., 2003; Kiefer, 2007). Equally important and coupled with DNA methylation is the DNA demethylation, which is carried out by either TET enzymes (Ten-eleven translocation methylcytosine dioxygenase) or AID/APOBEC enzymes (a group of cytidine deaminases). The DNA demethylation process is necessary for

epigenetic reprogramming and also directly involved in many important disease mechanisms such as tumor progression (Baylin, 2008; Egger, Liang, Aparicio, & Jones, 2004).

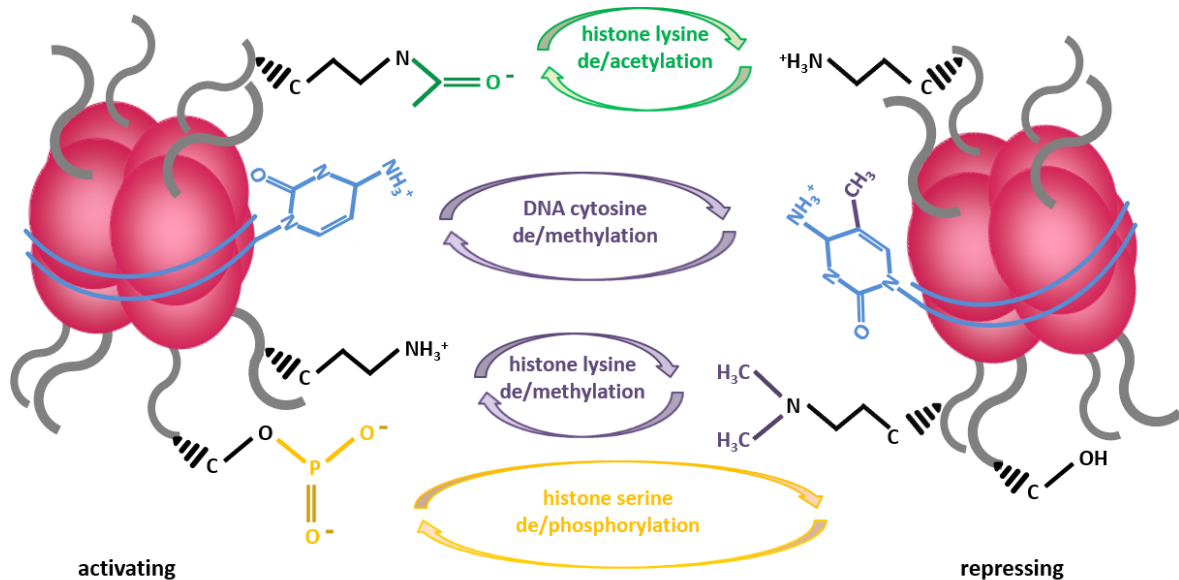


Figure 2. Epigenetic mechanisms. Modifications either on DNA or histone proteins trigger chromatin remodeling. Posttranslational modifications of specific amino acid residues within the N-terminal tails of core histone proteins such as lysine acetylation and serine phosphorylation are known to activate gene expression. In repressed chromatin regions, mainly DNA cytosine and histone lysine methylation can be found.

Along with DNA methylation there are specific modifications on the protein level which act as epigenetic mechanisms to alter chromatin structure, hence influencing transcription levels. These posttranslational modifications such as acetylation, methylation, ADP-ribosylation, ubiquitination, citrullination and phosphorylation are catalyzed by specific enzymes and are exerted on amino acid residues located within the N-terminal tails of nucleosomal histones (Figure 2). More than 30 sites within each of the four octameric histones are known to be accessible for distinct modifications which are not only stabilizing or destabilizing the interaction between histone proteins and the underlying DNA within the chromatin structure, but also serve to recruit other proteins from the regulatory machinery by specific recognition of the modified histone via distinct protein domains (Jenuwein & Allis, 2001; McNairn & Gilbert, 2003; Quina et al., 2006; Wolffe & Hayes, 1999). Individual histones may even acquire a series of modification marks in close proximity to each other. The collectivity of these histone marks, either at the local or the genomic level, and the appropriate prediction of the transcriptional state is known as the so-called '*histone code*' (Cosgrove &

Wolberger, 2005; Featherstone, 2002; Fischle et al., 2002; Fischle, Wang, & Allis, 2003; Jenuwein & Allis, 2001; Quina et al., 2006; Strahl & Allis, 2000; Turner, 2000). Major players in histone modification are the histone deacetylases (HDACs) which will later be discussed in detail.

With the discovery of non-coding RNA molecules new components involved in epigenetic processes were found (Baulcome, 2005; Filipowicz, 2005; Sontheimer & Carthew, 2005). These regulatory molecules are transcribed from DNA, but are not further translated into proteins, and comprise with their activities new controls for gene expression at the transcriptional and post-transcriptional level. The huge amount of non-coding RNAs can be divided into two major groups depending on their size. Small non-coding RNAs are not longer than 30 nucleotides and are sub-grouped into microRNAs (miRNAs), short interfering RNAs (siRNAs) and piwi-interacting RNAs (piRNAs). miRNAs mediate posttranscriptional gene silencing by binding with a complementary sequence to a specific target messenger RNA (mRNA) and inducing cleavage, degradation or blocking of translation. siRNAs function in a similar way as miRNAs and cause degradation of the targeted mRNA, but in addition siRNAs are able to induce heterochromatin formation. Last, but not least, piRNAs, which are so-called due to their interaction with the piwi family of proteins, primarily function in chromatin regulation and the suppression of transposon activity in germline and somatic cells. The other major group of non-coding RNAs comprises longer RNA molecules which are in general made up of more than 200 nucleotides. These can complex with chromatin-remodeling enzymes and recruit their catalytic activity to specific sites in the genome, thereby regulating transcription and posttranscriptional processes. However, both major groups, the small and large non-coding RNA molecules, find their role in epigenetic processes like heterochromatin formation, histone modification, DNA methylation targeting and gene silencing (Brennecke et al., 2007; Carthew & Sontheimer, 2009; Collins, Schönfeld, & Chen, 2011; Cui, Zhang, Ko, & Kim, 2009; Dogini et al., 2014; André Fischer, Sananbenesi, Schrick, Spiess, & Radulovic, 2004; Gavazzo, Vassalli, Costa, & Pagano, 2013; Hsieh & Gage, 2004; Hüttenhofer, Schattner, & Polacek, 2005; Kaikkonen, Lam, & Glass, 2011; Mercer & Mattick, 2013; Sontheimer & Carthew, 2005).

1.3 The family of histone deacetylases (HDACs) as epigenetic modifiers

It has been suggested that regulatory acetylation/deacetylation is considerably more widespread than presently appreciated, acting in a manner similar to phosphorylation and dephosphorylation (Gregoretto, Lee, & Goodson, 2004; Kouzarides, 2000). However, as an epigenetic mark, the acetylation state of core histones is strongly influencing the architecture of the chromatin, thus, modulating gene activity (Cress & Seto, 2000). In general, increased levels of acetylation (hyperacetylation) are associated with transcriptionally active genes, as it contributes to the decondensed chromatin state and maintains the unfolded structure of the nucleosome, whereas decreased levels of acetylation (hypoacetylation) usually mark inactive genes causing a repression of transcriptional activity (Davie et al., 2008; de Ruijter, van Gennip, Caron, Kemp, & van Kuilenburg, 2003; Delcuve, Khan, & Davie, 2012; Forsberg & Bresnick, 2001; Groth, Rocha, Verreault, & Almouzni, 2007; Ito, Barnes, & Adcock, 2000; Johnstone, 2002; Marmorstein, 2001; Shahbazian & Grunstein, 2007; Shogren-Knaak et al., 2006; Tse, Sera, Wolffe, & Hansen, 1998; X. Wang, He, Moore, & Ausio, 2001). Histone acetylation occurs mainly at lysine residues, located within the freely accessible N-terminal tails of the nucleosomal histone proteins. The balance between histone acetylation and deacetylation is mediated by opposing activities of two large protein families, the histone acetyltransferases (HATs) and the histone deacetylases (HDACs) (Delcuve et al., 2012; H.-J. Kim & Bae, 2011; Sweatt, Nestler, & Michael, 2013). There are about 30 known HATs in humans which can be grouped into five families based on subcellular localization, structure and function. As epigenetic regulators, HATs catalyze the direct transfer of an acetyl group from the co-factor acetyl-CoA to the ϵ -NH⁺ group of the lysine residues, thus, neutralizing the positive charge which increases DNA accessibility or serves as a binding site for chromatin remodeling complexes (Lau et al., 2000; Richman, Chicoine, Collini, & Cook R.G. Allis, 1988; Sweatt et al., 2013; Tanner, Langer, & Denu, 2000).

The counteracting enzymes are the histone deacetylases (HDACs). Like acetylation, the deacetylation of a lysine ϵ -amino group was first discovered on histones and gives the HDACs their name, which is actually a misnomer and the enzymes should be more accurately described as '*lysine deacetylases*' as lysine amino acid side chains are acetylated in a wide variety of cellular proteins besides just histones. Hence, HDACs have histones and non-histone proteins among their substrates including transcription factors, cytoskeletal proteins and numerous metabolic enzymes (Delcuve et al., 2012; Gregoretto et al., 2004; H.-J. Kim & Bae, 2011; Sweatt et al., 2013). In the sense

of epigenetic regulation, the predominant substrates of HDACs are of course the histone molecules. Acetylation and deacetylation takes exclusively place at lysine residues, which protrude in an N-terminal tail out of the histone molecules and the nucleosome. Predestined targets are distinct lysine residues of histone 3 (H3: H3K9, H3K14, H3K27)) and histone 4 (H4: H4K5, H4K8, H4K12, H4K16, H4K20) (Figure 3) (Jenuwein & Allis, 2001; Peleg et al., 2010; Turner, 2000). The removal of an acetyl group from lysine side chains of the histones reconstitutes their positive charge which in turn stabilizes the interaction between histones and the negatively charged DNA inducing the formation of a compacted, transcriptionally repressed chromatin structure. Indeed, HDACs are often found to be part of co-repressor complexes. However, this repressing model reflects an oversimplification of the role of HDACs in epigenetic regulation as genetic experiments in *Drosophila* and yeast have indicated that deacetylase activity can contribute to gene activation as well (Gregoret et al., 2004; Grozinger, Chao, Blackwell, Moazed, & Schreiber, 2001; Kurdistani & Grunstein, 2003; Marmorstein, 2001).

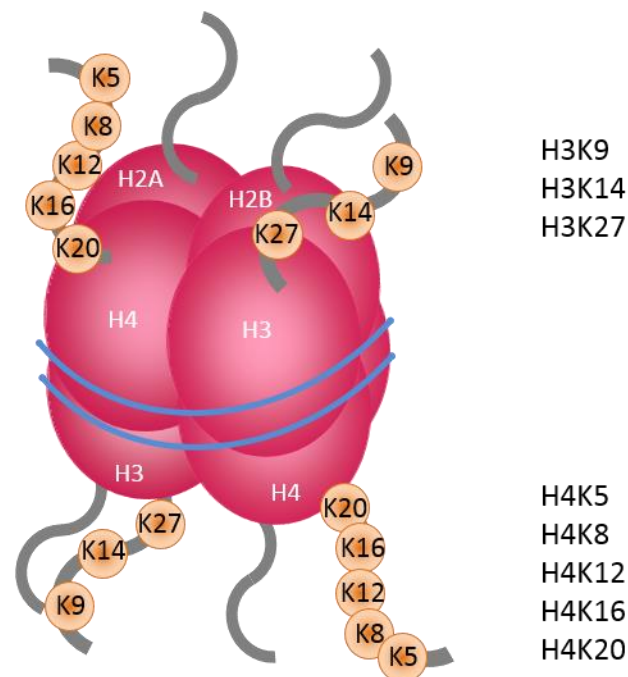


Figure 3. Predestined lysine side chains of histone molecules. Acetylation/deacetylation of histones takes exclusively place at lysine residues, located within the N-terminal tails, which protrude out of the nucleosome. Predominant targets are H3K9, H3K14, H3K27, H4K5, H4K8, H4K12, H4K16 and H4K20. [H = histone; K = lysine residue]

HDACs are members of an ancient enzyme family found in plants, animals, fungi, archaeobacteria and eubacteria. They can be divided into two main categories, the classical HDACs and the sirtuins, which are completely different in their characteristics and are only categorized into one and the same family of proteins due to their ability to deacetylate their substrates. The sirtuins will not be subject of discussion in the following and only for completeness they will be described briefly: seven members (Sirt1-7) belong to the group of sirtuins, which all deacetylate lysine ϵ -amino groups depending on NAD⁺ as cofactor, but they differ in their substrates and biological function (de Ruijter et al., 2003; Gregoretta et al., 2004; Grozinger et al., 2001; Grozinger, Hassig, & Schreiber, 1999; Leipe & Landsman, 1997; Marmorstein, 2001; Shore, 2000). In the following the term HDACs will refer to the eleven members of the conventional HDAC family and not to the sirtuins. All eleven classical HDACs are metalloenzymes and have in common to act in a Zn²⁺-dependent manner. Their catalytic domain is formed by a stretch of approximately 390 amino acids consisting of a set of highly conserved residues which form a gently curved tubular pocket with a wider bottom at the active site. Removal of an acetyl group from substrates occurs via a charge-relay system, consisting of two adjacent histidine residues, two aspartic residues (separated from one another by approximately 6 amino acid residues and located approximately 30 amino acid residues downstream from the two histidine residues) and one tyrosine residue (located approximately 123 amino acid residues downstream from the two aspartic residues). The Zn²⁺ ion as cofactor is an essential component of the charge-relay system and bound at the bottom of the pocket (Buggy et al., 2000; de Ruijter et al., 2003; Finnin et al., 1999; Sweatt et al., 2013). Members of the classical HDAC family can be divided into three classes based on their sequence similarity to yeast (*Saccharomyces cerevisiae*) counterparts (Figure 4). Class I HDACs, closely related to the transcriptional regulator RPD3 of *Saccharomyces cerevisiae*, comprise HDAC1, HDAC2, HDAC3 and HDAC8. Class II HDACs (HDAC4, HDAC5, HDAC6, HDAC7, HDAC9 and HDAC10) share domains with similarity to the yeast HDA1 and can be further phylogenetically divided into subclass IIa (HDAC4, HDAC5, HDAC7 and HDAC9) and subclass IIb (HDAC6 and HDAC10). Class IV consists of only one member, the HDAC11 protein. Class III resembles the class of the seven sirtuins described earlier (Bjerling et al., 2002; de Ruijter et al., 2003; Fischle, Dequiedt, et al., 2001; L. Gao, Cueto, Asselbergs, & Atadja, 2002).

As mentioned before, all members of classical HDACs share their common catalytic motif which is highly conserved and essential for their deacetylating activity (Figure 5.A), and they can be distinguished by their phylogenetic similarities to yeast counterparts which makes the differentiation into groups possible. Additionally a unique N-terminal sequence is only found in class II enzymes which results in high molecular weight proteins, whereas class I and class IV

enzymes are rather small proteins (Grozinger et al., 1999; H. Y. Kao et al., 2001; H. Y. Kao, Downes, Ordentlich, & Evans, 2000; Wade, 2001). Furthermore, the classes vary in their distribution within various tissue. Currently it is thought that HDACs of class I are expressed in most cell types and tissues, whereas the distribution of class II HDACs is more restricted, although recent studies show that most tissues express at least one member of class II enzymes. To exert their main function, the deacetylation of histone proteins, the HDAC enzymes are required to be in the cell nucleus, therefore, all classical HDACs, with few exceptions, comprise a nuclear localization signal (NLS) (Figure 5.B). A second way to translocate to the nucleus is the binding to other HDAC proteins, which is possible through a HDAC association domain (HAD) located in the N-terminal portions of the proteins which allows homo- or heterodimerization. Some HDACs, mainly members of class II, can be cytosolic as well and harbor therefore a nuclear export signal (NES). These enzymes are able to shuttle in and out of the nucleus in response to various internal and external stimuli of the cell (Figure 5.C) (Bertos, Wang, & Yang, 2001; Buggy et al., 2000; de Ruijter et al., 2003; Fischle, Dequiedt, et al., 2001; Gregoretta et al., 2004; W.-M. Yang, Tsai, Wen, Fejer, & Seto, 2002). In the following section, all eleven members of the classical HDAC family are described individually in more detail. The focus lies on two class I proteins, namely HDAC1 and HDAC3, as these two enzymes are the main subject of this work.

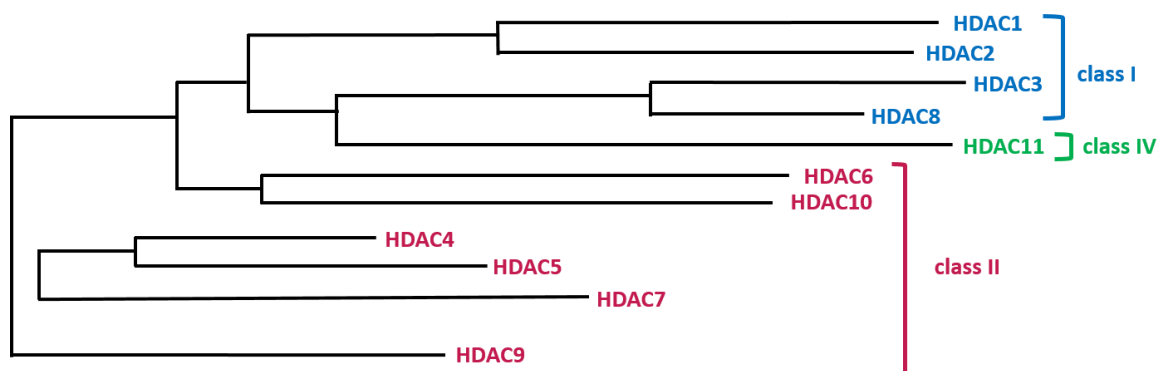


Figure 4. Evolutionary relationship between classical HDACs. Schematic representation of the phylogenetic division of all eleven classical HDAC members. Class I HDACs are depicted in blue and can be grouped together due to their high sequence similarity to the *Saccharomyces cerevisiae* protein RPD3. Class II HDACs are all highly homologous to their yeast counterpart HDA1 and can be divided into class IIa (HDAC6 and HDAC10) and class IIb (HDAC4, HDAC5, HDAC7, HDAC9). HDAC11 forms a separate class, but is more similar to class I members than class II members. Class III comprises the seven sirtuins and is therefore not depicted. Adapted from (de Ruijter et al., 2003; Gregoretta et al., 2004).

1.3.1 Describing the low molecular weight class I HDACs

1.3.1.1 HDAC1 and HDAC2 are exclusively nuclear proteins and important chromatin remodelers

HDAC1 (originally called HD1) was the first protein found to possess histone deacetylase activity in mammals. With its purification and cloning in 1996 a major breakthrough in the study of histone deacetylases was achieved (Kijima, Yoshida, Sugita, Horinouchi, & Beppu, 1993; Taunton, Hassig, & Schreiber, 1996; Yoshida, Horinouchi, & Beppu, 1995). The predicted amino acid sequence derived from the full-length cDNA sequence of HDAC1 revealed for both, the human and mouse HDAC1 protein, to be highly similar to the yeast transcriptional regulator RPD3 (Bartl et al., 1997; Furukawa et al., 1996; Vidal & Gaber, 1991). After the discovery of HDAC1, a transcriptional co-repressor protein also showing high homology to yeast RPD3 was identified in the same year from a yeast two-hybrid experiment and later called HDAC2 as it contains deacetylase activity as well (W M Yang, Inouye, Zeng, Bearss, & Seto, 1996; Wen Ming Yang, Yao, Sun, Davie, & Seto, 1997). HDAC1 and HDAC2 possess a high degree of similarity with an overall sequence identity in mammals of approximately 82% and an almost identical genomic organization (de Ruijter et al., 2003; Khier, Bartl, Schuettengruber, & Seiser, 1999). Indeed, HDAC1 and HDAC2 arose most probably from a relatively recent gene duplication (Gregoretta et al., 2004). The *Hdac1* gene maps to mouse chromosome 4 and human chromosome 1p34.1 and is about 30 kb in length, comprising 14 exons interrupted by 13 introns (Furukawa et al., 1996; Khier et al., 1999). The *Hdac1* open reading frame is 1446 bp long and encodes a protein of 482 amino acids with a molecular mass of approximately 55 kDa (Bartl et al., 1997; Furukawa et al., 1996; Taunton et al., 1996). The HDAC1 protein is mainly characterized by the catalytic domain at the N-terminus, which forms the major part of the protein (Figure 5.A). However, the structural and functional organization of the protein can be divided into three domains: (1) the N-terminal HDAC association domain (HAD; residues 1-53), which is essential for homo- and heterodimerization; (2) the central zinc-binding catalytic domain termed HDAC consensus motif (residues 25-303), which is highly conserved and forms the active site pocket; (3) the C-terminal lysine-rich domain (residues 438-482) which contains the nuclear localization signal (NLS) KKAKRVKT and the IACEE motif involved in the interaction with the pocket proteins pRb, p107 and p130, which are important enzymes for cell cycle regulation and progression, apoptosis and cell maturation (Figure 4.A and 4.B) (Brehm et al., 1998; Cress & Seto, 2000; Ferreira, Magnaghi-Jaulin, Robin, Harel-Bellan, & Trouche, 1998; H. Y. Kao et al., 2000; J. Li et al., 2000; Magnaghi-Jaulin et al., 1998; Taplick et al., 2001; Wade, 2001). The *Hdac2* gene located on mouse chromosome 10 and human chromosome 6q21 is similar in size compared to *Hdac1* and also consists of 14 exons

and 13 introns. The encoded protein comprises 488 amino acids with a molecular mass of approximately 55 kDa. The protein organization into the three functional and structural domains is identical with HDAC1 (Figure 4.A and 4.B) (Cress & Seto, 2000; de Ruijter et al., 2003; Wade, 2001).

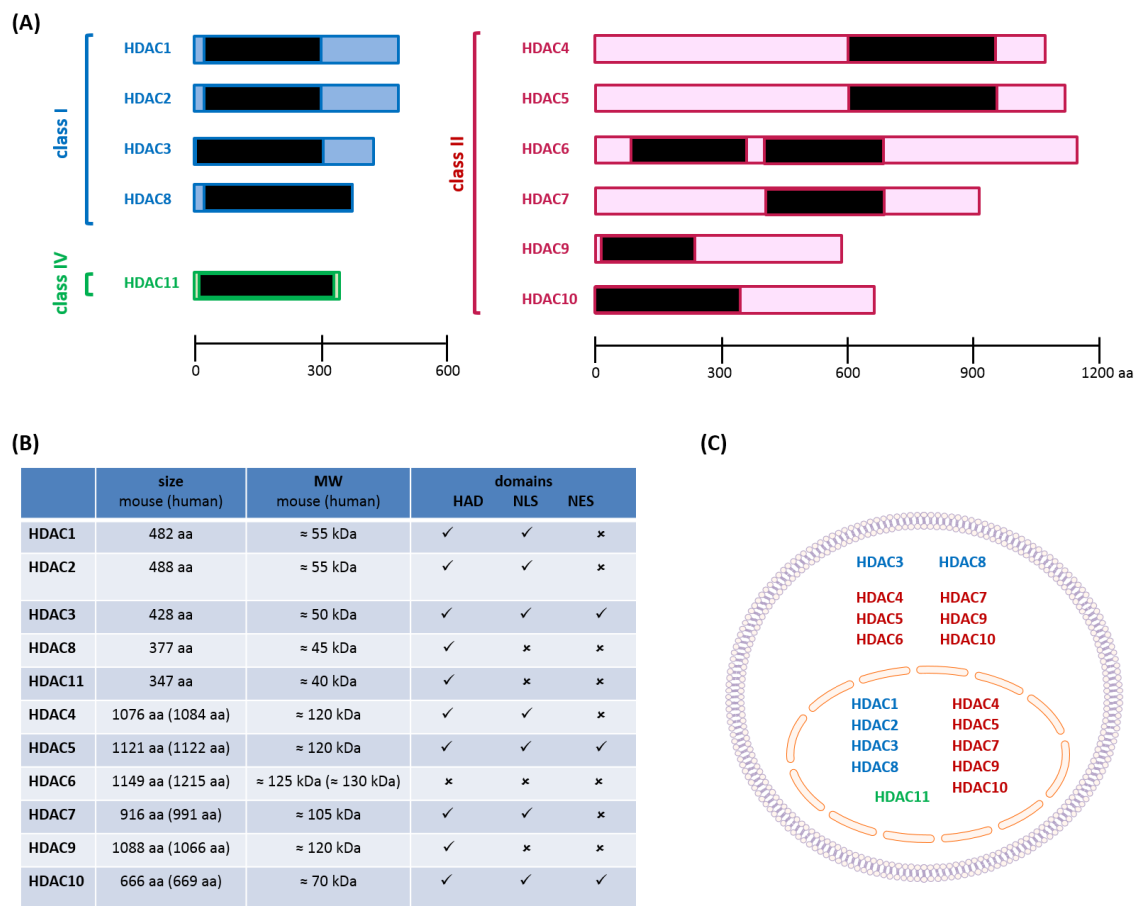


Figure 5. Characterization of the classical HDAC proteins. (A) Schematic representation of the structural composition of HDAC1-11. All classical HDACs have a highly conserved catalytic motif in common (depicted by black boxes), which is essential for the enzymes' ability to deacetylate their substrates. Members of class I HDACs (HDAC1, HDAC2, HDAC3 and HDAC8) and the class IV HDAC (HDAC11) are rather small proteins, whereas class II HDACs (HDAC4, HDAC5, HDAC6, HDAC7, HDAC9 and HDAC10) are high molecular weight proteins. (B) The human and murine homologues of class I and class IV enzymes comprise exactly the same number of amino acids, whereas class II enzymes differ all slightly in size comparing human and murine homologues. (C) Class I HDACs HDAC1 and HDAC2 are exclusively nuclear proteins. HDAC3 possesses an NLS and NES and thus, can shuttle in and out of the nucleus. The small HDAC8 is also found in both compartments although it exhibits neither an NLS nor an NES and can only shuttle due to specific non-HDAC interaction partners. Class II enzymes do have a distinct amount of cytoplasmic substrates and thus, can be found in both, the cytosol and nucleus. The only exception is HDAC6 which is only found in the cytoplasm, where it fulfills its function acting on non-nuclear substrates. [aa = amino acid; HAD = HDAC association domain; MW = molecular weight; NES = nuclear export signal; NLS = nuclear localization signal] Adapted from (de Ruijter et al. 2003; www.ensembl.org).

The localization of HDAC1 and HDAC2 is mainly nuclear, due to the lack of a nuclear export signal (NES) and both have the ability to homodimerize or heterodimerize with each other or further HDAC proteins (Figure 5.B and 5.C). Interestingly, Taplick and colleagues could show that a truncated HDAC1 protein lacking the NLS can still translocate into the nucleus through association with an intact HDAC1 protein suggesting that the homodimerization seems to play a pivotal role in enzyme activity (de Ruijter et al., 2003; Johnstone, 2002; Taplick et al., 2001). Furthermore, HDAC1 seems to influence the expression of HDAC2 and *vice versa*. The transcription of the *Hdac1* gene is highly regulated. Its promoter, lacking a TATA box consensus sequence, is rich in GC content and contains two other regulatory sequences (CCAAT and a distal GC box), both, promoting the assembly of transcription factors and thus being crucial for the full activity of the gene. Transcription factors of the NF-Y (nuclear factor Y) and SP (small protein) family have been found to regulate the transcriptional activation or repression of the *Hdac1* gene synergistically by recruiting either HATs or HDACs, respectively, to the *Hdac1* promoter, indicating that the *Hdac1* transcription is regulated by the balanced action of acetylating and deacetylating enzymes. In particular, the HDAC1 protein has been found to be recruited to its own promoter, suggesting the existence of a negative feedback loop to regulate its own expression level (Hauser, Schuettengruber, Bartl, Lagger, & Seiser, 2002; Schuettengruber, Simboeck, Khier, & Seiser, 2003). As briefly mentioned before, the often co-expressed HDAC1 and HDAC2 enzymes strongly dependent on homo- and heterodimerization to be active, but, the proteins are also target of various posttranslational modifications. Thus, phosphorylation of serine residues within the C-terminal portion of HDAC1 and HDAC2 seems to cause a slight, but significant increase in their enzymatic activity. Other known posttranslational modifications of HDAC1 and HDAC2 are sumoylation and acetylation (R. Cai et al., 2001; David, Neptune, & Depinho, 2002; de Ruijter et al., 2003; Galasinski, Resing, Goodrich, & Ahn, 2002; Goldberg, Allis, & Bernstein, 2007; Pflum, Tong, Lane, & Schreiber, 2001; Taplick et al., 2001).

In addition to the regulation of HDAC1 and HDAC2 by posttranslational modifications, a second means of regulating enzymatic activity is given via the availability of co-repressors and complex formation. HDAC1 is generally found together with HDAC2 in multi-protein complexes consisting of proteins necessary for modulating their deacetylase activity and for binding DNA. Within these complexes, various transcription factors can target HDAC1 and HDAC2 to specific promoters to exert their function (de Ruijter et al., 2003; Y Zhang et al., 1999). To date, three complexes containing HDAC1 and HDAC2 have been characterized in mammals: (1) the co-repressor complex SIN3 (named after its characteristic element mSin3A); (2) the NuRD (nucleosome remodeling and deacetylating) complex; (3) and the CoREST (co-repressor for elemnt-1-silencing transcription factor)

complex (Figure 6) (Ayer, 1999; de Ruijter et al., 2003; Grozinger et al., 2001; Hui Ng & Bird, 2000). The SIN3 complex and the NuRD complex consist of the same core complex containing HDAC1, HDAC2, retinoblastoma-associated protein 46 (RbAp46) and RbAp48, a protein originally co-purified with human HDAC1, which is able to bind histone H4 directly. Besides the core complex, additional cofactors are crucial to possess maximal HDAC activity. These are for the SIN3 complex mSin3A (transcriptional regulatory protein), SAP18 and SAP30, whereas the NuRD complex is enriched by Mi2 α /Mi2 β (also called CHD3/CHD4) and MTA2 (Ashburner, Westerheide, & Baldwin, 2001; Brehm et al., 1998; de Ruijter et al., 2003; Galasinski et al., 2002; Heinz et al., 1997; Taunton et al., 1996). In contrast, the CoREST complex is composed of HDAC1, HDAC2, CoREST and LSD1, a recently identified lysine-specific histone demethylase (Grozinger et al., 2001, 1999; Yujiang Shi et al., 2004).

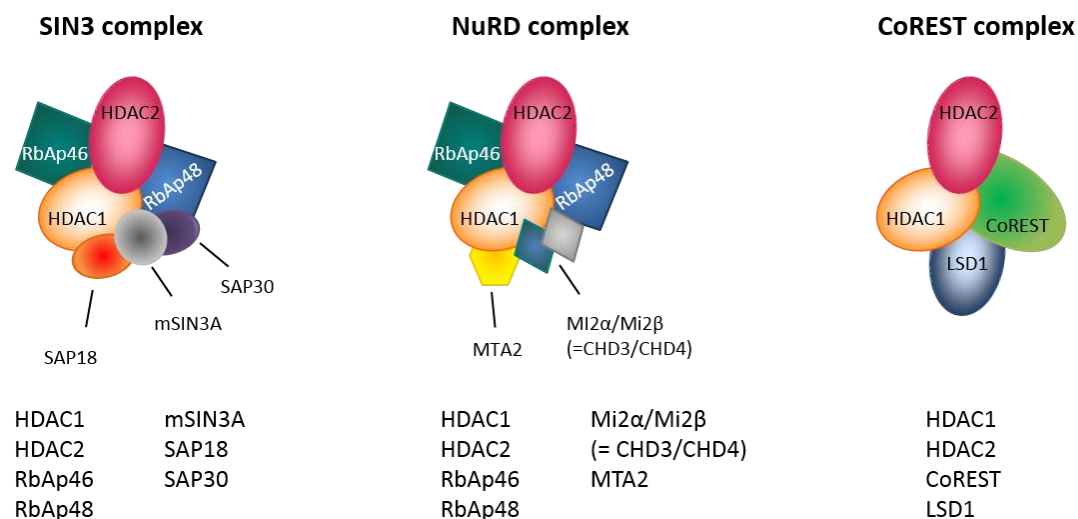


Figure 6. HDAC1 and HDAC2 containing multi-protein complexes. Generally both enzymes, HDAC1 and HDAC2, are found together in the same complexes: SIN3 complex, NuRD complex and COREST complex. Sin3 and NuRD complexes share the same core (HDAC1, HDAC2, RbAp46 and RbAp48). All complexes target HDAC1 and HDAC2 to specific promoters to exert their function. [RbAp = retinoblastoma-associated protein; CoREST = co-repressor for elemnt-1-silencing transcription factor; LSD = lysin-specific histone demethylase]

The repressive function of HDAC1 plays a critical role in various biological processes including cell cycle progression, proliferation and differentiation (Bartl et al., 1997; Lagger et al., 2002; Mal, Sturniolo, Schiltz, Ghosh, & Harter, 2001; Puri et al., 2001). However, increasing evidence indicates that HDAC1 also influences other cellular activities such as DNA replication and chromosome segregation via mechanisms that do not involve transcriptional repression (Austin & Marsh, 1998;

R. L. Cai, Yan-Neale, Cueto, Xu, & Cohen, 2000; David, Turner, Yao, Protopopov, & DePinho, 2003; Johnson, Padgett, Austin, & Turner, 2001; Tsai et al., 2000; Vaute, Nicolas, Vandiel, & Trouche, 2002). Analysis of knockout mouse models could prove an essential role for HDAC1 in mouse embryonic development as the disruption of both alleles leads to lethality before E10.5 (Lagger et al., 2002). Furthermore, there is evidence that HDAC1 is involved in cellular defense against viral infections and it plays a pivotal role in pathological processes such as tumor formation and progression (Glaser et al., 2003; Gwack, Byun, Hwang, Lim, & Choe, 2001; F. Lu et al., 2003). The biological roles of HDAC2 are similar to those of HDAC1 and in many functions the two enzymes can complement for each other. However, knockout studies of HDAC1 and HDAC2 show that there indeed need to be mechanisms which require essential roles of either HDAC1 or HDAC2 (Guan et al., 2009; Montgomery et al., 2007).

1.3.1.2 HDAC3 shuttles in and out of the nucleus

The excitement in the field of histone deacetylases did not end with the discoveries of HDAC1 and HDAC2. Shortly afterwards three research groups reported independently on the identification of an additional human enzyme with deacetylase activity, named HDAC3. It is the third member out of four belonging to class I HDACs sharing a high sequence similarity with the yeast RPD3 yet distinct from HDAC1 and HDAC2 (Emiliani, Fischle, Van Lint, Al-Abed, & Verdin, 1998; Wen Ming Yang et al., 1997). The *Hdac3* gene is localized on mouse chromosome 18 and human chromosome 5q31, spans over 13 kb and contains 15 exons (de Ruijter et al., 2003; Mahlknecht, Bucala, Hoelzer, & Verdin, 1999; Mahlknecht, Emiliani, Najfeld, Young, & Verdin, 1999). Its open reading frame comprises 1284 bp and encodes a protein of 428 amino acids with a molecular mass of approximately 50 kDa meaning that it is slightly smaller in size compared to HDAC1 and HDAC2 (Figure 5.B) (Emiliani et al., 1998; Mahlknecht, Emiliani, et al., 1999; Wen Ming Yang et al., 1997). HDAC3 has the same domain structure as described for HDAC1 and HDAC2 (Figure 5.A). The highly conserved catalytic domain in the N-terminal portion of the protein (amino acid residues 4-316) possesses high sequence similarities with the domains of HDAC1 (62.3% of identity) and HDAC2 (61.0% of identity). However, HDAC3 lacks a small segment corresponding to the extreme N termini of HDAC1 and HDAC2 and also regions that correspond to the C termini of HDAC1 and HDAC2 are absent (HDAC1: 399-482; HDAC2: 400-488) suggesting that both HDAC3 ends possess unique functions that are distinct from other class I HDACs. In addition to the nuclear localization signal (NLS) which is present in all class I HDACs, a functional nuclear export signal (NES) resides in HDAC3 between residues 180-313, allowing the HDAC3 protein to shuttle in and out of the nucleus in almost all cell

types to fulfill its function (Figure 5.B and 5.C) (de Ruijter et al., 2003; Takami & Nakayama, 2000; W.-M. Yang et al., 2002).

HDAC3 mainly self-associates in dimers and trimers to be active, but also hetero-oligomerization with other HDACs is possible, although only detected to a small extent. Endogenous HDAC3 only associates with HDAC4, whereas the oligomerization with other class II HDACs, namely HDAC5, HDAC7, HDAC9 and HDAC10 is only detected when HDAC3 is bound within one of the multi-protein complexes. These co-repressor multi-protein complexes relying on HDAC3 activity are NCoR (nuclear receptor corepressor) and SMRT (silencing mediator for retinoid and thyroid hormone receptors) (Bertos et al., 2001; Fischle, Dequiedt, et al., 2001; Fischle et al., 2002; Grozinger et al., 1999; H. Y. Kao et al., 2000; Tong, Liu, Bertos, & Yang, 2002; W.-M. Yang et al., 2002; Zhou, Richon, Rifkind, & Marks, 2000). However, NCoR and SMRT do not only bind HDAC3, but can also stimulate its activity via a conserved deacetylase-activating domain (DAD) (Guenther et al., 2000; Wen et al., 2000; J. Zhang, Kalkum, Chait, & Roeder, 2002).

After the discovery of HDAC3, its biological function has been extrapolated from the knowledge of HDAC1 and HDAC2. However, HDAC3 possesses many unique biological functions. With its repressive action on transcription it is not only involved in cell cycle control, but also critically regulates ribosome biogenesis. Embryonic lethality of knockout mice at E10.5 emphasizes its unique and important function in development (Dangond et al., 1998, 1999; Glaser et al., 2003; Robyr et al., 2002).

1.3.1.3 HDAC8, the smallest member of class I HDACs

In the year 2000 the fourth class I human HDAC was identified and called HDAC8, because at that time seven human HDACs had already been discovered falling into class I (HDAC1, HDAC2, HDAC3) and class II (HDAC4, HDAC5, HDAC6, HDAC7) (Buggy et al., 2000; Hu et al., 2000; Van den Wyngaert et al., 2000). The *Hdac8* gene is localized in mammals on the chromosome X and is organized into 11 exons over a total length of approximately 25 kb. The *Hdac8* open reading frame encodes a protein of 377 amino acid residues resulting in a size of approximately 45 kDa, thus, representing the smallest class I HDAC protein (Buggy et al., 2000; Van den Wyngaert et al., 2000). Phylogenetic tree analyses place HDAC8 closely to the evolutionary boundary between class I and class II HDACs (Figure 4) and this may represent a key point that distinguishes class I and class II HDACs in humans due to HDAC8 diverging early in evolution from other class I HDACs. However, amino acid sequence comparisons indicate that HDAC8 is most closely related to HDAC3 with an overall sequence

identity of 34% and exhibits the highest conservation within the catalytic domain. Compared with the three other class I HDACs, HDAC8 lacks 50-111 amino acids in the C-terminal portion of the enzyme (Figure 5.A). As this part is essential for multi-protein complex formation and modulation of enzymatic activity via posttranslational modifications within these other HDACs, this suggests that HDAC8 is regulated differently or entirely different regions of the protein surface are utilized for its recruitment and modulation (Buggy et al., 2000; David et al., 2002; de Ruijter et al., 2003; Finnin et al., 1999; Hu et al., 2000; Pflum et al., 2001; Somoza et al., 2004; Van den Wyngaert et al., 2000). In fact, HDAC8 is unlike all other class I HDACs posttranslationally modified within the N-terminal and not the C-terminal part of the protein (David et al., 2002; Galasinski et al., 2002; Hu et al., 2000; H. Lee, Rezai-Zadeh, & Seto, 2004; W.-M. Yang et al., 2002). Furthermore, due to the lack of the C-terminal extension, also the nuclear localization signal (NLS) is missing (Figure 5B.). However, overexpressing studies (necessary due to low abundance of HDAC8 under physiological conditions) could show, that HDAC8 resides within the nucleus, most probably due to a stretch of basic amino acid residues within the catalytic domain (Arg¹⁶⁴-Lys¹⁶⁸: RLRRK) (Figure 5.C) (Ayer, 1999; Hu et al., 2000; Van den Wyngaert et al., 2000; W.-M. Yang et al., 2002).

Further studies could show, that despite the possible existence of two HDAC8 mRNA species (a short transcript of approximately 2 kb and a longer with approximately 2.4 kb) an apparently unique HDAC8 protein exists. This was first thought to be ubiquitously expressed in various human tissues and cells, but later on it was proved that HDAC8 is rather expressed in a restricted manner, i.e. in normal human cells showing smooth muscle differentiation, skull, kidney, lung, heart and distinct regions of the brain. Unexpectedly, the enzyme has also been found to be predominantly cytosolic and co-localizes and associates with the smooth muscle actin cytoskeleton. This differences in protein subcellular localization in regard to earlier studies may have been the result of an improper folding of overexpressed N-terminally tagged protein constructs, possibly hindering the HDAC8 localization to the cytoplasm. Global deletion of HDAC8 in mice leads to perinatal lethality due to skull instability and underlines the role of HDAC8 in skull morphogenesis (Buggy et al., 2000; Haberland, Montgomery, & Olson, 2009; Hu et al., 2000; Van den Wyngaert et al., 2000; Waltregny et al., 2004, 2005).

1.3.2 Describing the high molecular weight class II HDACs

1.3.2.1 Class IIa HDACs, HDAC4, HDAC5 and HDAC7

The members of class II HDACs (HDAC4, HDAC5, HDAC6, HDAC7, HDAC9 and HDAC10) possess domains with significant sequence similarity to the deacetylase domain of the *yeast* histone deacetylase 1 (HDA1) and resemble rather large proteins compared to class I HDACs (Rundlett et al., 1996). HDAC4, HDAC5 and HDAC7 are found in the same branch of the phylogenetic tree and represent the HDAC subgroup class IIa (Figure 4). They share high sequence similarities with an overall identity of 70% between HDAC4 and HDAC5, followed by 58% identity for HDAC4 and HDAC7 and 57% identity for HDAC5 and HDAC7 (de Ruijter et al., 2003; Gregoretta et al., 2004). The genomic locus of HDAC4 is on mouse chromosome 1 and human chromosome 2, for HDAC5 on mouse chromosome 11 and human chromosome 17 and for HDAC7 on mouse chromosome 15 and human chromosome 12. They are all composed of 24-29 exons, corresponding almost exactly to homologous segments within the coding regions of the three genes. However, the loci themselves vary greatly in size, ranging from only approximately 18 kb for Hdac7 to 350 kb for Hdac4. The encoded proteins are all large in size (\approx 105-120 kDa) and share their general structural composition (Figure 5.A). Within the extended N-terminus, in all three proteins an NLS can be found, but only HDAC5 exhibits in addition an NES (Figure 5.B). Highly conserved domains within all three proteins are the binding domains for C-terminal binding protein (CtBP), myocyte enhancer factor 2 (MEF2) and 14-3-3 (a cytosolic anchor protein) located within the N-terminal half. The catalytic domain is located within the C-terminal portion of the proteins which makes them different in organization from the small class I HDACs (Figure 5.A) (Lemercier et al., 2000; Sparrow et al., 1999; A. H. Wang et al., 1999, 2000).

The functional role of HDAC4, HDAC5 and HDAC7 is strongly dependent on their interaction partners, posttranslational modifications, subcellular localization and tissue-specific expression levels (Figure 5.C). Numerous interactions are possible due to the large N-termini and allude a bewildering array of possible roles and regulation of various target promoters. Interestingly, HDAC4, HDAC5 and HDAC7 associate also with HDAC3 via co-recruitment to the SMRT/NCOR complex (Fischle, Kiermer, Dequiedt, & Verdin, 2001; Fischle et al., 2002; Fischle, Dequiedt, et al., 2001; W.-M. Yang et al., 2002). The enzymatic activity is furthermore regulated by posttranslational modifications as phosphorylation of the 14-3-3 binding sites within the N-terminal part of the proteins. HDAC4 was also identified to be conjugated to the small ubiquitin-like modifier-1 (SUMO-1) and to be cleaved by caspases 2 and 3 in response to pro-apoptotic stimuli (Kirsh et al., 2002; Liu,

Hu, D'ercole, & Ye, 2009; Paroni et al., 2004). The variable subcellular localization of HDAC4, HDAC5 and HDAC7 due to signal-dependent nucleoplasmic shuttling is a hallmark of the three class IIa HDACs and for differentiating muscle cells a clear model exists. The three proteins can shuttle in and out of the cell-nucleus in dependence of their phosphorylation status within different stages of muscle cell differentiation. Thus, HDAC4 is transported upon phosphorylation out of the nucleus and retained by 14-3-3 within the cytosol in pre-differentiating cells, while HDAC5 and HDAC7 still reside in the nucleus. These two proteins are transported into the cytosol only in differentiating cells in which HDAC4 is already dephosphorylated and translocated back to the nucleus. This model suggest that HDAC5 and HDAC7 complement for HDAC4 and *vice versa* to control the differential regulation of gene expression during various stages of differentiation in muscle cells (Bertos et al., 2001; Dressel et al., 2001; H. Y. Kao et al., 2001; Kumar et al., 2005; McKinsey, Zhang, Lu, & Olson, 2000; Miska et al., 2001; Wu, Li, Park, & Chen, 2001). It is widely known, that unlike the ubiquitously expressed class I HDACs, members of class IIa are expressed in a more tissue-restricted manner. However, further studies suggest that this assumption is not true and the reality is a bit more complex. Thus, class IIa HDACs are widely expressed, but they are clearly expressed much more strongly in a limited subset of cells. HDAC4 and HDAC5 are for example particularly expressed in brain, heart and skeletal muscle, whereas HDAC7 shows high expression levels within heart, thymus and lung. The transient expression of class IIa HDACs in specific cell types suggests that these enzymes might play important roles in the development of tissues with low overall expression levels such as in the heart, skeletal muscle and the immune system (Dequiedt et al., 2003; Fischle et al., 1999; Fischle, Dequiedt, et al., 2001; Grozinger et al., 1999; H. Y. Kao et al., 2000; Verdel & Khochbin, 1999; A. H. Wang et al., 1999; Zhou, Marks, Rifkind, & Richon, 2001; Zhou et al., 2000). For HDAC7 knockout studies exist, showing that global deletion of HDAC7 in mice results in the defects of endothelial cells-cells contacts and consequent dilation and rupture of blood vessels (Chang et al., 2006).

1.3.2.2 HDAC6 a rather unique enzyme among classical HDACs

With the characterization of HDAC6 in 1999 the first evidence of non-nuclear and non-histone-associated activity for an HDAC member was proved (Grozinger et al., 1999). As a class II HDAC member, HDAC6 resembles to the *yeast* HDA1, although the identity with other human HDACs is low and phylogenetic analyses indicate that it is evolutionarily most closely related to HDAC10 (Figure 4) (P. Marks et al., 2001; Yoshida et al., 2001). HDAC6 is like HDAC8 an X-linked HDAC with a gene size of 23 kb in humans comprising 29 exons. The open reading frame encodes a protein of

1215 amino acids resulting in a size of approximately 130 kDa (Figure 5.B). The protein resembles a rather unique enzyme within the classical HDAC family as it contains not only two tandem catalytic domains, but also a zinc finger motif that is absent in other HDAC members (Figure 5.A). This motif is also known as a BUZ (binding-of-ubiquitin zinc) finger or as a HUB (HDAC6-USP3, and Brap2-related zinc) finger and intriguingly is found almost exclusively in deubiquitinating enzymes, suggesting that HDAC6 might be functionally connected to protein ubiquitination (Bertos et al., 2001; de Ruijter et al., 2003; Grozinger et al., 1999; Hook, Orian, Cowley, & Eisenman, 2002; Kovacs et al., 2005). Among the 11 identified classical human HDAC members, HDAC6 is uniquely localized to the cytoplasm under most conditions and exerts its deacetylation function only on non-histone targets such as tubulin to regulate microtubule-dependent cell motility (Figure 5.C) (Hubbert et al., 2002; Yu Zhang et al., 2003). Global deletion of HDAC6 in mice suggests that HDAC6 is a critical component of stress granules involved in the cellular stress response (Kwon, Zhang, & Matthias, 2007).

1.3.2.3 HDAC9 is related in structure and function to class IIa HDACs

HDAC9 is a member of class II HDACs related to the subgroup IIa (HDAC4, HDAC5 and HDAC7). The mouse *Hdac9* is located on chromosome 12 with a size of 150 kb and 40 exons encode a protein consisting of 1088 amino acids (120 kDa), whereas the human gene is localized on chromosome 7 and covers 500 kb with 38 exons encoding a 1066 amino acid protein (120 kDa) (Figure 5.A and 5.B). Both species encode besides the long variant also shorter transcripts. The protein organization differs to the organization of the related class IIa HDACs, as HDAC9 exhibits its catalytic domain within the N-terminal part and inhabits a long C-terminal extension. In its features HDAC9 largely resembles HDAC4, HDAC5 and HDAC7 as it has also several interaction partners and is regulated by nucleocytoplasmic signaling. An important function in muscle cell differentiation is suggested for HDAC9 in line with class IIa HDACs (Bertos et al., 2001; de Ruijter et al., 2003; Grozinger et al., 1999; Pflum et al., 2001; Zhou et al., 2001). Furthermore, HDAC9 knockout studies in mice show that HDAC9 seems to play an important role in adipose tissue dysfunction and systemic metabolic disease during high-fat feeding (Chatterjee et al., 2014).

1.3.2.4 HDAC10 acts rather as recruiter than as deacetylase

HDAC10 as the latest identified class II HDAC is most similar to HDAC6, although they differ strongly in size (Guardiola & Yao, 2002). Human *Hdac10* could be identified on chromosome 22 with a size of only 6 kb, comprising 20 exons and encoding a protein of 669 amino acids resulting in a size of approximately 70 kDa (Figure 5.A and 5.B). The murine homologue is located on chromosome 15 and almost identical in size to human HDAC10 (D. D. Fischer et al., 2002). HDAC10 possesses its catalytic domain on the N-terminus and contains like HDAC6 a putative second catalytic domain. In HDAC10, however, this domain is not functional. The protein also harbors a nuclear export signal (NES) which allows the protein to locate not only within the nucleus, but also in the cytoplasm (Figure 5.C). When HDAC10 is found within the nucleus, it is mostly tethered to a promoter and represses transcription independently of its deacetylase activity. HDAC10 is found to interact with the class I HDACs HDAC1, HDAC2 and HDAC3 and with class II HDACs HDAC4, HDAC5 and HDAC7 suggesting a role as HDAC recruiter rather than as deacetylase (de Ruijter et al., 2003; Guardiola & Yao, 2002; H.-Y. Kao, Lee, Komarov, Han, & Evans, 2002; Tong et al., 2002).

1.3.3 Describing the sole class IV HDAC member HDAC11

With the discovery of HDAC11 in 2002, the latest member of eleven known classical HDACs was identified. Phylogenetic analyses could show, that HDAC11 appears to be most closely related to HDAC3 and HDAC8, but the overall sequence identity is limited (Figure 4). Thus, a new group with only HDAC11 as member was established. This group is called class IV HDAC as class III was already occupied by the sirtuins, which do not belong to the classical HDACs, but to the HDAC superfamily. The *HDAC11* gene maps to human chromosome 3, is 26 kb in size and possesses 10 exons encoding the smallest HDAC enzyme with only 347 amino acids and a molecular mass of 40 kDa (Figure 5.A and 45.B). The catalytic domain is situated within the N-terminal portion of the protein and contains conserved amino acid residues in the catalytic core regions shared by both, class I and class II HDACs. The subcellular localization of HDAC11 is within the nucleus, although it was found to interact with the mainly cytoplasmic HDAC6 (Figure 5.C) (Bertos et al., 2001; de Ruijter et al., 2003; L. Gao et al., 2002). Global deletion of HDAC11 in mice identified the enzyme to be a novel epigenetic regulator of myeloid derived suppressor cell expansion and to function in tumor growth (Sahakian et al., 2015).

1.4 HDAC inhibitors are useful epigenetic tools and therapeutic compounds

HDAC inhibitors (HDACi) are attractive therapeutic agents for the treatment of various diseases, especially used in anti-cancer therapy. Most anti-cancer drugs are cytotoxic agents that act in a rather non-selective manner, but HDAC inhibitors appear to interfere with the mechanisms underlying tumor development (Mahlknecht & Hoelzer, 2000; Tan, Cang, Ma, Petrillo, & Liu, 2010). Furthermore, HDACi contributed to the discovery of HDACs and were used as important tools for cloning HDAC cDNAs. Hence, the first HDAC was identified after isolation from a human T-cell line using a trapoxin-based affinity matrix (Bartl et al., 1997; Kijima et al., 1993; Taunton et al., 1996; Yoshida et al., 2001). The first studies concerning HDACs used HDACi and even today a large portion of our knowledge about HDAC functions is obtained via inhibitor studies. Similar to the HDAC proteins, the HDACi are structurally diverse. Their origin can be both, natural and synthetic, but all of them can be categorized into four structural groups: (1) the short-chain fatty acids; (2) the hydroxymates; (3) the benzamides; and (4) the cyclic tetrapeptides (Table 1) (Dokmanovic, Clarke, & Marks, 2007; Heerboth et al., 2014). The first compound described as inhibitor of HDAC activity is the synthetic HDACi sodium butyrate which belongs to group (1) of HDACi. To be effective, its concentration needs to reach more than millimolar levels which causes effects on other proteins than HDACs and might also perturb the cytoskeleton and cell membrane. In addition, its low specificity against distinct HDACs leads to many side effects and strongly suggests to use this HDACi with caution (Candido & Davie, 1978; André Fischer et al., 2010; Guan et al., 2009). In the early 1990s two natural HDACi, trichostatin A (TSA) and trapoxin (TPX) were identified when used as fungal antibiotics. Both inhibit effectively HDACs and need to reach only nanomolar concentrations. However, also these two compounds are not very specific, but act in a broad spectrum within the HDAC arena (Dokmanovic et al., 2007; Heerboth et al., 2014; Kijima et al., 1993; Richon et al., 1998; Yoshida, Kijima, Akita, & Beppu, 1990). The first HDACi which was approved for clinical use by the Food and Drug Administration is vorinostat, also known as SAHA (suberoylanilide hydroxamic acid). It blocks cancer cell proliferation effectively already when applied in nanomolar concentrations (Alarcón et al., 2004; Guan et al., 2009). However, vorinostat has multiple targets and also induces many side effects such as diarrhea, fatigue, nausea and anorexia (Dokmanovic et al., 2007; Duvic et al., 2007; Heerboth et al., 2014; P. A. Marks & Breslow, 2007; Richon, 2006). Another HDACi is valproic acid, primarily effective against class I HDACs and being one of the first compounds linking the field of epigenetic chromatin plasticity with various brain disorders and psychiatric diseases such as Alzheimer's disease, schizophrenia, bipolar disorders, seizure disorders and major

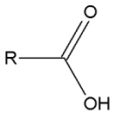
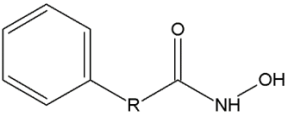
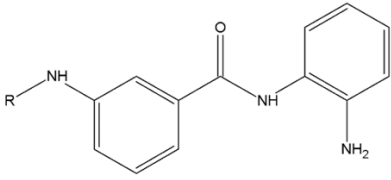
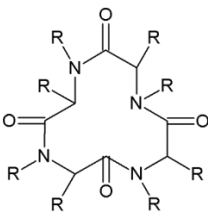
Group and structure	Compounds	Approved/Clinical trial
Short-chain fatty acid 	Valproic acid	
Hydroxamic acid 	TSA Vorinostat (SAHA) Sodium butyrate Panobinostat Belinostat	preclinical phase approved (2006) approved (2015) clinical trial phase II
Benzamide 	MS-275 RGFP 136 Chidamide	approved (2015)
Cyclic tetrapeptides 	Trapoxin (TPX) Romidepsin	approved (2009)

Table 1. HDAC inhibitors (HDACi). HDACi can be both, natural and synthetic, and they are structurally diverse. Thus, they can be categorized into four structural groups: short-chain fatty acids, hydroxamic acids, benzamides and cyclic tetrapeptides. Some compounds are already approved and used as therapeutic agents, others are in clinical trials or only used in research laboratories. [TSA = trichostatin A; SAHA = suberoylanilide hydroxamic acid]

depression (Casey et al., 2003; André Fischer et al., 2010; Andre Fischer, Sananbenesi, Wang, Dobbin, & Tsai, 2007; Flood, Choinski, Marino, & Gasior, 2009; Haddad, Das, Ashfaq, & Wieck, 2009; L. Li, Suzuki, Mori, & Greengard, 1993; Tremolizzo et al., 2005). Although HDACs appear widespread on DNA as chromatin structure remodelers, HDACi only affect 2-10% of expressed genes. Accordingly, this demonstrates the potential for specificity in using HDACi especially in the treatment of neuropsychiatric diseases to prevent extreme side effects as individual HDACs seem to serve distinct functions within the adult brain. Therefore, more specific HDACi like MS-275 (preferentially inhibits HDAC1) and RGFP136 (preferentially inhibits HDAC3) are currently in use in

several studies. Moreover, it is indispensable that more information of the distinct roles of each individual HDAC member is acquired (André Fischer et al., 2010; Guan et al., 2009; McQuown et al., 2011).

1.5 Neuroepigenetics – an emerging field with tremendous impact on brain development, learning, behavior and neuropathology

The role that epigenetic mechanisms play in phenomena such as cellular differentiation during embryonic development, X-chromosomal inactivation and cancer is well-characterized, but the field of neuroepigenetics, which is also referred to as behavioral epigenetics, meaning the roles of epigenetic mechanisms in the central nervous system (CNS) is just beginning to be understood and is one of the most exciting areas of today's molecular and behavioral neuroscience. A search for '*epigenetic*' in the pubmed database revealed at the beginning of 2016 more than 45957 papers, but only about 4427 are linked to brain-related studies. Dealing with neuroepigenetics means to shift our understanding of several fundamental concepts of traditional epigenetics and cognitive neurobiology. When thinking of heredity as the traditional aspect to define epigenetics, this leads immediately to a violation of mature neurons considering their non-dividing nature. Nevertheless, it is clear that epigenetic molecular mechanisms are active in non-dividing neurons in the nervous system and are implicated to be important mediators in numerous brain processes such as development, the brain-regulated maintenance of homeostasis within the body, sensorimotor ability, adult neurogenesis, modulation of neural behavior and neural plasticity, higher brain functions like cognition, memory and learning, and development of neurologic and psychiatric disorders (Bird, 2007; Farah & Hook, 2008; Ravi & Kannan, 2013; Sweatt et al., 2013; Volmar & Wahlestedt, 2014). Furthermore, nowadays studies in behavioral epigenetics could show that the historical dichotomy between '*nature*' (genes) and '*nurture*' (environment and experience) is a false one. Thus, the historic model with separate and distinct influences of genes and the environment is incorrect. Fundamental questions regarding animal behavior can be explained by putative factors such as early life stress, adversity, abuse and social interactions, and these behavioral patterns are not essentially ingrained, immutable and only determined by the genetic make-up. Genes and experience are mechanistically intertwined and epigenetic mechanisms contribute to this intertwining (Farah & Hook, 2008; Ravi & Kannan, 2013; Sweatt et al., 2013).

1.5.1 Epigenetic regulation during brain development with a special focus on HDAC involvement

The epigenetic mechanisms regulating transcription within the CNS upon organismal experience and cellular signaling are the same found in all other cells and tissue. Thus, the remodeling of

chromatin structure via several modifications of the DNA and associated histones displays the central aspect in regulating gene expression in neural cells and systems. Epigenetic molecular mechanisms drive neurodevelopment and stem cell fate. The CNS develops out of cells arisen from neuroepithelial cells and neural stem cells (NSC), which undergo diverse processes due to changes in their epigenetic state in response to extrinsic factors to form all the cell types found in the CNS. For instance a core process in the formation of neurons is given by the epigenetic regulation of promoters of genes that are essential to be expressed in neurons. These genes have a neuron-restrictive silencer element (NRSE) within their promoter regions which leads to a complete silencing within all other cell-types except neurons (L. Li et al., 1993; Maue, Kraner, Goodman, & Mandel, 1990; Mori, Schoenherr, Vandenberg, & Anderson, 1992; Sweatt et al., 2013). Thus, within neurons, the epigenetic machinery needs to be modified that the NRSE cannot fulfill its repressive function. The REST protein, which is ubiquitously expressed, was the first transcription factor found to bind to the NRSE to repress gene expression. REST is acting in concert with other repressive components and can be found in complexes together with SIN3A/HDAC1 or CoREST/HDAC2. Thus, the REST-dependent gene silencing involves a decrease in histone acetylation (Z. F. Chen, Paquette, & Anderson, 1998; Chong et al., 1995; Grimes et al., 2000; Y. Huang, Myers, & Dingledine, 1999; Naruse et al., 2004; Paquette, Perez, & Anderson, 2000; Ravi & Kannan, 2013; Sweatt et al., 2013). Furthermore, the brain development is influenced by the quality of the prenatal and early postnatal environment and has consequences on adult behavior. Thus, persisting epigenetic marks are acquired through early-life experiences via epigenetic mechanisms and these marks cause lasting cellular effects which are responsible for the basis of adult behavior including vulnerability to stress, susceptibility to diseases and cognitive deficits. HDACs are demonstrated to be often involved in these epigenetic processes. Hence, the positive effects of high-grooming maternal care on offspring brain development was not only linked to DNA methylation, but also to histone acetylation (André Fischer et al., 2010; Skinner, 2011; Weaver et al., 2004, 2005).

However, although global loss of HDAC1 leads to early embryonic lethality (E10.5), studies could show that HDAC1 has no individual role in neuronal development. Mice lacking HDAC1 or HDAC2 individually in neuronal precursor cells showed no overt histoarchitectural phenotype and the immature neurons could differentiate normally into mature neurons. Only the deletion of both, HDAC1 and HDAC2, caused abnormal development as differentiation of progenitors into mature neurons was not possible anymore. The severe effects of the neuronal double knockout (KO) of HDAC1 and HDAC2 lead to early embryonic lethality at E7.5 (Lagger et al., 2002; Montgomery, Hsieh, Barbosa, Richardson, & Olson, 2009). HDACs appear also to be involved in synapse development. Studies with differentiated murine hippocampal cells showed a pronounced increase

in the maturation of synaptic function as well as a modest increase in synapse number when treated with HDAC inhibitors (e.g. TSA, valproic acid). Mice with conditional null alleles for HDAC1 and HDAC2 could prove that these two enzymes form a developmental switch that controls excitatory synapse maturation and function. In addition also the knockdown of HDAC2 alone decreased the synaptic activity, but the loss of HDAC1 had no apparent effect in synapse development (Akhtar et al., 2009). Furthermore, analysis of cell type-specific and developmental stage-specific expression of HDAC1 and HDAC2 in the mouse cerebellum suggests a potential role for HDAC1 in cell proliferation and for HDAC2 in cell migration and differentiation within the developing cerebellum (Yoo, Larouche, & Goldowitz, 2013). The class II HDAC members HDAC5 and HDAC6 seem also to be involved in the development of the CNS. Hence, HDAC5 has been implicated in the proliferation of NSC via its co-recruitment with LSD1 to the promoter of target genes downstream of TLX (NR2E1), an essential regulator of the maintenance and self-renewal of neural stem cells in embryonic and adult brains (André Fischer et al., 2010; W. Li et al., 2008; Yanhong Shi et al., 2004; Sun et al., 2010). HDAC6 was demonstrated to be important for cellular processes such as neuronal transport and the cytoskeletal network during brain development (André Fischer et al., 2010; Y. Gao et al., 2007).

Furthermore, several contemporary studies concerning the roles of epigenetic mechanisms in the functioning of the adults' CNS are focusing on adult neurogenesis as the widely held dogma, that there is no new generation of neurons in the adult CNS, collapsed during the last decades due to new and fascinating studies (Eriksson et al., 1998; Sweatt et al., 2013).

1.5.2 The contribution of epigenetic mechanisms related to HDACs to memory formation and learning

In the last decade, epigenetic markers have also emerged as important regulators for consolidation and maintenance of memory and learning behavior. Numerous studies could prove that epigenetic marks, especially DNA methylation are actively and transiently regulated in post-mitotic neurons of adult rodents, honeybees, aplysia and drosophila during learning processes (Chwang, O'Riordan, Levenson, & Sweatt, 2006; Gupta et al., 2010; Kilgore et al., 2010; Levenson & Sweatt, 2005; Levenson et al., 2004; Lockett, Helliwell, & Maleszka, 2010; Lubin & Sweatt, 2007; Maddox & Schafe, 2011; C. A. Miller, Campbell, & Sweatt, 2008; L. Miller et al., 2011). But also other chromatin remodeling mechanisms like acetylation induce lasting changes in behavior due to stimulus-specific cellular and molecular changes and will consolidate a memory into an everlasting trace. Most

studies linking histone acetylation to learning processes and memory were conducted using HDAC inhibitors and could show that increased histone acetylation is associated with enhanced cognition (Korzus, Rosenfeld, & Mayford, 2004; Levenson & Sweatt, 2005; Swank & Sweatt, 2001; Volmar & Wahlestedt, 2014). Histone acetylation was especially shown to be involved in critical steps during the stabilization of short-term memory into long-term memory in wild-type mice (Korzus et al., 2004; Swank & Sweatt, 2001; Volmar & Wahlestedt, 2014). In aged mice or neurodegenerative mouse models linked to Alzheimer's disease the treatment with the pan-HDAC inhibitor sodium butyrate could restore a broad histone acetylation pattern which is usually found in mice with enhanced cognitive behavior due to environmental enrichment (Andre Fischer et al., 2007; Frick, Stearns, Pan, & Berger-Sweeney, 2003; F. L. Huang, Huang, Wu, & Boucheron, 2006; Peleg et al., 2010; Pereira et al., 2007).

However, different HDACs appear to have specific roles in different types of learning and memory. Guan and colleagues for instance identified HDAC2, but not HDAC1, to be a negative regulator of associative and spatial memory via overexpression and knockout studies (Guan et al., 2009). Furthermore, with the use of MS-275, a specific HDAC1 inhibitor, and virus-induced overexpression of HDAC1 within the hippocampal formation of adult mice, HDAC1 was proved to enhance the extinction of contextual fear memories (Bahari-Javan et al., 2012). HDAC3 was shown to act as negative regulator of long-term memory formation as the inhibition of HDAC3 enhances long-term object recognition memory in mice and this is linked to an increase in H4K8 acetylation (Malvaez, Sanchis-Segura, Vo, Lattal, & Wood, 2010; McQuown et al., 2011). The most recent finding of the role of class I HDACs in fear memory is that the phosphorylated form of a well-approved drug for treatment of multiple sclerosis, namely fingolimod (FTY720), inhibits members of class I HDACs and facilitates fear memories (Hait et al., 2014). For class II HDACs, the role of HDAC4 is described to be important for synaptic plasticity and thus, for memory formation. Studies where HDAC4 was silenced or truncated showed impairments in spatial learning and memory in mice (M.-S. Kim et al., 2012; Sando et al., 2012). HDAC5 was shown not to be involved in spatial learning, but to be crucial for context- and tone-dependent fear memory formation (Agis-Balboa, Pavelka, Kerimoglu, & Fischer, 2013; M.-S. Kim et al., 2012). In 2013 a novel HDAC inhibitor, crebinostat, was identified which inhibits the class I HDACs HDAC1, HDAC2 and HDAC3 as well as the class II HDAC HDAC6. Wild-type mice treated with this inhibitor showed improved fear learning. Cultured primary neurons of these mice showed on the molecular level an increase in Bdnf and granulin expression and more synapsin 1 punctae suggesting upregulation of its dendritic density (Fass et al., 2013).

1.5.3 Neuropsychiatric diseases triggered by epigenetic mechanisms involve HDACs

Considering all the important roles of epigenetic mechanisms in the CNS for normal brain function and behavior, it is not surprising that a dysregulation of the epigenetic machinery is associated with a variety of neuropsychiatric diseases. Hence, HDACs have been shown to be implicated in the pathogenesis of Alzheimer's disease, Huntington's disease, traumatic brain injury, post-traumatic stress disorder, addiction and depression (Agis-Balboa et al., 2013; Broide et al., 2007; Covington et al., 2009; Fass et al., 2013). The inhibition of distinct HDAC isoforms has for instance been reported to improve symptoms of depression, bipolar disorders and schizophrenia (Benes et al., 2007; Covington et al., 2009; Hobara et al., 2010; Kurita et al., 2012). Thus, the HDAC1 specific inhibitor MS-275 was shown to restore a normal acetylation state of histone H3K14 when applied to the nucleus accumbens of mice subjected to the chronic social defeat stress paradigm and elicited a significant antidepressant effect. Furthermore, the down-regulation of CAMKII, CREB, ERK, REST and nAChR expression which is associated with stress could be reversed by MS-275 treatment (Covington et al., 2009). Comprehensive studies and reports show a strong correlation between the histone acetylation pattern and the expression of distinct HDACs in response to commonly prescribed drugs for antidepressant treatment and mood stabilizer in specific brain regions such as the nucleus accumbens, striatum, cingulate cortex, amygdala and hippocampus (Benes et al., 2007; Hobara et al., 2010; Ookubo, Kanai, Aoki, & Yamada, 2013; Rudenko & Tsai, 2014; Volmar & Wahlestedt, 2014).

The expression of HDAC1 was shown to be elevated in neurons under hypoxia conditions, in post-mortem brain samples of schizophrenia patients and in a mouse model for Huntington's disease suggesting a specific role for HDAC1 in the pathogenesis of various brain disorders (Benes et al., 2007; André Fischer et al., 2010; Haberland et al., 2009; Sharma, Grayson, & Gavin, 2008; Z. Wang et al., 2011). In contrast to these findings, other studies implicated the loss of HDAC1 to be involved in neurodegeneration suggesting rather a neuroprotective than a neurotoxic function for HDAC1. Hence, inactivation of HDAC1 by p25 in the CK-25 mouse model of rapid neurodegeneration precedes Alzheimer's-like disease resulting in double-stranded DNA breaks, aberrant cell-cycle protein expression and neuronal death. Likewise, the HDAC1 gain-of-function was protective against ischemia-induced neuronal death in a stroke model and furthermore, HDAC1 was also found to be neuroprotective in a *Caenorhabditis elegans* model of Huntington's disease (Bates, Victor, Jones, Shi, & Hart, 2006; Cruz, Tseng, Goldman, Shih, & Tsai, 2003; André Fischer et al., 2010; D. Kim et al., 2008). However, HDAC1 inhibition appears to be advantageous in some cases, whereas

in other situations the inhibition contributes to disease progression. About other class I HDACs and their involvement in neurological diseases only little is known. HDAC3 was shown to be neurotoxic in Huntington's disease and the expression of HDAC8 is significantly correlated with the occurrence of neuroblastoma (Bates et al., 2006; André Fischer et al., 2010; Oehme, Deubzer, Lodrini, Milde, & Witt, 2009; Oehme, Deubzer, Wegener, et al., 2009). The class II HDAC member HDAC4 seems to exert a neurotoxic function under certain conditions. Thus, the specific overexpression of HDAC4 in cerebellar granular neurons promotes neuronal cell death and recent studies revealed for HDAC4 a role in regulating muscle gene transcription in response to neural activity at the neuromuscular junction and therefore implicated HDAC4 in the etiology of neuromuscular diseases such as ALS (amyotrophic lateral sclerosis). Furthermore, a genetic association study found an HDAC4 SNP (single nucleotide polymorphism) to be associated with schizophrenia in a Korean population (Bolger & Yao, 2005; Cohen et al., 2007, 2009; André Fischer et al., 2010; T. Kim, Park, Kim, Chung, & Kim, 2010; Williams et al., 2009). Another class II HDAC member, HDAC5, appears to be a critical regulator of adaptive responses to chronic stress and cocaine consumption, whereas HDAC6 is described to be both, neuroprotective and neurotoxic dependent of the disorder it is implicated with (Ding, Dolan, & Johnson, 2008; Fiesel et al., 2010; André Fischer et al., 2010; Kwiatkowski et al., 2009; J. Y. Lee, Nagano, Taylor, Lim, & Yao, 2010; Ling et al., 2010; Pandey et al., 2007; Perez et al., 2009; Renthal et al., 2007; Tsankova et al., 2006).

2 AIM OF THE THESIS

The role that epigenetic mechanisms play in phenomena such as cellular differentiation during embryonic development, X-chromosomal inactivation and cancer is well-characterized, but the field of neuroepigenetics, which is also referred to as behavioral epigenetics, meaning the roles of epigenetic mechanisms in the central nervous system (CNS) is just beginning to be understood and is one of the most exciting areas of today's molecular and behavioral neuroscience. When thinking of heredity as the traditional aspect to define epigenetics, this leads immediately to a violation of mature neurons considering their non-dividing nature. Nevertheless, it is clear that epigenetic molecular mechanisms are active in non-dividing neurons in the nervous system and are implicated to be important mediators in numerous processes which are regulated by the brain such as development, the maintenance of homeostasis within the body, sensorimotor ability, adult neurogenesis, modulation of neural plasticity, higher brain functions like cognition, memory and learning, emotional behavior and development of neurologic and psychiatric disorders (Bird, 2007; Farah & Hook, 2008; Ravi & Kannan, 2013; Sweatt et al., 2013; Volmar & Wahlestedt, 2014).

There are many epigenetic mechanisms and enzymes to study, but we focus on histone deacetylases (HDACs) as it has been suggested that regulatory acetylation/deacetylation is considerably more widespread than presently appreciated, acting in a manner similar to phosphorylation and dephosphorylation (Gregoretto et al., 2004; Kouzarides, 2000). However, as an epigenetic mark, the acetylation state of core histones is strongly influencing the architecture of the chromatin, thus, modulating gene activity (Cress & Seto, 2000). Therefore, we define the following aims of the thesis:

- (1) Up to date, the expression of classical HDACs within the adult brain is for rodents only described in rats (Broide et al., 2007), but for mice a detailed description is missing. Therefore, we intend to conduct a comprehensive gene expression mapping of the eleven classical HDACs (class I: HDAC1, HDAC2, HDAC3 and HDAC8; class II: HDAC4, HDAC5, HDAC6, HDAC7, HDAC9 and HDAC10; class IV: HDAC11) throughout the adult murine brain. With the development of an HDAC1-11 gene expression atlas we would like to provide some information to answer the following questions: Are all classical HDAC members generally expressed in the murine brain and if yes, do they have specific expression patterns? How is the expression level of individual HDACs? Which HDACs are present in distinct brain regions?

- (2) Transgenic overexpression or knockout mouse models are frequently used in many research laboratories since decades. Especially in neurobiology the generation of mouse mutants harboring targeted inactivation of a desired gene or overexpression of a distinct gene in specific brain regions is used as a powerful tool to analyze a gene's role in complex brain functions such as learning, memory, emotional behavior, synaptic plasticity as well as neurogenesis and neuronal cell death (Anagnostopoulos, Mobraaten, Sharp, & Davisson, 2001; Bolivar, Cook, & Flaherty, 2000; C. Chen & Tonegawa, 1997; Erdmann, Schütz, & Berger, 2007). However, often the disruption of a gene is detrimental and causes embryonic or developmental abnormalities leading up to embryonic or postnatal lethality. Therefore, the overexpression or knockout of genes often requires spatial and/or temporal control. An elegant and most frequently used tool to bypass severe side effects of overexpression or knockout studies is the spatio-temporal control via the Cre/loxP system. In neurobiology and especially when working in behavioral analyses of mice, the induction of the gene knockout or overexpression via the activation of the Cre/loxP system is often a critical step as the activating agent tamoxifen is applied to mice by injections or gavaging which both impose considerable stress on mice. Therefore, we aim to establish the application of tamoxifen via food pellets to induce stress-free gene ablation or overexpression. To gain more information about the optimal duration and the efficacy of tamoxifen treatment via food, we intend to apply the tamoxifen via food to mice for different durations and to analyze comprehensively the mice's drinking and feeding behavior as well as their body weight change.
- (3) Analysis of knockout mouse models could prove an essential role for HDAC1 in mouse embryonic development as the disruption of both alleles leads to lethality before E10.5 (Lagger et al., 2002). The biological roles of HDAC1 and HDAC2 are often described to be redundant and it is known that they often complement for each other. However, especially in the brain it was shown, that there indeed need to be mechanism which require essential roles of either HDAC1 or HDAC2 (Guan et al., 2009; Montgomery et al., 2007). Therefore, we are interested in generating a conditional HDAC1 knockout mouse model to dissect the brain-specific functions of HDAC1. In a first step we intend to analyze HDAC1-lacZ reporter mice to define the HDAC1 expression throughout the adult murine brain and throughout various tissues and organs of the whole body. Furthermore, we would like to establish a spatio-temporal controlled HDAC1 disruption in mice with the use of a tamoxifen inducible Cre/loxP system driven by the Camk2a promoter. With the use of this mouse model and its

behavioral phenotyping, we hope to gain insights in HDAC1 function in the adult forebrain especially in regard to emotional behavior, stress compensation and memory formation.

- (4) Shortly after the discovery of HDAC1 and HDAC2, a third enzyme with deacetylating activity was identified (HDAC3). The biological function of HDAC3 has been extrapolated from the knowledge on HDAC1 and HDAC2. However, HDAC3 possesses many unique biological functions and embryonic lethality of knockout mice at E10.5 emphasizes its unique function in development (Dangond et al., 1998, 1999; Emiliani et al., 1998; Glaser et al., 2003; Robyr et al., 2002; Wen Ming Yang et al., 1997). Like previously described for HDAC1, we also want to gain more insight into roles of HDAC3 concerning the CNS and its functions via conditional knockout mouse models. With the generation of lacZ reporter mice we intend to gain more insights in HDAC3 expression throughout the adult murine brain and throughout various tissues and organs of the whole body. Furthermore, we are interested in specific roles of HDAC3 in the adult forebrain in regard to emotional behavior, stress compensation and memory formation. Therefore, we intend to generate and phenotype a conditional HDAC3 knockout mouse model which is spatio-temporally controlled via the use of a tamoxifen inducible Cre/loxP system driven by the Camk2a promoter.

3 MATERIAL AND METHODS

3.1 Material

3.1.1 Buffers and Solutions

All buffers and solutions were prepared using Millipore Q-distilled water ($\text{H}_2\text{O}_{\text{bidest}}$). Chemicals were purchased from Sigma-Aldrich (Munich, Germany), Carl Roth (Karlsruhe, Germany) and Merck (Darmstadt, Germany) unless indicated otherwise.

3.1.1.1 Buffers for agarose gel electrophoresis

1x TRIS acetate EDTA (TAE) buffer

4.84 g tris(hydroxymethyl)-aminomethan (TRIS)

1.142 ml acetic acid

20 ml 0.5 M ethylenediaminetetraacetic acid (EDTA), pH 8.0

800 ml $\text{H}_2\text{O}_{\text{bidest}}$

adjusted to pH 8.3

adjusted to a volume of 1 liter with $\text{H}_2\text{O}_{\text{bidest}}$

6x DNA loading buffer (orange)

1 g orange G

10 ml 2 M Tris-HCl, pH 7.5

150 ml glycerol

adjusted to a volume of 1 liter with $\text{H}_2\text{O}_{\text{bidest}}$

3.1.1.2 Buffers and solutions for *in situ* hybridization (ISH)

Diethylpyrocarbonate (DEPC)- H_2O

1 ml DEPC

adjusted to a volume of 1 liter with $\text{H}_2\text{O}_{\text{bidest}}$

2x autoclaved

10x phosphate buffered saline (PBS)/DEPC-H₂O

1.37 M NaCl

27 mM KCl

200 mM Na₂HPO₄ x 12 H₂O

20 mM KH₂PO₄

adjusted to pH 7.4

adjusted to a volume of 1 liter with DEPC-H₂O

incubated overnight

2x autoclaved

20% paraformaldehyde (PFA)

20% (w/v) PFA

adjusted to pH 7.4

adjusted to a volume of 1 liter with 1x PBS/DEPC-H₂O

10x triethanolamine (TEA)

1 M TEA

adjusted to pH 8.0

adjusted to a volume of 1 liter with DEPC-H₂O

incubated overnight

2x autoclaved

20x standard saline citrate (SSC)

3 M NaCl

300 mM sodium citrate

adjusted to pH 7.4

adjusted to a volume of 1 liter with DEPC-H₂O

incubated overnight

2x autoclaved

Hybridization-mix (hybmix)

50 ml formamide
1 ml 2 M Tris-HCl, pH 8.0
1.775 g NaCl
1 ml 0.5 M EDTA, pH 8.0
10 g dextransulphate
0.02 g ficoll 400
0.02 g polyvinylpyrrolidone 40 (PVP40)
0.02 g bovine serum albumin (BSA)
5 ml tRNA (10 mg/ml)
1 ml carrier DNA (salmon sperm, 10 mg/ml)
4 ml 5 M dithiothreitol (DTT)
stored as 1 to 5 ml aliquots at -80°C

Hybridization chamber fluid

250 ml formamide
50 ml 20x SSC
200 ml H₂O_{bidest}

5 M DTT/DEPC

7.715 g DTT
4 ml DEPC-H₂O
the falcon tube was shaken until the powder was nearly dissolved
adjusted to a volume of 10 ml with DEPC-H₂O

10x proteinase K buffer/DEPC

500 ml 1 M Tris-HCl, pH 7.5
100 ml 0.5 M EDTA, pH 8.0
adjusted to a volume of 1 liter with DEPC-H₂O
autoclaved

5x NTE

146.1 g NaCl

50 ml 1 M Tris-HCl, pH 8.0

50 ml 0.5 M EDTA, pH 8.0

adjusted to a volume of 1 liter with DEPC-H₂O

incubated overnight

autoclaved

3.1.1.3 Buffers and solutions for Western blottingRadio-immune precipitation (RIPA) lysis buffer

50 mM Tris, pH 8.0

150 mM NaCl

0.1% SDS

1.0% Nonidet P40 (NP40)

0.5% sodium deoxycholate

4x loading buffer

50% glycerol

125 mM Tris-HCl, pH 6.8

20% sodium dodecyl sulfate (SDS)

1% bromphenol blue

5% β-mercaptoethanol

12% resolving gel for SDS PAGE (10 ml)

3.3 ml H₂O_{bidest}

4.0 ml 30% acrylamide mix

2.5 ml 1.5 M Tris-HCl, pH 8.8

0.1 ml 10% SDS

0.1 ml 10% ammonium persulfate (APS)

0.004 ml tetramethylethylenediamine (TEMED)

5% stacking gel for SDS PAGE (1 ml)

0.68 ml H₂O_{bidest}

0.17 ml 30% acrylamide mix

0.13 ml 1.0 M Tris-HCl, pH 6.8

0.01 ml 10% SDS

0.01 ml 10% APS

0.004 ml TEMED

10x running buffer for SDS PAGE

30.3 g Tris

144 g glycine

50 ml 20% SDS

adjusted to a volume of 1 liter with H₂O_{bidest}

Transfer buffer

400 ml methanol

6.06 g Tris

28.8 g glycine

adjusted to pH 8.3

adjusted to a volume of 2 liter with H₂O_{bidest}

10x TBS

12.11 g Tris

87.66 g NaCl

adjusted to pH 7.6

1x TBS-T

900 ml H₂O_{bidest}

100 ml 10x TBS

0.1 ml tween-20

(for 5% milk solution 5 g of milk powder were dissolved in 100 ml TBS-T)

3.1.1.4 Buffers and solutions for lacZ staining

LacZ-fix

4% PFA/PBS, pH 7.4

0.005 M ethylene glycol tetraacetic acid (EGTA)

0.001 M MgCl₂

adjusted to a volume of 50 ml with 0.1 M PBS, pH 7.4

LacZ wash buffer

0.002 M MgCl₂

0.01% deoxycholate

0.02% Nonidet P40 (NP40)

adjusted to a volume of 0.5 liter with 0.1 M PBS, pH 7.4

LacZ staining solution

0.1% X-Gal

0.005 M potassium-ferrocyanide

0.005 M potassium-ferricyanide

adjusted to a volume of 50 ml with lacZ wash buffer

3.1.1.5 Other buffers and solutions

10x phosphate buffered saline (PBS)

1.37 M NaCl

27 mM KCl

200 mM Na₂HPO₄ x 12 H₂O

20 mM KH₂PO₄

adjusted to pH 7.4

adjusted to a volume of 1 liter with H₂O_{bidest}

incubated overnight

2x autoclaved

Cryoprotection solution

125 ml ethyleneglycol

125 ml glycerol

250 ml 1x PBS

3.1.2 Media for bacterial cultures

Lysogeny broth (LB) medium

1% (w/v) bacto-tryptone (BD)

0.5% (w/v) bacto-yeast-extract (BD)

1.5% (w/v) NaCl

adjusted to pH to 7.4

autoclaved

LB agar plates

1% (w/v) bacto-tryptone (BD)

0.5% (w/v) bacto-yeast-extract (BD)

1.5% (w/v) NaCl

1.5% (w/v) bacto-agar (BD)

adjusted to pH 7.4

autoclaved

3.1.3 Oligonucleotides

3.1.3.1 Primers used for *ISH* probe cloning procedures

name	sequence	PCR product
Hdac1_cDNA_F3	5'-AAGGAGGAGAAGCCAGAAGC-3'	503 bp
Hdac1_cDNA_R3	5'-CAAAAAGGAAGCTAGGCTATCAA-3'	
Hdac1_cDNA_delta_F2	5'-GTCCTCACAAAGCCAATGCT-3'	151 bp
Hdac1_cDNA_delta_R2	5'-CCATCAAACACCGGACAGT	
Hdac2_cDNA_F2	5'-TATTATGGCCAGGGTCATCC-3'	518 bp
Hdac2_cDNA_R3	5'-GTCATCACGCGATCTGTTGT-5'	
Hdac3_cDNA_F2	5'-TATGGTTTTCCCAGGTCTGA-3'	547 bp
Hdac3_cDNA_R	5'-TCATCTGTTTCCTTTTCACATCA-3'	
Hdac3_cDNA_delta_F2	5'-GAAACTGGGCAGTCATCA-3'	159 bp
Hdac3_cDNA_delta_R2	5'-GATCGTCTTCAAGCCTTACCA-3'	
Hdac4_cDNA_F1	5'-CTGATTGAGGCGAAAAGTGTGAG AAGGAAG-3'	566 bp
Hdac4_cDNA_R1	5'-GACTGTGGGATTGTGGGTAAGAA TCAAATGTTAAGC-3'	
Hdac5_cDNA_F2	5'-CCACTGGGTGGCTATTCTGT-3'	498 bp
Hdac5_cDNA_R2	5'-TCACAATGATGAAGCCCAGA-3'	
Hdac6_cDNA_F2	5'-TGGAGGTCAGGACATGAACA-3'	647 bp
Hdac6_cDNA_R2	5'-CCCGTTGTCTCCTTCAATGT-3'	
Hdac7_cDNA_F2	5'-GTGGCCTTCTCAGGTTCTG-3'	561 bp
Hdac7_cDNA_R2	5'-ATACCCTCTGCACGCACTC-3'	
Hdac8_cDNA_F2	5'-ACAGAGGAGCAGGAACTGGA-3'	565 bp
Hdac8_cDNA_R2	5'-CCAGGACAGCATCATTGAGA-3'	
Hdac9_cDNA_F2	5'-CTGGGAATGTGACCGAAAAT-3'	598 bp
Hdac9_cDNA_R2	5'-TGGATCTGCTGCTGGTATTG-3'	
Hdac10_cDNA_F1	5'-CAGAGGAAGAGTTGGGCTTG-3'	561 bp
Hdac10_cDNA_R1	5'-GAAAGGCAGCCAAATAGTCG-3'	
Hdac11_cDNA_F1	5'-TGAAAACACGTTTGGGATGA-3'	569 bp
Hdac11_cDNA_R3	5'-GTCTGGTCCAGGTCAGTGGT-3'	

3.1.3.2 Primers used for genotyping

name	sequence	PCR product
Hdac1_EU_wt_F	5'-TCCAGTGCCCCTCTGGCTCC-3'	wild-type: 472 bp
Hdac1_EU_frt_F	5'-TACCGCGTCGAGAAAGTTCCT-3'	lacZ: 219 bp
Hdac1_EU_R1	5'-AATGTAAGCCAAAACACCAAGC-3'	floxed: 617 bp
HDAC1_DEL_F1	5'-GCCAAGGCTACAGAGAAAGTC-3'	floxed: 732 bp and 1158 bp knockout: 392 bp
HDAC1_DEL_R1	5'-CTTACATCTCTGCATCTGCTTG-3'	
HDAC1_DEL_R2	5'-GGTGGGACCACCTCATCTCAAAG-3'	
Hdac3_EU_frt_F1	5'-CACTGGGTGAAGGTGCCTGCC-3'	wild-type: 756 bp
Hdac3_EU_frt_R1	5'-GCCACCCAAGTACCTTGGGC-3'	lacZ: 341 bp
Hdac3_EU_frt_R2	5'-CCCCGGCCTCCCAGTGATTG-3'	floxed: 890 bp
Hdac3_EU_frt_F1	5'-CACTGGGTGAAGGTGCCTGCC-3'	floxed: 890 bp and 1321 bp knockout: 473 bp
Hdac3_EU_frt_R2	5'-CCCCGGCCTCCCAGTGATTG-3'	
Hdac3_EU_Cre_R1	5'-GCACACGCTGCCCTCCTAC-3'	
Flipase_fwd	5'-TTCGAATCATCGGAAGAAGC-3'	flp: 413 bp
Flipase_rev	5'-TTGCCGGTCTATTTACTCG-3'	
i-Cre1	5'-GGTTCTCCGTTTGCACTCAGGA-3'	wild-type: 290 bp
i-Cre2	5'-CTGCATGCACGGGACAGCTCT-3'	i-Cre-mutant: 375 bp
i-Cre3	5'-GCTTGCAGGTACAGGAGGTAGT-3'	

3.1.4 Riboprobes for *in situ* hybridization (ISH)

name	antisense transcript	vector	accession no.	bp
Hdac1-3	T7	pCRII-TOPO	NM_008228	1479 - 1981
Hdac1-delta	T7	pCRII-TOPO	NM_008228	248 - 398
Hdac2-2	T7	pCRII-TOPO	NM_008229	278 - 795
Hdac3-2	T7	pCRII-TOPO	NM_010411	1422 - 1968
Hdac3-delta	T7	pCRII-TOPO	NM_010411	210 - 368
Hdac4-1	SP6	pCRII-TOPO	NM_207225	3216 - 3781
Hdac5-2	T7	pCRII-TOPO	NM_001284248	3725-4222
Hdac6-2	SP6	pCRII-TOPO	NM_010413	3390 - 4036
Hdac7-2	T7	pCRII-TOPO	NM_001204278	3549 - 4109
Hdac8-2	T7	pCRII-TOPO	NM_027382	212 - 776
Hdac9-2	T7	pCRII-TOPO	NM_024124	1178 - 1775
Hdac10-1	SP6	pCRII-TOPO	NM_199198	419 - 979
Hdac11-3	T7	pCRII-TOPO	NM_144919	1854 - 2422
LacZ	SP6	pCRII-TOPO	NM_00404	192 - 569

3.1.5 Antibodies

name	species	denotation	company
anti-HDAC1	rabbit	PA1-860	Thermo Scientific, Darmstadt, Germany
anti-HDAC3	rabbit	ab16047	Abcam, Cambridge, UK
anti- β -actin	rabbit	4967	Cell Signaling Technology, Darmstadt, Germany
anti-rabbit-IgG HRP	mouse	7074	Cell Signaling Technology, Darmstadt, Germany

3.1.6 *Escherichia coli* (*E. coli*) strains

strain	genotype	company
DH5 α	fhuA2 Δ (argF-lacZ)U169 phoA glnV44 Φ 80 Δ (lacZ) M15 gyrA96 recA1 endA1 thi1 hsdR17	Invitrogen, Darmstadt, Germany

3.1.7 Animals

Female and male C57BL/6 mice were used as wild-type mice for breeding, *in situ* hybridization and lacZ staining.

Conditional HDAC1 knockout mice were obtained by breeding HDAC1-lacZ reporter mice from the European Conditional Mouse Mutagenesis Program (EUComm; <http://www.knockoutmouse.org/about/eucomm>). This heterozygous *Hdac1*^{+/lacZ} reporter mice were generated following a targeted trapping strategy of the *Hdac1* gene locus using the ES cell clone with the following clone ID: EPD0028_5_A01.

Conditional HDAC3 knockout mice were obtained by breeding HDAC3-lacZ reporter mice from the European Conditional Mouse Mutagenesis Program (EUComm; <http://www.knockoutmouse.org/about/eucomm>). This heterozygous *Hdac3*^{+/lacZ} reporter mice were generated following a targeted trapping strategy of the *Hdac3* gene locus using the ES cell clone with the following clone ID: EPD0028_3_D01.

In the chronic social defeat stress paradigm dominant male CD1 mice were used as resident.

3.2 Methods

3.2.1 Microbiological methods

3.2.1.1 Preparation of electrocompetent bacteria

For cloning of plasmid DNA, electrocompetent *Escherichia coli* (*E. coli*) bacteria of the conventional strain DH5 α were used and prepared as follows. An overnight 50 ml culture was inoculated with the frozen glycerol-stock of DH5 α . After vigorous shaking overnight at 37 °C, the pre-culture was transferred to 500 ml LB medium and incubated on an orbital shaker at 37 °C. The growth of the bacteria solution was checked regularly with a spectrophotometer (DU 530 Life Science UV/Vis Spectrophotometer, Beckman) at 600 nm wavelength until it reached an optical density (OD) of 0.5-0.6. The bacteria suspension was split into four 250 ml centrifugation bottles and cooled down on ice for 30 minutes. From here, all procedures were performed at 4 °C. The tubes were centrifuged at 4000x g for 15 min at 4 °C. The supernatants were discarded and each of the pellets was carefully resolved in 150 ml of ice-cold H₂O_{bidest.} Bacteria were centrifuged again at 4000x g for 15 min at 4 °C. Each of the bacteria pellets were resolved a second time in 80 ml of ice cold H₂O_{bidest.} and centrifuged again at 4000x g for 15 min at 4 °C. Each pellet was then carefully resolved in 6 ml of 10% glycerol diluted in H₂O_{bidest.} Bacteria suspensions were then transferred to two 30 ml centrifugation plastic tubes and centrifuged at 4000x g for 15 min at 4 °C. Each pellet was dissolved in 1 ml of 10% glycerol in H₂O_{bidest.} Bacteria suspensions were combined and split in 20 μ l aliquots, frozen on dry-ice and stored at -80 °C. The transformation efficiency (# of colonies/ μ g plasmid DNA) was determined for each batch by transformation of 10 pg and 100 pg pUC18 control plasmid. Usually, preparations of electrocompetent bacteria had a transformation efficiency of 10⁸-10⁹ colonies/ 1 μ g plasmid DNA.

3.2.1.2 Transformation of electrocompetent bacteria

For one transformation, one aliquot of electrocompetent *E. coli* was thawed on ice and 1-2 μ l of a ligation reaction or 10-100 pg of circular plasmid DNA were added. The suspension was mixed carefully and then transferred into a 1 mm electroporation cuvette (VWR). Electroporation was carried out using a Biorad electroporation system following the manufacturer's instructions (1800 V, 25 μ F capacitance, 200 Ω resistance). After the electroporation pulse bacteria were transferred immediately to 1 ml pre-warmed LB medium and incubated at 37 °C, shaking vigorously, for 30-60 min. Afterwards dilutions of the electroporated bacteria were plated on LB agar plates containing

the appropriate antibiotic for selection and incubated overnight at 37°C. Typically, 100 µg ampicillin or 50 µg kanamycin per ml LB medium were used for selection of transformed clones.

3.2.1.3 Glycerol stocks

For long-term storage, 750 µl of an overnight bacteria culture was mixed with 250 µl 80% glycerol and frozen at -80°C.

3.2.2 Preparation and analysis of nucleic acids

3.2.2.1 RNA isolation

Total RNA was prepared from brain tissue using TRIzol reagent according to the manufacturer's protocol (Invitrogen, Darmstadt, Germany). cDNA was derived from this RNA using Reverse Transcriptase Superscript II from Invitrogen and oligo-dT primers following the manufacturer's protocol (Invitrogen, Darmstadt, Germany). Aliquots of the cDNA were utilized as templates for cloning riboprobes.

3.2.2.2 Preparation of plasmid DNA from bacteria

Plasmid DNA was isolated from transformed bacteria using plasmid isolation kits from Qiagen (Hilden, Germany) following the manufacturer's instructions. The Qiagen MiniPrep Kit was used for screening of correctly transformed clones and the Qiagen Plasmid Maxi Kit, Qiagen HiSpeed Plasmid Maxi Kit, or Qiagen Plasmid Maxi Kit Plus were used for higher yield plasmid preparations.

For MiniPreps, a single colony was inoculated in 5 ml LB medium with the appropriate antibiotic overnight at 37°C. For MaxiPreps, either 500 µl of an overnight MiniPrep culture, or the appropriate glycerol-stock of bacteria was added to 250 ml LB medium with antibiotic and incubated overnight at 37°C with vigorous shaking.

3.2.2.3 DNA preparation from mouse tail tissue

For PCR genotyping of transgenic mice, tail tissue was digested in 100 μ l 50 mM NaOH for 30 min at 99°C followed by a neutralization step using 30 μ l 1 M Tris-HCl (pH 7.0) and stored at 4°C. 1-2 μ l of the tail lysates were used as template for PCRs.

3.2.2.4 Agarose gel electrophoresis

For separation of DNA by gel electrophoresis, agarose (Invitrogen, Darmstadt, Germany) was boiled in 1x TAE buffer with agarose concentration depending on DNA fragment size. For fragments between 100 and 1000 bp 2% agarose gels were chosen. For larger fragments 0.8-1% agarose gels were applied. 0.1 μ g/ml ethidiumbromide was added to boiled and liquid agarose in 1x TAE which was split in a gel electrophoresis chamber (PeqLab, Erlangen, Germany). DNA were mixed with 6x sample buffer and loaded onto the gel. As size marker the smart ladder (Eurogentec, Brussels, Belgium) was used. Electrophoresis was carried out with 80-140 V for 1-2 h. Separated DNA fragments were detected with a UV light camera (Biometra, Göttingen, Germany).

3.2.2.5 Photometric measurement of DNA and RNA concentrations

DNA or RNA concentration was measured in duplicates in a UV photometer Gene Quant II (Pharmacia Biotech, Uppsala, Sweden) at 260 nm. Samples were diluted in H₂O_{bidest.} At a wavelength of 260 nm and a cuvette thickness of 1 cm an optical density (OD) of 1 corresponds to a concentration of 50 μ g/ml for double stranded DNA, 33 μ g/ml for single stranded DNA and 40 μ g/ml for RNA. The concentration of the sample (X) was therefore $OD_{260} \times T \times \text{dilution factor} = X \mu\text{g/ml}$, with T being 50 μ g/ml for double stranded DNA, 33 μ g/ml for single stranded DNA and 40 μ g/ml for RNA.

3.2.2.6 Restriction digest of plasmid DNA and PCR products for analytical purposes

For digestion of plasmid DNA or PCR products 2-4 units (U) per restriction enzyme (Fermentas, Darmstadt, Germany or New England Biolabs (NEB), Ipswich, USA) were used per μ g of DNA or per 25 μ l PCR reaction. The reaction conditions and the type of buffer were chosen following the manufacturer's instructions. The restriction digest was incubated for 1 hour at 37°C (unless a

different temperature was recommended for the used enzyme) and fragment sizes were subsequently analysed using agarose gel electrophoresis.

3.2.2.7 Sequencing

Sequencing reactions were carried out by Sequiserve (Vaterstetten, Germany) or GATC-Biotech (Konstanz, Germany). The sequencing results were analysed using the software *Vector NTI Advance 11* (Invitrogen, Darmstadt, Germany).

3.2.3 Polymerase Chain Reaction (PCR)

For genotyping PCRs and to amplify specific cDNA fragments for expression vector cloning, polymerase chain reactions (PCRs) were performed using the Thermoprime Plus DNA polymerase (ABgene, Hamburg, Germany) as follows:

PCR reaction:

1 µl	cDNA/genomicDNA
1 µl	primer forward (10 pmol)
1 µl	primer reverse (10 pmol)
1 µl	dNTPs (dATP, dTTP, dGTP; 10 mM each; Roche, Basel Switzerland)
5 µl	10x reaction buffer IV (ABgene/ThermoScientific, Darmstadt, Germany)
3 µl	MgCl ₂ solution (25 mM; ABgene/ThermoScientific, Darmstadt, Germany)
0.5 µl	Thermoprime Plus DNA polymerase (5 U/µl; ABgene/ThermoScientific, Darmstadt, Germany)
37.5 µl	H ₂ O _{bidest}
50 µl	final volume

PCR was carried out in a thermocycler (GeneAmp PCR Sytem 9700, Applied Biosystems, Darmstadt, Germany) with the following temperature settings:

PCR program:

94°C	2 min	

94°C	30 sec	
x1°C	30 sec	(35 cycles)
72°C	x2 sec	

72°C	5 min	
4°C	∞	

Annealing temperature (x1) and elongation time (x2) were chosen in dependence of the melting temperature of the primers and the amplicon size.

3.2.4 Cloning techniques

3.2.4.1 Restriction digest of plasmid DNA and PCR products for preparative purposes

For digestion of plasmid DNA or PCR products 2-4 units (U) per restriction enzyme (Fermentas, Darmstadt, Germany or NEB, Ipswich, USA) were used per µg of DNA or per 25 µl PCR reaction. The reaction conditions and the type of buffer were chosen following the manufacturer's instructions. The restriction digest was incubated overnight at 37°C (unless a different temperature was recommended for the used enzyme). Desired fragments were purified either by using a PCR Purification Kit from Qiagen (Hilden, Germany) following the manufacturer's instructions or by gel extraction.

3.2.4.2 DNA gel extraction

For purification of DNA fragments out of an agarose gel a gel with 1% agarose was poured and fragments were separated. The desired DNA fragment was cut out under UV light and purified using the QIAquick Gel Extraction Kit from Qiagen (Hilden, Germany) following the manufacturer's instructions. DNA was eluted using 30 µl of H₂O_{bidest.} Extracted DNA concentration was estimated using agarose gel electrophoresis and different amounts of the DNA marker smart ladder.

3.2.4.3 Ligation of DNA fragments

For the ligation of the linearized vector and the insert, a molar ratio of 1:3, 1:6 or 1:9 of vector:insert was used. In general, 100 ng of vector DNA and 3x, 6x or 9x of insert, in molar ratio, were mixed. For very short inserts (<500 bp) a molar ratio of 1:15 was used. T4 DNA ligase buffer and 5 U of T4 DNA ligase (Fermentas, Darmstadt, Germany) were added in a total volume of 10-15 µl. The reaction was incubated overnight at 16°C. Afterwards, 1-2 µl of the ligation reaction were used for transformation into electrocompetent bacteria.

3.2.4.4 TOPO TA cloning

TOPO TA cloning from Invitrogen (Darmstadt, Germany) is based on the biochemical properties of DNA topoisomerase type I. PCR products with A-overhangs, derived from PCR reactions carried out with Taq DNA polymerase (Roche, Basel, Switzerland) are inserted into a cut vector which carries T-overhangs with covalently bound topoisomerase.

Probes for *ISH* were cloned into the pCRII-TOPO vector (Invitrogen, Darmstadt, Germany) following manufacturer's instructions. The pCRII-TOPO vector contains among others SP6 and T7 promoters which allow *in vitro* transcription.

For blue-white selection of the colonies, 40 µl of 40 mg/ml X-Gal in dimethylformamide (DMF) solution were previously added to LB-agar plates. After overnight incubation at 37°C white colonies were picked for screening.

3.2.5 *In situ* hybridization (*ISH*)

ISH using ³⁵S-labeled cRNA probes was performed following a protocol which is a modified version of the procedure described from Dagerlind and colleagues (Dagerlind, Friberg, Bean, & Hökfelt, 1992) and is well-established at the MPI of Psychiatry.

3.2.5.1 Tissue preparation

2-3 months old male mice were sacrificed by an overdose of isoflurane (Forene, Abbott, Wiesbaden, Germany) followed by decapitation. Brains were carefully removed, immediately shock-frozen on dry-ice and stored at -80°C.

For quantitative and qualitative *ISH* frozen brains were mounted in different directions on polyfreeze tissue freezing medium (Polyscience Inc., Warrington, PA, USA) for subsequent cutting with a HM 560 M cryostat (Microm/ThermoScientific, Darmstadt, Germany). Consecutive sections were prepared with a thickness of 20 µm in coronal or sagittal orientation, mounted on super frost plus microscope slides (Menzel/ThermoScientific, Darmstadt, Germany), dried on a 37°C warming plate and stored at -20°C until further processing.

3.2.5.2 Preparation of radioactive riboprobes

All cDNA inserts used as templates for the generation of the radiolabeled cRNA probes were cloned in pCRII-TOPO vectors and contain SP6 and T7 promoters. Therefore, for template amplification PCRs SP6 and T7 primers were used in the following protocol.

PCR for template amplification:

1 µl	plasmid template
1 µl	primer forward (10 pmol)
1 µl	primer reverse (10 pmol)
1 µl	dNTPs (dATP, dTTP, dGTP; 10 mM each; Roche, Basel Switzerland)
5 µl	10x reaction buffer IV (ABgene/ThermoScientific, Darmstadt, Germany)
3 µl	MgCl ₂ solution (25 mM; ABgene/ThermoScientific, Darmstadt, Germany)
0.5 µl	Thermoprime Plus DNA polymerase (5 U/µl; ABgene/ThermoScientific, Darmstadt, Germany)
37.5 µl	H ₂ O _{bidest}
50 µl	final volume

PCR program:

94°C	3min	

94°C	30 sec	
67°C	30 sec	(35 cycles)
72°C	60 sec	

72°C	5 min	
4°C	∞	

To prevent RNA degradation all possible precautions were taken to avoid RNase activity.

In vitro transcription and radiolabeling:

x µl (200 ng)	PCR product
x µl	H ₂ O-DEPC
3 µl	10x transcription buffer (Roche, Basel, Switzerland)
3 µl	NTP-mix (rATP, rCTP, rGTP; 10 mM each; Roche, Basel, Switzerland)
1 µl	0.5 M DTT
1 µl	RNasin (RNase-inhibitor; 40 U/µl; Roche, Basel, Switzerland)
6 µl	³⁵ S-thio-rUTP (12.5 mCi/mM; 1250 Ci/mml; Perkin Elmer, Waltham, MA, USA)
1 µl	T7 or SP6 RNA polymerase (20 U/µl; Roche, Basel, Switzerland)
30 µl	final volume

After pipetting, the reaction samples were gently mixed by tapping the Eppendorf tubes and spun down quickly. Then the samples were incubated for a total of 3 hours at 37°C. After 1 hour another 0.5 µl of RNA polymerase was added.

To destroy the DNA template after the incubation, 2 µl of RNase-free DNase I (10 U/µl; Roche, Basel, Switzerland) were added and samples were incubated another 15 min at 37°C. Afterwards the radiolabeled riboprobes were purified with the use of the Qiagen RNeasy Kit (Qiagen, Venlo, Netherlands). RNA was diluted in 100 µl of RNase-free water and for quantification purposes, 1 µl of each probe was measured in 2 ml scintillator solution (Zinsser Analytic, Frankfurt, Germany) in a beta-counter (LS 6000 IC, Beckmann Coulter). For *ISH* 35,000 to 70,000 cpM/µl and 90 µl/slide (7 Mio/slide) were necessary.

3.2.5.3 Pre-treatment of brain slices

Cryo-slides with brain slices were taken out from their storage at -20°C and warmed up for about 1 hour at room temperature while still sitting in their boxes. Then they were spread out on a clean tissue and dried for another 15 minutes before they were placed in special racks for further treatment.

Pre-treatment procedure:

1. fixation	10 min	4% PFA/PBS/DEPC-H ₂ O	ice-cold (4°C)
2. rinsing	3x 5 min	PBS/DEPC-H ₂ O	
3.	10 min	0.1 M TEA-HCl (pH 8.0)	add 600 µl acetic anhydride to 200 ml of rapidly rotating TEA
4. rinsing	2x 5 min	2x SSC/DEPC-H ₂ O	
5. dehydration	1 min	60% ethanol/DEPC-H ₂ O	
6.	1 min	75% ethanol/DEPC-H ₂ O	
7.	1 min	95% ethanol/DEPC-H ₂ O	
8.	1 min	100% ethanol	
9.	1 min	chloroform	
10.	1 min	100% ethanol	
11.	1 min	95% ethanol/DEPC-H ₂ O	
12. air-drying (dust free)			

3.2.5.4 Hybridization of riboprobes

An appropriate amount of hybridization mix (hybmix) containing the riboprobe was prepared. 90 to 100 µl hybmix containing 3.5 to 7 million counts per slide were required.

The riboprobe in hybmix was incubated for 2 minutes at 90°C, shortly cooled down on ice and then put on room temperature. The solution was pipetted onto each slide and coverslips were carefully put on top while avoiding air bubbles on brain slices between cryo-slide and coverslip.

The slides were carefully placed in a hybridization chamber containing hybridization chamber fluid to prevent drying out of the hybmix and the chamber was sealed with adhesive tape. The chambers were put overnight (up to 20 hours) into an oven with 55-68°C.

3.2.5.5 Washing of brain slices

After the hybridization procedure, the coverslips were removed from the cryo-slides and the brain slices were washed.

Washing procedure:

- | | | | | |
|-----|------------------------|--|------|---|
| 1. | 4x 5min | 4x SSC | RT | |
| 2. | 20 min | NTE (20 µg/ml RNaseA) | 37°C | add 500 µl RNaseA
(10 mg/ml) to 250 ml |
| 3. | 2x 5min | 2x SCC/1 mM DTT | RT | 50 µl of 5 M DTT to 250 ml |
| 4. | 10 min | 1x SCC/1 mM DTT | RT | 50 µl of 5 M DTT to 250 ml |
| 5. | 10 min | 0.5x SCC/1 mM DTT | RT | 50 µl of 5 M DTT to 250 ml |
| 6. | 2x 30 min | 0.1x SCC/ 1 mM DTT | 64°C | 50 µl of 5 M DTT to 250 ml |
| 7. | 2x 10 min | 0.1x SCC | RT | |
| 8. | 1 min | 30% EtOH in 300 mM NH ₄ OAc | RT | |
| 9. | 1 min | 50% EtOH in 300 mM NH ₄ OAc | RT | |
| 10. | 1 min | 70% EtOH in 300 mM NH ₄ OAc | RT | |
| 11. | 1 min | 95% EtOH in 300 mM NH ₄ OAc | RT | |
| 12. | 2x 1 min | 100% EtO | RT | |
| 13. | air-drying (dust free) | | | |

3.2.5.6 Autoradiography

Dried *ISH* sections were exposed to a special high performance X-ray film (BioMax MR from Kodak, Rochester, NY, USA) for one to three days dependent on signal intensity.

3.2.5.7 Dipping radiolabeled brain slices in silver staining solution

For qualitative expression analysis, slides were dipped for about 4 seconds in a pre-warmed KODAK NTB2 photographic emulsion (KODAK, Rochester, NY, USA) and air-dried overnight at RT. The next day, slides were packed into light-tight black boxes with sufficient desiccant (silica gel capsules), labelled and sealed with tape. Depending on signal intensity detected on the X-ray film, the slides were stored in the dark at 4°C for three to four weeks and then developed.

For development of silver stained slices, the boxes were equilibrated to room temperature for 2 hours while still sealed. The slides were developed in KODAK D 19 developer (SIGMA P5670) for 3 min at room temperature, rinsed for 30 sec under the tap and fixed with KODAK fixer for 5 min. Afterwards slides were rinsed under running tap water for another 25 minutes. With the use of a strong razor blade the emulsion was scratched from the back side of slides and the slides were air-dried at room temperature in the light.

3.2.5.8 Nissl staining

Brain sections on developed slides were counterstained with the synthetic dye cresyl violet. This basic aniline dye is able to stain the RNA of the rough endoplasmic reticulum, called Nissl substance, in the cytoplasm of neurons within the brain sections.

Staining procedure:

1. 20 min 0.5% Cresyl violet acetate
2. 1 min water
3. 2x 1 min 70% ethanol
4. 1 min 96% ethanol + 1 ml of acetic acid
5. 2x 1 min 96% ethanol
6. 2x 1 min 100% ethanol
7. 2x 5min xylol

3.2.5.9 Figure preparation

Photomicrographs (brightfield for brain sections on X-ray film; darkfield for dipped brain sections) were taken on a Zeiss Axioplan microscope equipped with a Zeiss AxioCam MRc digital camera. Image processing in Adobe Photoshop included adjustments of total tonal value, brightness, contrast, sharpness and image size (no partially modifications, only on whole section).

3.2.6 Western blot analysis

Tissue was lysed in RIPA buffer containing protease inhibitors (complete protease inhibitor tablets, Roche, Basel, Switzerland). Protein concentrations were measured using Bradford assay and the

adequate amount of loading buffer was added. Samples were incubated at 95°C for 5 min to denature the proteins and subsequently put on ice. 30 µl of each sample and 10 µl of the pre-stained protein ladder PageRuler™ (Fermentas, Darmstadt, Germany) were separated on a 12% SDS-PAGE gel for 3 hours at RT, 100 V and subsequently transferred onto a PVDF membrane (Millipore, Darmstadt, Germany) overnight at 4°C, 25 V. For both steps, WB chambers from Bio-Rad (Hercules, CA, USA) were used. The next day, membranes were blocked for 1 hour in 5% milk powder in TBS-T at RT. Incubation of the first antibody, diluted in 5% milk in TBS-T, was carried out overnight at 4°C while rotating. Afterwards, membranes were washed 3x 10 min with TBS-T and followed by the incubation with the secondary antibody (Cell Signaling, Cambridge, UK), diluted in 5% milk powder in TBS-T, for 1 hour at RT at a rotator. Afterwards, membranes were washed 3x 10 min with TBS-T and immunoreactive bands were detected using ECL detection kit (Millipore, Darmstadt, Germany) and a Kodak film was developed using an automated development machine (XP 2000, Kodak, Rochester, NY, USA).

3.2.7 Animal housing

In all experiments mice were housed under standard laboratory conditions (12 hours light-dark cycle with lights on between 7:00 a.m. and 7:00 p.m.; 22±1°C; 55±5% humidity) with food and water *ad libitum*. All animal breeding and experiments were conducted in accordance with the 'Guide for the Care and Use of Laboratory Animals of the Government of Bavaria'.

Litters at the age of 3 to 4 weeks were separated from dams, numbered by ear-punching and a small tail biopsy was taken for genotyping. Mice were housed at three to five animals per cage with the same gender, when not in breeding.

3.2.8 Behavioral testing

In all experiments male mice in the adult age between two and three months were separated and habituated to single housing and test room conditions for a period of two weeks. At the same time the mice were fed with tamoxifen chow (LASvendi, Soest, Germany) for 7 days when knockout/recombination via the Cre/loxP system was desired, followed by a 7 day wash-out phase with standard diet prior to behavioral experiments. In addition, animals underwent a few days before testing a general health check including fur and general physical conditions as well as

bodyweight analysis to ensure that behavioral findings are not confounded by the animals' health conditions. The testing procedure occurred between 8:00 a.m. and 1:00 p.m. to minimize the influence of hormonal circadian variations (Lightman et al., 2008). Before the introduction of each mouse, all behavioral apparatus were cleaned with water to eliminate sensory traces. To limit additional stress effects induced by each test itself, the order of tests was performed from least to most stressful (Kalueff & Murphy, 2007). Random distribution of genotype, condition and treatment groups excluded an apparatus bias. Animal tracking was accomplished by an automated video tracking software (Anymaze; Stoelting Co., Wood Dale, IL, USA).

3.2.8.1 Open field (OF) test

The open field (OF) test, first described for rats' emotional behavior testing by Hall in 1934, is a common test used for the characterization of locomotor activity and explorative behavior in a novel environment. The test is based on creating a conflict between the mice exploratory drive and its natural fear of an unprotected novel environment (Prut & Belzung, 2003). The apparatus consists of an enclosed square arena (50 x 50 x 40 cm) and is made of grey polyvinylchloride (PVC). The arena is virtually divided into two zones, an inner zone (25 x 25 cm) and an outer zone. During testing, both arenas were illuminated equally with less than 15 lux. All mice were placed in the upper left corner of the apparatus, facing the wall at the beginning of the trial. Testing duration was 30 or 15 minutes (depending on number of animals to be tested at the same day), usually only the first 15 minutes divided into three segments of five minutes were used for analyzing. Parameters of interest included the total distance travelled, inner zone exploration time and the time of immobility.

3.2.8.2 Elevated plus maze (EPM) test

The elevated plus maze (EPM) test is one of the most validated tests of anxiety in rodents. Derived from Montgomery's studies in 1955 on the relationship between novelty, fear and exploration in rodents, Huddle and Mithani developed this test in 1984, creating a typical approach-avoidance conflict. The natural explorative tendency of mice is in opposition to the innate fear of illuminated, elevated and unprotected areas (R. J. Rodgers & Dalvi, 1997).

The apparatus was made of grey PVC and consists of a plus-shaped platform with two opposing open arms (30 x 5 x 0.5 cm) and two opposing enclosed arms (30 x 5 x 15 cm) which are connected by a central arm (5 x 5 cm). The whole device is elevated 50 cm above the floor. Illumination was 25 Lux within the open arms and less than 10 lux within the closed arms. The trial duration was set to 5 or 10 minutes (depending in number of animals to be tested at the same day) and usually only the first 5 minutes were analyzed. Animals were placed in the center zone of the apparatus facing the left closed arm. Parameters of interest included open arm time versus closed arm time, latency until first open arm entry (four paw criterion), number of open arm entries, time of immobility and total distance travelled.

3.2.8.3 Dark/light box (DaLi) test

The dark/light box (DaLi) test is based on the innate aversion of rodents to brightly illuminated areas and on the spontaneous exploratory behavior of rodents in response to mild stressors, that is, novel environment and light to assess anxiety-related behavior (J. Crawley & Goodwin, 1980). The apparatus is a box consisting of one compartment (30 x 20 x 25 cm) made of black PVC (dark) and a second compartment (30 x 20 x 25 cm) made of white PVC (light) which are connected through a tunnel (4 x 7 x 10 cm). The black compartment was illuminated with less than 5 lux and the white compartment was brightly illuminated with an intensity of 680-700 lux. Each animal was placed into the dark compartment facing the upper left corner. The trial duration was set to 5 minutes and the following parameters were analyzed to assess anxiety-like behavior: time spent in lit compartment versus dark compartment, latency until the first full entry (four paw criterion) and the number of full entries into the lit compartment.

3.2.8.4 Forced swim test (FST)

The forced swim test (FST) introduced by Porsolt in 1977, is one of the most frequently used model to assess stress-coping/depression-like behavior in rodents (Cryan & Mombereau, 2004; Porsolt, Bertin, & Jalfre, 1977). The test is based on the observation that mice develop an immobile posture in an inescapable cylinder filled with water after an initial period of escape-directed movements. Three behavioral patterns are classified in this paradigm: floating (interpreted as despair), swimming (interpreted as neutral behavior) and struggling (interpreted as escape-orientated behavior) (Ohl, 2005).

Each animal was gently placed into a glass beaker (diameter: 13 cm, height: 24 cm, filled with 2 liter of water, temperature: $21\pm 1^{\circ}\text{C}$) and the behavior during a 6 minutes test period was recorded. The animals were removed from the cylinder, dried with a towel and put back in their home cages.

The parameters floating (immobile posture with only small movements to keep balance), swimming (directed locomotion by movement of the hind legs) and struggling (strong escape-orientated action) were scored by an experienced observer, blind to genotype, condition or treatment of the animals.

3.2.8.5 Social approach/avoidance (SA) test

The social approach/avoidance (SA) test was established by Berton and colleagues (Berton et al., 2006). The test consists of two trials. In the first trial, each test mouse was introduced for 2.5 minutes into an enclosed square arena (50 x 50 x 40 cm), made up of grey polyvinylchloride (PVC), containing a very small empty wire mesh cage which was located at the middle of one side of the arena. The small field around the cage is marked as the interaction zone). During the second trial an unfamiliar male CD1 mouse was put into the wire mesh cage, allowing for nose contact between the bars, but prevented fighting. The time spent within the interaction zone in the first trial and the time spent interacting with unfamiliar mouse in the second trial were analyzed.

3.2.8.6 Female urine sniffing test (FUST)

The female urine sniffing test (FUST) designed for reward-seeking behavior was adopted and performed according to the protocol from Malkesman and colleagues (Malkesman et al., 2010). Animals were habituated to a sterile cotton-tip in their home cages one hour before testing. The test comprised three stages, all conducted under non-aversive conditions (2-3 lux) within the animal's home cages. In the first trial (water trial) the animals were exposed for 3 minutes to a cotton tip dipped in sterile water. After an interval of 45 minutes, the mice were exposed to a second cotton tip dipped in fresh female urine, which was previously collected from the females' estrus (urine trial). The sniffing time of both, water and urine trial were analyzed.

3.2.8.7 Chronic social defeat stress (CSDS) paradigm

The chronic social defeat stress (CSDS) paradigm was established by the research group of Matthias Schmidt at the MPI of Psychiatry, based on the protocol of Berton and colleagues (Berton et al., 2006; Wagner et al., 2011). To describe briefly, test mice were submitted to chronic social defeat stress for 21 consecutive days. Therefore, they were introduced into the home cage of a dominant CD1 resident mouse for no longer than 5 min and subsequently defeated. Following defeat, animals spent 24 hours within the same cage, but separated via a holed steel partition, enabling sensory, but not physically contact. Every day chronically defeated mice were exposed to a new unfamiliar resident. Control animals were housed in their home cages throughout the course of the experiment. All animals were handled daily, as well as the body weight was assessed daily and the fur status was checked every 3-4 days. The fur was evaluated as describe before by Mineur and colleagues (Mineur, Prasol, Belzung, & Crusio, 2003).

3.2.8.8 Acute stress response and sampling during CSDS paradigm

On day 19 of the chronic social defeat stress procedure, test animals were subjected to an acute stress challenge in form of the FST for 6 minutes. Blood samples were collected by tail cut 15 minutes after the start of the FST and corticosterone plasma concentrations were measured using a radioimmune assay according the manufacturer's manual (sensitivity 6.25 ng/ml; MP Biomedicals Inc., Santa Ana, CA, USA). Animals were sacrificed by an overdose of isoflurane (Forene, Abbott, Wiesbaden, Germany) followed by decapitation on day 21 of the experiment. In order to obtain basal corticosterone levels, trunk blood was collected and processed. Thymus and adrenal glands were removed and stored in Ringer's solution. In order to determine the organ weight, additional surrounding tissue was removed and the thymi and adrenal glands were weighted.

3.2.8.9 Water Cross Maze (WCM) test

The water cross maze (WCM) test was used to assess spatial learning via allocentric navigation of mice and it was established by the research group of Carsten Wotjak at the MPI of Psychiatry, based on Tolman's work from 1946 (Kleinknecht et al., 2012; Tolman, Ritchie, & Kalish, 1946). The used material for the plus-shaped maze is 1 cm thick clear acrylic glass to allow for visual orientation via distant extra-maze cues in the experimental room. Each of the four maze arms were equal in size

(50 x 10 x 30 cm) and clockwise labeled as North, East, South and West. When using the spatial learning protocol, in all trials a submerged platform (8 x 8 x 10 cm) was positioned at the end of the West arm and the maze was filled with fresh tap water ($21\pm 1^\circ\text{C}$) up to 11.5 cm level each day prior before testing. A metal grid (9 x 9 cm) was used to remove the animal from the maze after the end of each trial. The testing room was dimly illuminated (15-20 lux) and the room contained several distant visual cues such as a sink, a chair, a cupboard, doors and a clock.

Animals were gently put into the water at the starting position described within the particular protocol, facing the wall of the maze. The experimenter remained standing motionless behind the current starting arm during the total time of the trial. Parameters of each trial were recorded and as soon as the animal reached the platform, the animal was placed back into its home cage, which was subsequently put under an infrared light to dry and warm the animals. After each run, the walls of the maze were wiped dry and the water was stirred between the four arms every three runs in order to avoid urine and pheromones influence on swimming paths. Animal feces were removed with the use of a metal strainer. Each animal was tested on five consecutive days, six times a day in groups of six, resulting in an intertrial interval of about 10 minutes for each animal. The platform was in all trials located at the end of the West arm, while the starting point of the mice altered between North and South arm in a pseudorandom manner displayed in Table 2. Thus, to perform accurately, mice needed to orientate spatially.

Parameters used as performance indicators are the accuracy and the number of accurate learners. The accuracy indicated the success or failure of the mouse to swim the correct path to the platform. Specifically, the mouse is counted as accurate if it does not enter other arms except the goal arm (platform arm), but enters the goal arm right away and climbs onto the platform within a distinct period of time. In this case, the run is given the value 1 (= accurate), otherwise the mouse is counted as 0 (= not accurate). The sum of correct runs is divided by the total number of runs and the percentage calculated ($\text{sum of correct runs} / 6 * 100$). Given the natural tendency of mice to explore, one error is permitted, which then manifests in an accuracy of 83.3% as the bottom threshold for a mouse to be considered as accurate. The second parameter is given by the number of accurate learners and indicates the percentage of animals of a particular group performing accurately.

day	run 1	run 2	run 3	run 4	run 5	run 6
1	S	N	N	S	S	N
2	N	S	S	N	N	S
3	S	N	N	S	S	N
4	N	S	S	N	N	S
5	S	N	N	S	S	N

Table 2. Training protocol for spatial learning using the water cross maze (WCM). Mice were tested 6 runs a day on five consecutive days. The starting position varied for every trial and every day between South (S) and North (N) arm and therefore was not foreseeable for mice.

3.2.9 Statistics

Data output and statistical analysis were performed with the use of the computer programs GraphPad Prism 5 and SPSS 16.0. All results are shown as means \pm standard error of the mean (SEM). Significance was accepted with $p < 0.05$. Data sets were tested by the appropriate analysis of variance (ANOVA) model. To examine performance in the basal behavioral screen, One-way ANOVA and Student's t-test was employed, whereas effects of genotype and stress on behavior and neuroendocrine data Two-way ANOVA and repeated-measures ANOVA (for comparison of multiple time points) were used. To examine performance in the WCM task Two-way repeated measures ANOVA was employed. The appropriate post-hoc test was performed after acceptance of significant p-values.

4 RESULTS

4.1 Distribution of the classical HDACs throughout the adult murine brain

Up to date, the expression of classical HDACs within the adult brain for rodents has only been described in rats (Broide et al., 2007), but for mice a detailed description is missing. Therefore, a comprehensive gene expression mapping of the eleven classical HDACs (class I: HDAC1, HDAC2, HDAC3 and HDAC8; class II: HDAC4, HDAC5, HDAC6, HDAC7, HDAC9 and HDAC10; class IV: HDAC11) was conducted throughout the adult murine brain using radioactive *in situ* hybridization (*ISH*) and exposure to photo emulsion. For each single HDAC member a highly specific sequence was chosen for designing respective riboprobes to detect endogenous *Hdac1-11* mRNA levels. The sequences were selected carefully using external data base information as all eleven classical HDACs display high homologies to each other (Table 3). The highest homology among cDNA sequences exists for *Hdac1* and *Hdac2*, two class I HDACs, which most probably arose from a relatively recent gene duplication (Gregoretta et al., 2004). The smallest homology was observed for two class II HDACs, *Hdac6* and *Hdac7*, but it still reaches a value of 51% identity among cDNA sequences. Nevertheless, for all eleven HDACs a specific probe which only detects the distinct member was identified (Figure 7). All probes are similar in size, ranging from 500-650 bp and were chosen to hybridize within the translated region of the mRNA. However, for some probes a highly-specific region could only be found within the 3' untranslated region (3'UTR).

With the use of these carefully designed antisense riboprobes radioactive high-resolution *ISH* was performed. For a first glance, probes were hybridized on sagittal brain sections which proved that all eleven classical *Hdacs* are expressed within the adult murine brain (Figure 8). Interestingly, no expression pattern looks like the other and the *Hdac* isoforms showed both, overlapping and distinct expression patterns throughout the murine brain. This supports the idea that each HDAC isoform inhabits a crucial and non-redundant role within the adult mammalian brain. Having a closer, but still overall look, the expression pattern of the only class IV member, *Hdac11*, attracts attention as this member is the highest expressed *Hdac* regarding signal intensity and number of brain regions where it is expressed suggesting that HDAC11 is a predominant and important player among HDACs in the adult brain. In expression strength *Hdac11* is directly followed by the class II HDAC member *Hdac5*, whereas the class I HDAC member, *Hdac3* ranks place three. Thus, from each class of classical HDACs one member is present among the top three of highest expressed *Hdacs*.

The lowest expression could be detected for *Hdac10* (class II), which is not only generally low in expression levels, but also within respect to the number of brain regions showing expression at all. It should also be noted, that *Hdac1*, *Hdac2*, *Hdac3*, *Hdac5*, *Hdac7*, *Hdac8*, *Hdac9* and *Hdac11* are broadly expressed, whereas *Hdac4*, *Hdac6* and *Hdac10* seem rather to be expressed in very distinct brain regions.

For a detailed description of the expression levels of *Hdac1-11*, series of coronal brain slices throughout the brain were generated and analyzed at least from three separate animals (Figures 9-11). Qualitative and quantitative analysis of signal intensity of each *Hdac* was performed for more than 50 brain regions of the adult murine brain with the use of autoradiographs and assessment of silver grains following exposure of radiolabeled brain sections to photoemulsion (Table 4). Signal intensities were scored from low to high (0-5) and global expression levels were calculated as the sum of regional expression values, with the rank order of expression levels listed below (Table 4).

<i>Hdac</i>	1	2	3	4	5	6	7	8	9	10	11
1	100	68	61	64	62	67	67	54	61	53	58
2		100	56	63	60	67	63	53	60	53	57
3			100	67	64	69	67	53	61	55	58
4				100	65	54	60	65	67	62	60
5					100	51	59	65	66	62	60
6						100	53	66	57	67	64
7							100	67	59	63	62
8								100	59	56	58
9									100	58	55
10										100	55
11											100

Table 3. Classical *Hdacs* show high degree of sequence homology. cDNA sequences of *Mus musculus Hdac1-11* were aligned using the freely available web program ClustalW2 to determine the degree of homology in % (<http://www.ebi.ac.uk/Tools/msa/clustalw2/>). cDNA sequences were obtained from the public data base Ensembl (<http://www.ensembl.org>). [Gene Accession Number/Ensembl transcript IDs: *Hdac1* NM_008228/ENSMUST00000102597; *Hdac2* NM_008229/ENSMUST00000019911; *Hdac3* NM_010411/ENSMUST00000043498; *Hdac4* NM_207225/ENSMUST00000008995; *Hdac5* NM_001284248/ENSMUST000000107152; *Hdac6* NM_10413/NM_ENSMUST00000115642; *Hdac7* NM_001204278/ENSMUST00000116408; *Hdac8* NM_027382/ENSMUST00000087916; *Hdac9* NM_024124/ENSMUST00000110819; *Hdac10* NM_199198/ENSMUST00000082197; *Hdac11* NM_144919/ENSMUST00000041736;]

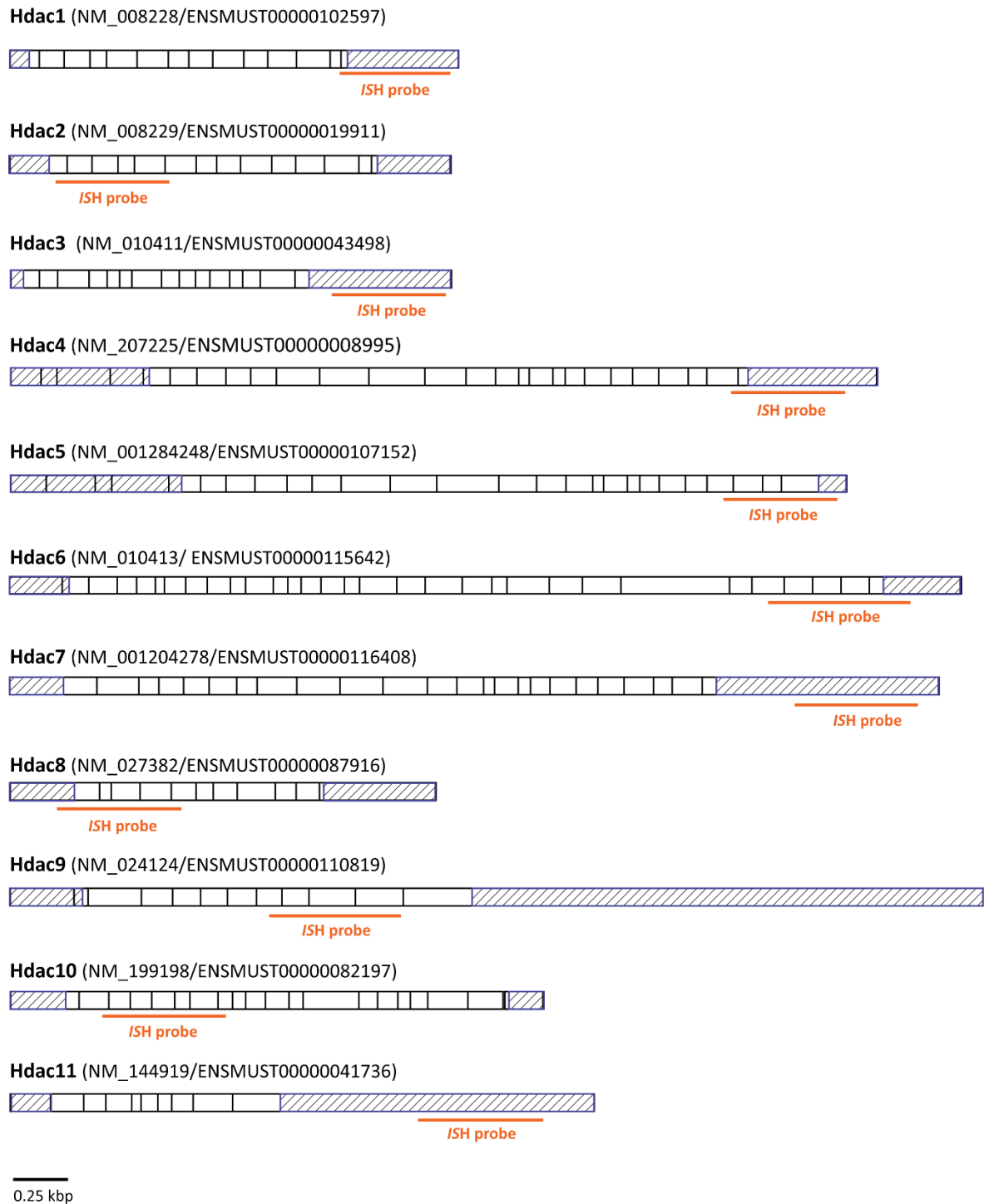


Figure 7. Localization of antisense nucleotide probes designed for ISH of *Mus musculus* Hdac1-11. Each ISH probe (depicted in orange) is highly specific for the corresponding *Hdac*. Some riboprobes were chosen to hybridize to the 3' untranslated region (UTR) as no other specific sequence of 500-650 bp in length could be found. cDNA sequences were obtained from the public data base Ensembl (<http://www.ensembl.org>). [Gene Accession Number and Ensembl Transcript IDs are depicted in parentheses; black rectangles represent exons; blue and shaded rectangles represent 5' and 3' UTRs.]

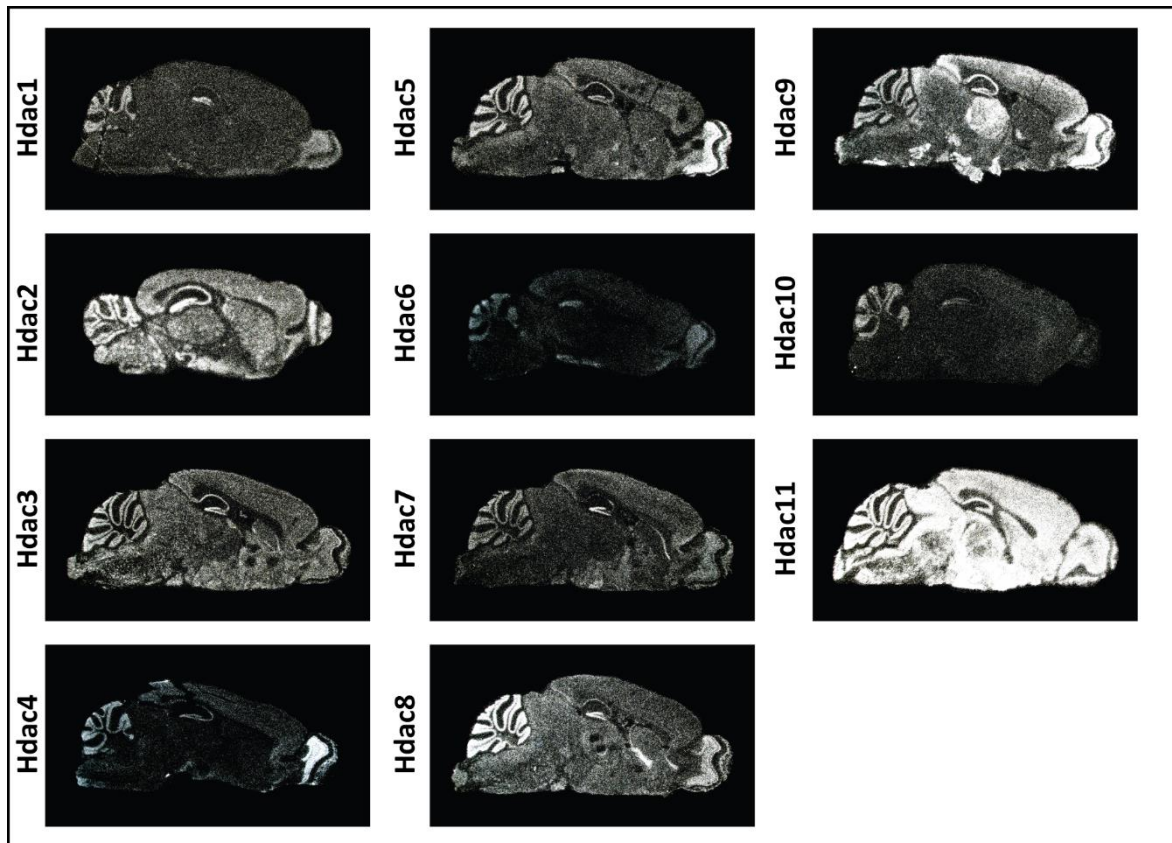


Figure 8. Distribution of *Hdac1-11* mRNA within the adult murine brain. The expression of *Hdac1-11* was analyzed by ISH using ^{35}S -labeled riboprobes highly specific for the respective *Hdac* member. Depicted are representative dark-field photomicrographs of 20 μm -thick sagittal brain sections hybridized with the indicated probe, showing the expression pattern through the whole mouse brain from the olfactory bulb to the brain stem for each classical *Hdac* member. As a control experiment brain sections were in addition hybridized with the appropriate sense probe of all used riboprobes (data not shown).

Three members of class I HDACs, *Hdac2*, *Hdac3* and *Hdac8*, are globally expressed with a moderate expression intensity throughout the adult murine brain and only one member, *Hdac1*, shows a low expression brain-wide and a distinct expression in a few brain regions. The highest expression of *Hdac1* scores a value of 2.5 and is found in the granular cell layer of the dentate gyrus (DG) and the medial habenula of the thalamus. The second highest expression (score 2.0) is present in the granular cell layers of the olfactory bulb and the cerebellum, the choroid plexus and the paraflocculus. Scores with values of 1.5 prove the expression of *Hdac1* in the glomerular layer of the olfactory bulb and the hippocampus (CA1, CA2 and CA3 pyramidal layer). However, all other analyzed brain-wide expression reaches a value of 1.0 except brain regions with no expression like the radiatum cell layer and the lacunosum moleculare of the hippocampus and the molecular layer and purkinje cell layer of the cerebellum (Figure 8 and 9, Table 4). HDAC1 and HDAC2 are known to

be arisen from a relatively recent gene duplication event and the two enzymes are found within the same multi-protein complexes, thus being often redundant in function. However, throughout the brain, *Hdac2* is definitely expressed to a higher extent within mice proposing a broader significance for this enzyme than for HDAC1 within brain processes and function. Besides its overall higher expression, *Hdac2* is specifically expressed within the granular cell layer of the olfactory bulb and the hippocampal formation (CA1, CA2 and CA3 pyramidal layer and dentate gyrus) with scores between 3 and 3.5 (Figure 8 and 9, Table 4). Medium expression of *Hdac2* (scores 2 and 2.5) were detected in the glomerular layer of the olfactory bulb, cortical structures like perirhinal cortex, visual cortex, entorhinal cortex and piriform cortex, the amygdala, the medial habenula, the hypothalamus (medial and lateral preoptic nucleus and dorsomedial nucleus) and in the granule cell layer of the cerebellum. Low expression was found in the anterior olfactory nucleus of the olfactory bulb, the dorsal tenia tecta, several cortical structures, the septum, the choroid plexus, in almost all analyzed thalamic structures, in all analyzed regions of the pons and the medulla and in the purkinje cell layer of the cerebellum.

Hdac3 ranks in the list of all eleven Hdacs as the one with the third highest expression level when considering the overall expression in the brain. Distinct areas where HDAC3 seems to fulfill important roles due to its high expression level are especially within the granular cell layer of the olfactory bulb (3.0), cortical structures (all analyzed regions score a value of 2.0-2.5), the caudate putamen (2.0), the nucleus accumbens (2.0), the globus pallidus (2.0), the septum (2.0), the hippocampal formation (CA1, CA2 and CA3 pyramidal cell layer and granular cell layer of the dentate gyrus: 2.5-3.0), parts of the pons (dorsal raphe nucleus, interpeduncular nucleus, pedunculopontine tegmental: 2.0-2.5), the cerebellum (granular cell layer: 2.5) and all parts of the medulla except the facial nucleus (Figure 8 and 9, Table 4).

Hdac3 is followed in expression intensity by the fourth member of class I HDACs, *Hdac8*, which is highly expressed especially in the glomerular layer of the olfactory bulb (3.0) and the cerebellum (granular cell layer and purkinje cell layer) reaching score values of 4. Moderate expression levels are present in brain regions like the granular cell layer of the olfactory bulb (2.0), the nucleus accumbens (2.5) the hippocampus (CA1, CA2 and CA3 pyramidal cell layer and molecular cell layer of the DG: 2.0-2.5), the medial habenula (2.0), the periventricular nucleus of the hypothalamus (2.0) and the facial nucleus of the medulla (2.0). All other analyzed brain structures show low expression of *Hdac8* except the olfactory tubercle and the molecular layer of the cerebellum where no expression was identified (Figure 8 and 9, Table 4).

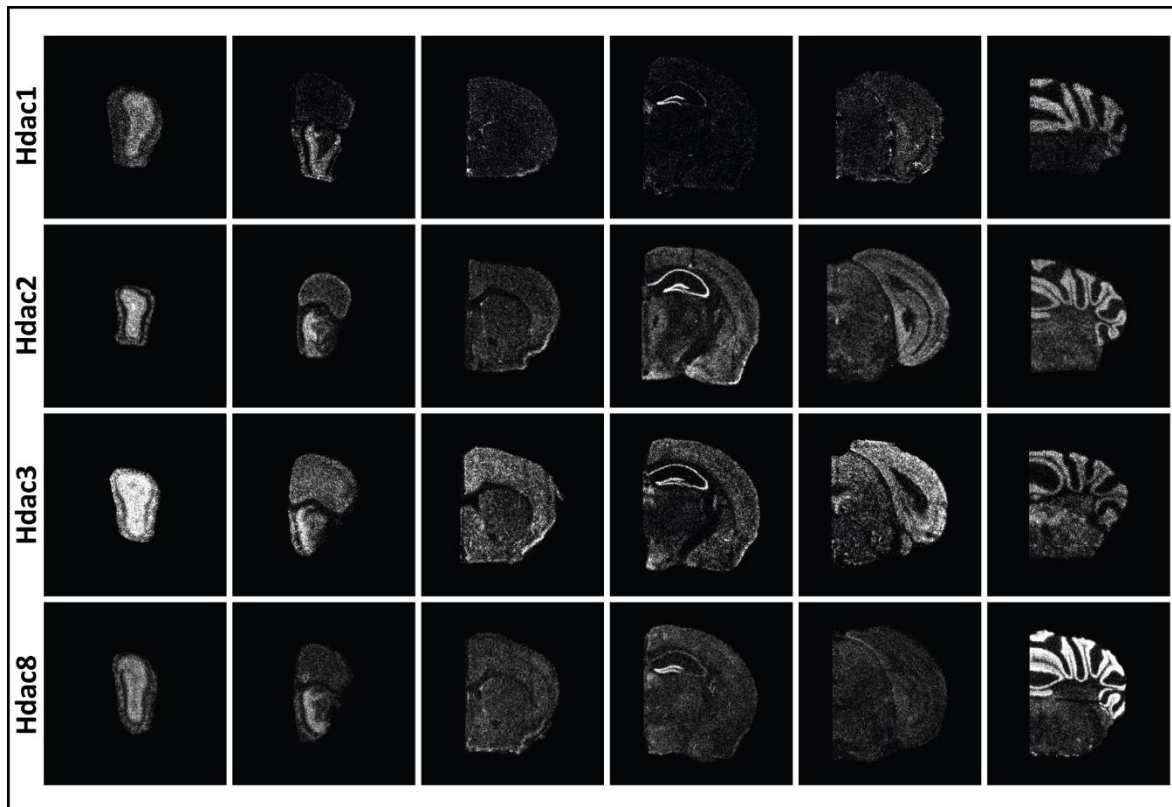


Figure 9. Detailed representation of the expression pattern of class I *Hdacs*. Qualitative ISH analysis of *Hdac1*, *Hdac2*, *Hdac3* and *Hdac8* mRNA using specific ^{35}S -labeled riboprobes. Depicted are representative dark-field photomicrographs of a series of 20 μm -thick coronal brain sections hybridized with the indicated probe. As a control experiment brain sections were in addition hybridized with the appropriate sense probe of all used riboprobes (data not shown).

Class II HDACs (*Hdac4*, *Hdac5*, *Hdac6*, *Hdac7*, *Hdac9* and *Hdac10*) include with *Hdac5* the *Hdac* isoform which ranks place two in expression intensity, but with *Hdac10* also the lowest expressed isoform (autoradiographic material with a longer incubation time was taken to enhance signal for visualization). *Hdac4*, *Hdac6* and *Hdac10* show a low expression level throughout the adult murine brain and if expression is present, it is only detectable in distinct brain areas. Thus, *Hdac4* is specifically expressed to a high level in the glomerular and granular cell layer of the olfactory bulb (3.0-4.0), whereas *Hdac6* shows its highest expression with a score value of 2.5 in the granular cell layer of the DG of the hippocampal formation. *Hdac10*'s highest expression reaches only a score of 1.5, which was found in the granular cell layer of the DG of the hippocampal formation and the granular cell layer of the cerebellum (Figure 8 and 10, Table 4).

The other class II members *Hdac5*, *Hdac7* and *Hdac9* show brain-wide a higher expression. *Hdac5* expression reaches top values of 5.0 and 4.5 in the olfactory bulb (glomerular and granular cell

layer), the medial habenula and the granular cell layer of the cerebellum. Expression levels of 3.0 were detected in all analyzed cortical structures, the hippocampal formation (CA1, CA2 and CA3 pyramidal cell layer and granular cell layer of the DG), the periaqueductal grey of the pons and the facial nucleus of the medulla. The rest of the analyzed regions show expression levels around 2.0 and 2.5 (Figure 8 and 10, Table 4).

Hdac7's highest expression is present in the granular cell layer of the DG of the hippocampus (3.5), which is followed by the expression in the glomerular and granular cell layer of the olfactory bulb (2.0), all analyzed cortical structures (2.0), the CA2 pyramidal cell layer of the hippocampus (2.0), the paraventricular nucleus of the midbrain (2.0) and the cerebellum (granular and purkinje cell layer: 2.0). All other regions show only expression levels with a score of 0.5-1.5 (Figure 8 and 10, Table 4).

Hdac9 expression levels are also of top scores with a value of 5.0 in the olfactory bulb (glomerular and granular cell layer). The moderate expression level lies between 3.0 and 3.5 and was detected in cortical structures, the hippocampus (CA1, CA2 and CA3 pyramidal cell layer), the paraventricular nucleus of the thalamus and the cerebellum (granular and purkinje cell layer). Furthermore, *Hdac9* expression with scores of 2.5 were identified in the anterior olfactory nucleus and the medial habenula. All other analyzed regions show only low expression with values of 0.5 and 1.0 (Figure 8 and 10, Table 4).

Having a closer look on the only class IV HDAC member, *Hdac11*, it is clear, that this isoform scores not only values of 5, but is also expressed in almost all analyzed brain regions. Being the highest expressed classical HDAC suggesting that it serves highly important functions within the adult murine brain. To better visualize the specific expression pattern of *Hdac11* signal intensities were decreased in the depicted photomicrographs (Figure 8 and 11, Table 4).

With these experiments we could establish an atlas of *Hdac1-11* expression throughout the adult murine brain, which shows highly specific and distinct expression patterns for each *Hdac* suggesting for each member a crucial, non-redundant role within neurological processes and brain functions. This indicates the importance to characterize each single HDAC to identify potential drug targets for the treatment of neuropsychiatric diseases without creating severe side effects through disturbances of other HDAC members.

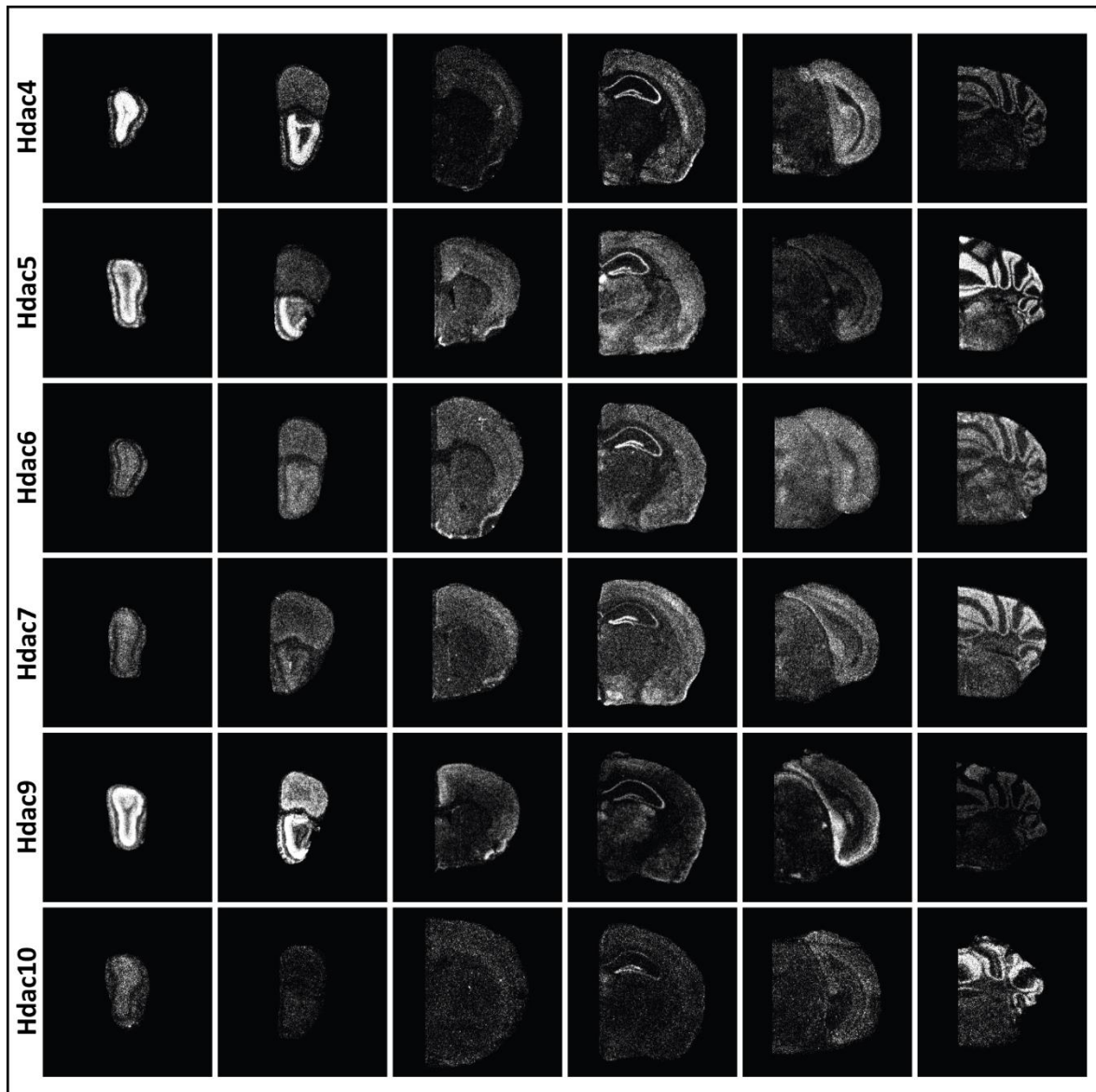


Figure 10. Detailed representation of the expression pattern of class II *Hdacs*. Qualitative *ISH* analysis of *Hdac4*, *Hdac5*, *Hdac6*, *Hdac7*, *Hdac9* and *Hdac10* mRNA using specific ^{35}S -labeled riboprobes. Depicted are representative dark-field photomicrographs of a series of 20 μm -thick coronal brain sections hybridized with the indicated probe. For *Hdac10* autoradiographic material with a longer incubation time was used to enhance the signal for visualization. As a control experiment brain sections were in addition hybridized with the appropriate sense probe of all used riboprobes (data not shown).

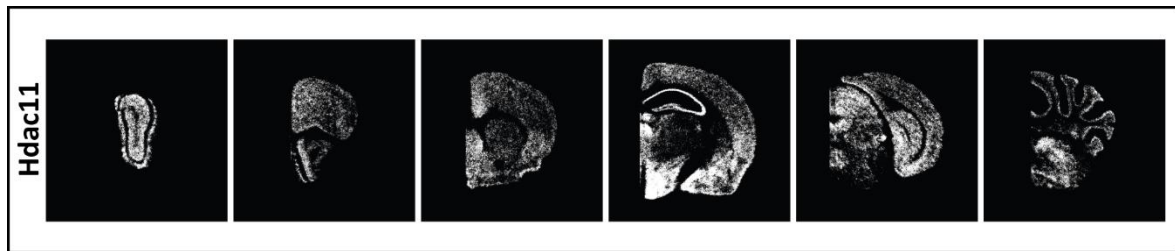


Figure 11. Detailed representation of the expression pattern of *Hdac11* as the only class IV member. Qualitative *ISH* analysis of *Hdac11* mRNA using a specific ^{35}S -labeled riboprobe. Depicted are representative dark-field photomicrographs of a series of 20 μm -thick coronal brain sections hybridized with the *Hdac11* specific probe. To better visualize the specific expression pattern of *Hdac11* signal intensities were decreased in the depicted photomicrographs. As a control experiment brain sections were in addition hybridized with the appropriate sense probe (data not shown).

brain region	Hdac1	Hdac2	Hdac3	Hdac4	Hdac5	Hdac6	Hdac7	Hdac8	Hdac9	Hdac10	Hdac11
olfactory bulb											
glomerular layer	1.5	2	2	3	4.5	1	2	3	5	1	4.5
granular cell layer	2	3	3	4	4.5	1	2	2	5	1	4.5
anterior olfactory nucleus	0	1	1.5	0.5	2.5	1	1	1.5	2.5	0	4.5
olfactory tubercle											
dorsal tenia tecta	1	0	0	0	0	1	0	0	0	0	0
dorsal tenia tecta	1	1.5	1.5	1	1.5	0	1	1.5	1	0	4.5
cortex											
frontal cortex area 3	1	1.5	2	2	3	1.5	2	1.5	3	0.5	4.5
motor cortex											
primary motor cortex	1	1.5	2	1.5	3	1.5	2	1.5	3	0.5	4.5
secondary motor cortex	1	1.5	2	1.5	3	1.5	2	1.5	3	0.5	4.5
somatosensory cortex	1	1.5	2	1.5	3	1.5	2	1.5	3	0.5	4.5
insular cortex	1	1.5	2	1.5	3	1.5	2	1.5	3	0.5	4.5
cingulate cortex	1	1.5	2	1.5	3	1.5	2	1.5	3.5	0.5	4.5
auditory cortex	1	1.5	2.5	1.5	3	1.5	2	1.5	3	0.5	4.5
perirhinal cortex	1	2	2.5	1.5	3	1.5	2	1.5	3	0.5	4.5
visual cortex	1	2	2.5	1.5	3	1.5	2	1.5	3	0.5	4.5
ectrorhinal cortex	1	2	2.5	1.5	3	1.5	2	1.5	3	0.5	4.5
piriform cortex	1	2	2.5	1.5	3	1.5	2	1.5	3	0.5	4.5
caudate putamen (=striatum)											
nucleus accumbens	1	1.5	2	0.5	2.5	0.5	0.5	1.5	0.5	0	3
nucleus accumbens	1	0	2	0.5	2	0	0.5	2.5	1	0	0
globus pallidus	1	1.5	2	0.5	2	0.5	0.5	1.5	0.5	0	2.5
BNST (bed nucleus of stria terminalis)	1	0	1.5	0.5	2	0.5	1.5	1.5	0.5	0	4.5
septum	1	1.5	2	0.5	2	1.5	1	1.5	0.5	0	4.5
amygdala	1	2	1.5	0.5	2	1.5	0.5	1.5	0.5	0	3
hippocampus											
CA1 pyramidal layer	1.5	3.5	2.5	2	3	1.5	1.5	2	3.5	1	5
CA2 pyramidal layer	1.5	3.5	2.5	2	3	1.5	2	2	3.5	1	5
CA3 pyramidal layer	1.5	3.5	2.5	2.5	3	1.5	1.5	2	3.5	1	5
radiatum cell layer	0	0	0	0	0.5	0	0.5	1	0.5	0	0
lacunosum moleculare	0	0	0	0	0.5	0	0.5	1	0.5	0	0
DG granular layer	2.5	3.5	3	2	3	2.5	3.5	2.5	3	1.5	5
DG molecular layer	0	0	0	0	0.5	0	0.5	1	0	0	0
choroid plexus	2	1.5	2	1	1	0.5	1	1.5	0	0	3
thalamus/midbrain											
medial habenula	2.5	2.5	2	1.5	4.5	1.5	0.5	2	2.5	1	5
paraventricular nucleus	1	1	2	0.5	2.5	1.5	2	1.5	3.5	0	4
central medial thalamic nucleus	1	1.5	1.5	0.5	2.5	0.5	1	1.5	0.5	0	4
ventral tegmental area	1	1	0	0.5	2	0.5	0	1.5	0.5	0	0
substantia nigra-compacta	1	1	0	0.5	0	1	0.5	1.5	0.5	0	3
hypothalamus											
medial preoptic nucleus	1	2	2	0.5	2	0.5	1.5	1.5	0.5	0	4.5
lateral preoptic nucleus	1	2	2	0.5	2	0.5	1	1.5	0.5	0	4.5
paraventricular nucleus	1	1	2	0.5	2	0.5	1.5	1.5	0.5	0	1
periventricular nucleus	1	0	2	0.5	2	0.5	0	2	0.5	0	4.5
dorsomedial nucleus	1	2	2	1	2.5	1.5	1	1.5	0.5	0	5
ventromedial hyp. nucleus	1	1.5	2	0.5	2	0.5	1	1.5	0.5	0	4.5
zona incerta	1	1	2	0.5	2.5	0.5	0.5	1.5	0.5	0	3
pons											
pontine nucleus	1	1	0	1.5	2	0.5	1	0.5	0.5	0	1
dorsal raphe nucleus	1	1	2.5	0.5	2	0.5	2	2	0.5	0	4
interpeduncular nucleus	1	1	2	0.5	2	1	1	1.5	0	0	2
pedunculopontine tegmental	1	1	2	0.5	2	0.5	1	1.5	0.5	0	2.5
periaqueductal grey	1	1	1.5	0.5	3	0.5	1	1.5	0.5	0	4
superior cerebellar peduncle	1	1	0	0.5	2	0.5	0.5	1.5	0.5	0	3
cerebellum											
granule cell layer	2	2.5	2.5	1	5	1	2	4	3	1.5	3
molecular layer	0	0	0	0.5	0	0	0.5	0	0.5	0	0
purkinje cell layer	0	2	0	1	0	1	2	4	3.5	0	4
paraflocculus	2	-	-	-	-	-	-	-	-	-	-
medulla											
principal sensory trigeminal nucl	1	1	2.5	0.5	2	0.5	0.5	1.5	0.5	0	2
reticular nuclei	-	-	2	0.5	2	0.5	0.5	1	1	0	3.5
locus coeruleus	1	1	2.5	0.5	2	1	0.5	1.5	0.5	0	0
solitary nucleus	-	-	2	0.5	2	0.5	0.5	1	0.5	0	3.5
facial nucleus	1	1	0	0.5	3	0.5	0.5	2	0.5	-	3
SUM	58	78	95	54.5	128.5	50.5	67.5	90	88.5	14.5	186.5
RANK ORDER	8	6	3	9	2	10	7	4	5	11	1

Table 4. Determination of expression levels of *Hdac1-11* within the adult murine brain. Semi-quantitative expression analysis was conducted throughout more than 50 brain regions using 20 μm -thick coronal and sagittal brain sections hybridized with ^{35}S -labeled antisense riboprobes against *Hdac1-11* mRNA and exposed to autoradiographic photo emulsion. Expression intensity was scored from low to high (0-5). For expression levels which were not uniform within the indicated brain region, the intensity depicted corresponds to an estimated overall mean in this region.

4.2 Establishing the oral application of tamoxifen via chow to activate the Cre/loxP system in conditional transgenic mouse models

The Cre/loxP system is the most frequently used tool for spatio-temporal overexpression or inactivation of genes by-passing embryonic and postnatal lethality. In order to achieve a tight temporal control, the recombinase Cre has been fused to a mutated estrogen receptor (ER) ligand-binding domain which is insensitive to endogenous estrogen, but sensitive to tamoxifen. In the absence of tamoxifen, the fusion protein is retained in the cytoplasm through binding of the ER ligand-binding domain to the heat-shock protein 90 (HSP90) complex (Figure 12) (Feil, Wagner, Metzger, & Chambon, 1997). Upon tamoxifen binding to the ER ligand binding domain, the fusion protein is released from the complex and translocates due to the nuclear localization signal (NLS) artificially fused to Cre into the nucleus, where Cre-mediated recombination between loxP sites takes place. To obtain spatial control of gene overexpression or deletion, Cre expression can additionally be regulated by a specific promoter.

At the beginning of the thesis, there was no stress-free method for tamoxifen administration in mice available. In rodents, the most frequently used chemical form of tamoxifen is 4-hydroxytamoxifen (4-OHT), dissolved in alcohol and/or oil, administered usually by repeated intraperitoneal (i.p.) injections, supplied by gavaging or via the drinking water. However, i.p. injections and gavaging impose considerable stress on mice, whereas administration via drinking water is hampered by poor solubility (0.5 mg/ml at 37°C). Thus, feeding the animals with tamoxifen enriched chow would be an elegant way to reduce handling distress on mice, effort and costs. There are studies which describe the use of tamoxifen enriched chow, but high 4-OHT doses (2.5 mg/g) are needed meaning that mice consume up to 20% of the acute lethal dose. Even there are no severe side-effects described so far, the administration via 4-OHT chow is limited by poor acceptance in mice due to the bitter taste of the food pellets (Agger, Santoni-Rugiu, Holmberg, Karlström, & Helin, 2005; Brocard et al., 1997; Casanova et al., 2002; Forde, Constien, Gröne, Hämmerling, & Arnold, 2002; Indra et al., 2005; Kostetskii et al., 2005; Leone et al., 2003; M. Li et al., 2000; Metzger & Chambon, 2001; Mijimolle et al., 2005; Moosmang et al., 2003; Petrich, Molkentin, & Wang, 2003; Sohal et al., 2001; Xiao et al., 2001; Yu, Dews, Park, Tobias, & Thomas-Tikhonenko, 2005).

Kiermayer and colleagues described the use of soy-free chow containing another chemical form of tamoxifen (tamoxifen citrate salt (TCS)) produced by LASvendi (Soest, Germany) (Kiermayer,

Conrad, Schneider, Schmidt, & Brielmeier, 2007). In this chow, the tamoxifen dose can be kept at a minimum level of 400 mg/kg due to the use of TCS and the absence of the tamoxifen antagonist soy genistein which can be found in high concentrations in conventional chow. Thus, the total tamoxifen uptake can be minimized and the chow is more accepted by the rodents as the bitter taste is kept within a limit compared to high concentration 4-OHT soy-rich chow.

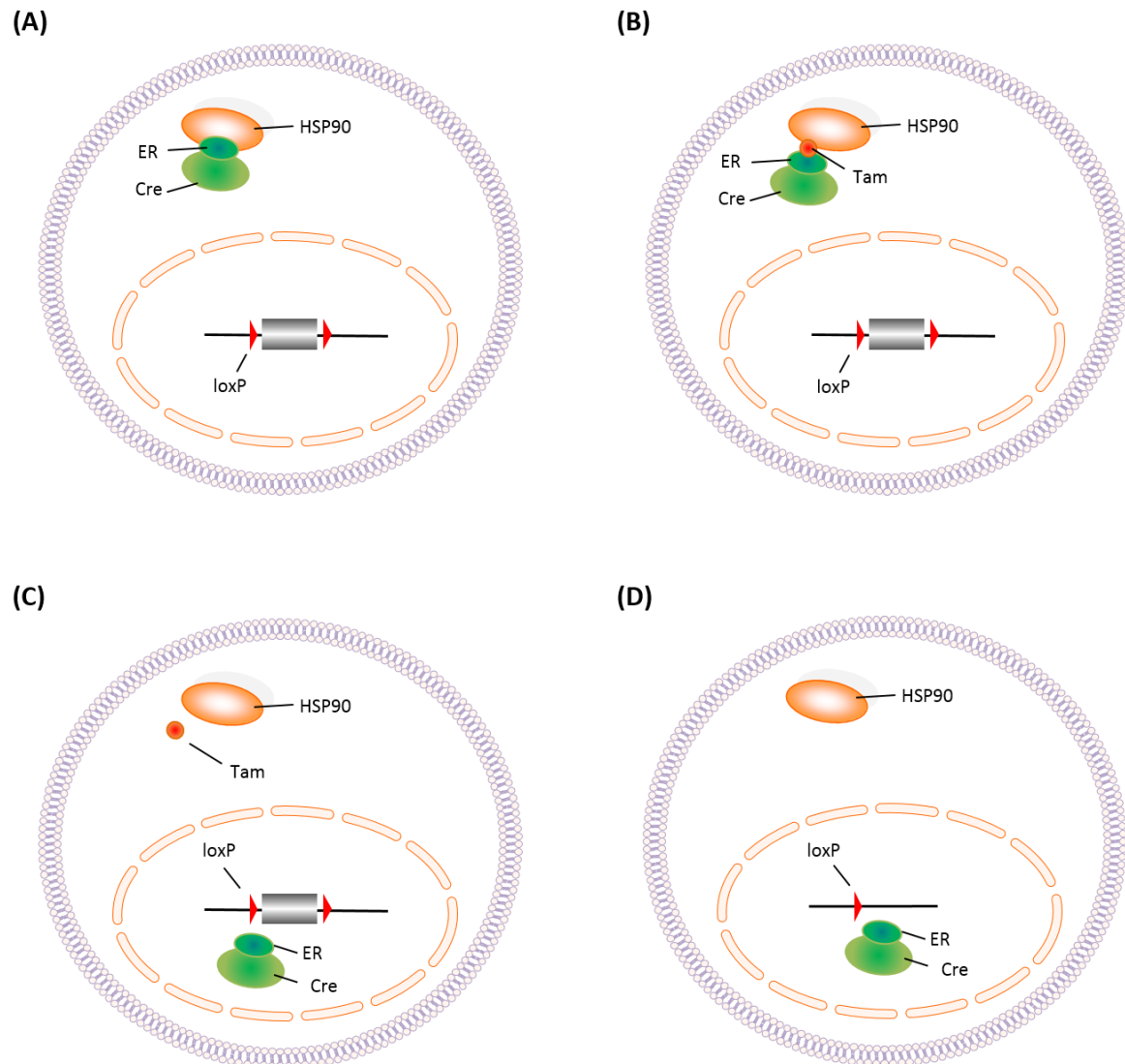


Figure 12. Activation of the Cre/loxP system using tamoxifen administration. (A) Cre recombinase fused to a mutant estrogen receptor ligand-binding domain (ER) associates within the cell with the heat-shock protein 90 (HSP90) and the complex is retained within the cytoplasm. (B) Tamoxifen (Tam) interrupts the complex and leads to free Cre-ER. (C) When Cre-ER is not bound to HSP90 anymore, it immediately translocates due to a nuclear localization signal (NLS) to the cell nucleus. (D) Cre-ER causes recombination between loxP sites, e.g. deletion of loxP-flanked DNA sequences.

The TCS enriched soy-free chow was shown to be effective in a heart-specific inactivation of thioredoxin reductase 2 (Kiermayer et al., 2007). To extend the use of the described TCS chow to brain-specific gene overexpression or disruption, we addressed the question, if the tamoxifen administered via the described TCS food pellets will result in efficient CreER^{T2}- mediated recombination within the central nervous system (CNS).

4.2.1 Oral tamoxifen administration via food pellets in CRH overexpressing mice

To establish the oral application of tamoxifen via TCS chow to activate the Cre/loxP system within the CNS, we used the conditional transgenic mouse line CRH-COE^{IFB} (corticotropin-releasing hormone conditional overexpression inducible forebrain) which was previously developed in our lab (Figure 13) (Erdmann et al., 2007; A. Lu et al., 2008; Refojo et al., 2011). Therefore, the conditional *Crh* overexpressing mouse line (CRH-COE) which combines a knockin of a single copy of the murine *Crh* cDNA into the *ROSA26* locus with the Cre/loxP system, was bred to the Camk2a-CreER^{T2} (calcium/calmodulin-dependent protein kinase type 2 alpha chain promoter driven Cre fused to estrogen receptor ligand binding domain type 2) mouse line (Refojo et al., 2011). To allow a spatio-temporal control of *Crh* overexpression, a Stop cassette flanked by loxP sites (parallel orientation) was introduced upstream of the *Crh* sequence. Upon CreER^{T2}-mediated recombination in CRH-COE^{IFB} animals, *Crh* will be specifically expressed in principle forebrain neurons. Furthermore, the *Crh* sequence is followed by an *IRES-lacZ* reporter gene, which can be detected by *ISH* analysis to monitor induction of Cre activity. The Cre mouse line is described in more detail in chapters 4.3. and 4.4.

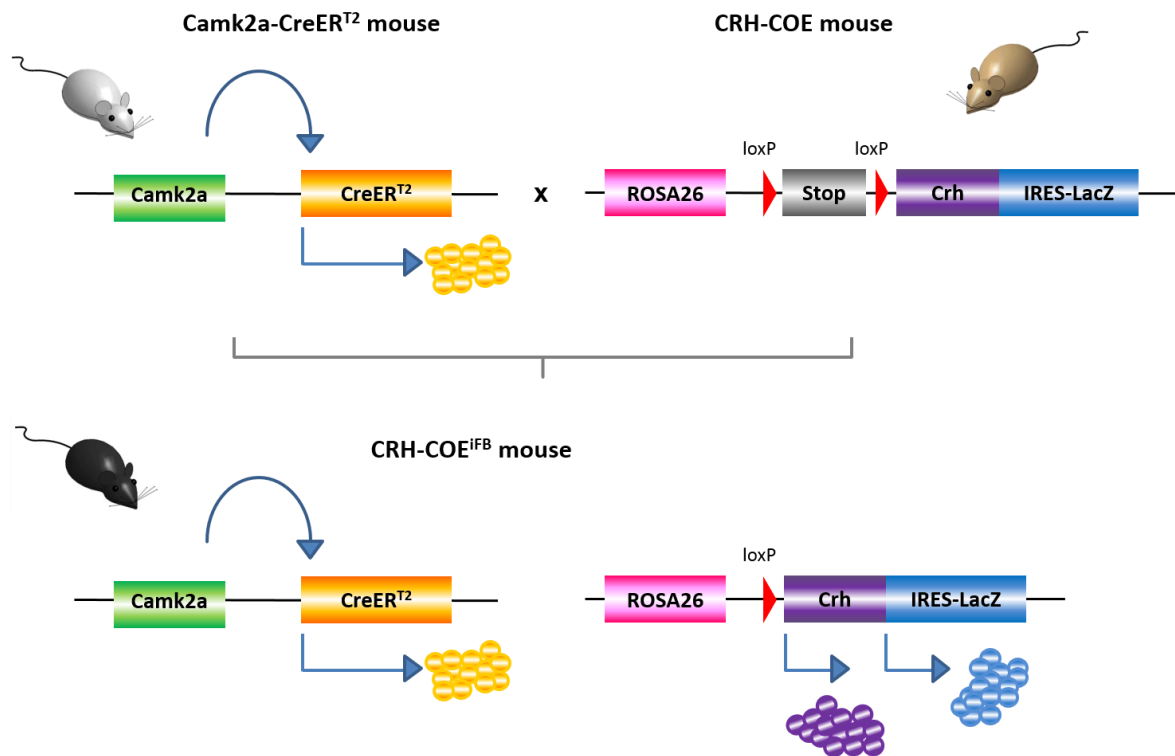


Figure 13: Description of the CRH-COE^{iFB} mouse line. The mouse line was generated by breeding Camk2a-CreER^{T2} mice to the CRH-COE mouse line. The Camk2a-CreER^{T2} mouse is expressing the CreER^{T2} fusion protein under the control of the regulatory elements of the mouse Camk2a gene. The CRH-COE mouse line harbors a knock-in of *Crh* followed by *IRES-lacZ* in the *ROSA26* locus. A floxed stop cassette preceding the *Crh* cDNA prohibits *Crh* and *lacZ* overexpression prior to Cre-mediated recombination. Within the CRH-COE^{iFB} mice, the overexpression is induced by Cre-mediated excision of the Stop cassette.

4.2.1.1 Tamoxifen administration via food pellets results in efficient CreER^{T2}-mediated recombination in the CNS

In a first approach we divided male animals of the line CRH-COE^{iFB} in eight groups differing in the time fed with TCS chow (Table 5). Each group consisted of four littermates, two overexpressing mice CRH-COE^{iFB} (homozygous for *Crh* knock-in, hemizygous for Camk2a-CreER^{T2}) and two control mice CRH-COE^{CTRL} (homozygous for *Crh* knock-in, no Camk2a-CreER^{T2}). Animals were sacrificed immediately after tamoxifen treatment.

group	tamoxifen administration
1	4 days
2	8 days
3	12 days
4	16 days
5	20 days
6	4 weeks
7	5 weeks
control	no tamoxifen

Table 5: First approach of tamoxifen administration via food pellets. Animals of the CRH overexpressing mouse line were grouped differing in the duration of tamoxifen treatment. Each group consisted of two overexpressing CRH-COE^{iFB} and two control CRH-COE^{CTRL} male mice. Animals were fed with TCS chow for the indicated period of time.

For determination of the efficacy of tamoxifen applied to mice by oral administration, the mRNA expression of *lacZ* was analyzed using *in situ* hybridization (ISH) on brain sections. A radiolabeled *lacZ* riboprobe was used for indirect determination of the *Crh* overexpression as the *lacZ* gene as well as the transgenic *Crh* gene are only transcribed upon successful deletion of the Stop cassette by CreER^{T2}. CRH-COE^{iFB} mice of all groups except the control group (no tamoxifen) displayed high *lacZ* mRNA expression within the dentate gyrus, CA1 region, CA2 region and CA3 region of the hippocampus as well as in the cortex without showing a hemispheric difference (Figure 14). Thus, the tamoxifen administered by TCS chow crossed the blood-brain barrier and activated Cre-mediated overexpression of *Crh* and *lacZ* already within 4 days of tamoxifen treatment. Animals of the control group displayed only a background signal indicating inactive CreER^{T2} as no tamoxifen was applied. No *lacZ* signal was detected in CRH-COE^{CTRL} mice lacking CreER^{T2} (data not shown).

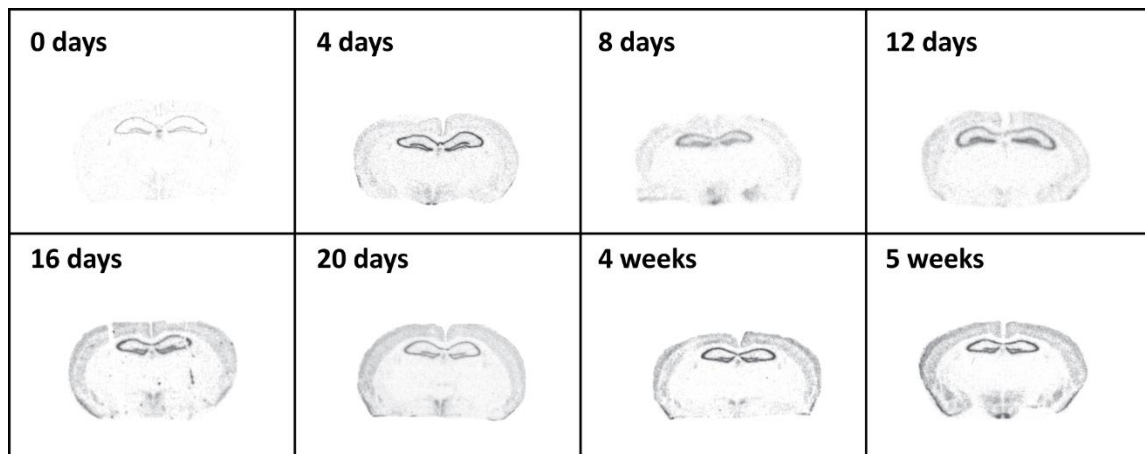


Figure 14. Analysis of *lacZ* expression upon tamoxifen treatment (first approach). Expression of *lacZ* is demonstrated by *in situ* hybridization (*ISH*) using a *lacZ*-specific radiolabeled riboprobe detecting transgenic *lacZ* mRNA expression. Depicted are representative bright-field photomicrographs of autoradiographs of 20 μm -thick coronal brain sections CRH-COE^{IFB} mice which were fed with TCS chow for the indicated periods of time. All animals except the control (0 days) display high *lacZ* mRNA expression within the dentate gyrus, CA1 region, CA2 region and CA3 region of the hippocampus as well as in the cortex, being characteristic for CreER^{T2} expression under the control of the Camk2a promoter.

group	tamoxifen administration	tamoxifen wash-out
1A	2 days	7 days
1B	2 days	-
2A	4 days	7 days
2B	4 days	-
3A	6 days	7 days
3B	6 days	-
4A	8 days	7 days
4B	8 days	-
control	no tamoxifen	15 days

Table 6: Second approach of tamoxifen administration via food pellets. Animals of the CRH-overexpressing mouse line were grouped differing in the duration of tamoxifen treatment and tamoxifen wash-out time with standard diet. Each group consisted of four overexpressing CRH-COE^{IFB} and four control CRH-COE^{CTRL} male mice. Animals were fed with TCS chow and/or standard diet (tamoxifen wash-out) for the indicated period of time.

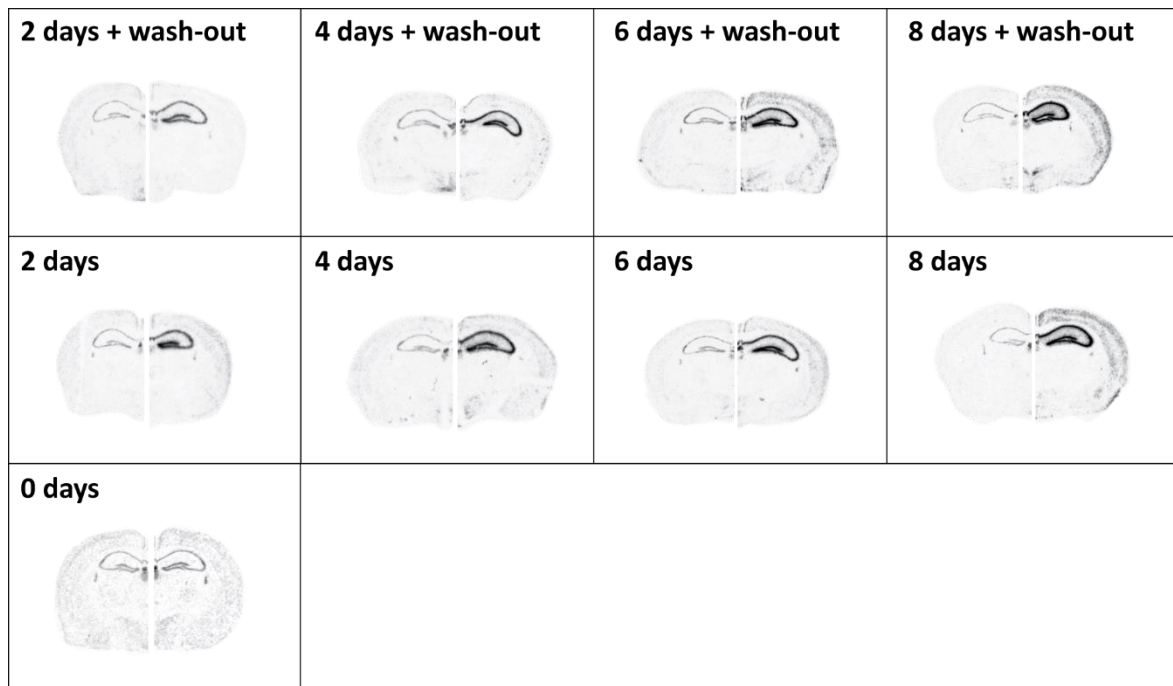


Figure 15. Analysis of *lacZ* expression upon tamoxifen treatment (second approach). Expression of *lacZ* is demonstrated by *in situ* hybridization (*ISH*) using a *lacZ*-specific radiolabeled riboprobe detecting transgenic *lacZ* mRNA expression. Depicted are representative bright-field photomicrographs of autoradiographs of 20 μm -thick coronal brain sections of the hippocampus and cortex of overexpressing CRH-COE^{iFB} (half brain slice on right side) and control CRH-COE^{CTRL} (half brain slice on left side) mice for each group. Groups were fed with TCS chow for indicated periods of time. Mice of several groups (upper row) were exposed to an additional wash-out time of seven days by using standard diet. Animals of the other groups (second row) were sacrificed immediately after TCS chow treatment. The lower row displays the control group with standard diet only. All CRH-COE^{iFB} animals except the control (0 days TCS chow) display high *lacZ* mRNA expression within the dentate gyrus, CA1 region, CA2 region and CA3 region of the hippocampus. Animals with longer TCS chow treatment also show *lacZ* expression within the cortex.

According to these results, we performed a second screening experiment, narrowing down the time window of TCS chow treatment to gain more insights into the temporal control of CreER^{T2} activity. Thus, we divided mice of the line CRH-COE^{iFB} in nine groups, each consisting of four overexpressing CRH-COE^{iFB} and four control CRH-COE^{CTRL} animals. The groups differed in time exposed to TCS chow with/without a seven-day wash-out phase by using standard diet (Table 6).

To verify that even these short-term tamoxifen administrations are able to induce CreER^{T2}-mediated *Crh* overexpression in CRH-COE^{iFB} mice, we analyzed the *lacZ* expression by *ISH* on brain sections using the same radiolabeled *lacZ*-specific riboprobe as described in the first approach. Overexpressing CRH-COE^{iFB} mice of all tested groups displayed a distinct *lacZ* expression within the dentate gyrus, CA1 region, CA2 region and CA3 region of the hippocampus, which is increasing with

the treatment time (Figure 15). Hence, two days of tamoxifen administration (with/without wash-out time) already caused CreER^{T2}-mediated recombination. However, broader expression covering also the cortex was only detected in animals treated for six and eight days with tamoxifen (with/without wash-out time) suggesting that it is possible to induce with short tamoxifen administration (2-4 days) a hippocampus-specific recombination. Control CRH-COE^{CTRL} mice presented for all groups only a background signal (probably due to unspecific binding of the riboprobe) which was also observed in mice of the control group with 0 days tamoxifen treatment, but 15 days standard diet.

4.2.1.2 Tamoxifen administration via food pellets changes feeding behavior of CRH overexpressing mice

Due to tamoxifen enrichment the TCS chow displays a characteristic bitter taste, which might cause problems in feeding behavior of adult mice habituated to standard diet. For that reason we studied in the previously described more detailed second approach also the food intake and water consumption of mice treated with TCS chow.

All tested animals displayed a food intake of $20 \pm 10\%$ of their own body weight within 24 hours regardless of the offered chow meaning that all mice accept the TCS chow in general without having severe problems in feeding (Figure 16). Looking closer at the feeding data, we detected within this $20 \pm 10\%$ range a difference between TCS chow and standard diet. Mice realized that they were exposed to a different kind of food pellets and consumed less chow during tamoxifen treatment (Figure 16.A) (2 days Tam: Repeated-measures ANOVA, post-hoc test, ## $p < 0.01$; 8 days Tam: Repeated-measures ANOVA, post-hoc test, ### $p < 0.01$). Animals transferred back to standard diet after TCS chow (with wash-out time) exhibited all a peak in food intake within the first 24 hours after pellet exchange coming then back to a slightly higher mean value compared to the TCS treatment suggesting that the mice preferred standard diet. However, also the control group (no tamoxifen) shows changes in food intake probably due to the weekly cage change for hygienic reasons.

Since tamoxifen treatment causes *Crh* overexpression in half of all analyzed animals (CRH-COE^{iFB}), we wanted to make sure, that there is no genotype-specific effect in feeding behavior. Thus, we analyzed the data in more detail in dependence of the animals' genotype (Figure 17). We could not observe any differences in food intake between the overexpressing CRH-COE^{iFB} and control CRH-

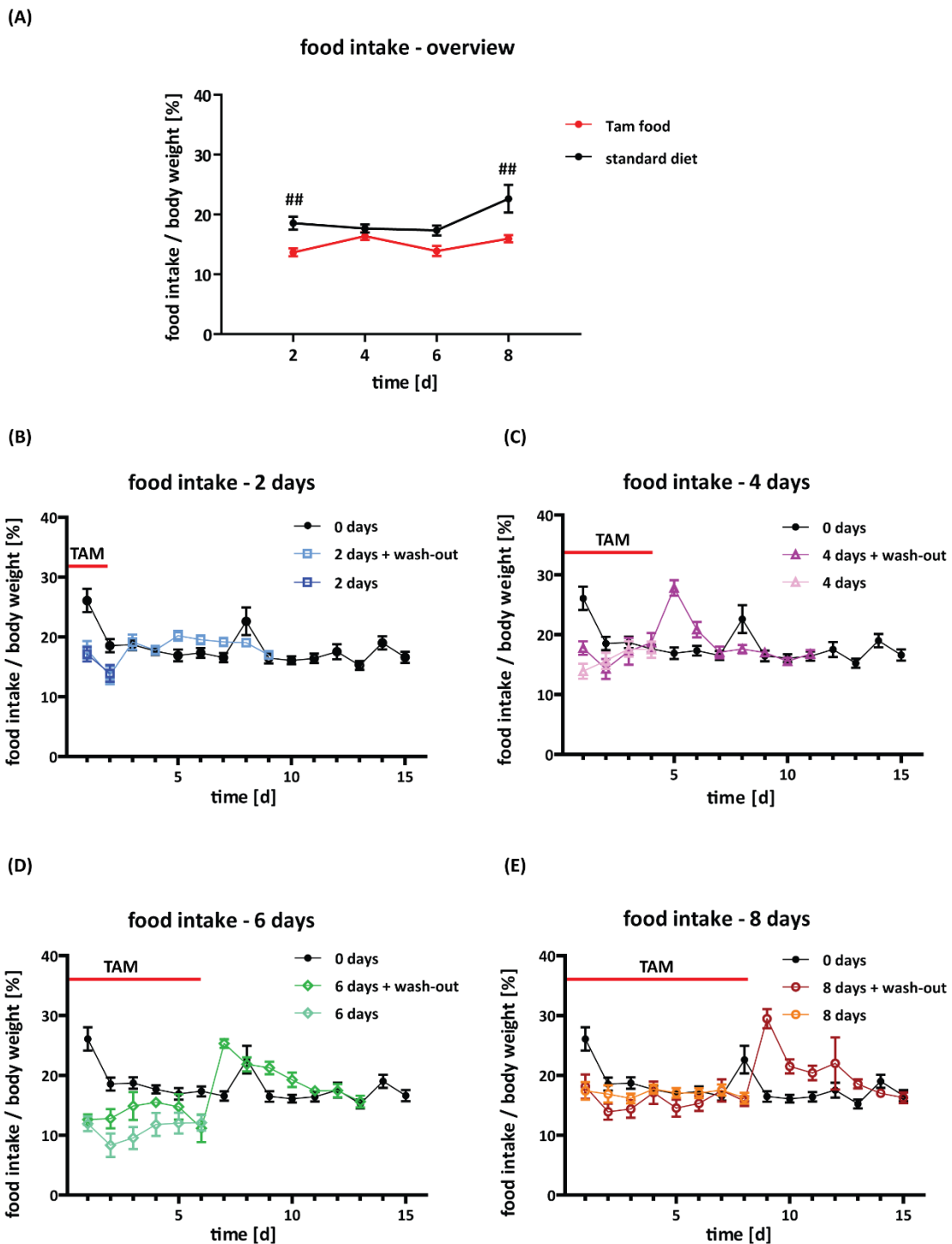
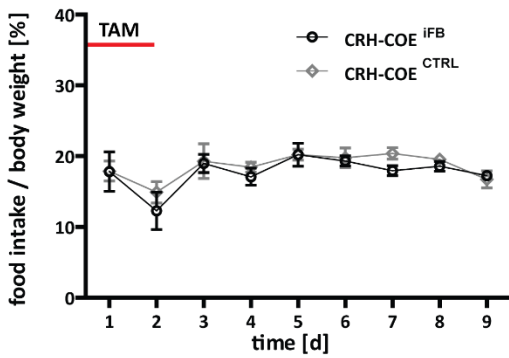


Figure 16. Determination of food intake of CRH-COE^{IFB} mice treated with TCS chow. The food intake is presented in % of the body weight (taken before treatment start) over the time. (A) An accumulative description and overview of all groups, which are represented in detail in B-E. All animals accept the TCS chow, but consume significantly less food at day 2 and day 8 when compared to the feeding behavior of animals treated with standard diet. (B-E) Mice of all groups show a slightly decreased food intake when fed with TCS and a sudden increase when TCS chow is exchanged by standard diet. | Data are presented as mean \pm SEM; n = 8-64; ## p < 0.01, Repeated-measures ANOVA, post-hoc test; Tam = tamoxifen.

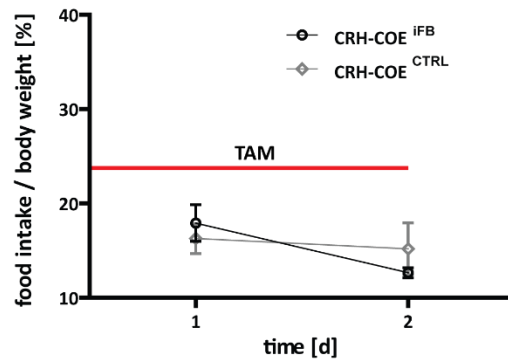
(A)

food intake - 2 days + wash-out



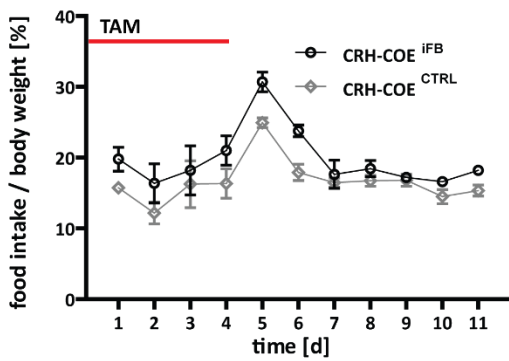
(B)

food intake - 2 days



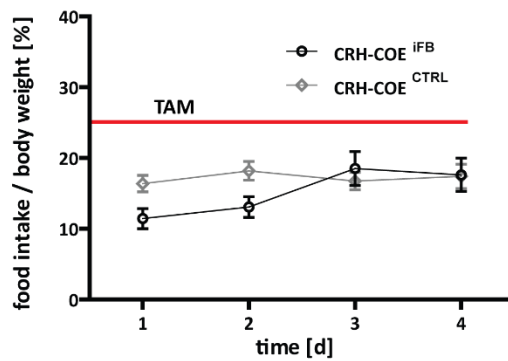
(C)

food intake - 4 days + wash-out



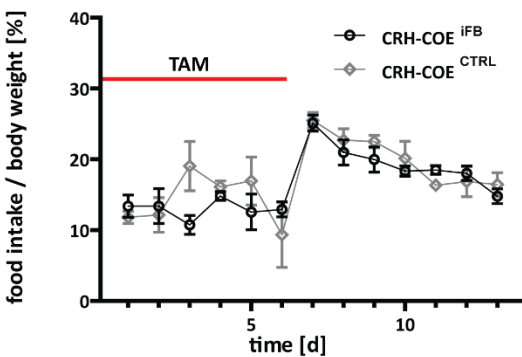
(D)

food intake - 4 days



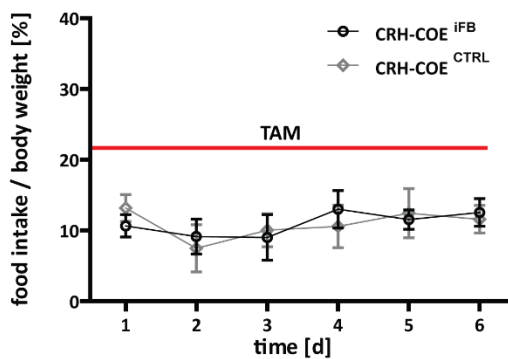
(E)

food intake - 6 days + wash-out



(F)

food intake - 6 days



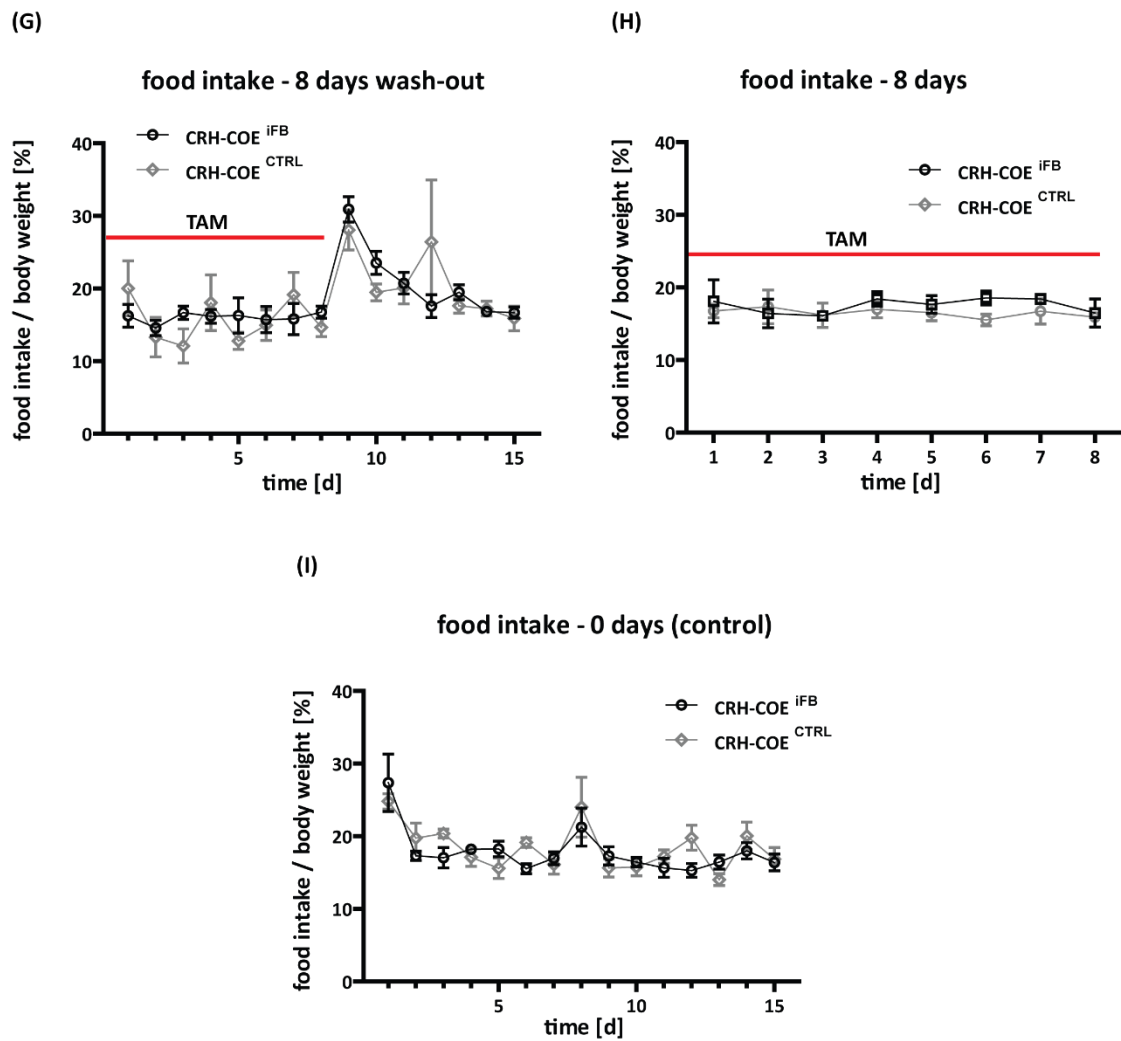


Figure 17. Excluding effects of CRH overexpression on food intake. The food intake is presented as percent of the body weight (taken before treatment start) over the time. *Crh* overexpressing (CRH-COE^{iFB}) mice display the same characteristics in food intake as their control (CRH-COE^{CTRL}) littermates. (A,C,E,G) Mice of groups with a seven day wash-out time by standard diet. Animals of both genotypes present in each group a specific peak when TCS chow is exchanged by standard diet. (B,D,F,H) Mice of groups without wash-out time but sacrificed immediately after TCS chow treatment do also not present any genotype effect. (I) Animals of control group. | Data are presented as mean \pm SEM; n (CRH-COE^{iFB}) = 4; n (CRH-COE^{CTRL}) = 4; Repeated-measures ANOVA.

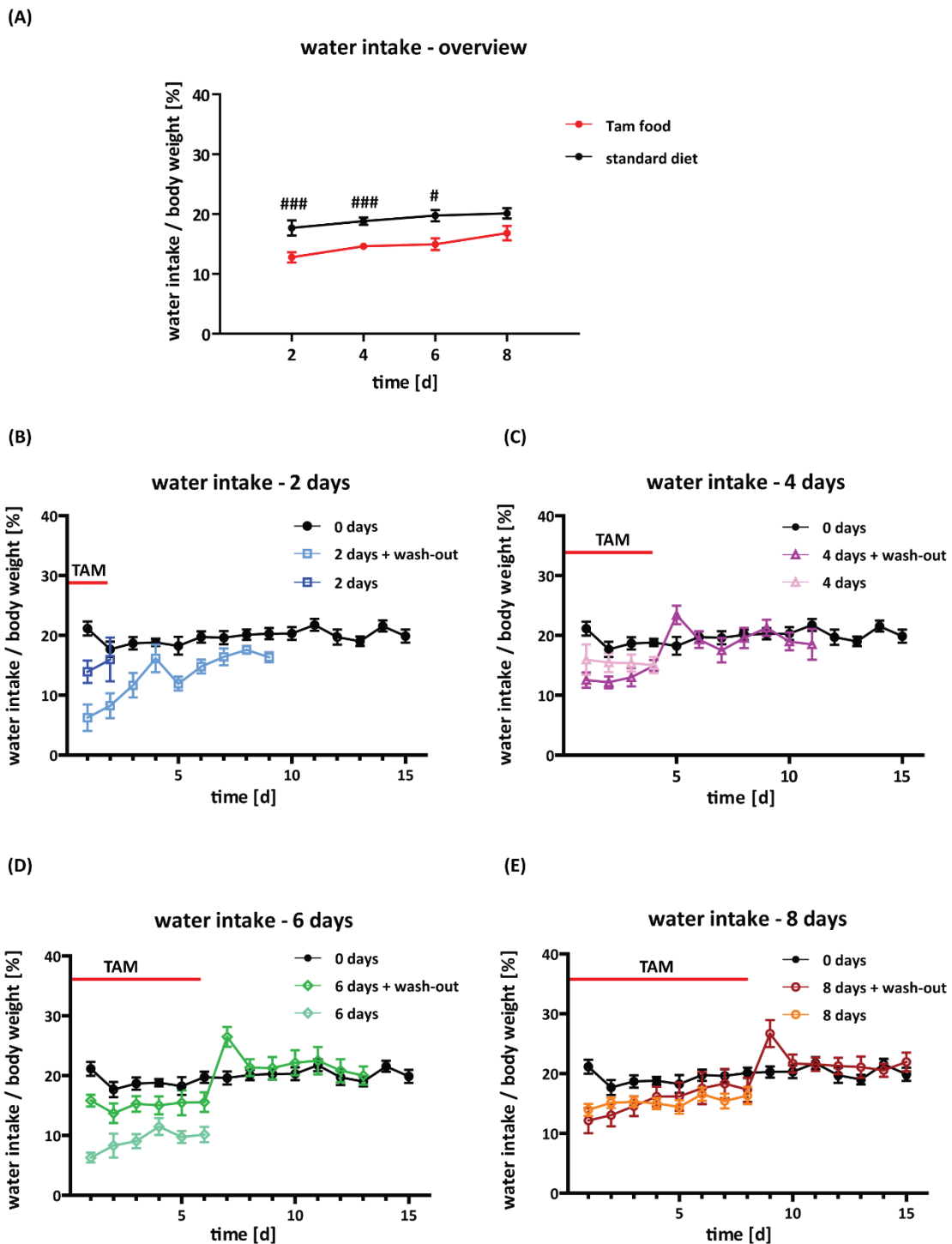
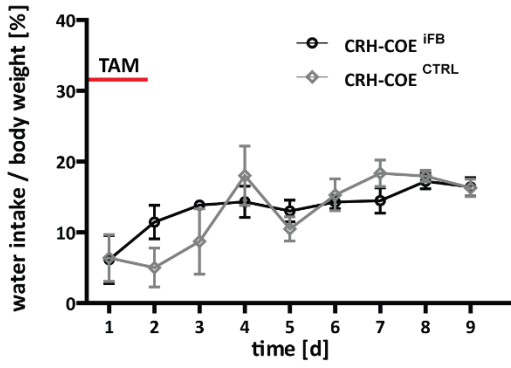


Figure 18. Determination of water intake of CRH-COE^{IFB} mice treated with TCS chow. The water intake is presented as percent of the body weight (taken before treatment start) over the time. (A) An accumulative description and overview of all groups, which are represented in detail in B-E. Animals fed with TCS chow consume significantly less water at day 2, 4 and 6 days of TCS chow treatment when compared to animals treated with standard diet. (B-E) Mice show a sudden increase in water intake when TCS chow is exchanged by standard diet. | Data are presented as mean \pm SEM; $n = 8-64$; # $p < 0.05$, ### $p < 0.001$, Repeated-measures ANOVA, post-hoc test; Tam = tamoxifen.

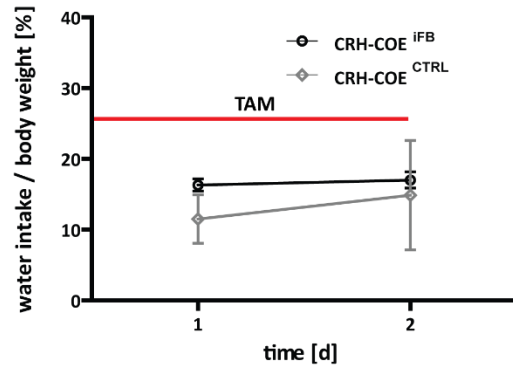
(A)

water intake - 2 days + wash-out



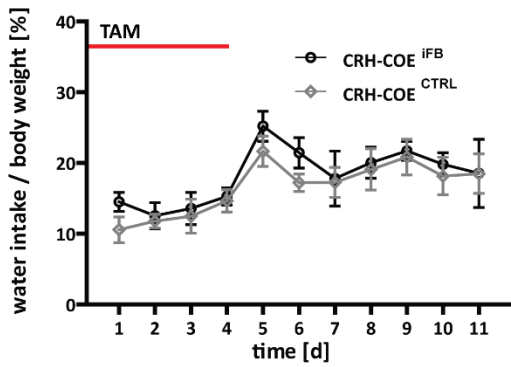
(B)

water intake - 2 days



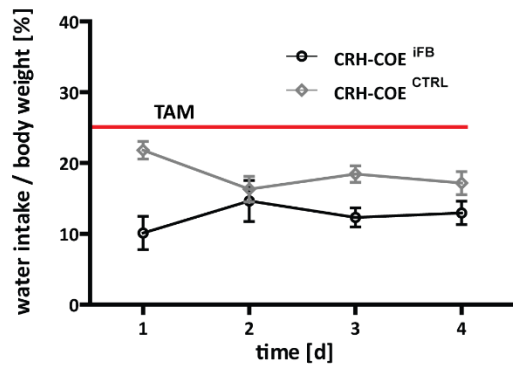
(C)

water intake - 4 days + wash-out



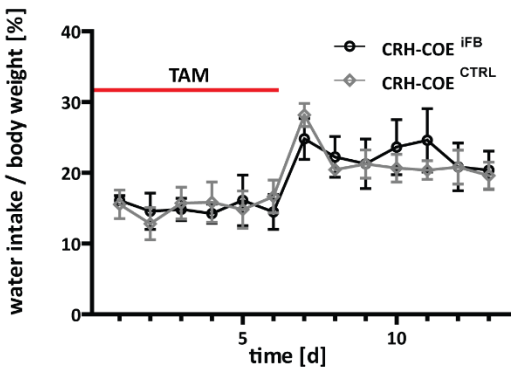
(D)

water intake - 4 days



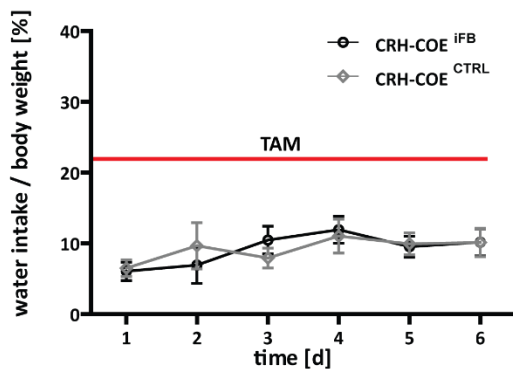
(E)

water intake - 6 days + wash-out



(F)

water intake - 6 days



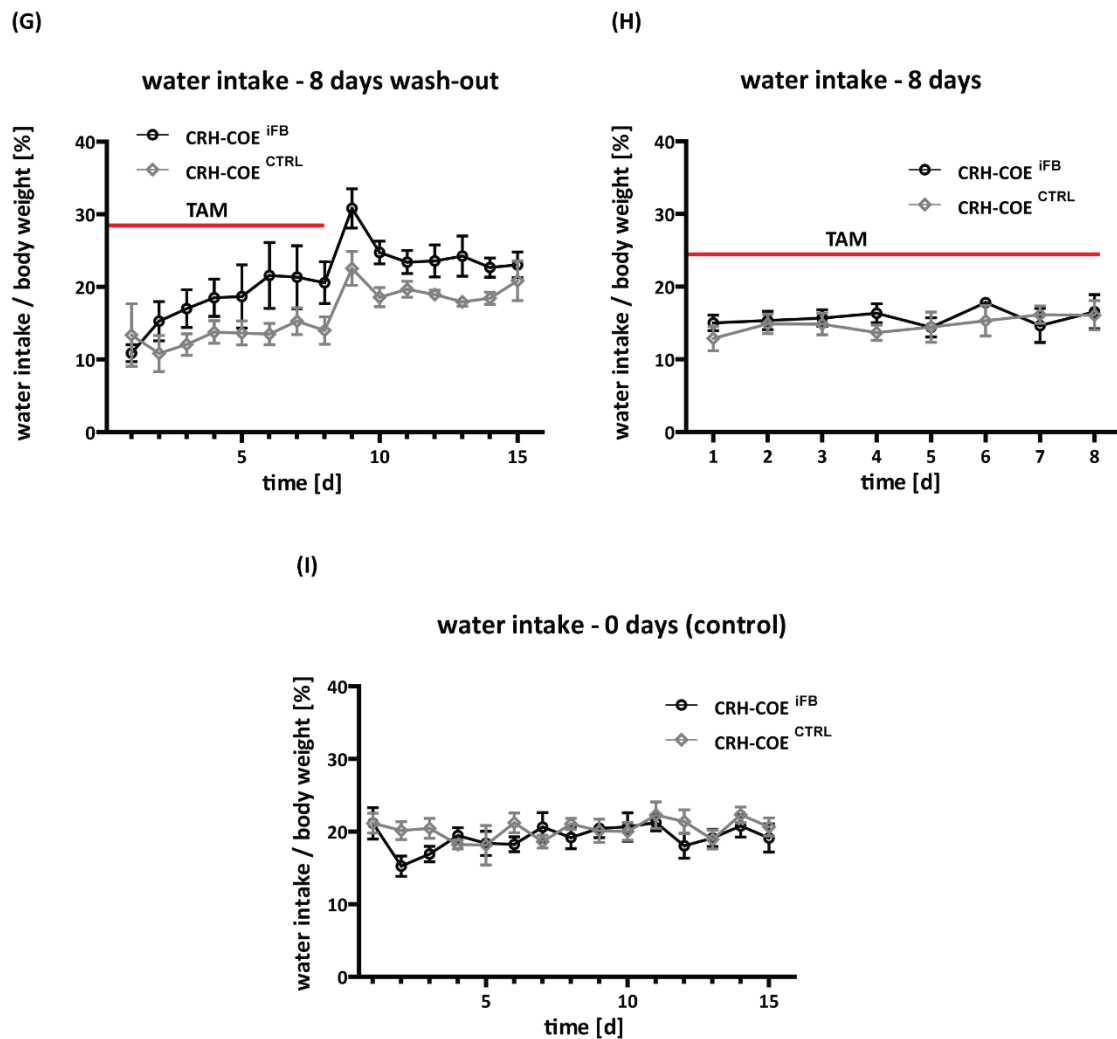


Figure 19. Excluding effects of CRH overexpression on water intake. The water intake is presented as percent of the body weight (taken before treatment start) over the time. *Crh* overexpressing (CRH-COE^{iFB}) mice display the same characteristics in water consumption as their control (CRH-COE^{CTRL}) littermates. (A,C,E,G) Mice of groups with a seven day wash-out time by standard diet. Animals of both genotypes present in each group the specific peak when TCS chow is exchanged by standard diet. (B,D,F,H) Mice of groups without wash-out time but sacrificed immediately after TCS chow treatment do also not present any genotype effect. (I) Animals of control group. | Data are presented as mean \pm SEM; n (CRH-COE^{iFB}) = 4; n (CRH-COE^{CTRL}) = 4; Repeated-measures ANOVA.

Furthermore, we analyzed the water consumption of these mice (Figure 18). Animals of all groups tested (no consideration of genotype) displayed a water intake of $15 \pm 5\%$ of their own body weight. However, we detected within this range for treatments of 2, 4 and 6 days a significant decrease in water consumption for animals treated with TCS chow (Figure 18.A) (2 and 4 days Tam: Repeated-measures ANOVA, post-hoc test, ### $p < 0.001$; 6 days Tam: Repeated-measures ANOVA, post-hoc test, # $p < 0.05$). As the animals still consume enough water, this should not display any problems. We described for feeding behavior, that animals exhibit a peak in food intake within the first 24 hours after pellet exchange which was also observed for water consumption (Figure 18) as well as the genotypic independence of the results (Figure 19).

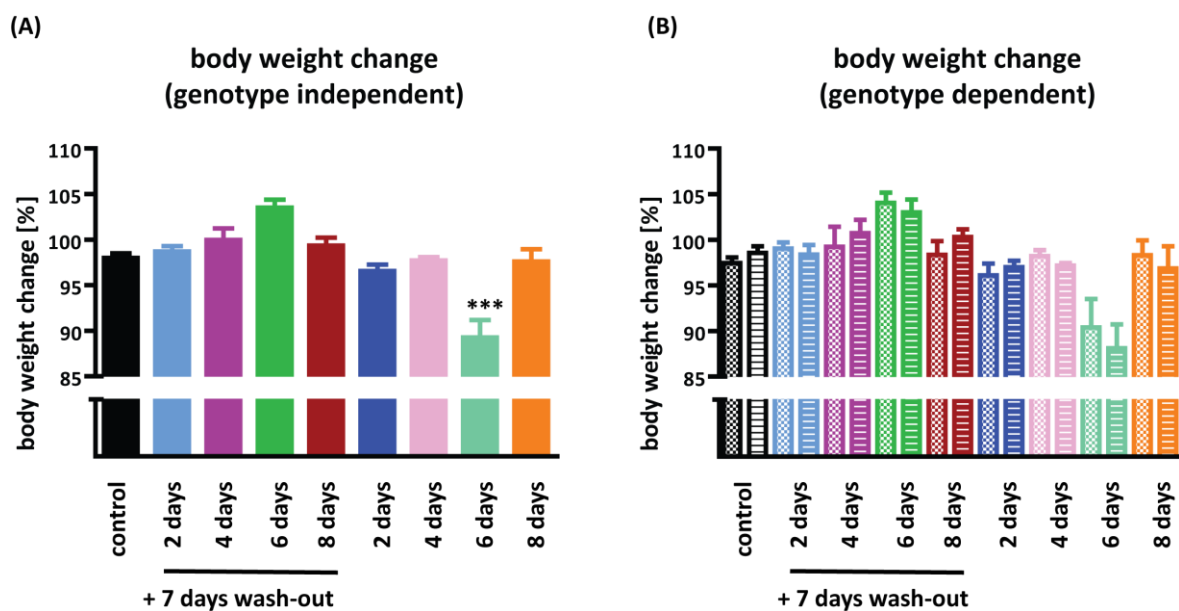


Figure 20. Body weight change of CRH-COE^{IFB} mice treated with TCS chow. Illustration of body weight change in percent during test time. (A) No severe body weight changes were detected during test time except for the group which was fed 6 days with Tam chow. Data are presented as mean \pm SEM; $n = 8$; *** $p < 0.001$, Student's t-test. (B) All groups were additionally split into the two genotypes overexpressing (CRH-COE^{IFB}) (depicted by striped columns) and control (CRH-COE^{CTRL}) (depicted by dotted columns) to assess whether there is any genotype-specific effect. | Data are presented as mean \pm SEM; n (CRH-COE^{IFB}) = 4; n (CRH-COE^{CTRL}) = 4; Student's t-test.

In line with the described feeding behavior (food intake and water consumption) the body weights of mice did not significantly change during treatment except for the group which was fed six days with TCS chow. These mice did not show any habituation to the food compared to mice of all other groups (Figure 20.A). No genotype-effect related to CRH overexpression was detected for body weight changes (Figure 20.B).

To summarize the findings in establishing the oral application of tamoxifen via chow to activate the Cre/loxP system in conditional transgenic mice, we can conclude that already short times (2 days) of TCS chow treatment are sufficient to enable CreER^{T2}-mediated recombination within the CNS. Furthermore, we demonstrated that there is a correlation between recombination efficacy and time of Tam treatment reaching a saturation after about 6 days of treatment. In addition, we could show, that there is no need to be concerned, that TCS chow treatment caused severe disturbances in feeding behavior or body weight change. Therefore, we recommend to treat animals 7 days with Tam chow followed by a 7 days wash-out phase with standard diet prior testing to obtain efficient recombination within brain cells.

4.3 Genetically dissecting brain-specific functions of histone deacetylase 1 (HDAC1)

4.3.1 Generation of conditional Hdac1 knockout mice

As we could show in chapter 4.1, that classical HDACs are widely expressed throughout the adult murine brain and they show all a distinct and unique pattern which suggests a specific role for each single HDAC member. However, HDAC1 and HDAC2 arose most probably from a recent gene duplication event and therefore, one could imagine that they fulfill similar functions (Gregoretto et al., 2004). Indeed, HDAC1 and HDAC2 are often found within the same multi-protein complexes, but embryonic lethality of total HDAC1 knockout animals and the divergent expression patterns of HDAC1 and HDAC2 strongly suggest that HDAC1 and HDAC2 cannot be redundant in all of their functions (de Ruijter et al., 2003; Lagger et al., 2002; Y Zhang et al., 1999). Therefore, we generated conditional Hdac1 knockout animals to specifically investigate the neuronal function of HDAC1.

4.3.1.1 Analysis of *Hdac1*-expression using lacZ reporter mice

We obtained Hdac1-lacZ reporter mice ($Hdac1^{tm1a(EUCOMM)wtsi}$) from the European Conditional Mouse Mutagenesis Program (EUCOMM; <http://www.knockoutmouse.org/about/eucomm>; tm1a = targeted mutation 1a; wtsi = Wellcome Trust Sanger Institute) and used them for generation of conditional knockout mice lacking HDAC1 in principal forebrain neurons in adulthood. Hdac1-lacZ mice are viable only as heterozygotes ($Hdac1^{tm1a(EUCOMM)wtsi}$) as the reporter allele disrupts *Hdac1* and HDAC1 homozygous knockout animals die at E10.5 (Lagger et al., 2002). The murine wild-type locus of *Hdac1* is located on chromosome 4 and spans about 30 kb. The gene comprises 14 exons and 13 introns and exhibits an open reading frame of 1446 bp (Bartl et al., 1997; Furukawa et al., 1996; Khier et al., 1999; Taunton et al., 1996). The mutant reporter allele was generated using a targeted trapping strategy (Figure 21.A). The gene trap cassette is integrated into intron 2 and consists of a splice acceptor (*engrailed 2 splice acceptor: En2 SA*), a *lacZ* gene driven by an internal ribosomal entry site (*IRES-lacZ*), a *phosphoglycerate kinase (PGK)* promoter driven *neomycin resistance* gene (*neo*) and a poly-adenylation signal (*simian virus 40 poly-adenylation signal: SV40 pA signal*). This cassette is flanked by two frt sites in parallel orientation followed by two loxP sites in parallel orientated flanking exon 3. The *splice acceptor (SA)* and the *internal ribosomal entry site (IRES)* of the *lacZ* gene is necessary that the lacZ-reporter is driven by the endogenous *Hdac1* promoter elements. Thus, the first two exons of *Hdac1* are transcribed, but no functional HDAC1 protein can be translated from this fusion transcript. β -galactosidase (expressed by the *lacZ* gene)

and the *neomycin* make up a fusion protein. The *frt* sites are recognized by the yeast enzyme Flp and *loxP* sites are recognition sites for the yeast Cre recombinase.

To genotype mice for the presence of the reporter allele, a triple-primer genotyping PCR was established using two forward primers and one reverse primer (Figure 21.B). Forward primer 1 (F1: Hdac1_EU_wt_F) and reverse primer 1 (R1: Hdac1_EU_R1) anneal to a DNA sequence present within the wild-type DNA sequence of *Hdac1* and produce a PCR product of 472 bp within the wild-type locus (Figure 21.C). In general, this primer pair can also create a PCR product in the *lacZ* mutant allele, but the sequence to be amplified is more than 5 kb long and the extension time of the PCR product is set to produce only smaller products up to 700 bp. Thus, the *lacZ* allele is only detected with the second gene trap cassette targeting vector-specific forward primer (F2: Hdac1_EU_frt_F) which amplifies together with R1 a PCR product of 219 bp (Fig. 21.B and C).

We used the Hdac1-*lacZ* reporter mice to shed light on *Hdac1* expression in addition to the *ISH* described earlier (Figure 22.A-C). A *lacZ*-based reporter mouse line enables a straight-forward screening of expression of a gene of interest. Expression analysis can be performed on sections or even whole organs. Heterozygous male Hdac1-*lacZ* reporter mice ($Hdac1^{tm1a(EUCOMM)wt/si}$) were sacrificed at the age of 2-3 months, various organs were removed and subsequently stained for *lacZ* expression (Figure 22.A). We could show that *Hdac1* is more or less ubiquitously expressed and detectable in many tissues (e.g. heart, kidney, adrenal gland, liver, lung, pituitary, skin, spinal cord, spleen, thymus) which goes in line with the literature which describes, that class I HDACs are broadly expressed within various tissues and especially HDAC1 was shown to be important for heart physiology (Montgomery et al., 2007). Furthermore, we used the Hdac1-*lacZ* ($Hdac1^{tm1a(EUCOMM)wt/si}$) reporter mice to determine the expression level of HDAC1 throughout the adult murine brain (Figure 22.B). *LacZ* staining confirms the *ISH* for *Hdac1* mRNA (Figure 22.C). In particular the low expression throughout the entire brain is clearly visible. In addition, distinct expression with high intensity is only detected in a few brain regions such as the granular cell layer of the dentate gyrus (DG), the olfactory bulb (data not shown) and the cerebellum (Fig. 22.B).

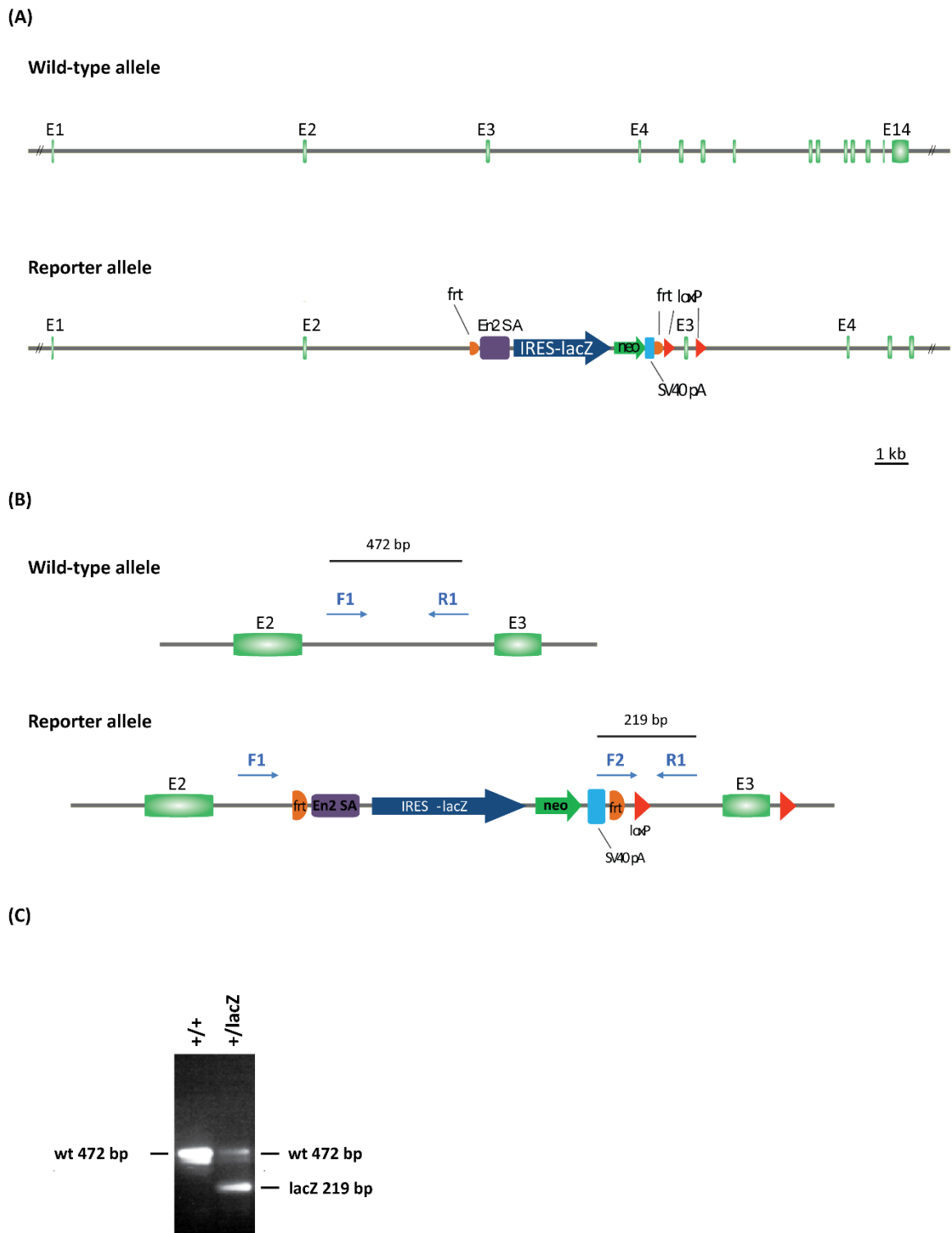


Figure 21. Schematic representation of the *Hdac1* wild-type locus and the *lacZ* reporter allele generated by targeted trapping. (A) *Hdac1* wild-type allele with 14 exons (E: depicted in light green) and respective reporter allele which was generated using a targeted trapping strategy of the *Hdac1* gene locus. | flt = Flp recognition target: depicted in orange; *EN2 SA* = *engrailed 2 splice acceptor*: depicted in violet; *IRES-lacZ* = *internal ribosomal entry site-lacZ*: depicted in blue; *PGK neo* = *phosphoglycerate kinase promoter driven neomycin resistance gene*: depicted in green; *SV40 pA* = *simian virus 40 poly-adenylation signal*:

depicted in light blue; Cre recognition target = *loxP* site: depicted in yellow; (B) Schematic representation of genotyping strategy to identify mice carrying the Hdac1-lacZ reporter allele. Identification of wild-type and mutant alleles by genotyping PCR using a forward primer (F1: Hdac1_EU_wt_F) and a reverse primer (R1: Hdac1_EU_R1) annealing to wild-type sequences, whereas a third primer (forward primer 2; F2: Hdac1_EU_frt_F) anneals to a sequence within the gene trap cassette. (C) Genotyping of Hdac1-lacZ reporter mice by PCR depicting results of a wild-type and a heterozygous reporter mouse, respectively. Primer F1 and R1 produce a 472 bp wild-type product and primer F2 and R1 produce a 219 bp lacZ product. [EUComm; <http://www.knockoutmouse.org/about/eucomm>]

(A)

+ / lacZ	colon 	diaphragm 	duodenum 	fat 	heart 	kidney, adrenal gland
+ / +	colon 	diaphragm 	duodenum 	fat 	heart 	kidney, adrenal gland
+ / lacZ	liver 	lung 	pancreas 	pituitary 	SG 	skin (ear)
+ / +	liver 	lung 	pancreas 	pituitary 	SG 	skin (ear)
+ / lacZ	spinal cord 	spleen 	stomach 	testis, bladder 	thymus 	tongue
+ / +	spinal cord 	spleen 	stomach 	testis, bladder 	thymus 	tongue

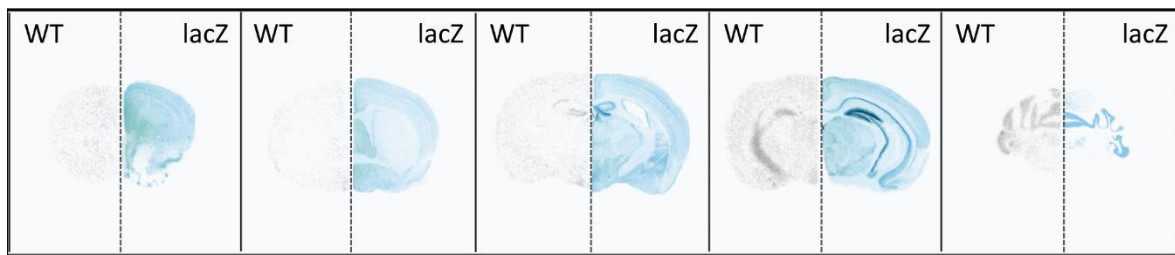
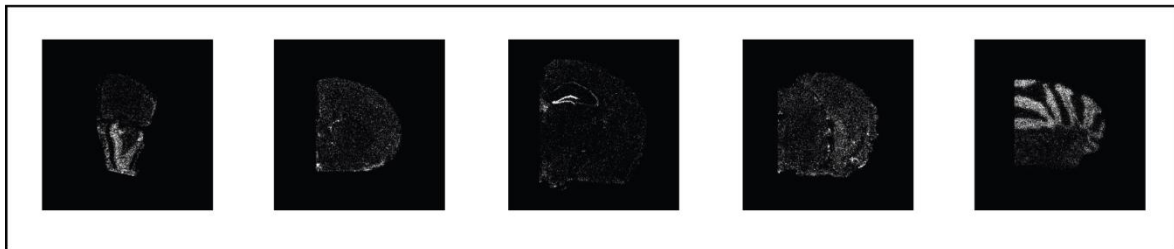
(B)**(C)**

Figure 22. *Hdac1* expression revealed by *Hdac1-lacZ* reporter mice. (A) Whole mount lacZ staining of various organs of heterozygous *Hdac1-lacZ* reporter mice. Organs were removed from heterozygous male *Hdac1-lacZ* reporter mice and wild-type mice after animals were sacrificed and subsequently lacZ stained. As β -galactosidase is expressed under the control of the *Hdac1* promoter the staining resembles the endogenous HDAC1 expression pattern. Unspecific staining was excluded by positive controls like colon and stomach which contain bacteria expressing naturally β -galactosidase and therefore show a positive staining for both, reporter and wild-type mice. (B) LacZ staining of 40 μ m-thick coronal brain sections of wild-type mice (left side) and *Hdac1-lacZ* reporter mice (right side). The lacZ staining in reporter mice resembles HDAC1 expression. (C) For comparison qualitative ISH analysis of *Hdac1* using a specific radiolabeled riboprobe was performed. Depicted are representative dark-field photomicrographs of a series of 20 μ m-thick coronal brain sections of a wild-type mouse hybridized with the indicated probe to show *Hdac1* expression on mRNA level.

4.3.1.2 Establishment of conditional *Hdac1* knockout mice

To establish conditional *Hdac1* knockout mice, we bred heterozygous *Hdac1-lacZ* (*Hdac1*^{tm1a(EUCOMM)wtst}) reporter mice to Flp-Deleter mice (Figure 23) (Rodriguez et al., 2000). Bred with the *Hdac1-lacZ* reporter mice, the Flp recombinase recognizes the two parallel orientated frt sites within the *Hdac1* locus and deletes the enframed sequence including the reporter cassette between the two frt sites (Figure 24.A). Thus, in the heterozygous offspring carrying the Flp recombinase the *Hdac1* gene is not disrupted anymore, however the loxP sites flanking the critical exon three (“floxed” exon) are still present and thus provide the means for a conditional inactivation. In these heterozygous floxed mice (*Hdac1*^{+lox}, Flp deleter) the *Hdac1* gene can be properly transcribed from both alleles. To generate conditional knockout mice and to by-pass embryonic lethality linked to constitutive loss of HDAC1, we bred the heterozygous floxed mice with

tamoxifen inducible Cre line. As a Cre driver, we chose Camk2a-CreER^{T2} mice (Erdmann et al., 2007). By the choice of the Camk2a-CreER^{T2} line we achieved temporally controlled somatic mutagenesis by the use of tamoxifen administration in the adult stage and exclude developmental effects, adaptive changes and in particular embryonic lethality. Furthermore, the CreER^{T2} is expressed under the control of the regulatory element of the *Camk2a* gene and therefore we have a spatially restricted Cre expression to induce the Hdac1 knockout only in principal neurons of the adult forebrain. Conditional Hdac1 knockout mice (Hdac1^{lox/lox}Camk2a-CreER^{T2} referred to as Hdac1-cKO) and control littermates (Hdac1^{lox/lox} referred to as Hdac1-CTRL) were obtained by the breeding strategy depicted in Figure 23.

Upon tamoxifen treatment via the strategy developed in chapter 4.2, Cre recombination was achieved in all principal forebrain neurons deleting *Hdac1* exon three which leads to a frame-shift and to a premature stop codon resulting in a non-functional HDAC1 enzyme.

The above mentioned triple-primer genotyping PCR was not only used to genotype mice for the presence of the *Hdac1* wild-type and lacZ reporter allele, but also to assess the floxed allele (Figure 24.B and C). Therefore, the forward primer 1 (F1: Hdac1_EU_wt_F) and reverse primer 1 (R1: Hdac1_EU_R1) were used to amplify also a PCR product in the floxed allele which is bigger than the allele of the wild-type locus (617 bp versus 472 bp). The second forward primer (F2: Hdac1_EU_frt_F) still creates together with R1 only in the lacZ locus a product with a size of 219 bp. Thus, the triple PCR is able to distinguish genotypes of Hdac1^{+/+} (wild-type), Hdac1^{+/lacZ} (heterozygous reporter), Hdac1^{+/lox} (heterozygous floxed) and Hdac1^{lox/lox} (homozygous floxed). Two additional PCRs to detect the Flp and CreER^{T2} were performed on genomic tail DNA of each animal (data not shown).

For successful disruption of Hdac1 within principal neurons of the adult murine forebrain, mice were fed seven days with tamoxifen chow and sacrificed after another seven days of wash-out. Brain slices were analyzed via ISH using a riboprobe detecting specifically exon 3 of the *Hdac1* mRNA (Figure 25). We could demonstrate especially in the hippocampus the loss of *Hdac1* expression in conditional Hdac1 knockout animals on mRNA level. The conditional knockout of Hdac1 was further validated on protein level. Western blot (WB) analysis clearly reveals reduced HDAC1 expression in hippocampal lysates of Hdac1-cKO mice compared to Hdac1-CTRL littermates. However, the small amount of remaining HDAC1 protein in the knockout animals detected by WB analysis originate from cells (i.e. glia cells) which do not express CreER^{T2}. In all subsequent experiments, we used Hdac1^{lox/lox} Camk2a-CreER^{T2} mice (Hdac1-cKO) and their control littermates (Hdac1^{lox/lox} Camk2a-CreERT2 = Hdac1-CTRL).

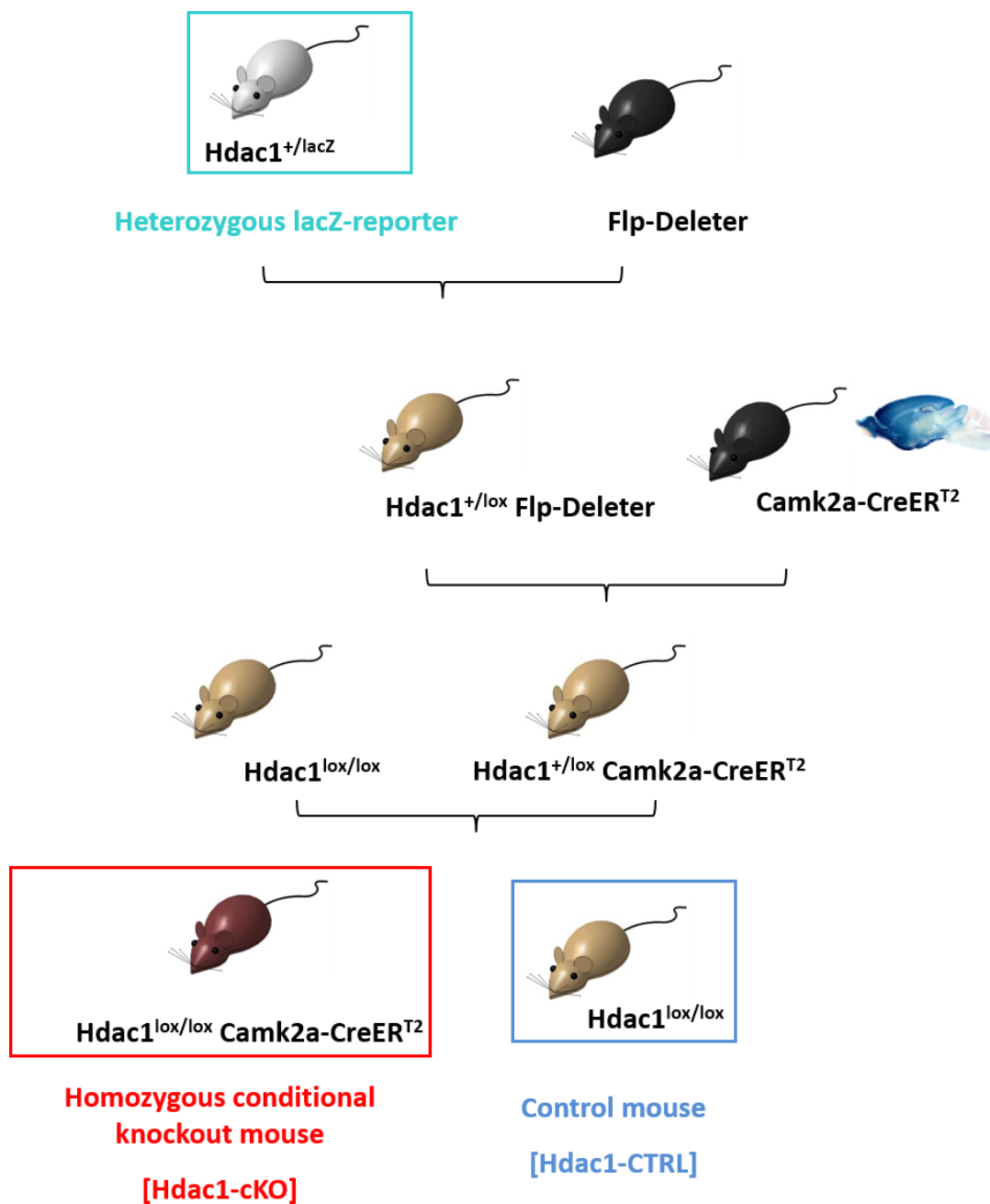
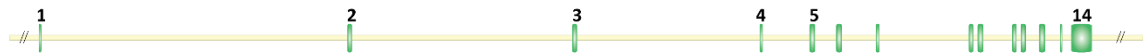


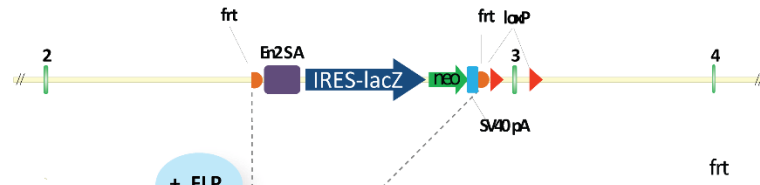
Figure 23. Breeding scheme to generate conditional *Hdac1* knockout mice. Heterozygous *Hdac1-lacZ* reporter mice ($Hdac1^{+/lacZ}$) were bred to Flp-Deleter mice for removal of the selection cassette. Recombination between the two *frt* sites restored *Hdac1* expression and left the critical exon 3 flanked by *loxP* sites ("floxed"). $Hdac1^{+/lox}$ Flp-Deleter mice were bred to the hemizygous inducible Cre-driver *Camk2a-CreER^{T2}* resulting in $Hdac1^{+/lox}$ *Camk2a-CreER^{T2}* which were bred to homozygous floxed mice ($Hdac1^{lox/lox}$) to finally obtain homozygous conditional *Hdac1* knockout mice ($Hdac1^{lox/lox}$ *Camk2a-CreER^{T2}* = Hdac1-cKO) and within the same breeding control littermates ($Hdac1^{lox/lox}$ = Hdac1-CTRL).

(A)

Wild-type allele



Reporter allele

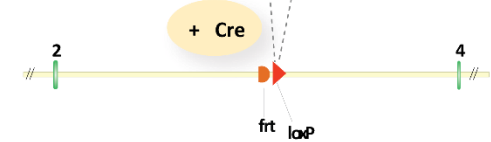


+ FLP

Floxed allele



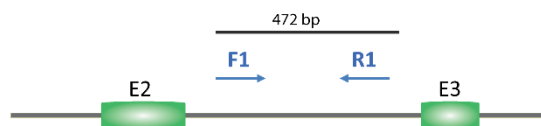
Knockout allele



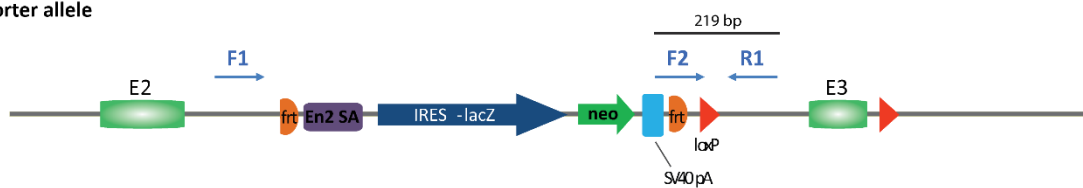
1 kb

(B)

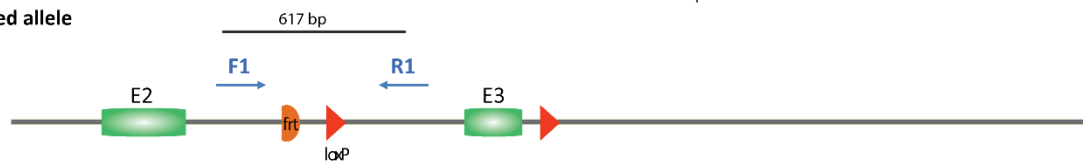
Wild-type allele



Reporter allele



Floxed allele



(C)

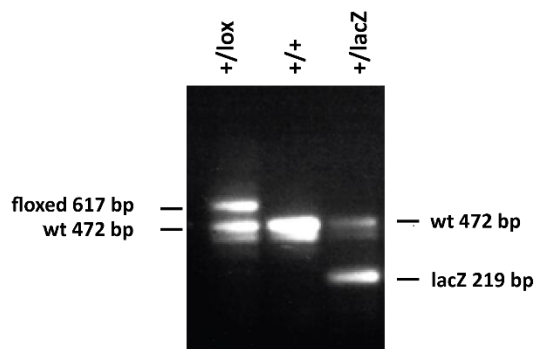


Figure 24. Schematic representation of the *Hdac1* wild-type locus, lacZ allele, floxed allele and knockout allele generated by targeted trapping and subsequent excision via Flp and Cre. (A) *Hdac1* wild-type allele comprising 14 exons (E: depicted in light green), reporter allele generated by the targeted trapping strategy, floxed allele obtained via Flp-mediated recombination of the reporter allele and knockout allele after further Cre-mediated recombination. | frt = Flp recognition target: depicted in orange; EN2 SA = engrailed 2 splice acceptor: depicted in violet; IRES-lacZ = internal ribosomal entry site-lacZ: depicted in blue; PGK neo = phosphoglycerate kinase promoter driven neomycin resistance gene: depicted in green; SV40 pA = simian virus 40 poly-adenylation signal : depicted in light blue; Cre recognition target = loxP site: depicted in yellow; (B) Schematic representation of genotyping strategy to identify mice carrying the *Hdac1* wild-type allele, lacZ reporter allele or floxed allele. Identification of wild-type, reporter and floxed alleles was possible by genotyping PCR using a forward primer (F1: *Hdac1*_EU_wt_F) and a reverse primer (R1: *Hdac1*_EU_R1) annealing to wild-type sequences, whereas a third primer (forward primer 2; F2: *Hdac1*_EU_frt_F) anneals to a sequence within the gene trap cassette. (C) Genotyping of *Hdac1*-lacZ reporter mice and floxed *Hdac1* mice by PCR depicting results of a heterozygous floxed mouse, a wildtype mouse and a heterozygous reporter mouse, respectively. Primer F1 and R1 produce a 472 bp wild-type product and a 617 bp floxed product, whereas primer F2 and R1 produce a 219 bp lacZ product.

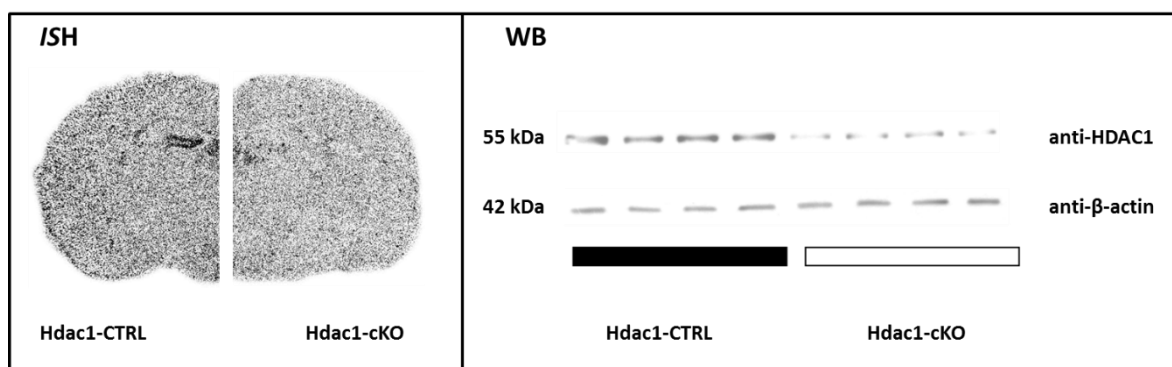


Figure 25. Verification of HDAC1 disruption in conditional *Hdac1* knockout mice upon tamoxifen treatment. *Hdac1*-cKO and *Hdac1*-CTRL mice were fed for 7 days with tamoxifen chow and analyzed after a 7 day wash-out phase via *in situ* hybridization (ISH) and Western Blot analysis (WB). The left panel shows qualitative ISH analysis using a radiolabeled riboprobe which specifically detects exon 3 of the *Hdac1* mRNA. Depicted are representative bright-field photomicrographs of autoradiographs of 20 μ m-thick coronal brain slices of control (left side) and conditional knockout (right side) mice. The right panel shows WB against HDAC1 of hippocampal lysates of control and conditional knockout animals.

4.3.2 Behavioral characterization of conditional Hdac1 knockout mice lacking HDAC1 in principal forebrain neurons

4.3.2.1 Basal behavioral screening of conditional Hdac1 knockout mice

For a comprehensive basal behavioral characterization of mice lacking HDAC1 in principal forebrain neurons, Hdac1-cKO mice and Hdac1-CTRL littermates were tested. To assess the same conditions for all mice, both genotypes were fed 7 days with tamoxifen chow followed by a 7 day wash-out phase using standard diet prior testing. Four tests were conducted within seven days following the schedule depicted in Figure 26 to assess locomotion and explorative, anxiety-related, depression-related and stress-coping behavior.

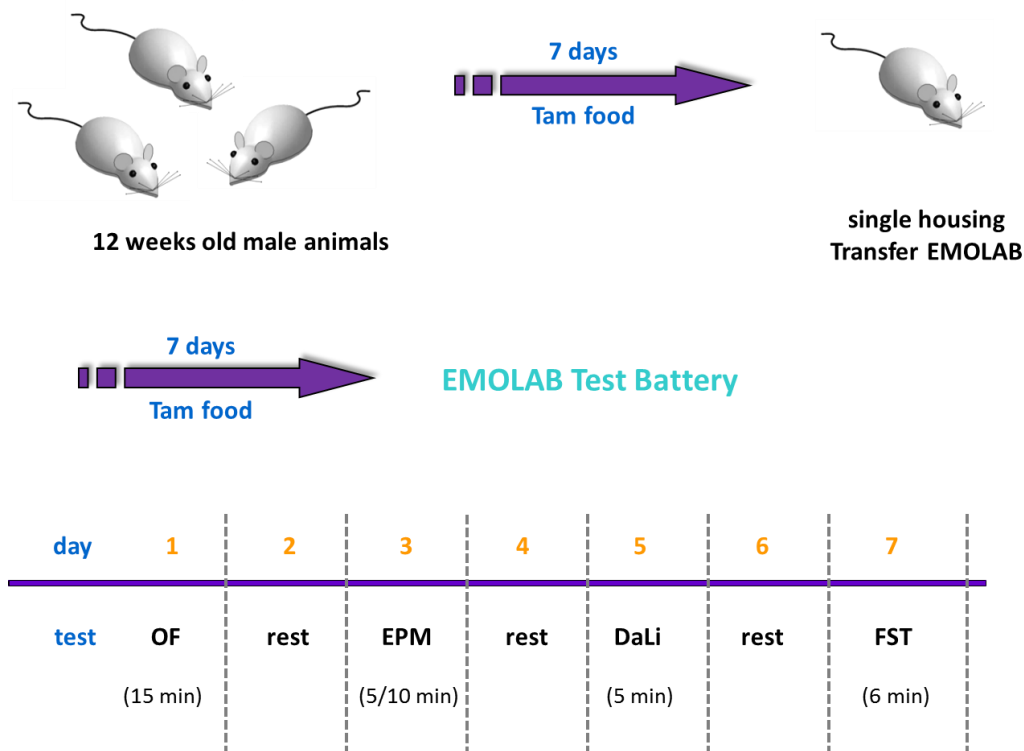


Figure 26. Testing schedule for basal emotionality screen of conditional Hdac1 knockout mice. Each test was followed by one day rest for the animals before conducting the next test. | EMOLAB = emotionality lab; OF = open field test; EPM = elevated plus maze test; DaLi = dark/light box test; FST = forced swim test.

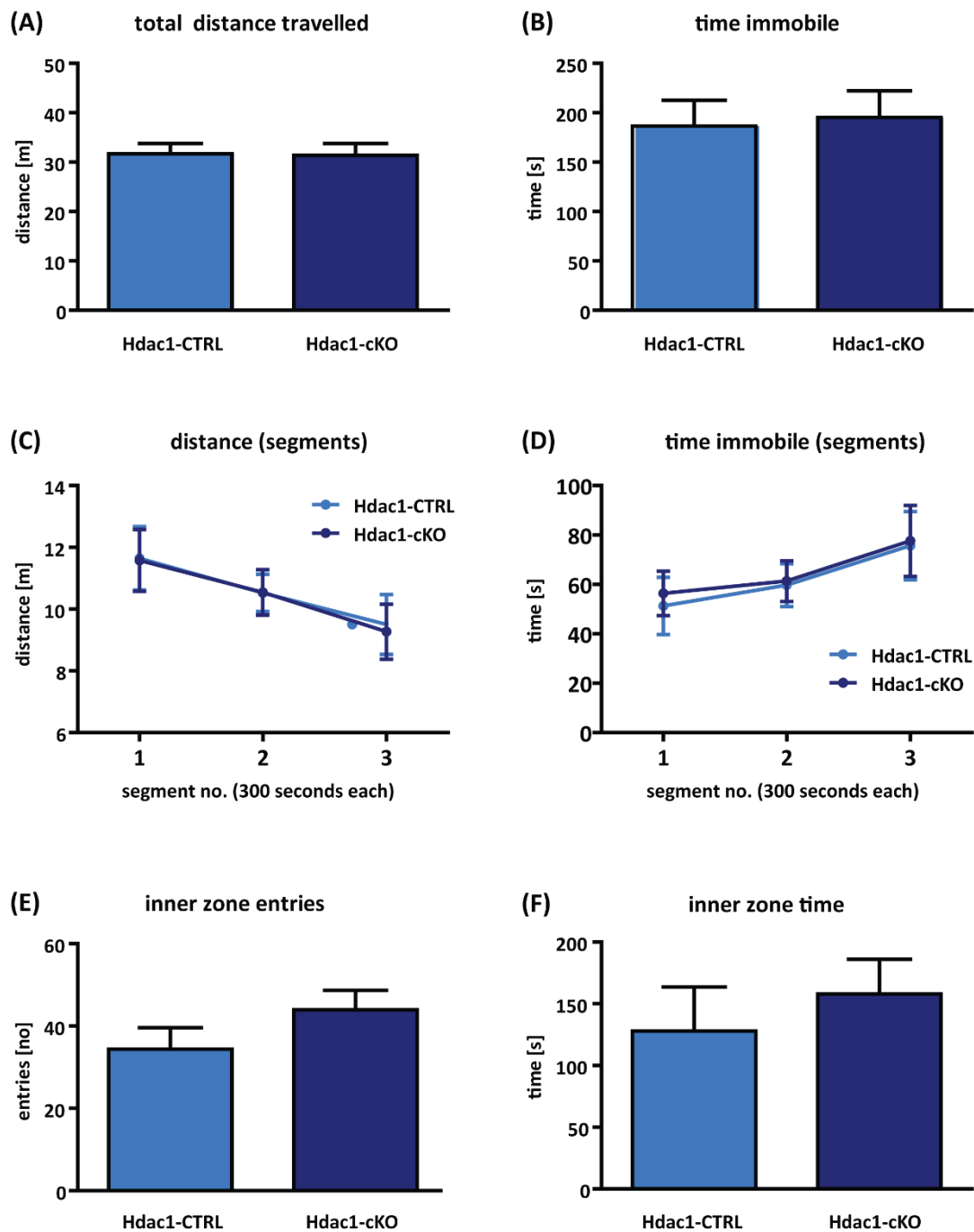


Figure 27. Analysis of conditional Hdac1 knockout mice in the open field (OF) test. (A) No significant difference was observed in total distance travelled (B) nor in time spent immobile. (C-D) The total test was also analyzed in segments of 5 minutes. Also here, no significant difference was revealed between the two genotypes. (E-F) To observe anxiety-related and explorative behavior, the number of inner zone entries and inner zone time was analyzed. Again no difference was observed. | Test duration analyzed: 15 minutes; Data are presented as means \pm SEM; n = 10-12; Hdac1-CTRL = control littermate; Hdac1-cKO = conditional Hdac1 knockout mouse.

The open field (OF) test was used to assess locomotor activity as well as explorative behavior and anxiety-related behavior. Analysis of data for the first 15 minutes of the OF test indicated that there was no difference in locomotion of conditional Hdac1 knockout mice compared to control littermates, neither in total distance travelled (Figure 27.A), nor when split into segments of five minutes (Figure 27.C). Anxiety-related behavior was assessed using parameters such as total time spent immobile (Figure 27.B), time spent immobile within segments of five minutes (Figure 27.D), number of entries to the inner zone (Figure 27.E) and total time spent in the inner zone (Figure 27.F), which all revealed no significant difference between the two genotypes as well.

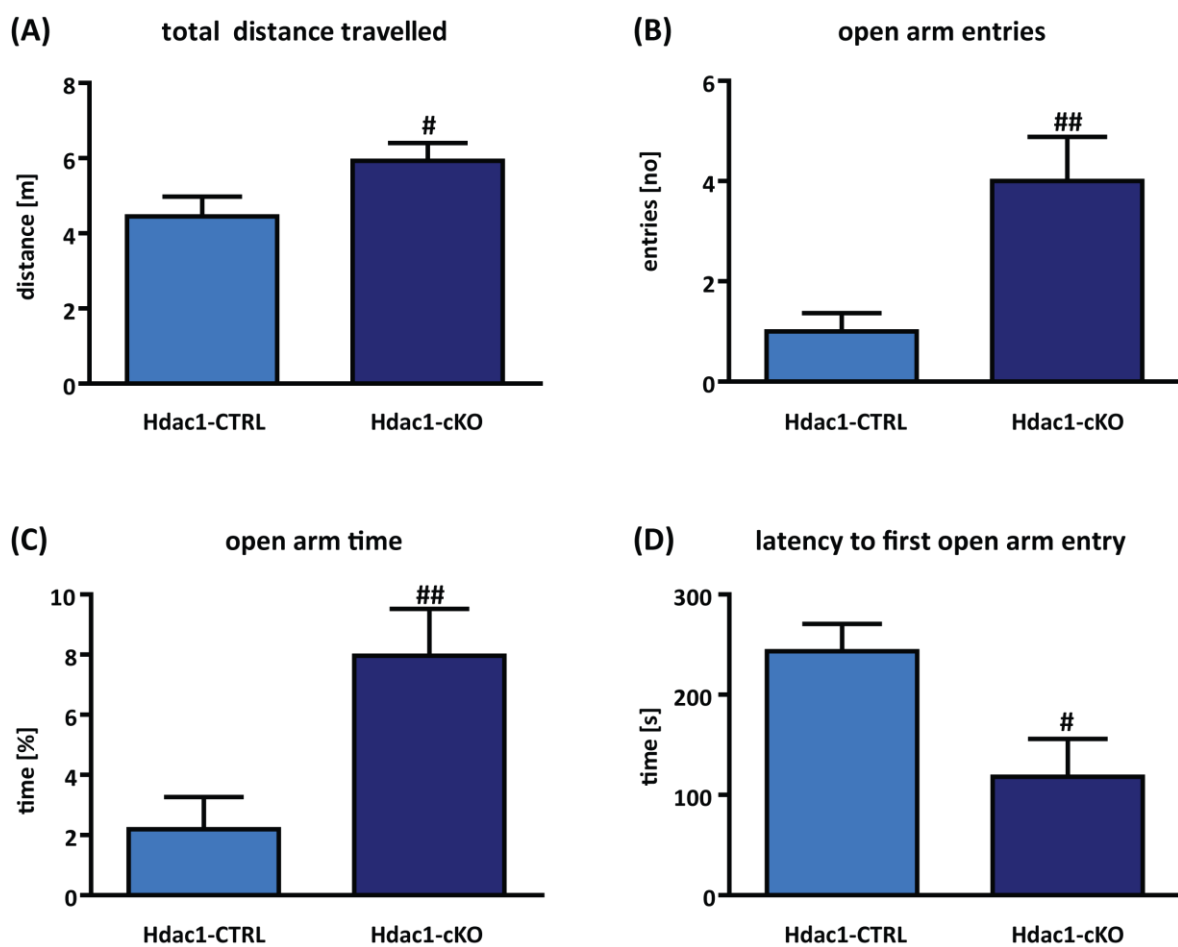


Figure 28. Analysis of conditional Hdac1 knockout mice in the elevated plus maze (EPM) test. (A) Hdac1-cKO mice showed an increase in total distance travelled within the EPM test. (B) HDAC1-cKO mice entered more often the open arm and (C) the open arm time was significantly increased as well. (D) Furthermore, the measurement of the latency to the first open arm entry revealed an earlier entry of Hdac1-cKO mice. | Test duration analyzed: 5 minutes; Data are presented as means \pm SEM; n = 10-12; # p < 0.05, ## p < 0.01, Student's t-test; Hdac1-CTRL = control littermate; Hdac1-cKO = conditional Hdac1 knockout mouse.

The elevated plus maze (EPM) test was used to assess anxiety-related behavior. Test data was analyzed for a duration of five minutes. A Student's t-test revealed a significant increase of total distance travelled (# $p < 0.05$) (Figure 28.A), number of open arm entries (## $p < 0.01$) (Figure 28.B), open arm time (### $p < 0.01$) (Figure 28.C) and a decrease of the latency to first open arm entry (# $p < 0.05$) (Figure 28.D) for the conditional *Hdac1* knockout mice compared to control littermates suggesting a decrease in anxiety-related behavior due to the loss of *Hdac1* expression.

The dark/light box (DaLi) test was used as an additional test to assess anxiety-related behavior in conditional *Hdac1* knockout mice. As this test is more aversive than the EPM test, the DaLi test was performed afterwards. However, in comparison to the EPM test, the DaLi test revealed no significant difference in the innate aversion of mice to brightly illuminated areas between conditional *Hdac1* knockout mice and control littermates (Figure 29.A). Also the other analyzed parameters such as entries into the lit compartment (Figure 29.B), latency to first lit compartment entry (Figure 29.C), the total distance travelled (Figure 29.D) and the distance travelled either in the lit compartment (Figure 29.E) or in the dark compartment (Figure 29.F) did not reveal any difference in anxiety-related behavior between the two genotypes.

To assess stress-coping and depression-related behavior in conditional *Hdac1* knockout mice, the forced swim test (FST) was performed. The analysis of the FST using the Student's t-test revealed that conditional *Hdac1* knockout mice differ in the two active stress-coping parameters in their behavior. Knockout mice struggled significantly less (# $p < 0.05$) (Figure 30.A), but increased their time swimming (### $p < 0.001$) (Figure 30.B) compared to control mice, whereas the time of behavioral immobility (floating) did not differ significantly between the two genotypes (Figure 30.C).

In summary of the behavioral results of the basal emotionality screen it emerges that conditional *Hdac1* knockout mice did not show any deficits in locomotor activity, but showed a decreased anxiety-related behavior in the EPM test, although this phenotype was not observed in the DaLi test. Furthermore, conditional *Hdac1* knockout mice differed from control littermates in their active stress-coping behavior in the FST showing a lower amount of struggling with a simultaneously increased swimming time.

To rule out, that the tamoxifen chow or the Cre recombinase caused an overall effect and might influence the obtained data, we conducted two additional control experiments in the same behavioral test battery (tamoxifen chow data not shown; Cre recombinase data shown in supplements).

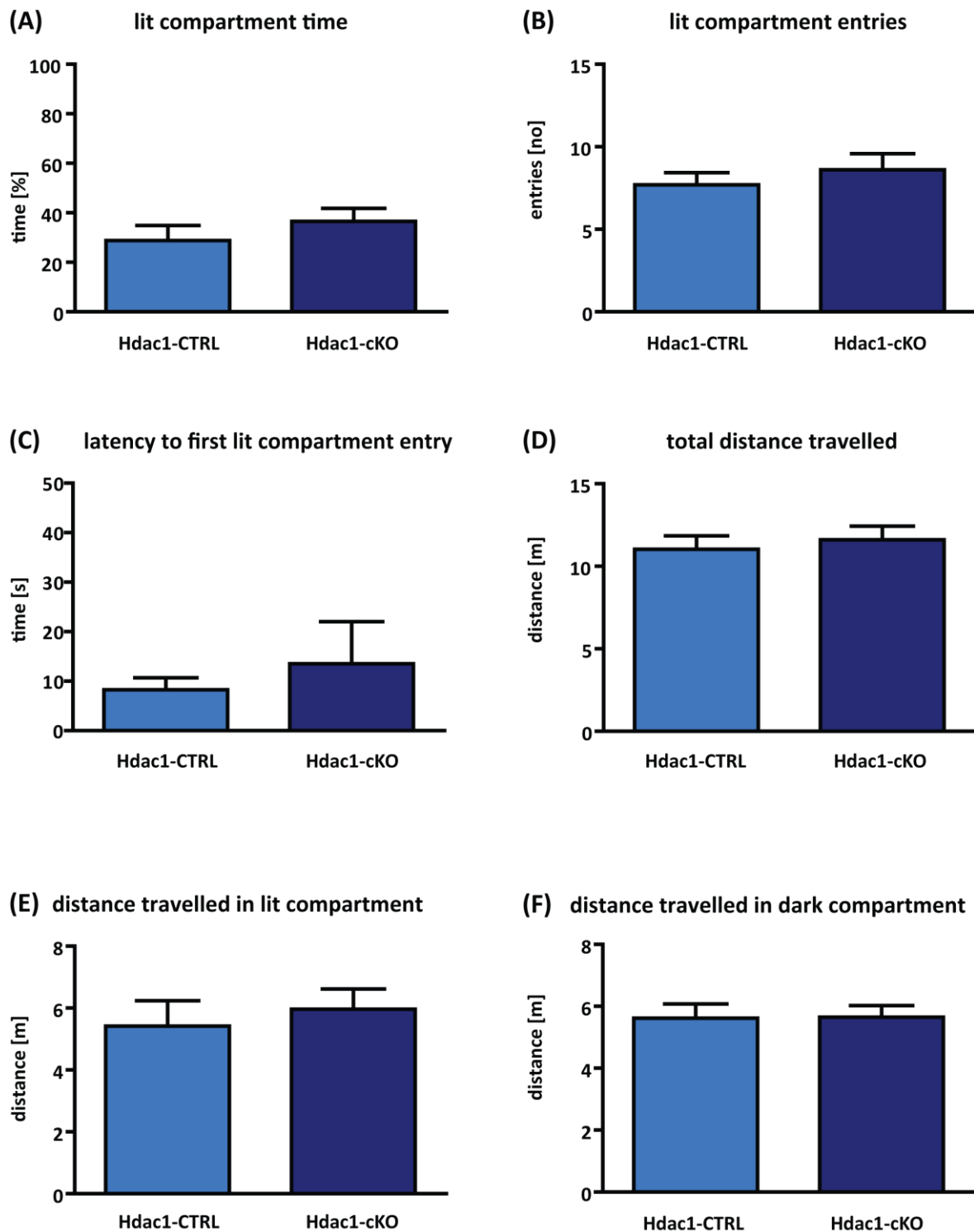


Figure 29: Analysis of conditional Hdac1 knockout mice in the dark/light box (DaLi) test. (A) The time spent in the lit compartment, (B) the number of entries to the lit compartment and (C) the latency to first lit compartment entry revealed no difference between Hdac1-cKO and Hdac1-CTRL mice. (D) The total distance travelled during the whole test, as well as the (E) distance travelled either in the lit or (F) in the dark compartment did not differ between the two genotypes. | Test duration analyzed: 5 minutes; Data are presented as means \pm SEM; n = 10-12; Hdac1-CTRL = control littermate; Hdac1-cKO = conditional Hdac1 knockout mouse.

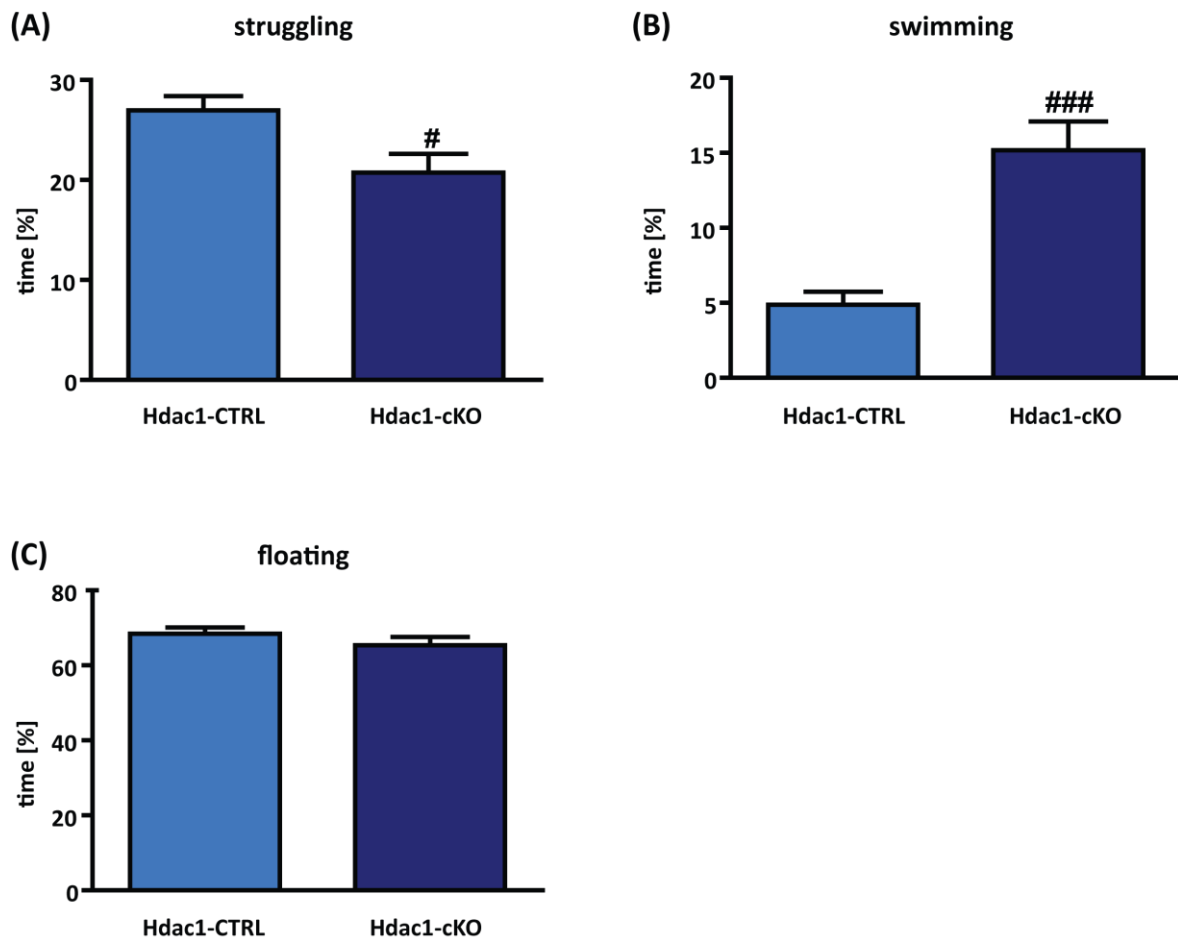


Figure 30: Analysis of conditional Hdac1 knockout mice in the forced swim test (FST). (A) The time Hdac1-cKO mice spent struggling was significantly decreased, (B) whereas the time the Hdac1-cKO mice spent swimming to cope with the situation was significantly increased compared to the control group. (C) However, most of the time, animals of both groups were floating, a passive stress coping behavior to overcome the desperate situation. | Test duration analyzed: 6 minutes; Data are presented as means \pm SEM; $n = 12$; # $p < 0.05$, ## $p < 0.01$, ### $p < 0.001$, Student's t-test; Hdac1-CTRL = control littermate; Hdac1-cKO = conditional Hdac1 knockout mouse.

4.3.2.2 Effects of chronic social defeat stress (CSDS) on conditional Hdac1 knockout mice

Since HDACs are main epigenetic mediators and thus, play a pivotal role in gene x environment interactions, we subjected conditional Hdac1 knockout mice to three weeks of chronic social defeat stress (CSDS) to assess whether the Hdac1 knockout in principal neurons of the forebrain in adulthood has any impact on the animals' stress response (Berton et al., 2006; Wagner et al., 2011). Therefore, animals were categorized into four groups having the two genotypes Hdac1-CTRL and Hdac1-cKO and two different conditions (basal: undefeated; stress: defeated). All animals were fed seven days with tamoxifen chow starting at the day of the first defeat and followed by a seven day wash-out phase prior testing (Figure 31).

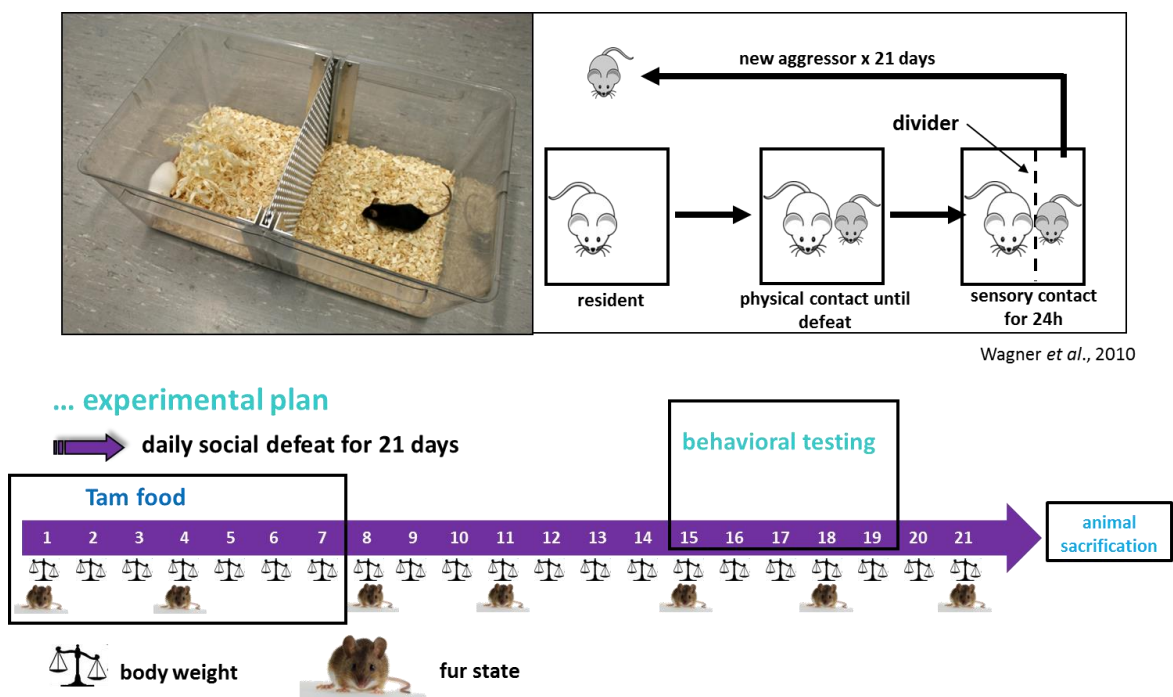


Figure 31. Schematic representation of the chronic social defeat stress (CSDS) paradigm and behavioral phenotyping of conditional Hdac1 knockout mice. Animals were submitted to CSDS for 21 consecutive days. Therefore, they were introduced into the home cage of a dominant CD1 resident mouse until defeated, but for no longer than 5 min. Following defeat, animals spent 24 hours within the same cage, but separated via a holed steel partition, enabling sensory, but not physically contact. Every day chronically defeated mice were exposed to a new unfamiliar resident. Control animals were housed in their home cages throughout the course of the experiment. All animals were handled daily, the body weight was assessed daily and the fur status was checked every 3-4 days. The fur was evaluated as describe before by Mineur and colleagues (Mineur et al., 2003). Tam application via food pellets was performed within the first 7 days of the defeat. Behavioral phenotyping included OF test, SA test, FUST, EPM and FST. | CSDS = chronic social defeat stress; Tam = tamoxifen; OF = open field; SA = approach/avoidance; FUST = female urine sniffing test; EPM = elevated plus maze; FST = forced swim test.

In order to control for the effectiveness of the CSDS paradigm, physiological parameters such as body weight progression, fur state and weight of adrenal glands and thymus were assessed. Both genotypes of mice (Hdac1-CTRL and Hdac1-cKO) showed similar characteristic physiological changes evoked by the CSDS (Figure 32). These included a progressive increase in body weight (Repeated-measures ANOVA, * $p < 0.05$) (Figure 32.A), a decrease in fur quality (Repeated-measures ANOVA, * $p < 0.05$) (Figure 32.B), an enlargement of adrenal glands (One-Way ANOVA, *** $p < 0.001$) (Figure 32.C) and an atrophy of the thymus (One-Way ANOVA, ** $p < 0.01$) (Figure 32.D).

Furthermore, it is known that stress enhances plasma corticosterone levels. Therefore, basal levels of corticosterone were assessed in all four groups in blood plasma during the circadian nadir in the morning (Figure 33.A). Blood samples were taken 15 and 90 minutes after the onset of a forced swim test as acute stressor to obtain corticosterone levels as response to the stressor (Figure 33.B) and the subsequent recovery from this stressful event (Figure 33.C). However, statistical analysis showed no significant differences in the corticosterone levels, no genotype, nor a condition effect was observed.

The chronic social defeat stress (CSDS) paradigm was established by the research group of Mathias Schmidt at the MPI of Psychiatry, based on the protocol of Berton and colleagues (Berton et al., 2006; Wagner et al., 2011). To describe briefly, test mice were submitted to chronic social defeat stress for 21 consecutive days (Figure 31). Therefore, they were introduced into the home cage of a dominant CD1 resident mouse for no longer than 5 min. During this time the intruder was defeated.

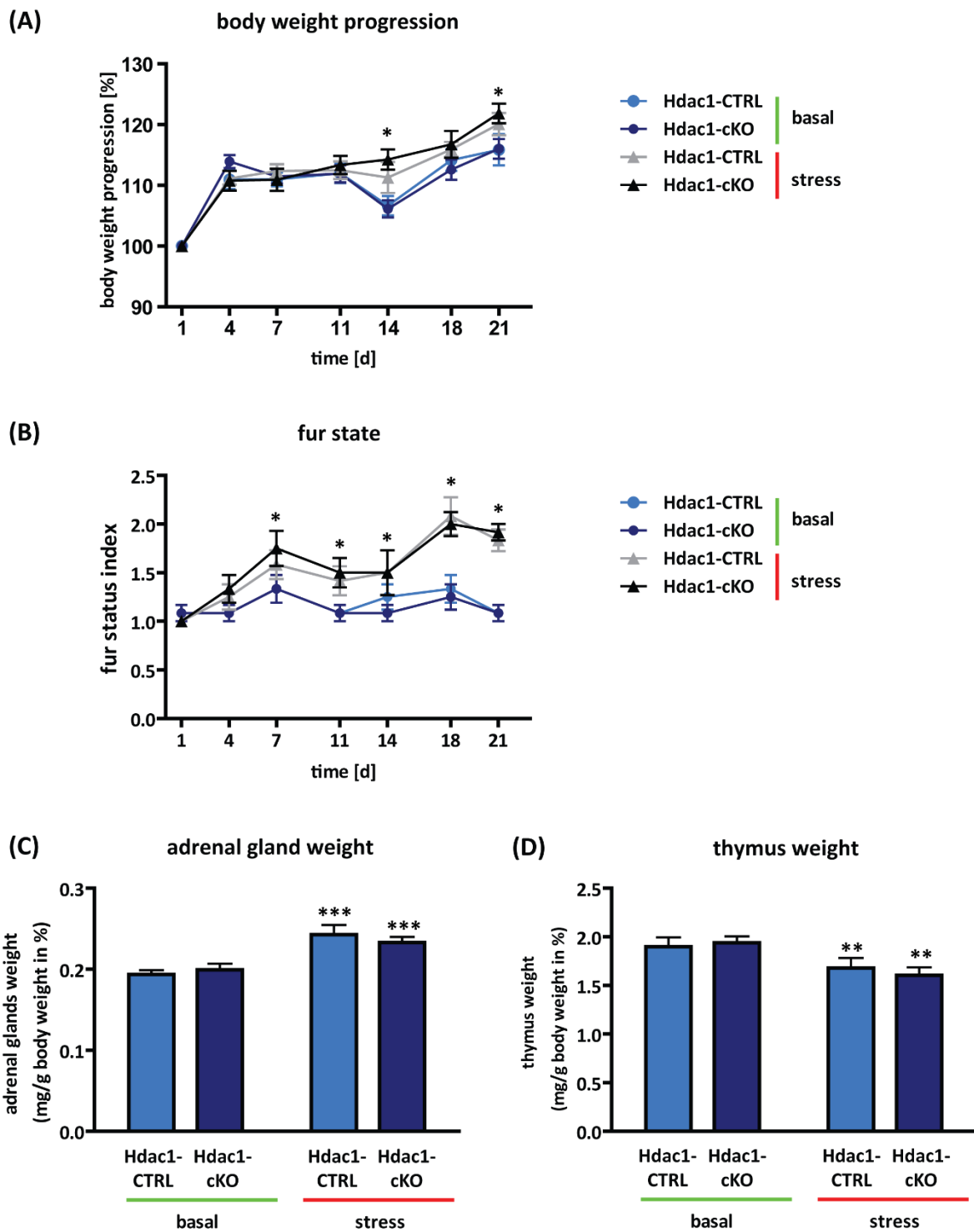


Figure 32. Analysis of physiological parameters of conditional Hdac1 knockout mice during and after the chronic social defeat stress (CSDS) paradigm. (A) Body weight of mice was assessed every day and is depicted as percentage of the starting weight at day one of defeat. Animals of all groups gained body weight throughout the experiment, especially within the first days. However, animals of both stressed groups gained significantly body weight compared to basal groups at day 14 and 21 of the experiment, whereas both basal groups showed a steady body weight progression throughout week 2 and 3 of the. (B) The fur status index was assessed every three or four days. An increase in fur state index is associated with a decrease in fur

quality. Fur state index reached a significantly higher score for both stressed groups compared with the basal groups. (C) After mice were sacrificed, adrenal glands and (D) thymi were dissected at day 21 and analyzed in relation to the animal's body weight. The weight of adrenal glands was significantly increased for both stressed groups, whereas the thymus weight was significantly decreased. | Data are presented as means \pm SEM; $n = 12$; * significantly different from control condition of same genotype, * $p < 0.05$, ** $p < 0.01$, *** $p < 0.001$, for (A) and (B) Repeated-measures ANOVA, for (C) and (D) One-Way ANOVA; CSDS = chronic social defeat stress; Hdac1-CTRL = control littermate; Hdac1-cKO = conditional Hdac1 knockout mouse.

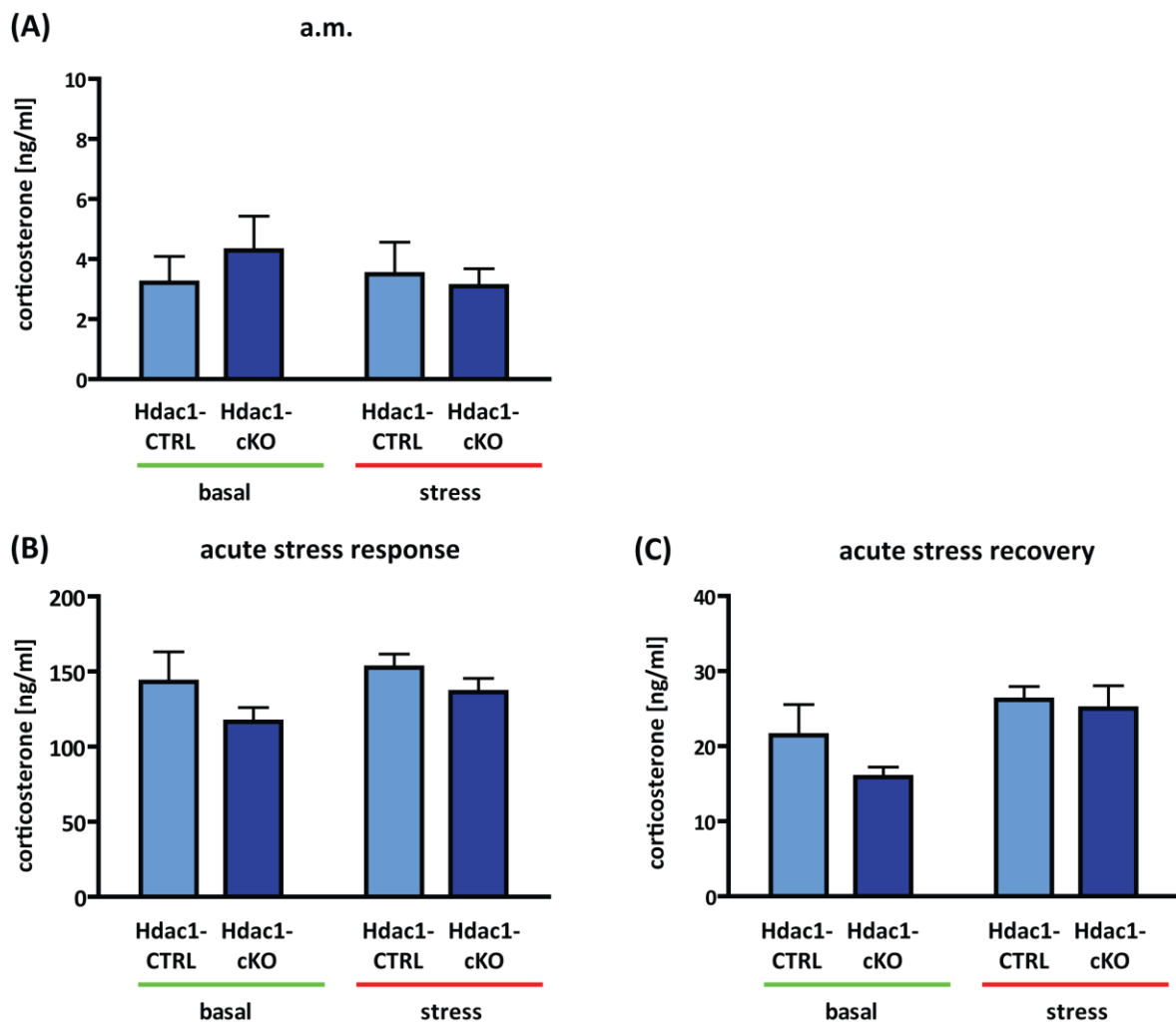


Figure 33. Analysis of corticosterone levels of conditional Hdac1 knockout mice subjected to the chronic social defeat stress (CSDS) paradigm. (A) Plasma corticosterone levels were analyzed for all four groups in the morning (a.m.) to obtain basal values. No genotype or condition effect was assessed. (B) Corticosterone levels were analyzed 15 min after the onset of the forced swim test (FST) as acute stressor. No genotype or condition effect was assessed. (C) 90 min after the start of the FST, corticosterone levels were analyzed. All groups recovered well from the stress indicated by low corticosterone levels. | Data are presented as means \pm SEM; $n = 12$; Two-Way ANOVA; CSDS = chronic social defeat stress; FST = forced swim; Hdac1-CTRL = control littermate; Hdac1-cKO = conditional Hdac1 knockout mouse.

Five behavioral tests were conducted in week three of the CSDS paradigm within five consecutive days (Figure 31) to assess locomotion, explorative, social, reward-seeking, anhedonic, anxiety-related, depression-like and stress-coping behavior.

The open field (OF) test was used to identify locomotor activity and explorative behavior as well as anxiety-related behavior. Test data were analyzed for the first 15 minutes of the test and revealed a condition effect for locomotion indicated by total distance travelled (Two-Way-ANOVA, * $p < 0.05$) (Figure 34.A) as well as a condition effect for time immobile (Two-Way-ANOVA, * $p < 0.05$) (Figure 34.B), inner zone entries (Two-Way-ANOVA, * $p < 0.05$) (Figure 34.E) and time spent in the inner zone (Two-Way-ANOVA, * $p < 0.05$) (Figure 34.F) indicating an increased anxiety-related behavior of defeated mice independent of genotype (Hdac1-CTRL versus Hdac1-cKO). A detailed analysis of the total distance travelled (Figure 34.C) and time immobile (Figure 34.D) in three segments of five minutes each, proved only an overall condition effect over the total duration of the test. A genotype effect was not observed for any of the analyzed parameters.

A variety of neurological and psychiatric disorders are characterized by deficits in social behavior. Therefore, we were interested in testing the defeated conditional Hdac1 knockout mice in the social approach/avoidance (SA) test. However, the analysis showed that the social behavior was not disrupted or influenced by the Hdac1 knockout or CSDS paradigm (Figure 35.A+B).

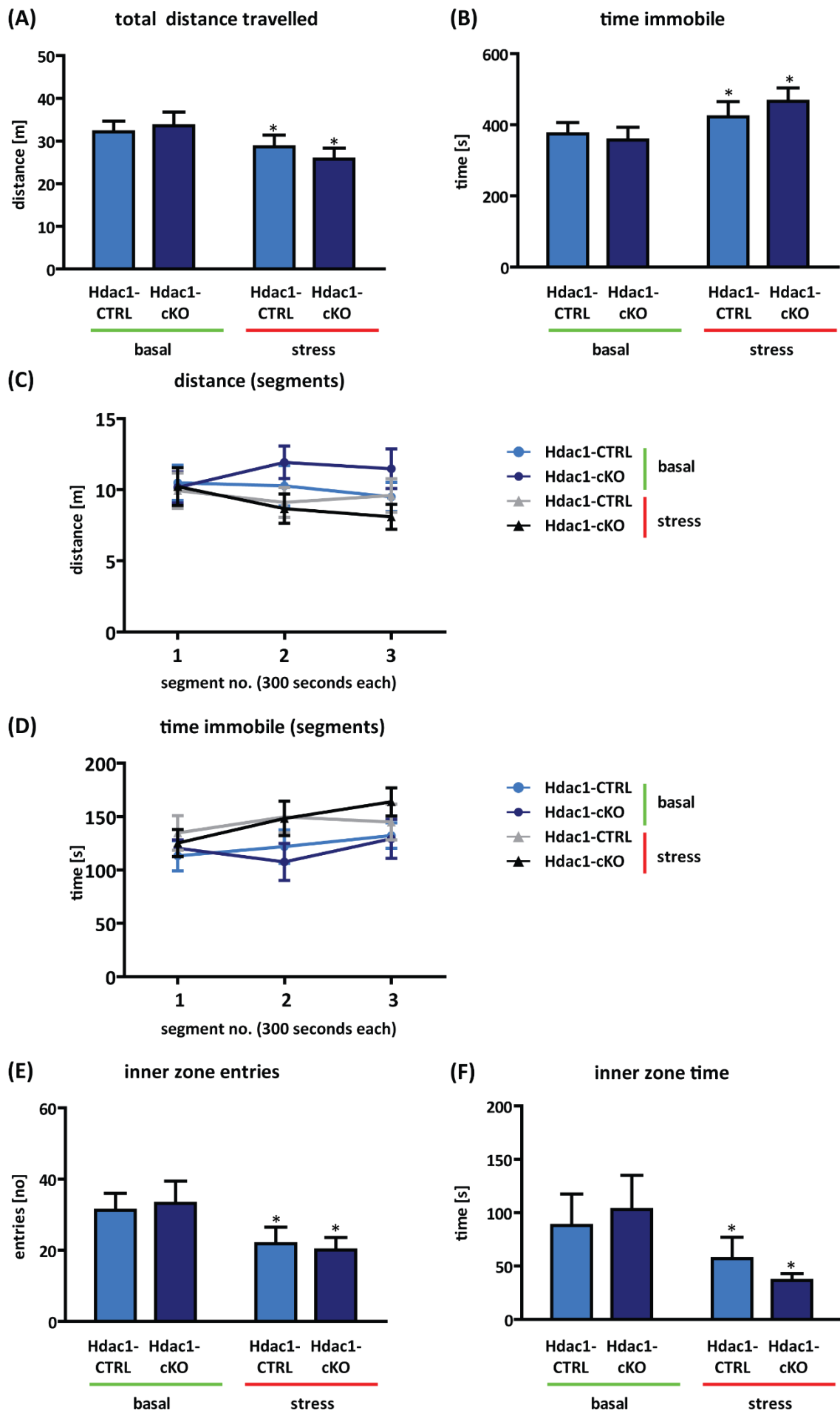


Figure 34. Analysis of the behavior of conditional Hdac1 knockout mice in the open field (OF) during the chronic social defeat stress (CSDS) paradigm. (A) A significant difference was observed in total distance travelled and (B) time immobile between the two conditions (basal and stress), but no genotype effect was detected. (C-D) The total test was also analyzed in segments of 5 minutes. However, for the single segments no significance was reached. (E-F) To observe anxiety-related and explorative behavior, the number of inner zone entries and inner zone time was analyzed and exhibited a condition effect as well. | Test duration analyzed: 15 minutes; data are presented as means \pm SEM; n = 12; * significantly different from control condition of same genotype, * p < 0.05, Two-Way ANOVA; OF = open field; CSDS = chronic social defeat stress; Hdac1-CTRL = control littermate; Hdac1-cKO = conditional Hdac1 knockout mouse.

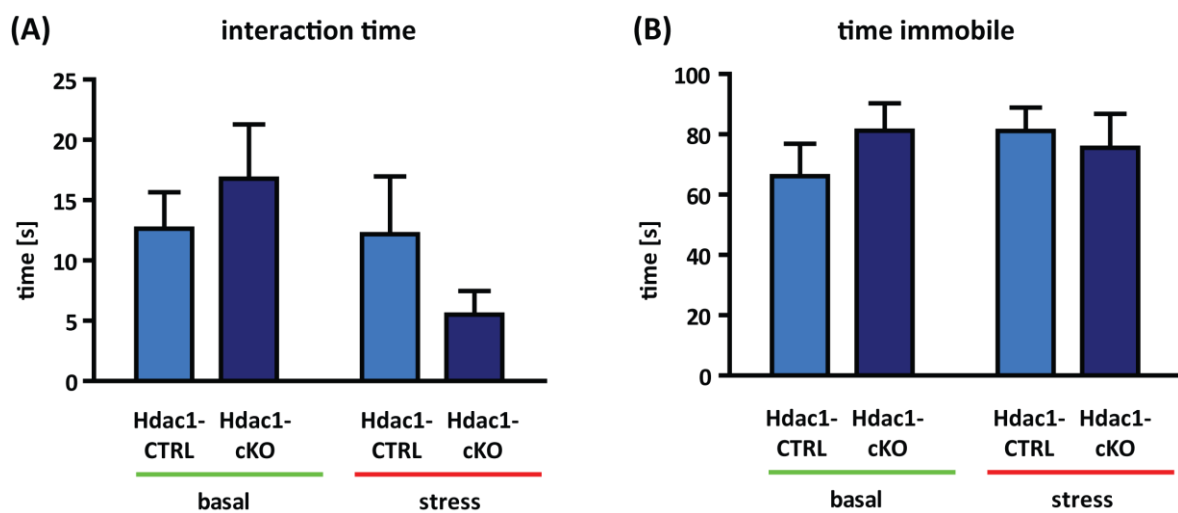


Figure 35. Analysis of conditional Hdac1 knockout mice in the social approach/avoidance (SA) test during the chronic social defeat stress (CSDS) paradigm. (A) No significant difference was observed for the interaction time with the social target in the second part of the test. (B) The time immobile showed no difference in regard to condition or genotype as well. | Test duration analyzed: 2.5 minutes; data are presented as means \pm SEM; n = 12; SA = social approach/avoidance; CSDS = chronic social defeat stress; Hdac1-CTRL = control littermate; Hdac1-cKO = conditional Hdac1 knockout mouse.

To gain more insight into behavioral alterations caused by the interaction of the missing HDAC1 enzyme and chronic stress, anhedonic behavior was assessed using the female urine sniffing test (FUST). Already within the first trial, when the cotton tips were soaked with water, mice with the control genotype exhibited a significant stress effect in sniffing time (Two-Way-ANOVA, ** p < 0.01) (Figure 36.A), whereas the conditional Hdac1 knockout mice seemed to compensate this effect and did not show a condition effect in this trial. However, analyzing the urine trial, control mice seemed to minimize the condition effect evoked in the water trial, but the conditional Hdac1 knockout mice showed a decreased sniffing time proposing a dramatic increase in anhedonic behavior between

undefeated and defeated mice in relation to the deleted HDAC1 enzyme (Hdac1-CTRL: Two-Way-ANOVA, * $p < 0.05$; Hdac1-cKO: Two-Way-ANOVA, *** $p < 0.001$) (Figure 36.B).

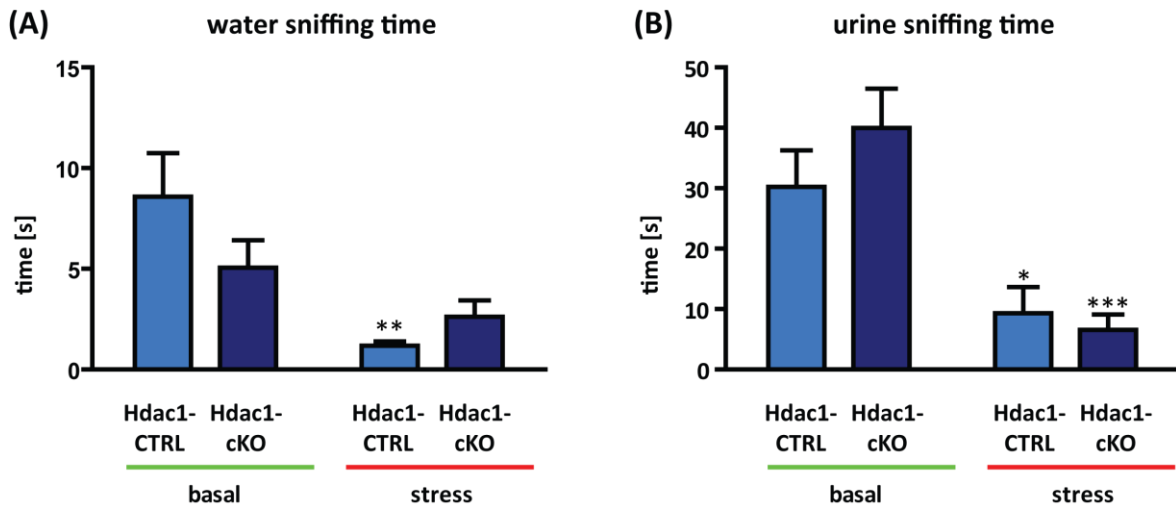


Figure 36. Analysis of conditional Hdac1 knockout mice in the female urine sniffing test (FUST) during the chronic social defeat stress (CSDS) paradigm. (A) In the water trial, defeated mice from the control group sniffed significantly less at the water-soaked tip compared to the undefeated control mice. No condition effect was observed for the Hdac1-cKO mice. (B) However, the urine trial showed still a condition effect for mice with Hdac1-CTRL genotype and also a highly significant condition effect for Hdac1-cKO mice. | Test duration analyzed: 3 minutes; data are presented as means \pm SEM; $n = 12$; * significantly different from control condition of same genotype, * $p < 0.05$, ** $p < 0.01$, *** $p < 0.001$, Two-Way ANOVA; FUST = female urine sniffing test; CSDS = chronic social defeat stress; Hdac1-CTRL = control littermate; Hdac1-cKO = conditional Hdac1 knockout mouse.

The elevated plus maze (EPM) test was used to assess anxiety-related behavior in chronically stressed animals. We could detect condition effects for parameters like total distance travelled (Two-Way-ANOVA, ** $p < 0.05$) (Figure 37.A), open arm entries (Two-Way-ANOVA, * $p < 0.05$) (Figure 37.B) and open arm time (Two-Way-ANOVA, * $p < 0.05$) (Figure 37.C) for both genotypes indicating that chronically stressed animals explore less and revealed increased anxiety-related behavior. Analysis of the latency to first open arm entry revealed a condition effect for the Hdac1-cKO animals (Two-Way-ANOVA, ** $p < 0.01$), a genotype effect under basal conditions (Two-Way-ANOVA, post-hoc test, ## $p < 0.01$), i.e. a genotype by condition interaction (Figure 37.D) and that the decrease of anxiety-related behavior in Hdac1-cKO mice observed under basal conditions in the previous experiment of the basal emotionality screen is reverted when mice are exposed to stress (compare Figure 28). However, the basal groups do not show the strong effect observed before

(Figure 28), but the same trend in the direction of decreased anxiety-related behavior in Hdac1-cKO mice is still visible. The loss of the strong effect with respect to decreased anxiety-related behavior of basal groups might be explained by the daily handling of the animals which might influence the behavior in comparison to totally naive animals.

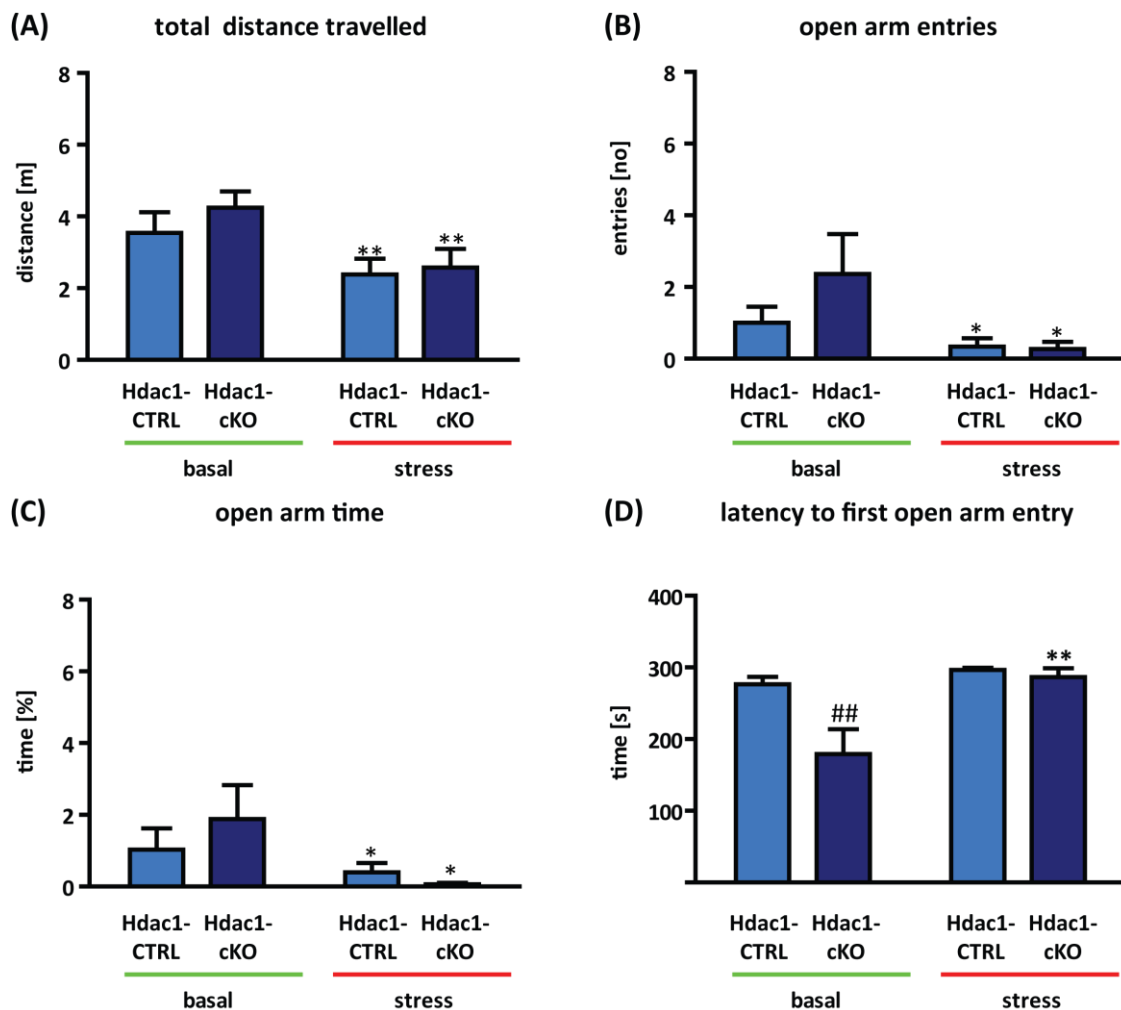


Figure 37. Analysis of conditional Hdac1 knockout mice in the elevated plus maze (EPM) test during the chronic social defeat stress (CSDS) paradigm. (A) The total distance travelled was decreased in both groups of defeated animals compared to the groups under basal conditions. (B) Also the open arm entries and (C) open arm time underscore a condition effect for both genotypes. (D) For the latency to the first open arm entry, a condition effect was observed for the Hdac1-cKO mice, but not for the Hdac1-CTRL mice. Under basal conditions a genotype effect could be detected as well. | Test duration analyzed: 5 minutes; Data are presented as means \pm SEM; n = 12; * significantly different from control condition of same genotype, * p < 0.05, ** p < 0.01, Two-Way ANOVA; # significantly different from control genotype of same condition, ## p < 0.01, Two-Way ANOVA, post-hoc test; EPM = elevated plus maze; CSDS = chronic social defeat stress; Hdac1-CTRL = control littermate; Hdac1-cKO = conditional Hdac1 knockout mouse.

The last test in the battery during the third week of the CSDS was the forced swim test (FST) to get an idea of depression-related or stress-coping behavior of defeated and undefeated conditional Hdac1 knockout mice. While assessing the two active stress-coping behavior types (struggling and swimming), we could show that both genotypes showed a condition effect in the amount of struggling which was higher for the defeated groups compared with undefeated groups (Two-Way-ANOVA, * $p < 0.05$) (Figure 38.A). Furthermore, we could show for both conditions a genotype effect with a significant decrease in the struggling amount of Hdac1-cKO mice compared to control groups (Two-Way-ANOVA, post-hoc test, # $p < 0.05$). The parameter swimming revealed only a condition effect for the knockout animals (Two-Way-ANOVA, * $p < 0.05$) (Figure 38.B). The third analyzed parameter, the passive stress-coping behavior floating showed no effects at all (Figure 38.C). Comparing the basal groups of Fig. 38 with the first basal screen of emotionality (Figure 30), Hdac1-cKO mice show the same effect in struggling, a trend in the same direction of the effect in swimming and a missing effect in both screens with regard to floating.

To summarize the main finding: when conditional Hdac1 knockout mice were exposed to chronic stress by using the CSDS paradigm, stressed mice with no regard to genotypes showed a decrease in locomotor activity and an increase in anxiety-related as well as active stress-coping and anhedonic behavior. Furthermore, in the elevated plus maze test, an inverted phenotype was detected when conditional Hdac1 knockout mice were chronically stressed (CSDS): Hdac1-cKO mice showed decreased anxiety-related behavior compared to control mice under basal conditions. But when subjected to stress, the Hdac1-cKO mice expressed increased anxiety-related behavior. The forced swim test revealed a decrease in struggling time for Hdac1-cKO mice compared with Hdac1-CTRL mice for both conditions (basal and CSDS).

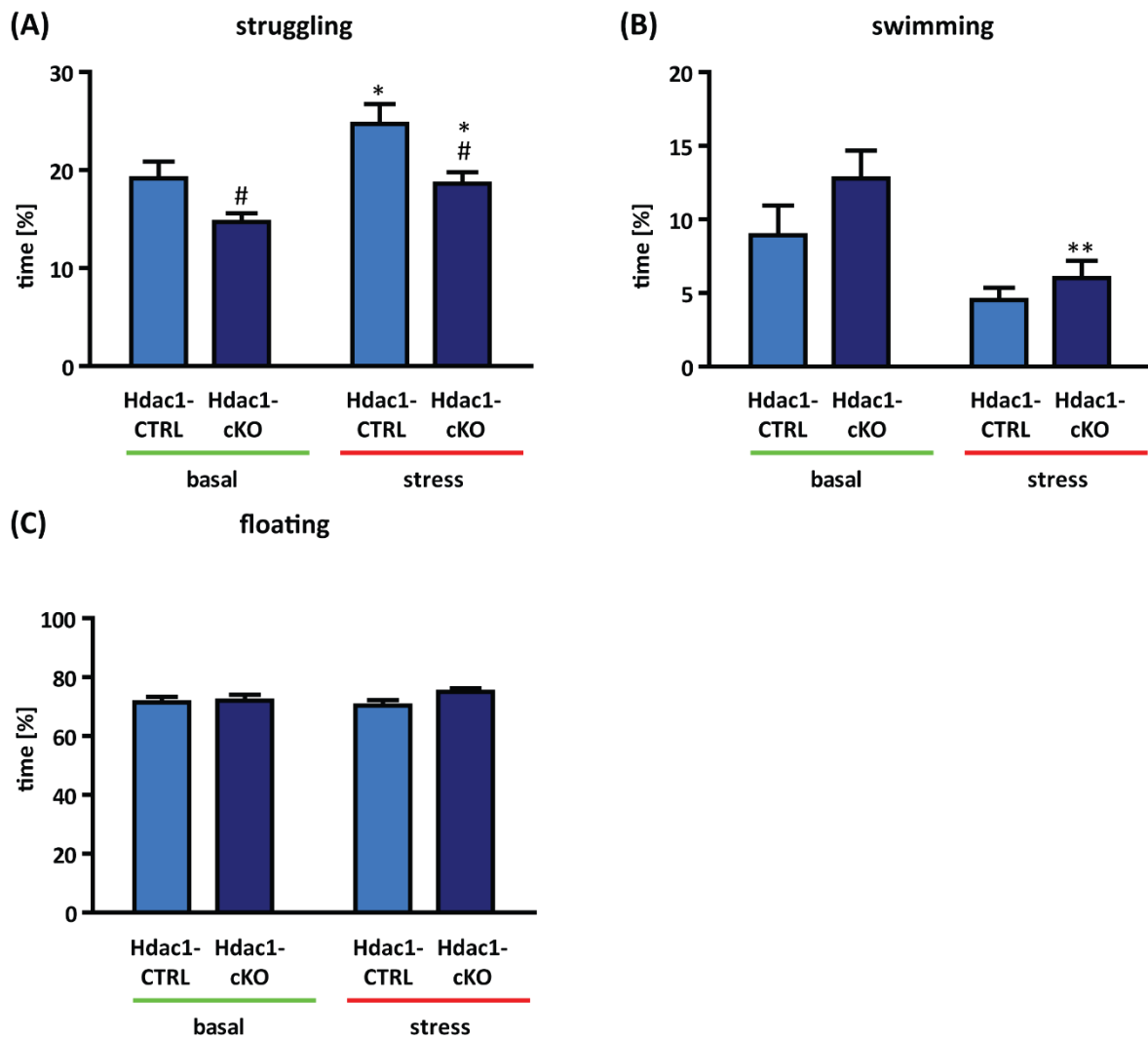


Figure 38: Analysis of conditional Hdac1 knockout mice in the forced swim test (FST) during the chronic social defeat stress (CSDS) paradigm. (A) For the active stress-coping behavior struggling, data analysis revealed a condition effect for both genotypes, as well as a decreased amount in struggling for Hdac1-cKO mice compared to Hdac1-CTRL mice of same conditions. (B) For the second active stress-coping behavior, swimming, only a genotype effect under defeated conditions was observed, whereas (C) the passive stress-coping behavior showed no effect at all. | Test duration analyzed: 6 minutes; Data are presented as means \pm SEM; $n = 12$; * significantly different from control condition of same genotype, * $p < 0.05$, ** $p < 0.01$, Two-Way ANOVA; # significantly different from control genotype of same condition, # $p < 0.05$, Two-Way ANOVA, post-hoc test; FST = forced swim test; CSDS = chronic social defeat stress; Hdac1-CTRL = control littermate; Hdac1-cKO = conditional Hdac1 knockout mouse.

4.3.2.3 Cognitive performance of conditional Hdac1 knockout mice

Epigenetic mechanisms and especially HDACs have emerged as important regulators for consolidation and maintenance of memory and learning behavior (Korzus et al., 2004; Levenson & Sweatt, 2005; Swank & Sweatt, 2001; Volmar & Wahlestedt, 2014). Numerous studies could prove that epigenetic marks are actively and transiently regulated in post-mitotic neurons of adult rodents, honeybees, aplysia and drosophila during learning processes (Chwang et al., 2006; Gupta et al., 2010; Kilgore et al., 2010; Levenson & Sweatt, 2005; Levenson et al., 2004; Lockett et al., 2010; Lubin & Sweatt, 2007; Maddox & Schafe, 2011; C. A. Miller et al., 2008; L. Miller et al., 2011). Therefore, chromatin remodeling mechanisms like acetylation induce lasting changes in behavior due to stimulus-specific cellular and molecular changes and will consolidate a memory into an everlasting trace. Most studies linking histone acetylation to learning processes and memory were conducted using HDAC inhibitors and could show that increased histone acetylation is associated with enhanced cognition (Korzus et al., 2004; Levenson & Sweatt, 2005; Swank & Sweatt, 2001; Volmar & Wahlestedt, 2014). Histone acetylation was especially shown to be involved in critical steps during the stabilization of short-term memory into long-term memory in wild-type mice (Korzus et al., 2004; Swank & Sweatt, 2001; Volmar & Wahlestedt, 2014). Furthermore, HDACs have been implicated in the pathogenesis of neurodegenerative diseases like Alzheimer's disease (Agis-Balboa et al., 2013; Broide et al., 2007; Covington et al., 2009; Fass et al., 2013). To get a first glance at the impact of HDAC1 loss in the murine forebrain in adulthood on memory and learning processes, we analyzed conditional Hdac1 knockout mice in the water cross maze (WCM) applying a protocol to assess hippocampus-dependent spatial learning.

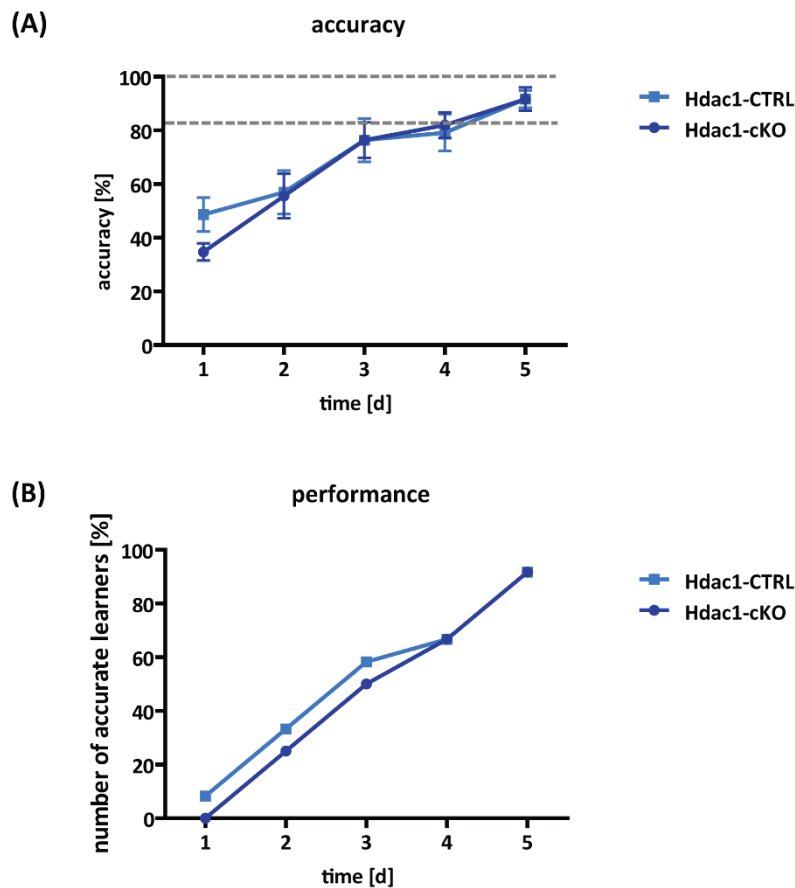


Figure 39: Analysis of conditional Hdac1 knockout mice in the water cross maze (WCM). (A) Spatial memory was evaluated by the accuracy indicating the success or failure of the mouse to swim the correct path to the platform. (B) A second parameter to interpret performance in the WCM is given by the number of accurate learners per group per day. | Data are presented as means \pm SEM; $n = 12$; Repeated-measures ANOVA; area between grey dashed lines = accuracy; WCM = water cross maze; Hdac1-CTRL = control; Hdac1-cKO = conditional Hdac1 knockout mouse.

The analysis of the performance of Hdac1-cKO mice in the WCM is indicated by the percent of accuracy (Figure 39.A). Given the natural tendency of mice to explore, one error within six trials per training day is permitted, which then manifests in an accuracy of 83.3% as the bottom threshold for a mouse to be considered as accurate. This threshold value was exceeded at training day five for both groups, Hdac1-cKO mice and Hdac1-CTRL mice, indicating that the mice did not suffer from any deficits in learning ability when Hdac1 is lacking in principal forebrain neurons. A second parameter to assess the cognitive behavior in the WCM was provided by the number of accurate learners of each group displaying a high learning performance for all animals independent of genotype (Figure 39.B).

In summary, it emerges in a first cognitive screen, that the HDAC1 enzyme missing in the murine forebrain in adulthood did not cause any deficits in memory and learning processes indicating that HDAC1 probably does not inhabit a crucial role in spatial learning.

4.4 Genetically dissecting brain-specific functions of histone deacetylase 3 (HDAC3)

4.4.1 Generation of conditional Hdac3 knockout mice

Compared to the ubiquitous Hdac1 expression throughout the adult murine brain, we showed in chapter 4.1 a distinct expression pattern for another class I HDAC, namely Hdac3. Hdac3 ranks among all eleven classical HDACs as the third highest expressed one within the adult murine brain. However, not only the expression intensity scores a high value, but also the number of brain regions where it is expressed is high. Like HDAC1, also HDAC3 seems to be detrimental in mouse development and knockout mice of Hdac3 die at E10.5 (Dangond et al., 1998, 1999; Glaser et al., 2003; Robyr et al., 2002). Therefore, we established conditional Hdac3 knockout animals to investigate the neuronal function of HDAC3.

4.4.1.1 Analysis of Hdac3-expression using lacZ reporter mice

As before described for HDAC1, we also obtained Hdac3-lacZ reporter mice ($Hdac3^{tm1a(EUCOMM)wtsi}$) from the European Conditional Mouse Mutagenesis Program (EUCOMM; <http://www.knockoutmouse.org/about/eucomm>; tm1a = targeted mutation 1a; wtsi = Wellcome Trust Sanger Institute) and used them for generation of conditional knockout mice lacking HDAC3 in principal forebrain neurons in adulthood. HDAC3 total knockout animals die at E10.5 (Dangond et al., 1998, 1999; Glaser et al., 2003; Robyr et al., 2002), therefore our Hdac3-lacZ mice are viable only as heterozygotes ($Hdac3^{tm1a(EUCOMM)wtsi}$) as the reporter allele disrupts the *Hdac3* allele. The murine wild-type locus of *Hdac3* is located on chromosome 18 and spans about 13 kb. The gene comprises 15 exons and 14 introns and exhibits an open reading frame of 1284 bp (de Ruijter et al., 2003; Mahlknecht, Bucala, et al., 1999; Mahlknecht, Emiliani, et al., 1999). The LacZ mutant allele with an inserted cassette was generated using a targeted trapping strategy of the wild-type locus of *Hdac3* (Figure 40). The gene trap cassette is the same used for HDAC1 and is integrated into intron 2 of *Hdac3*. It also consists of a splice acceptor (*engrailed 2 splice acceptor: En2 SA*), a *lacZ* gene driven by an internal ribosomal entry site (*IRES-lacZ*), a *phosphoglycerate kinase (PGK)* promoter driven *neomycin resistance* gene (*neo*) and a poly-adenylation signal (*simian virus 40 poly-adenylation signal: SV40 pA signal*). This cassette is flanked by two *frt* sites in parallel orientated followed by two *loxP* sites in parallel orientated flanking the critical exon 3. The *splice acceptor (SA)* and the *internal ribosomal entry site (IRES)* of the *lacZ* gene is necessary that the lacZ-reporter is driven by the endogenous *Hdac3* promoter elements. Thus, the first two exons of *Hdac3* are

transcribed and afterwards the translation is disrupted due to a premature stop codon. β -galactosidase (expressed by the *lacZ* gene) and the *neomycin* make up a fusion protein. The *frt* sites are recognized by the yeast enzyme Flp and *loxP* sites are recognition sites for the yeast Cre recombinase.

Similar to the procedure for HDAC1, a triple-primer genotyping PCR was established using one forward primer and two reverse primers to genotype mice for the presence of the reporter allele (Figure 40.B). Forward primer 1 (F1: Hdac3_EU_frt_F1) and reverse primer 1 (R1: Hdac3_EU_frt_R1) anneal to a DNA sequence present within the wild-type DNA sequence of *Hdac3* and produce a PCR product of 756 bp within the wild-type locus (Figure 40.C). In general, this primer pair can also create a PCR product in the *lacZ* mutant allele, but the sequence to be amplified is more than 5 kb long and the extension time of the PCR product is set to produce only smaller products up to 1 kb. Thus, the *lacZ* allele is only detected with the second gene trap cassette targeting vector-specific reverse primer (R2: Hdac3_EU_frt_R2) which amplifies together with F1 a PCR product of 341 bp (Fig. 40.B and C).

To describe the expression pattern of *Hdac3*, we used not only the earlier described *ISH* analysis (chapter 4.1), but also used the Hdac3-*lacZ* reporter mice (Figure 41.A-C). As mentioned in chapter 4.3 for HDAC1, a *lacZ*-based reporter mouse line enables a straight-forward screening of expression of a gene of interest. Expression analysis was therefore performed on brain sections and whole organs. Heterozygous male Hdac3-*lacZ* reporter mice ($Hdac3^{tm1a(EUCOMM)wtsi}$) were sacrificed at the age of 2-3 months, various organs were removed and subsequently stained for *lacZ* expression (Figure 41.A). We could show that *Hdac3* is more or less ubiquitously expressed and detectable in many tissues (e.g. diaphragm, heart, kidney, adrenal gland, liver, lung, pituitary, spinal cord, spleen, thymus, tongue) which goes in line with the literature which describes, that class I HDACs are broadly expressed within various tissues (de Ruijter et al., 2003). Furthermore, we used the Hdac3-*lacZ* ($Hdac3^{tm1a(EUCOMM)wtsi}$) reporter mice to determine the expression level and pattern of HDAC3 throughout the adult murine brain (Figure 41.B). *LacZ* staining confirms the *ISH* for *Hdac3* mRNA (Figure 41.C). HDAC3 as the third highest expressed classical HDAC shows a high expression level in intensity as well as numerous brain regions, where it is expressed. However, the highest expression could be detected in cortical structures, the hippocampal formation and the cerebellum (Fig. 41.B).

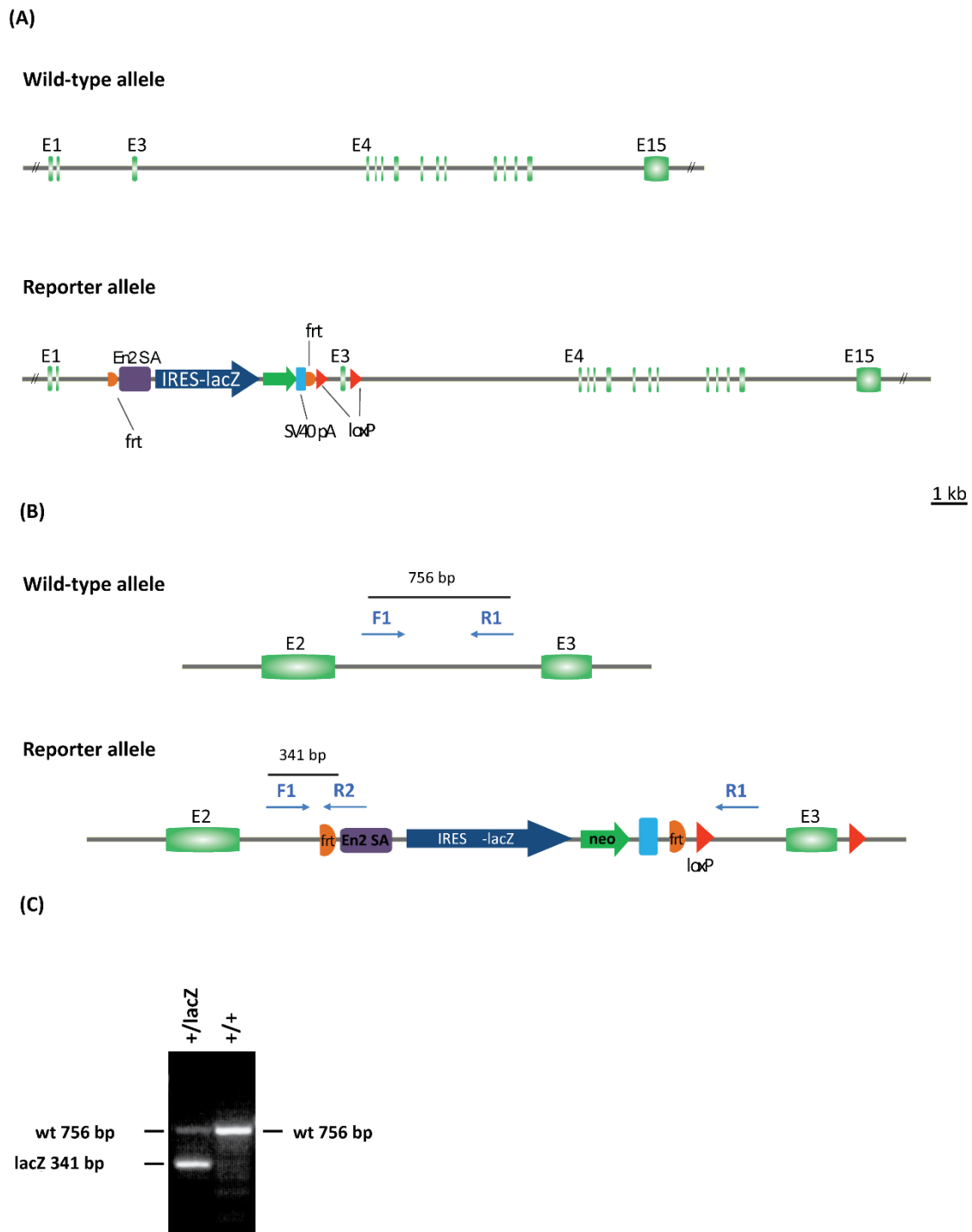





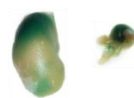
































Figure 40. Schematic representation of the *Hdac3* wild-type locus and the *lacZ* reporter allele generated by targeted trapping. (A) *Hdac3* wild-type allele with 15 exons (E: depicted in light green) and respective reporter allele which was generated using a targeted trapping strategy of the *Hdac3* gene locus. | frt = Flp recognition target: depicted in orange; *EN2 SA* = *engrailed 2 splice acceptor*: depicted in violet; *IRES-lacZ* = *internal ribosomal entry site-lacZ*: depicted in blue; *PGK neo* = *phosphoglycerate kinase promoter driven neomycin resistance gene*: depicted in green; *SV40 pA* = *simian virus 40 poly-adenylation signal*: depicted in light blue; Cre recognition target = *loxP* site: depicted in yellow; (B) Schematic representation of genotyping strategy to identify mice carrying the *Hdac3-lacZ* reporter allele. Identification of wild-type and

mutant alleles by genotyping PCR using a forward primer (F1: Hdac3_EU_frt_F1) and a reverse primer (R1: Hdac3_EU_frt_R1) annealing to wild-type sequences, whereas a third primer (reverse primer 2; R2: Hdac3_EU_frt_R2) anneals to a sequence within the gene trap cassette. (C) Genotyping of Hdac3-lacZ reporter mice by PCR depicting results of a wild-type and a heterozygous reporter mouse, respectively. Primer F1 and R1 produce a 756 bp wild-type product and primer F1 and R2 produce a 341 bp lacZ product. [EUComm; <http://www.knockoutmouse.org/about/eucomm>]

(A)

+/<i>lacZ</i>	colon 	diaphragm 	duodenum 	fat 	heart 	kidney, adrenal gland 
+/+	colon 	diaphragm 	duodenum 	fat 	heart 	kidney, adrenal gland 
+/<i>lacZ</i>	liver 	lung 	pancreas 	pituitary 	SG 	skin (ear) 
+/+	liver 	lung 	pancreas 	pituitary 	SG 	skin (ear) 
+/<i>lacZ</i>	spinal cord 	spleen 	stomach 	testis, bladder 	thymus 	tongue 
+/+	spinal cord 	spleen 	stomach 	testis, bladder 	thymus 	tongue 

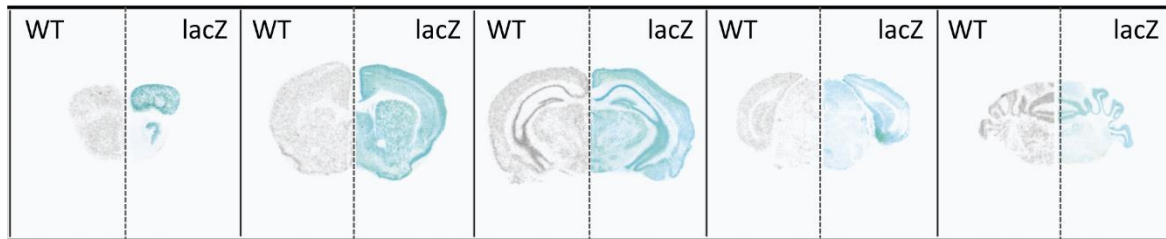
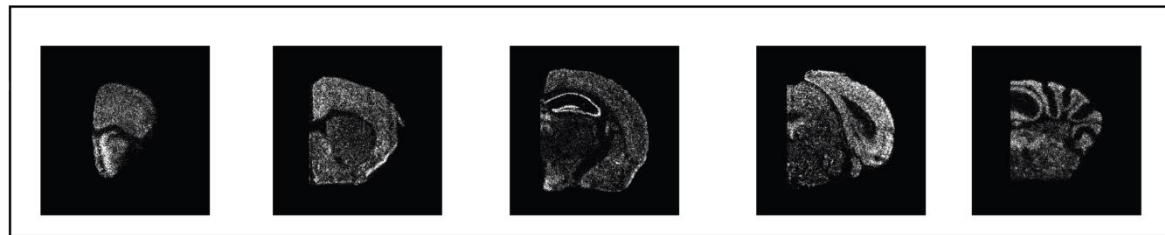
(B)**(C)**

Figure 41. *Hdac3* expression revealed by Hdac3-lacZ reporter mice. (A) Whole mount lacZ staining of various organs of heterozygous Hdac3-lacZ reporter mice. Organs were removed from heterozygous male Hdac3-lacZ reporter mice and wild-type mice after animals were sacrificed and subsequently lacZ stained. As β -galactosidase is expressed under the control of the *Hdac3* promoter the staining resembles the endogenous HDAC3 expression pattern. Unspecific staining was excluded by positive controls like colon and stomach which contain bacteria expressing naturally β -galactosidase and therefore show a positive staining for both, reporter and wild-type mice. (B) LacZ staining of 40 μ m-thick coronal brain sections of wild-type mice (left side) and Hdac3-lacZ reporter mice (right side). The lacZ staining in reporter mice resembles HDAC3 expression. (C) For comparison qualitative ISH analysis of *Hdac3* using a specific radiolabeled riboprobe was performed. Depicted are representative dark-field photomicrographs of a series of 20 μ m-thick coronal brain sections of a wild-type mouse hybridized with the indicated probe to show *Hdac3* expression on mRNA level.

4.4.1.2 Establishment of conditional Hdac3 knockout mice

We established conditional Hdac3 knockout mice by using the same strategy described for HDAC1 (chapter 4.3.1.2) and thus we only want to briefly mention it here: breeding of heterozygous Hdac3-lacZ reporter mice to Flp-Deleter mice (Figure 42 and 43.A) results in mice carrying the means for a conditional inactivation by the “floxed” exon three. These heterozygous floxed mice ($Hdac3^{+/lox}$, Flp deleter) were bred to mice of a tamoxifen inducible Cre line. As a Cre driver, we chose also here the Camk2a-CreER^{T2} mice (Erdmann et al., 2007). By the choice of the Camk2a-CreER^{T2} line we achieved temporally controlled somatic mutagenesis by the use of tamoxifen administration in the adult stage and exclude developmental effects, adaptive changes and in particular embryonic lethality. Furthermore, the CreER^{T2} is expressed under the control of the regulatory element of the *Camk2a* gene and therefore we have a spatially restricted Cre expression to induce the Hdac3 knockout only

in principal neurons of the adult forebrain. Conditional Hdac3 knockout mice ($Hdac3^{lox/lox}Camk2aCreER^{T2}$ referred to as Hdac3-cKO) and control littermates ($Hdac3^{lox/lox}$ referred to as Hdac3-CTRL) were obtained by the breeding strategy depicted in Figure 42.

Upon tamoxifen treatment via the strategy developed in chapter 4.2, Cre recombination was achieved in all principal forebrain neurons deleting *Hdac3* exon three which leads to a frame-shift and to a premature stop codon resulting in a non-functional HDAC3 enzyme.

The above mentioned triple-primer genotyping PCR was not only used to genotype mice for the presence of the *Hdac3* wild-type and lacZ reporter allele, but also to assess the floxed allele (Figure 43.B and C). Therefore, the forward primer 1 (F1: Hdac3_EU_frt_F1) and reverse primer 1 (R1: Hdac3_EU_frt_R1) were used to amplify also a PCR product in the floxed allele which is bigger than the allele of the wild-type locus (890 bp versus 756 bp). The second reverse primer (F2: Hdac3_EU_frt_R2) still creates together with F1 only in the lacZ locus a product with a size of 341 bp. Thus, the triple PCR is able to distinguish genotypes of $Hdac3^{+/+}$ (wild-type), $Hdac3^{+/lacZ}$ (heterozygous reporter), $Hdac3^{+/lox}$ (heterozygous floxed) and $Hdac3^{lox/lox}$ (homozygous floxed). Two additional PCRs to detect the Flp and CreER^{T2} were performed on genomic tail DNA of each animal (data not shown).

For successful disruption of Hdac3 within principal neurons of the adult murine forebrain, mice were fed seven days with tamoxifen chow and sacrificed after another seven days of wash-out. Brain slices were analyzed via ISH using a riboprobe detecting specifically exon 3 of the *Hdac3* mRNA (Figure 44). We could demonstrate especially in the hippocampus and cortical structures the loss of *Hdac3* expression in conditional Hdac3 knockout animals on mRNA level. The conditional knockout of Hdac3 was further validated on protein level. Western blot (WB) analysis clearly reveals reduced HDAC3 expression in hippocampal lysates of Hdac3-cKO mice compared to Hdac3-CTRL littermates. However, the small amount of remaining HDAC3 protein in the knockout animals detected by WB analysis originated from cells (i.e. glia cells) which do not express CreER^{T2}. In all subsequent experiments, we used $Hdac3^{lox/lox}Camk2aCreER^{T2}$ mice (Hdac3-cKO) animals and their control littermates ($Hdac3^{lox/lox}Camk2aCreERT2 = Hdac3-CTRL$).

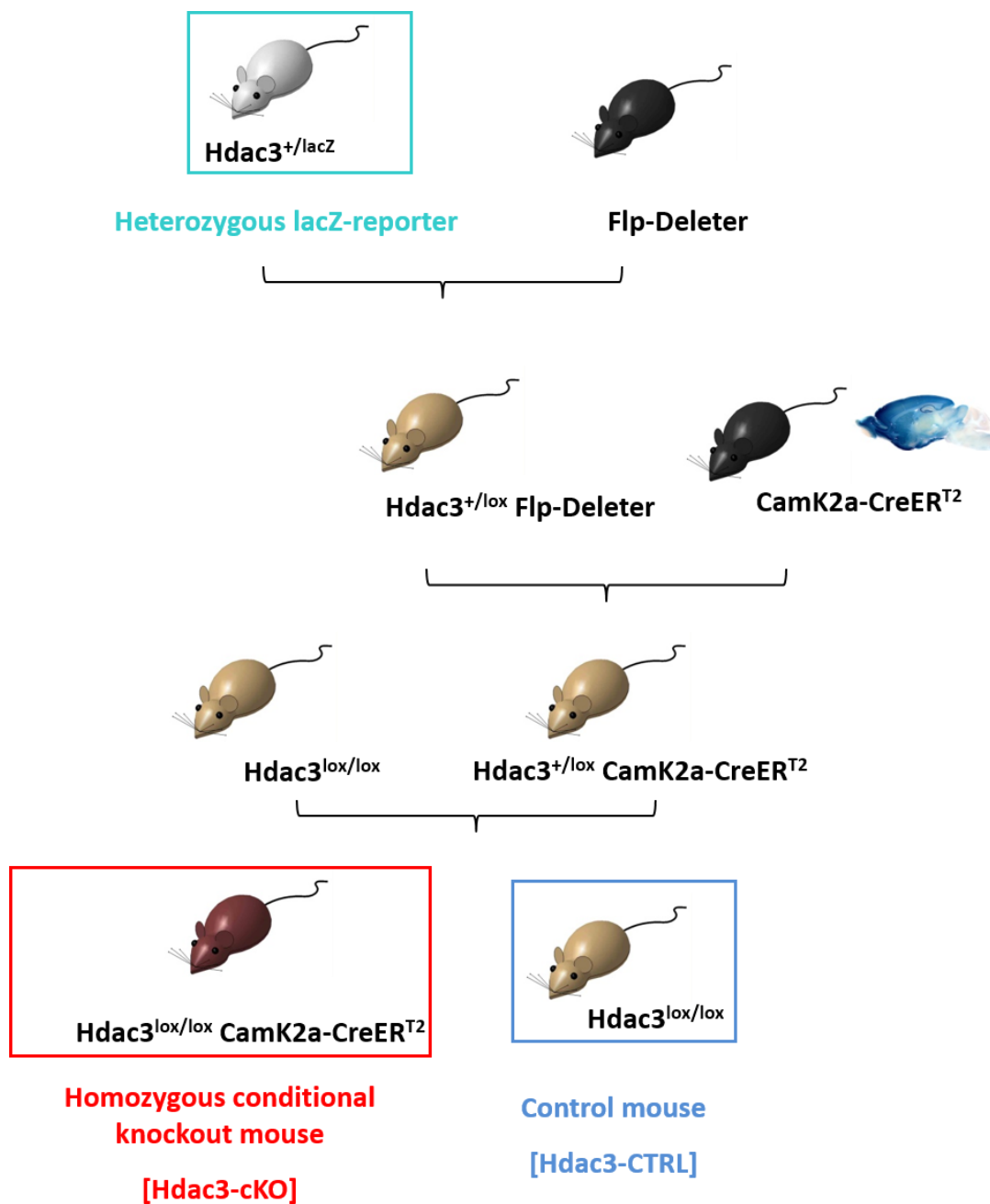
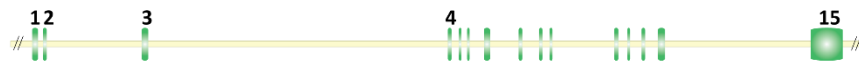


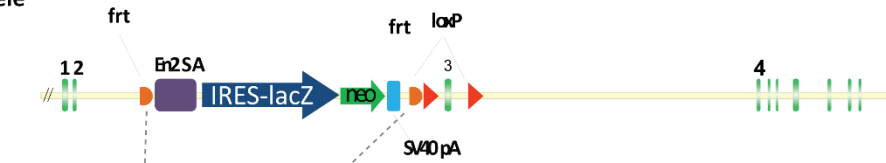
Figure 42. Breeding scheme to generate conditional *Hdac3* knockout mice. Heterozygous *Hdac3*-*lacZ* reporter mice ($Hdac3^{+/lacZ}$) were bred to Flp-Deleter mice for removal of the selection cassette. Recombination between the two *frt* sites restored *Hdac3* expression and left the critical exon 3 flanked by *loxP* sites ("floxed"). $Hdac3^{+/lox}$ Flp-Deleter mice were bred to the hemizygous inducible Cre-driver *Camk2a-CreER^{T2}* resulting in $Hdac3^{+/lox} Camk2a-CreER^{T2}$ which were bred to homozygous floxed mice ($Hdac3^{lox/lox}$) to finally obtain homozygous conditional *Hdac3* knockout mice ($Hdac3^{lox/lox} Camk2a-CreER^{T2}$ = *Hdac3*-cKO) and within the same breeding control littermates ($Hdac3^{lox/lox}$ = *Hdac3*-CTRL).

(A)

Wild-type allele

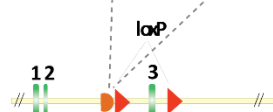


Reporter allele



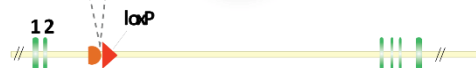
+ FLP

Floxed allele



+ Cre

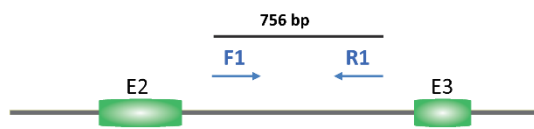
Knockout allele



1 kb

(B)

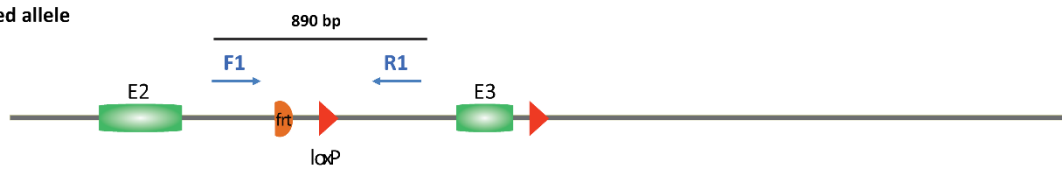
Wild-type allele



Reporter allele



Floxed allele



(C)

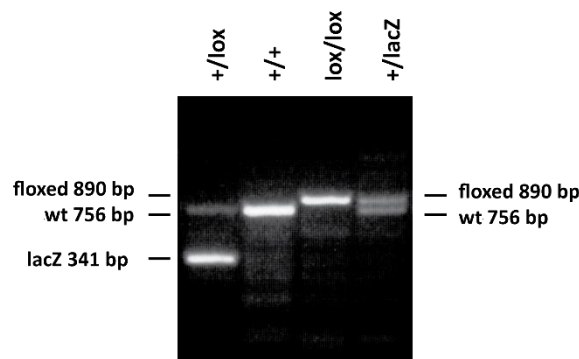


Figure 43. Schematic representation of the Hdac3 wild-type locus, lacZ allele, floxed allele and knockout allele generated by targeted trapping and subsequent excision via Flp and Cre. (A) Hdac3 wild-type allele comprising 15 exons (E: depicted in light green), reporter allele generated by the targeted trapping strategy, floxed allele obtained via Flp-mediated recombination of the reporter allele and knockout allele after further Cre-mediated recombination. | frt = Flp recognition target: depicted in orange; EN2 SA = engrailed 2 splice acceptor: depicted in violet; IRES-lacZ = internal ribosomal entry site-lacZ: depicted in blue; PGK neo = phosphoglycerate kinase promoter driven neomycin resistance gene: depicted in green; SV40 pA = simian virus 40 poly-adenylation signal : depicted in light blue; Cre recognition target = loxP site: depicted in yellow; (B) Schematic representation of genotyping strategy to identify mice carrying the Hdac3 wild-type allele, lacZ reporter allele or floxed allele. Identification of wild-type, reporter and floxed alleles was possible by genotyping PCR using a forward primer (F1: Hdac3_EU_frt_F1) and a reverse primer (R1: Hdac3_EU_frt_R1) annealing to wild-type sequences, whereas a third primer (reverse primer 2; R2: Hdac3_EU_frt_R2) anneals to a sequence within the gene trap cassette. (C) Genotyping of Hdac3-lacZ reporter mice and floxed Hdac3 mice by PCR depicting results of a heterozygous floxed mouse, a wildtype mouse and a heterozygous reporter mouse, respectively. Primer F1 and R1 produce a 756 bp wild-type product and a 890 bp floxed product, whereas primer F1 and R2 produce a 341 bp lacZ product.

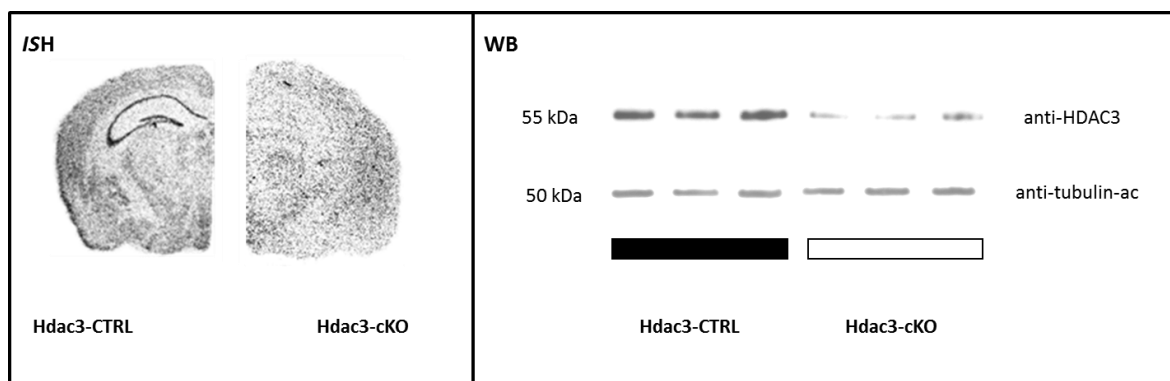


Figure 44. Verification of HDAC3 disruption in conditional Hdac3 knockout mice upon tamoxifen treatment. Hdac3-cKO and Hdac3-CTRL mice were fed for 7 days with tamoxifen chow and analyzed after a 7 day wash-out phase via *in situ* hybridization (ISH) and Western Blot analysis (WB). The left panel shows qualitative ISH analysis using a radiolabeled riboprobe which specifically detects exon 3 of the *Hdac3* mRNA. Depicted are representative bright-field photomicrographs of autoradiographs of 20 μ m-thick coronal brain slices of control (left side) and conditional knockout (right side) mice. The right panel shows WB against HDAC1 of hippocampal lysates of control and conditional knockout animals.

4.4.2 Behavioral characterization of conditional Hdac3 knockout mice lacking HDAC3 in principal forebrain neurons

4.4.2.1 Basal behavioral screening of conditional Hdac3 knockout mice

As we showed before for HDAC1 (chapter 4.3.2.1), we also performed a comprehensive basal behavioral characterization of conditional Hdac3 knockout mice. Therefore, mice lacking HDAC3 in principal forebrain neurons (Hdac3-cKO) and Hdac3-CTRL littermates were tested. To induce the knockout, we also used the previously described tamoxifen strategy (chapter 4.2.) and conducted four tests within seven days following the schedule depicted in Figure 45 to assess locomotion and explorative, anxiety-related, depression-related and stress-coping behavior.

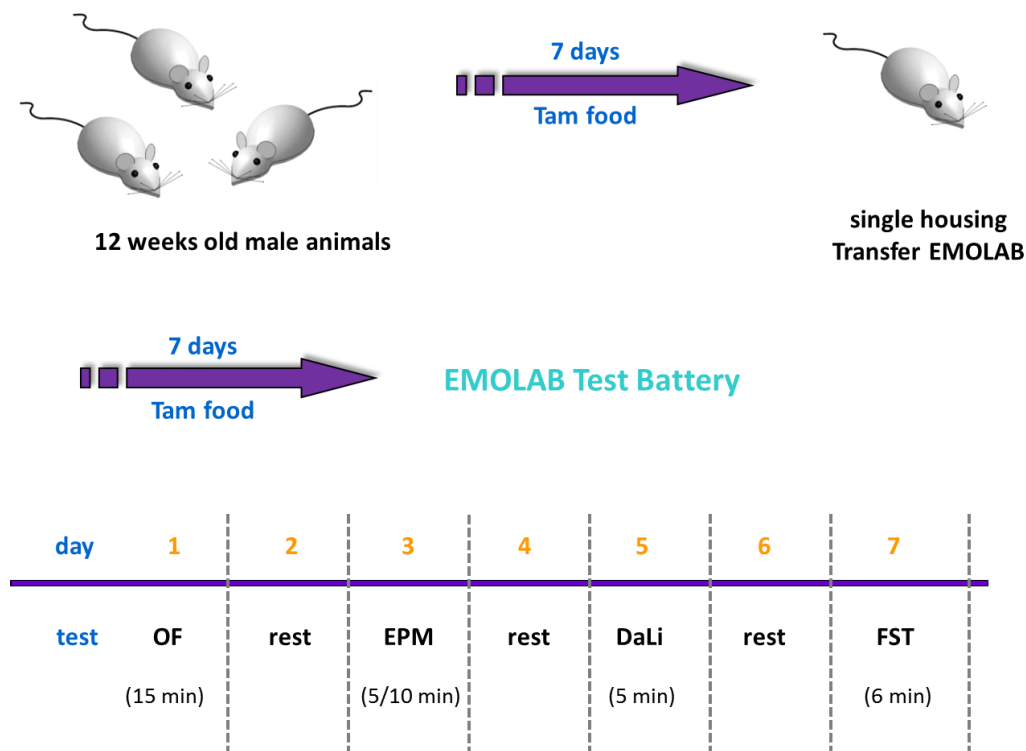


Figure 45. Testing schedule for basal emotionality screen of Hdac3 conditional knockout mice. Each test was followed by one day rest for the animals before conducting the next test. [OF = open field; EPM = elevated plus maze; DaLi = dark/light box; FST = forced swim test]

To assess locomotor activity as well as explorative behavior and anxiety-related behavior of conditional Hdac3 knockout mice and control littermates, we used the open field (OF) test. No difference in locomotion of conditional Hdac3 knockout mice compared to control littermates, neither in total distance travelled (Figure 46.A), nor when split into segments of five minutes (Figure 46.C) were found when data was analyzed for the first 15 min of the OF test. Anxiety-related behavior was assessed using parameters such as total time spent immobile (Figure 46.B), time spent immobile within segments of five minutes (Figure 46.D), number of entries to the inner zone (Figure 46.E) and total time spent in the inner zone (Figure 46.F), which all revealed no significant difference between the two genotypes as well.

Another test to assess anxiety-related behavior was the elevated plus maze (EPM) test. Mouse behavior was analyzed for five minutes, but no significant variation was observed between Hdac3-cKO and Hdac-CTRL mice as the values for the total distance travelled throughout the test (Figure 47.A), the number of open arm entries (Figure 47.B), the time spent on the open arm (Figure 47.C) and the latency to first open arm entry (Figure 47.D) did not reach significance in their difference.

Furthermore, a third test was used to analyze mice behavior in regard to anxiety-related behavior. This was the dark/light box (DaLi) test which is a more aversive test than the EPM test. The DaLi test revealed no significant difference in the time spent in the aversive surrounding of the lit compartment (Figure 48.A), but the Student's t-test showed that Hdac3-cKO mice visited the lit compartment more frequently than their control littermates ($\# p < 0.05$) (Figure 43.B). However, the latency to the first entry to the lit compartment was for both groups similar (Figure 48.C). The total distance mice travelled throughout the 5 minutes test time was also similar (Figure 48.D), but differed for the distance travelled within the lit compartment (Figure 48.E). Thus, the Student's t-test revealed a significantly higher value for the Hdac3-cKO mice ($\# p < 0.05$), whereas the distance travelled within the dark compartment was similar again (Figure 48.F).

To assess stress-coping and depression-related behavior in conditional Hdac3 knockout mice, the forced swim test (FST) was performed. However, Hdac3-cKO revealed neither a differences in active stress-coping behavior (struggling and swimming) (Figure 49.A and B) nor in the passive stress-coping parameter floating (Figure 49.C) when compared to Hdac3-CTRL mice.

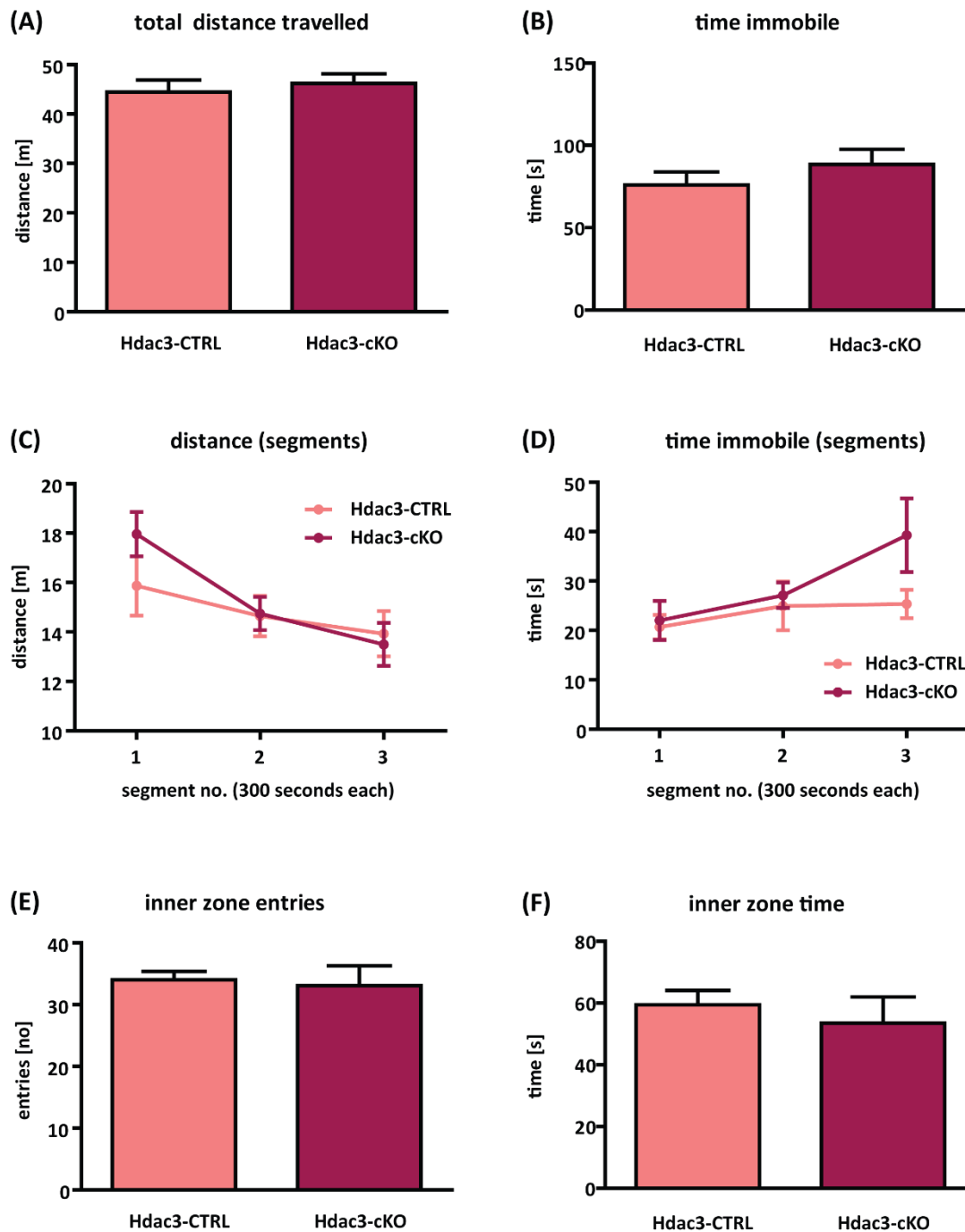


Figure 46. Analysis of conditional Hdac3 knockout mice in the open field (OF) test. (A) No significant difference was observed in total distance travelled (B) nor in time spent immobile. (C-D) The total test was also analyzed in segments of 5 minutes. Also here, no significant difference was revealed between the two genotypes. (E-F) To observe anxiety-related and explorative behavior, the number of inner zone entries and inner zone time was analyzed. Again no difference was observed. | Test duration analyzed: 15 minutes; Data are presented as means \pm SEM; n = 10-12; Hdac3-CTRL = control littermate; Hdac3-cKO = conditional Hdac3 knockout mouse.

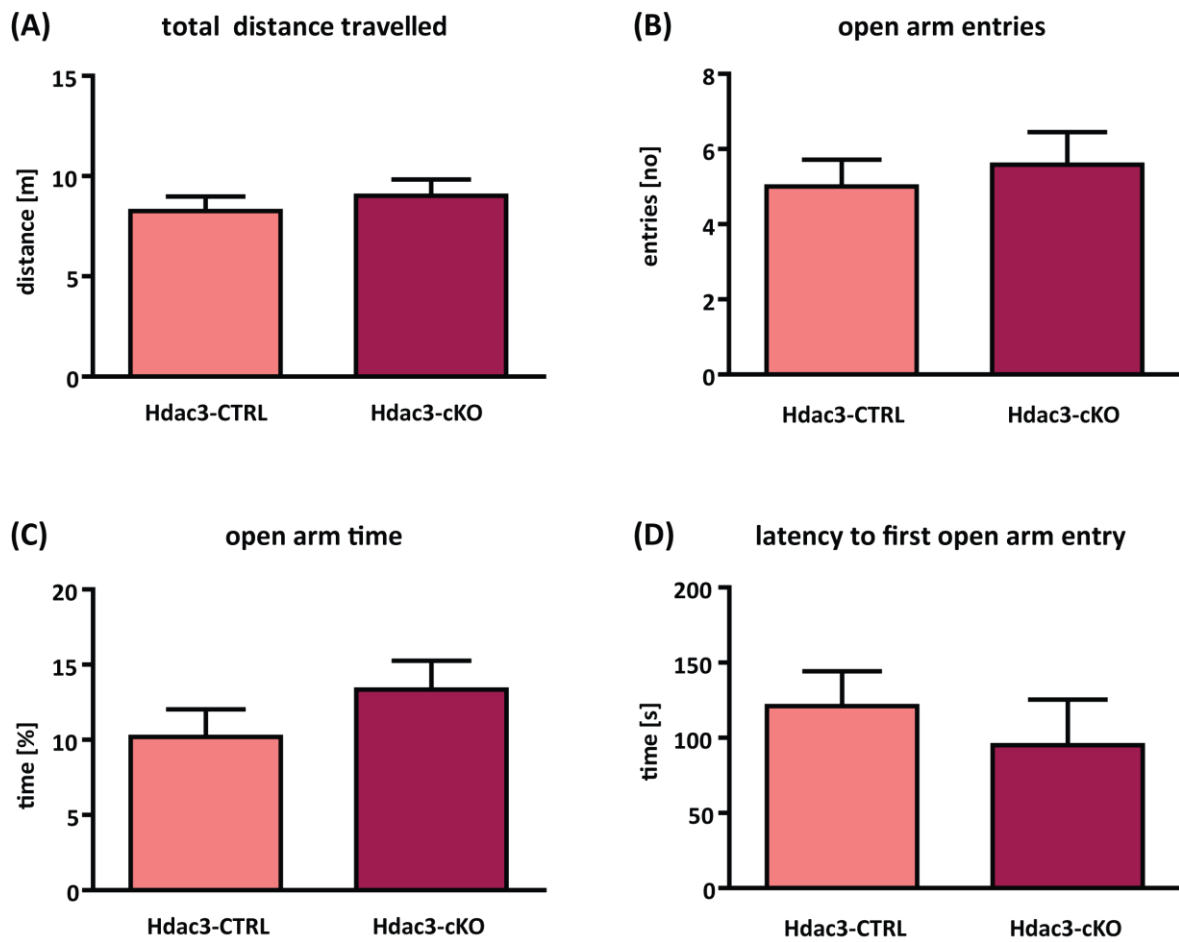


Figure 47. Analysis of conditional Hdac3 knockout mice in the elevated plus maze (EPM) test. (A) Hdac3-cKO mice showed no difference in total distance travelled within the EPM test when compared to Hdac3-CTRL mice, (B) nor did Hdac3-cKO differ from Hdac3-CTRL mice with respect to open arm entries or (C) time spent in the open arm. (D) Also the latency to the first open arm entry was not significantly different between the two genotypes. | Test duration analyzed: 15 minutes; Data are presented as means \pm SEM; $n = 11-13$; Hdac3-CTRL = control littermate; Hdac3-cKO = conditional Hdac3 knockout mouse.

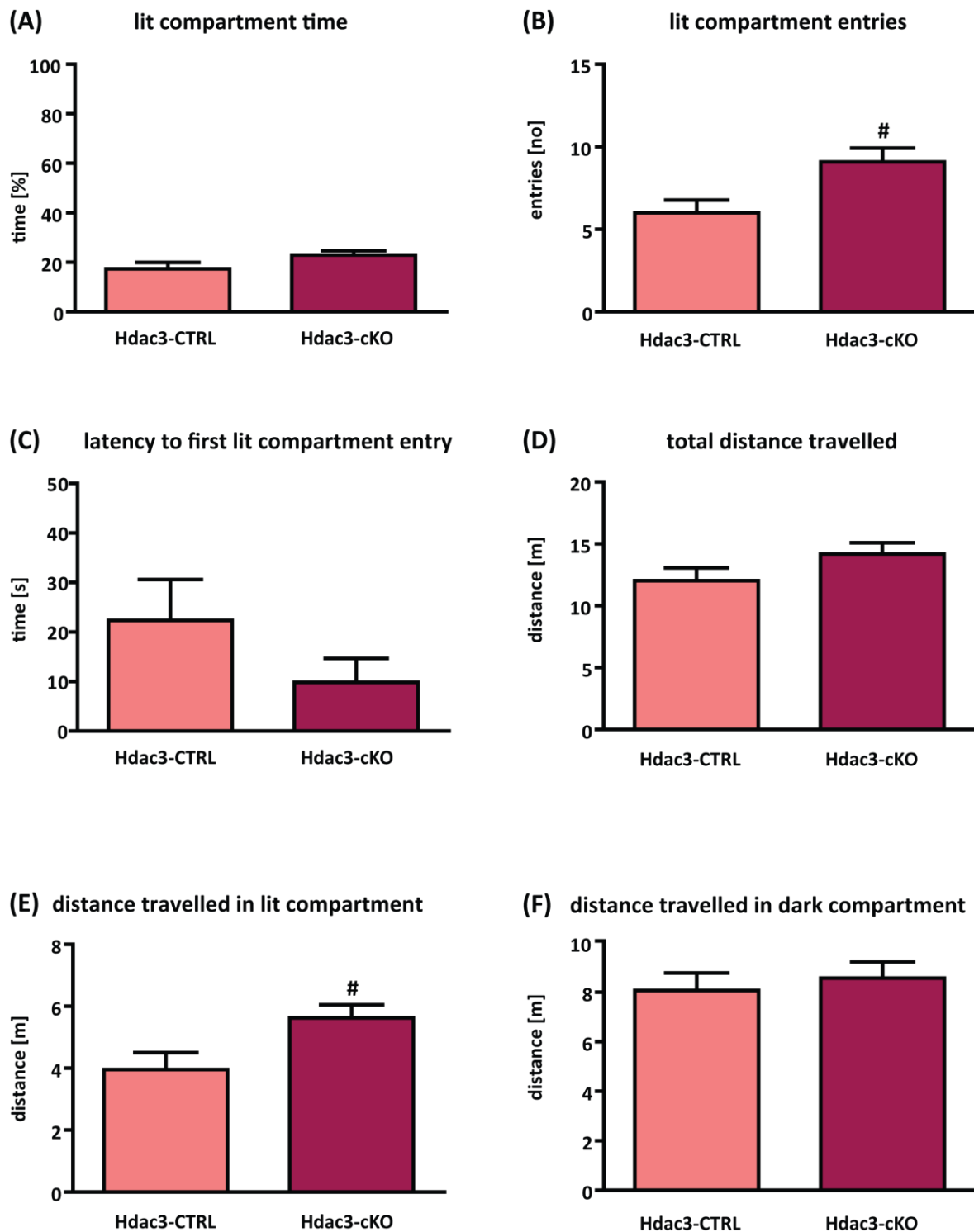


Figure 48: Analysis of conditional Hdac3 knockout mice in the dark/light box (DaLi) test. (A) The time spent in the lit compartment revealed no significant difference between Hdac3-cKO and Hdac3-CTRL mice. (B) The number of entries to the lit compartment reached a significantly higher value for Hdac3-cKO, but (C) the latency to first lit compartment entry was similar for both genotypes as well as (D) the total distance travelled during the whole test. (E) However, the distance travelled in the lit compartment was significantly higher for Hdac3-cKO mice, whereas (F) the distance travelled in the dark compartment again did not differ between

the two genotypes. | Test duration analyzed: 5 minutes; Data are presented as means \pm SEM; n = 9-13; # p < 0.05, Student's t-test; Hdac3-CTRL = control littermate; Hdac3-cKO = conditional Hdac3 knockout mouse.

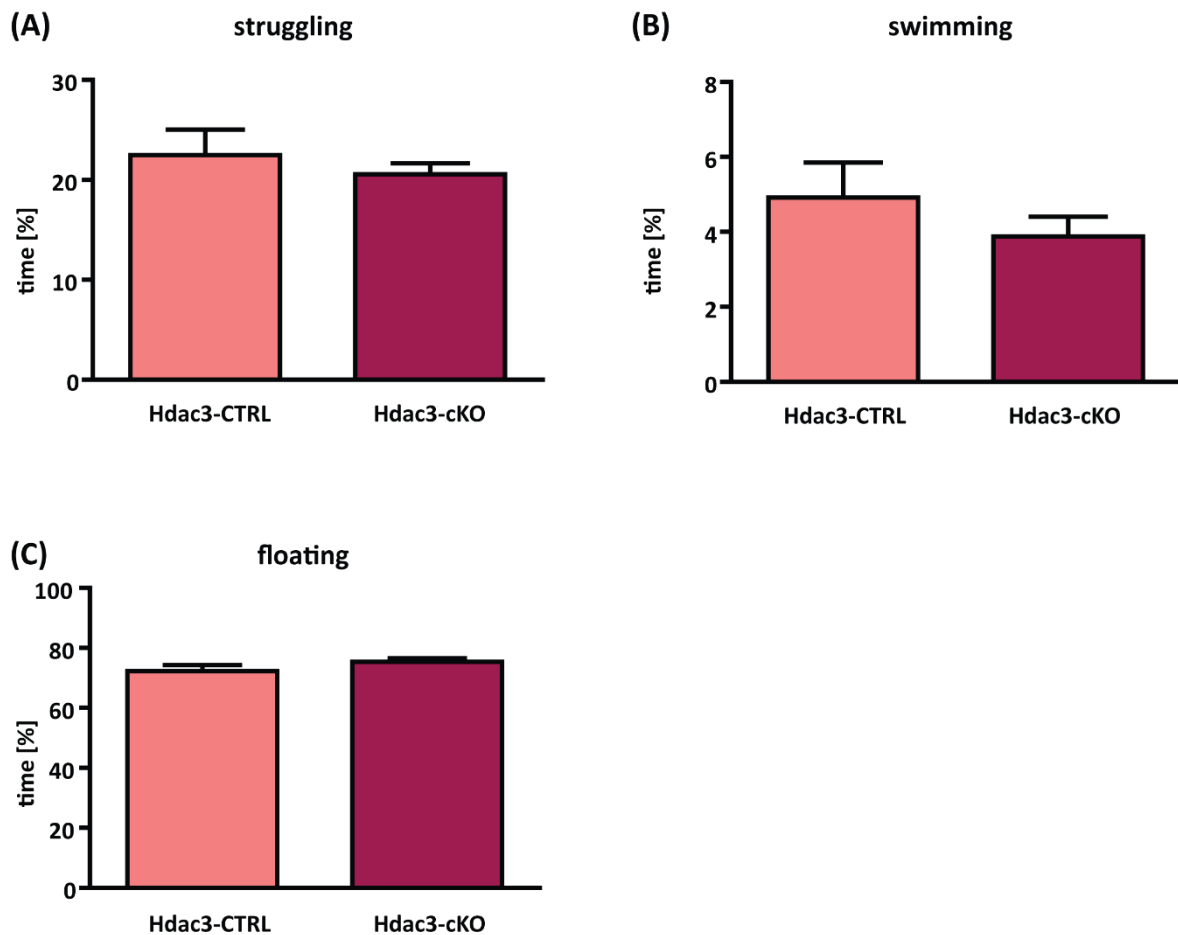


Figure 49: Analysis of conditional Hdac3 knockout mice in the forced swim test (FST). (A) Hdac3-cKO mice revealed no difference in active stress-coping behavior shown by struggling and (B) swimming when compared to Hdac3-CTRL. (C) Also the passive stress-coping parameter floating was not changed. | Test duration analyzed: 6 minutes; Data are presented as means \pm SEM; n = 11-13; Student's t-test; Hdac3-CTRL = control littermate; Hdac3-cKO = conditional Hdac3 knockout mouse.

In summary of the behavioral results of the basal emotionality screen it emerges that conditional Hdac3 knockout mice did not show any deficits in locomotor activity, nor in anxiety-related or stress-coping behavior.

To rule out, that the tamoxifen chow or the Cre recombinase did not cause an overall effect and might influence the obtained data, we conducted two additional control experiments in the same behavioral test battery (tamoxifen chow data not shown; Cre recombinase data shown in supplements).

4.4.2.2 Effects of chronic social defeat stress (CSDS) on conditional Hdac3 knockout mice

As we mentioned before, HDACs as main epigenetic mediators play a pivotal role in gene x environment interactions. Therefore, we also subjected conditional Hdac3 knockout mice to three weeks of chronic social defeat stress (CSDS) to assess whether the Hdac3 knockout in principal neurons of the forebrain in adulthood has any impact on the animals' stress response (Berton et al., 2006; Wagner et al., 2011). Therefore, animals were categorized into four groups having the two genotypes Hdac3-CTRL and Hdac3-cKO which were introduced earlier and two different conditions (basal: undefeated; stress: defeated). All animals were fed seven days with tamoxifen chow starting at the day of the first defeat and followed by a seven day wash-out phase prior testing (Figure 50).

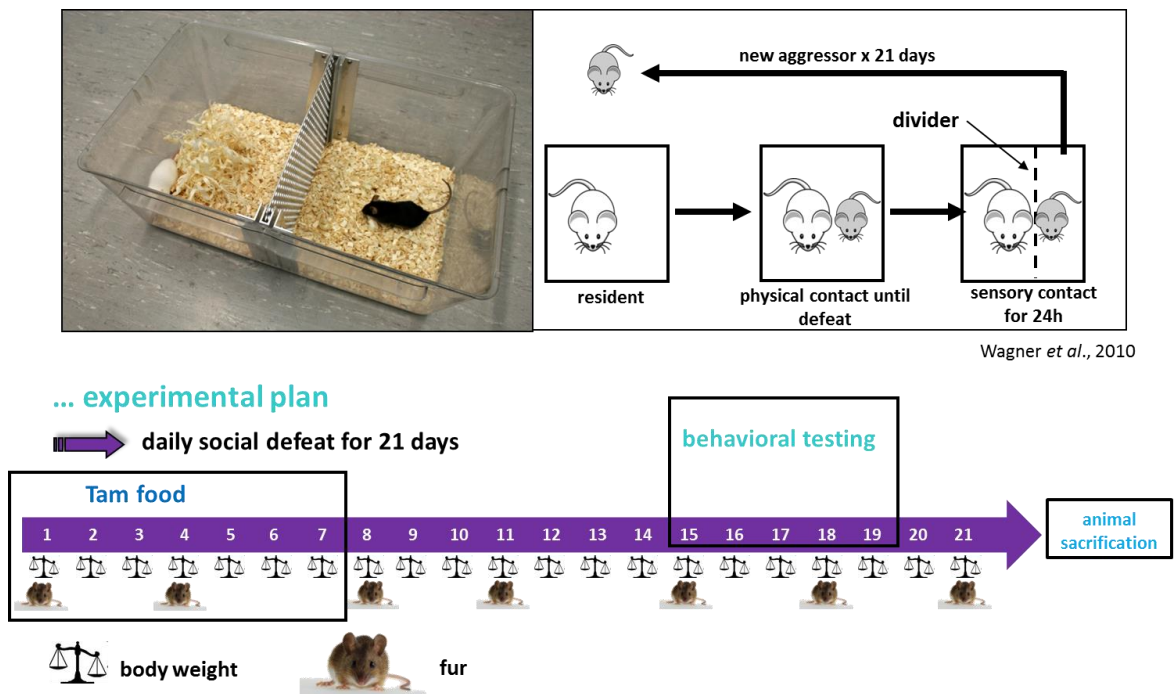


Figure 50. Schematic representation of the chronic social defeat stress (CSDS) paradigm and behavioral phenotyping of conditional Hdac3 knockout mice. Animals were submitted to CSDS for 21 consecutive days. Therefore, they were introduced into the home cage of a dominant CD1 resident mouse until defeated, but for no longer than 5 min. Following defeat, animals spent 24 hours within the same cage, but separated via a holed steel partition, enabling sensory, but not physically contact. Every day chronically defeated mice were exposed to a new unfamiliar resident. Control animals were housed in their home cages throughout the course of the experiment. All animals were handled daily, the body weight was assessed daily and the fur status was checked every 3-4 days. The fur was evaluated as describe before by Mineur and colleagues (Mineur et al., 2003). Tam application via food pellets was performed within the first 7 days of the defeat. Behavioral phenotyping included OF test, SA test, FUST, EPM and FST. | CSDS = chronic social defeat stress; Tam = tamoxifen; OF = open field; SA = approach/avoidance; FUST = female urine sniffing test; EPM = elevated plus maze; FST = forced swim test.

Physiological parameters such as body weight progression, fur state and weight of adrenal glands and thymus were assessed in order to control for the effectiveness of the CSDS paradigm (Figure 51). Although there were no effects visible for body weight progression nor for the weight of adrenal gland, the characteristic physiological changes evoked by the CSDS were visible for fur status and thymus weight. Thus, the fur quality was decreased for stressed control animals when compared to unstressed control littermates (Repeated-measures ANOVA, ** $p < 0.01$, *** $p < 0.001$) (Figure 51.B). Furthermore, the fur status indicated also a genotype effect for the stressed groups as Hdac3-cKO mice kept the state of fur quality whereas Hdac3-CTRL mice lost fur quality with the time (Repeated-measures ANOVA, ### $p < 0.001$, post-hoc test) (Figure 51.B). In addition, the thymus atrophy was observed as expected for both stressed groups (Two-Way ANOVA, *** $p < 0.001$) (Figure 51.D).

Moreover, it is known that stress enhances plasma corticosterone levels and therefore, we assessed in all four groups in blood plasma during the circadian nadir in the morning basal levels of corticosterone (Figure 52.A). Blood samples were taken 15 and 90 minutes after the onset of a forced swim test as acute stressor to obtain corticosterone levels as response to the stressor (Figure 52.B) and the subsequent recovery from this stressful event (Figure 52.C). However, statistical analysis showed no significant differences in the corticosterone levels between the two conditions (basal and stress) in the circadian nadir in the morning, but revealed a genotype effect with an increase of corticosterone level in Hdac3-cKO mice in response to CSDS (Repeated-measures ANOVA, # $p < 0.05$, post-hoc test) (Figure 52.A). The corticosterone levels after the acute stress and after the recovery from the acute stress event were unremarkable and showed no effect.

As mentioned before, the chronic social defeat stress (CSDS) paradigm was established by the research group of Mathias Schmidt at the MPI of Psychiatry, based on the protocol of Berton and colleagues (Berton et al., 2006; Wagner et al., 2011). To describe briefly, test mice were submitted to chronic social defeat stress for 21 consecutive days (Figure 50). Therefore, they were introduced into the home cage of a dominant CD1 resident mouse for no longer than 5 min. During this time the intruder was defeated

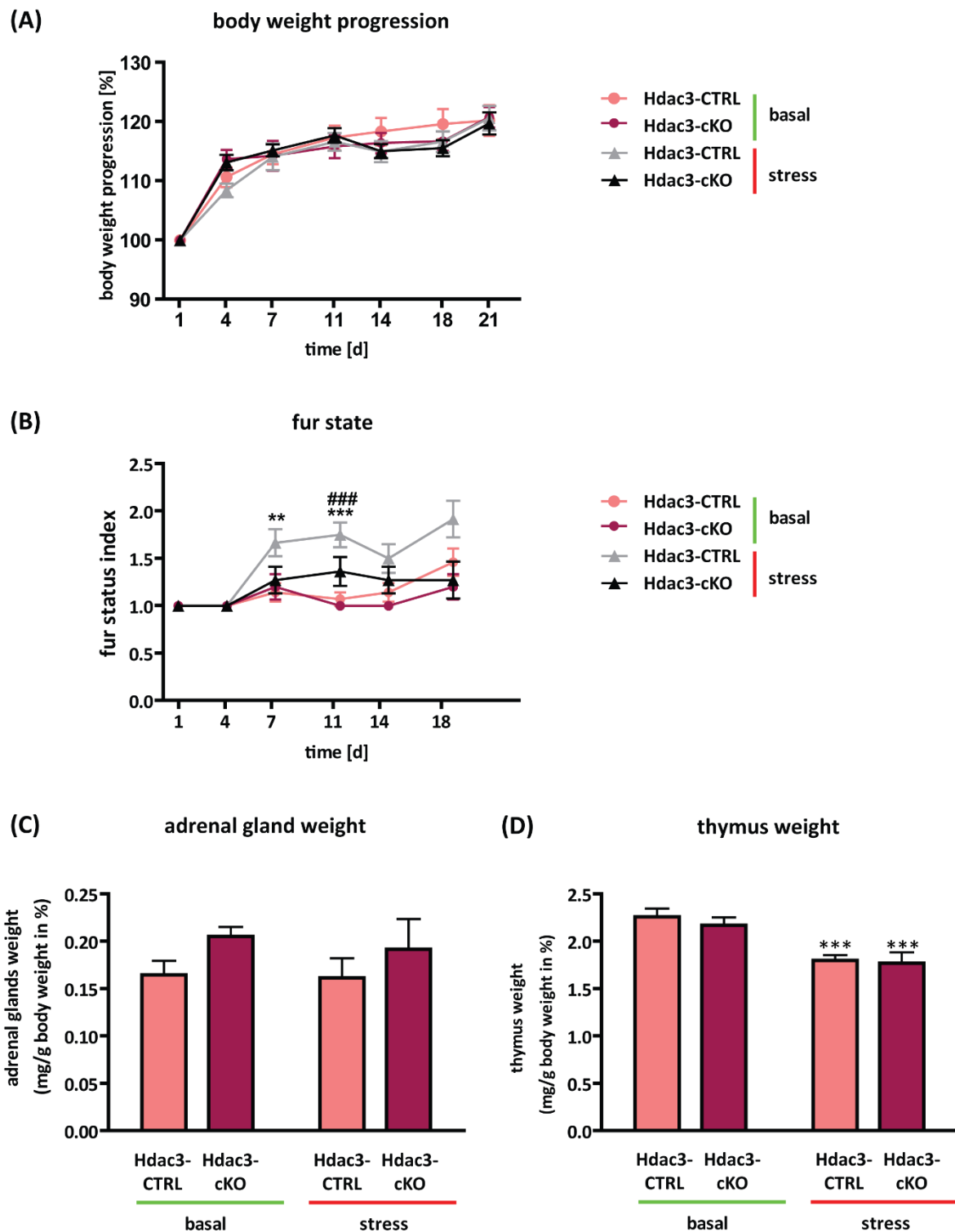


Figure 51. Analysis of physiological parameters of conditional Hdac3 knockout mice during and after the chronic social defeat stress (CSDS) paradigm. (A) Body weight of mice was assessed every day and is depicted as percentage of the starting weight at day one of defeat. Animals of all groups gained body weight throughout the experiment, but no significant changes were detected between groups. (B) The fur status index was assessed every three or four days. An increase in fur state index is associated with a decrease in fur quality. The fur state index reached a significantly higher score for the stressed Hdac3-CTRL group compared to the unstressed Hdac3-CTRL group and the stressed Hdac3-cKO group. (C) After mice were sacrificed, adrenal glands and (D) thymi were dissected at day 21 and analyzed in relation to the animal's

body weight. The weight of adrenal glands did not show any differences, whereas the thymus weight was significantly decreased in both stressed groups. | Data are presented as means \pm SEM; $n = 12$; * significantly different from control condition of same genotype, ** $p < 0.01$, *** $p < 0.001$, # significantly different from control genotype of same condition, ### $p < 0.001$, post-hoc test; for (A) and (B) Repeated-measures ANOVA, for (C) and (D) Two-Way ANOVA; CSDS = chronic social defeat stress; Hdac3-CTRL = control littermate; Hdac3-cKO = conditional Hdac3 knockout mouse.

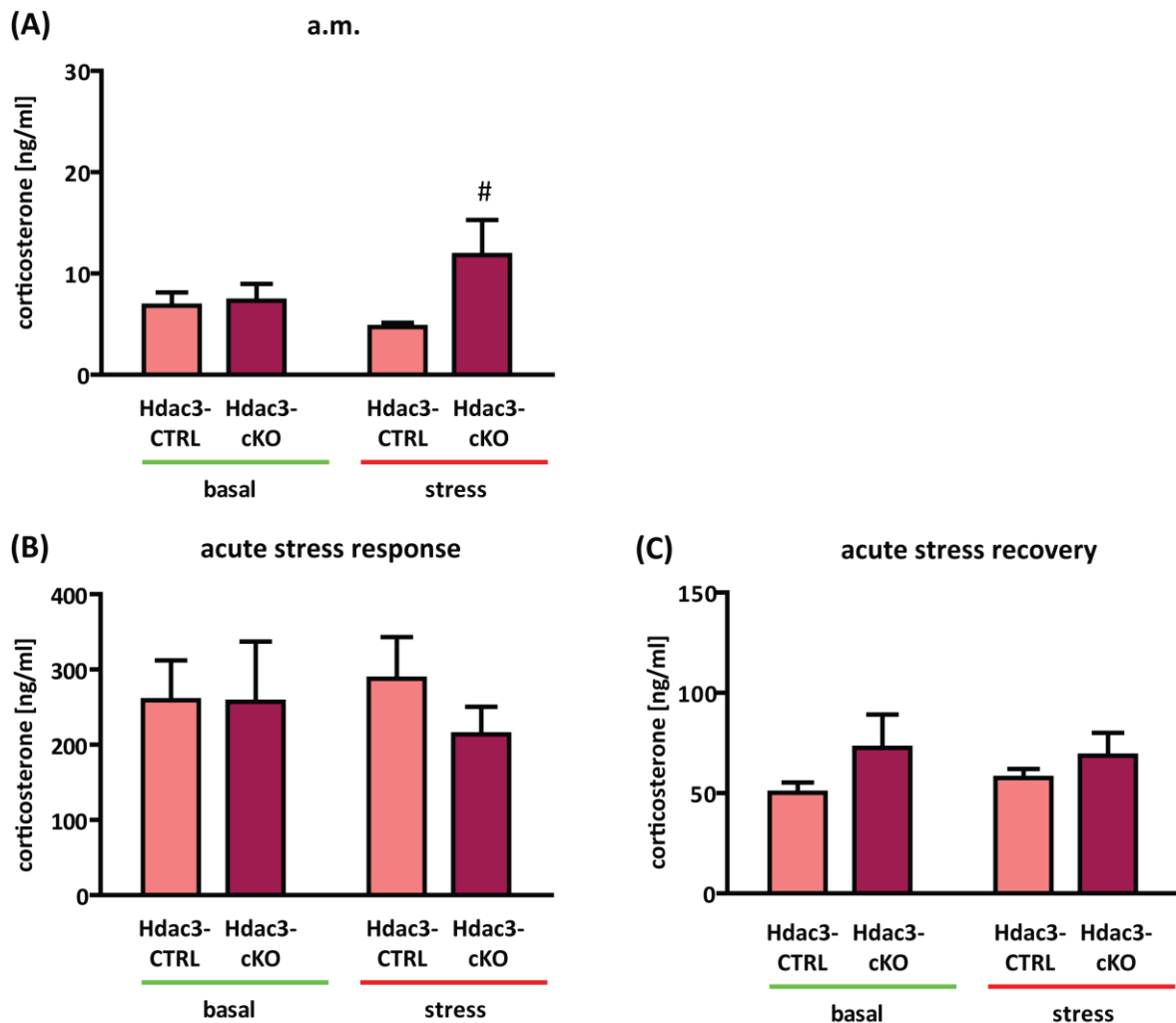


Figure 52. Analysis of corticosterone levels of conditional Hdac3 knockout mice subjected to the chronic social defeat stress (CSDS) paradigm. (A) Plasma corticosterone levels were analyzed for all four groups in the morning (a.m.) to obtain basal values. No condition effect was assessed, but a genotype effect between the two stressed groups. (B) Corticosterone levels were analyzed 15 min after the onset of the forced swim test (FST) as acute stressor. No genotype or condition effect was observed. (C) 90 min after the start of the FST, corticosterone levels were analyzed. All groups recovered well from the stress indicated by low corticosterone levels. | Data are presented as means \pm SEM; $n = 12$; # significantly different from control genotype of same condition, # $p < 0.05$, Two-Way ANOVA, post-hoc test; Hdac3-CTRL = control littermate; Hdac3-cKO = conditional Hdac3 knockout mouse.

The third week of the CSDS paradigm was used for behavioral experiments and five tests were conducted within five consecutive days (Figure 50) to assess locomotion, explorative, social, reward-seeking, anhedonic, anxiety-related, depression-like and stress-coping behavior.

The first test of the behavioral screening was the open field (OF) test to assess locomotor activity and explorative behavior as well as anxiety-related behavior. Mouse behavior was analyzed for the first 15 minutes of the test and revealed a condition effect for locomotion indicated by total distance travelled (Two-Way-ANOVA, * $p < 0.05$, *** $p < 0.001$) (Figure 53.A) as well as a condition effect for time immobile (Two-Way-ANOVA, * $p < 0.05$, ** $p < 0.01$) (Figure 53.B). Additionally, both parameters showed a genotype effect within the stressed groups indicating that Hdac3-cKO mice travelled more (Two-Way-ANOVA, ## $p < 0.01$, post-hoc) (Figure 53.A+C) and spent less time immobile (Two-Way-ANOVA, # $p < 0.05$, ## $p < 0.01$, post-hoc) (Figure 47.B+D). A more detailed analysis of both parameters in segments of five minutes showed, that the effects are caused in the middle and the end of the test (Two-Way-ANOVA, * $p < 0.05$, ** $p < 0.01$, *** $p < 0.001$) (Figure 53.C+D). For the amount of inner zone entries, only Hdac3-CTRL mice showed a condition effect (Two-Way-ANOVA, *** $p < 0.001$) (Figure 53.E), whereas for the time the animals spent in the inner zone a condition effect was again observed for both genotypes (Two-Way-ANOVA, ** $p < 0.01$) (Figure 53.F). In addition, the two stressed groups revealed for the parameter inner zone entries a genotype effect indicating that Hdac3-cKO mice entered more often the inner zone (Two-Way-ANOVA, # $p < 0.05$, post-hoc) (Figure 53.E).

The second test, the mice had to perform was the social approach/avoidance (SA) test, as various neurological and psychiatric disorders are characterized by deficits in social behavior. However, we could not observe any effect in the time the animals were interacting with the unfamiliar mouse (Figure 54.A), but the stressed animals of both genotypes showed an increase in immobility (Two-Way-ANOVA, * $p < 0.05$) (Figure 54.B).

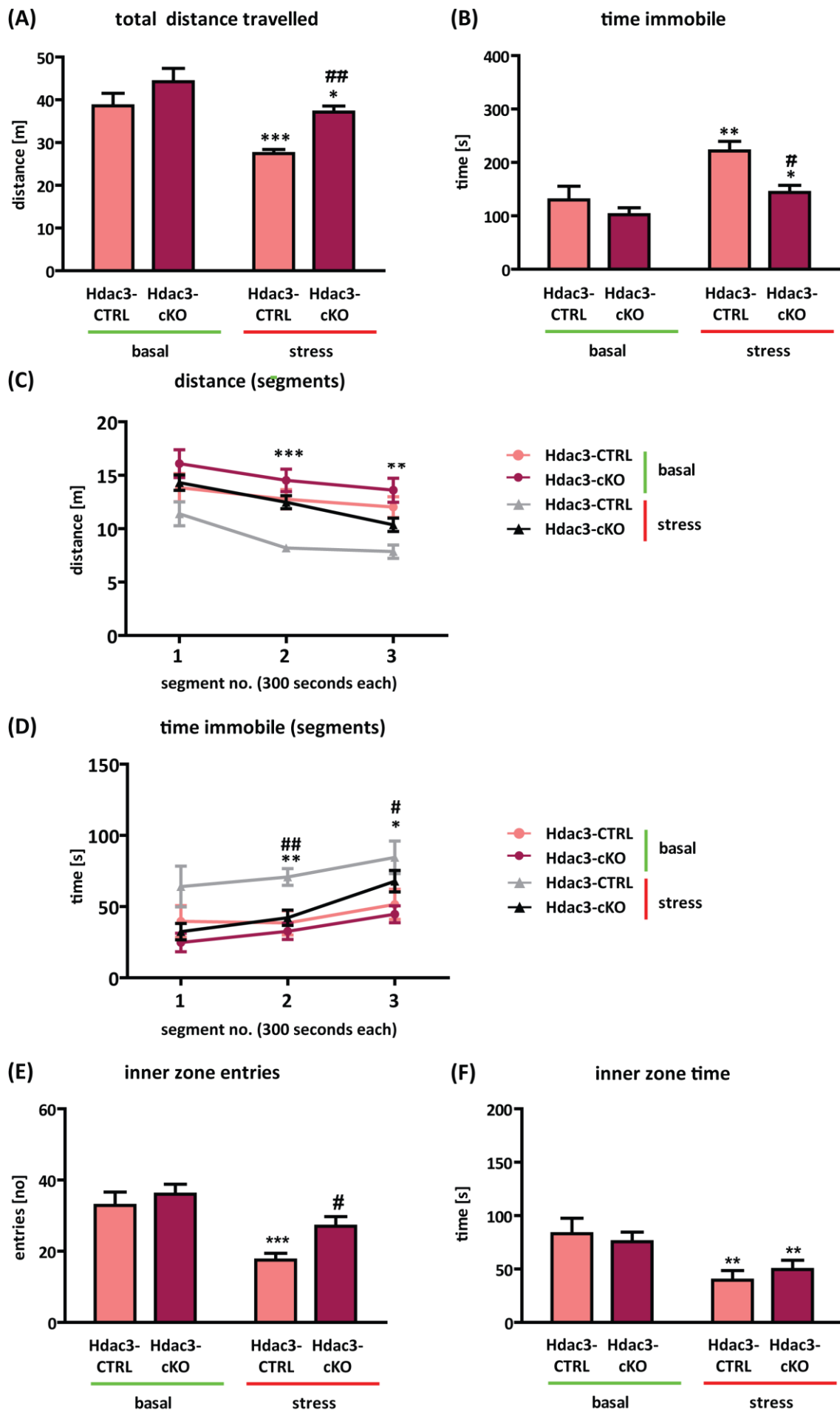


Figure 53. Analysis of the behavior of conditional Hdac3 knockout mice in the open field (OF) test during the chronic social defeat stress (CSDS) paradigm. (A) A significant difference was observed in total distance travelled and (B) time immobile between the two conditions (basal and stress). For both parameters an additional genotype effect was observed between the two stressed groups. (C-D) The total test was also analyzed in segments of 5 minutes with strong differences within segment two and three. (E-F) To observe anxiety-related and explorative behavior, the number of inner zone entries and inner zone time were analyzed. Inner zone entries revealed a condition effect for Hdac3-CTRL groups and a genotype effect for the stressed groups. The number of inner zone entries indicated a significant condition effect for both genotypes. | Test duration analyzed: 15 minutes; data are presented as means \pm SEM; n = 12; * significantly different from control condition of same genotype, * p < 0.05, ** p < 0.01, *** p < 0.001, Two-Way ANOVA; # significantly different from control genotype of same condition, # p < 0.05, ## p < 0.01, Two-Way ANOVA, post-hoc test; OF = open field; CSDS = chronic social defeat stress; Hdac3-CTRL = control littermate; Hdac3-cKO = conditional Hdac3 knockout mouse.

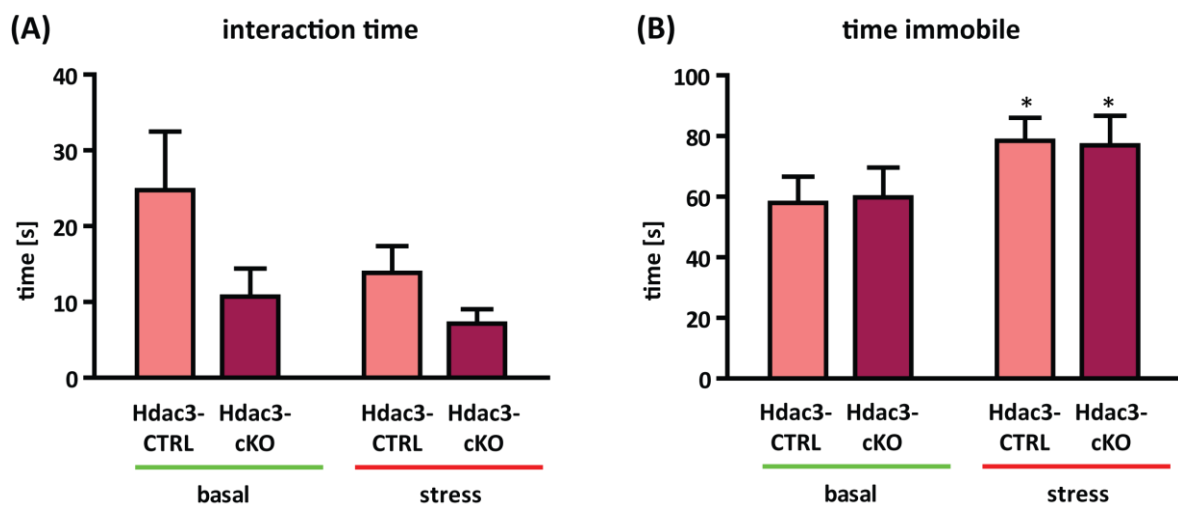


Figure 54. Analysis of conditional Hdac3 knockout mice in the social approach/avoidance (SA) test during the chronic social defeat stress (CSDS) paradigm. (A) No significant difference was observed for the interaction time with the social target in the second part of the test. (B) The time immobile showed a condition effect for both genotypes with an increase in time immobile for stressed animals. | Test duration analyzed: 2.5 minutes; data are presented as means \pm SEM; n = 12; * significantly different from control condition of same genotype, * p < 0.05, Two-Way ANOVA; SA = social approach/avoidance; CSDS = chronic social defeat stress; Hdac3-CTRL = control littermate; Hdac3-cKO = conditional Hdac3 knockout mouse.

With the use of the female urine sniffing test (FUST), we assessed anhedonic behavior in the conditional Hdac3 knockout mice. Already within the first trial, when the cotton tips were soaked with water, a genotype effect was observed under basal conditions indicating that Hdac3-cKO mice were less interested in the cotton tip compared to Hdac3-CTRL mice (Two-Way-ANOVA, # p < 0.05, post-hoc) (Figure 55.A). When analyzing the urine sniffing time, we observed an inverted genotype

effect for the basal groups with an increased sniffing time for Hdac3-cKO mice compared to control littermates (Two-Way-ANOVA, # $p < 0.05$, post-hoc) (Figure 55.B). Additionally, the Hdac3-cKO mice showed a condition effect with a decreased urine sniffing time for stress animals compared to the basal group of same genotype (Two-Way-ANOVA, ** $p < 0.01$) (Figure 55.B).

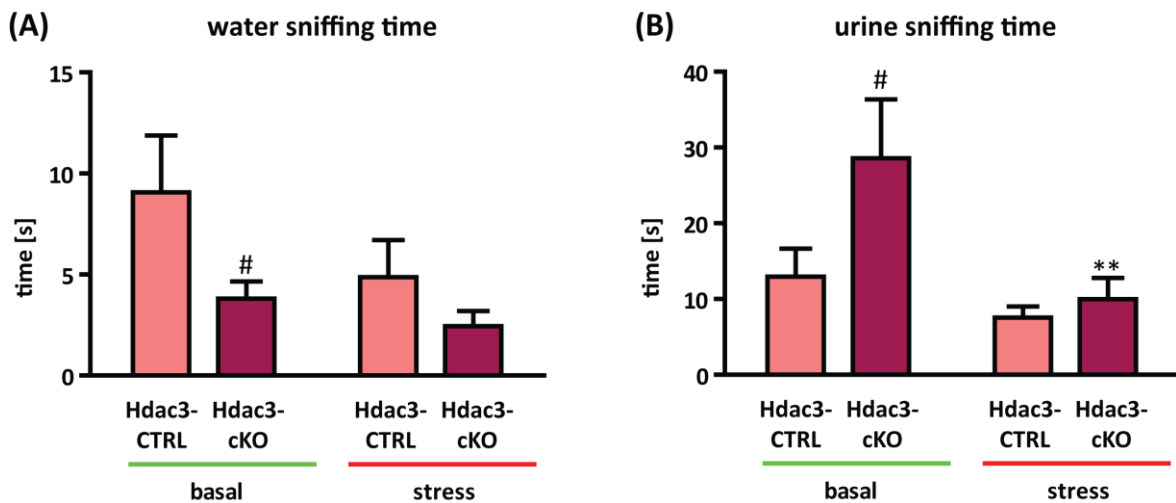


Figure 55. Analysis of conditional Hdac3 knockout mice in the female urine sniffing test (FUST) during the chronic social defeat stress (CSDS) paradigm. A) In the water trial we could observe a genotype effect under basal condition with a significantly lower sniffing time for the Hdac3-cKO mice, but no effect for the stressed mice was visible. (B) However, the urine trial showed still a condition effect for Hdac3-cKO mice which behaved more anhedonic when stressed and a genotype effect under basal conditions with a less anhedonic behavior for the Hdac3-cKO mice. | Test duration analyzed: 3 minutes; data are presented as means \pm SEM; $n = 12$; * significantly different from control condition of same genotype, ** $p < 0.01$, Two-Way ANOVA; # significantly different from control genotype of same condition, # $p < 0.05$, Two-Way ANOVA, post-hoc test; FUST = female urine sniffing test; CSDS = chronic social defeat stress; Hdac3-CTRL = control littermate; Hdac3-cKO = conditional Hdac3 knockout mouse.

To gain more insight into anxiety-related behavior, mice were conducted to the elevated plus maze (EPM) test. As we could not detect any condition effect, nor a genotype effect in the EPM test within the first five minutes (Figure 56), we analyzed all parameters additionally for a test duration of 10 minutes (Figure 57). However, the additional analysis revealed no condition effects and only a genotype effect for the parameter total distance travelled indicating the stressed Hdac3-cKO mice travelled significantly more compared to stressed Hdac3-CTRL mice (Two-Way-ANOVA, post-hoc test, ### $p < 0.01$) (Figure 57.A). Thus, stressed Hdac3 knockout animals showed an increase in locomotor activity during the EPM test. Anxiety-related behavior indicated by latency to first open

arm entry (Figure 57.B), open arm time (Figure 57.C) and latency to first open arm time (Figure 57.D) did not show any effects.

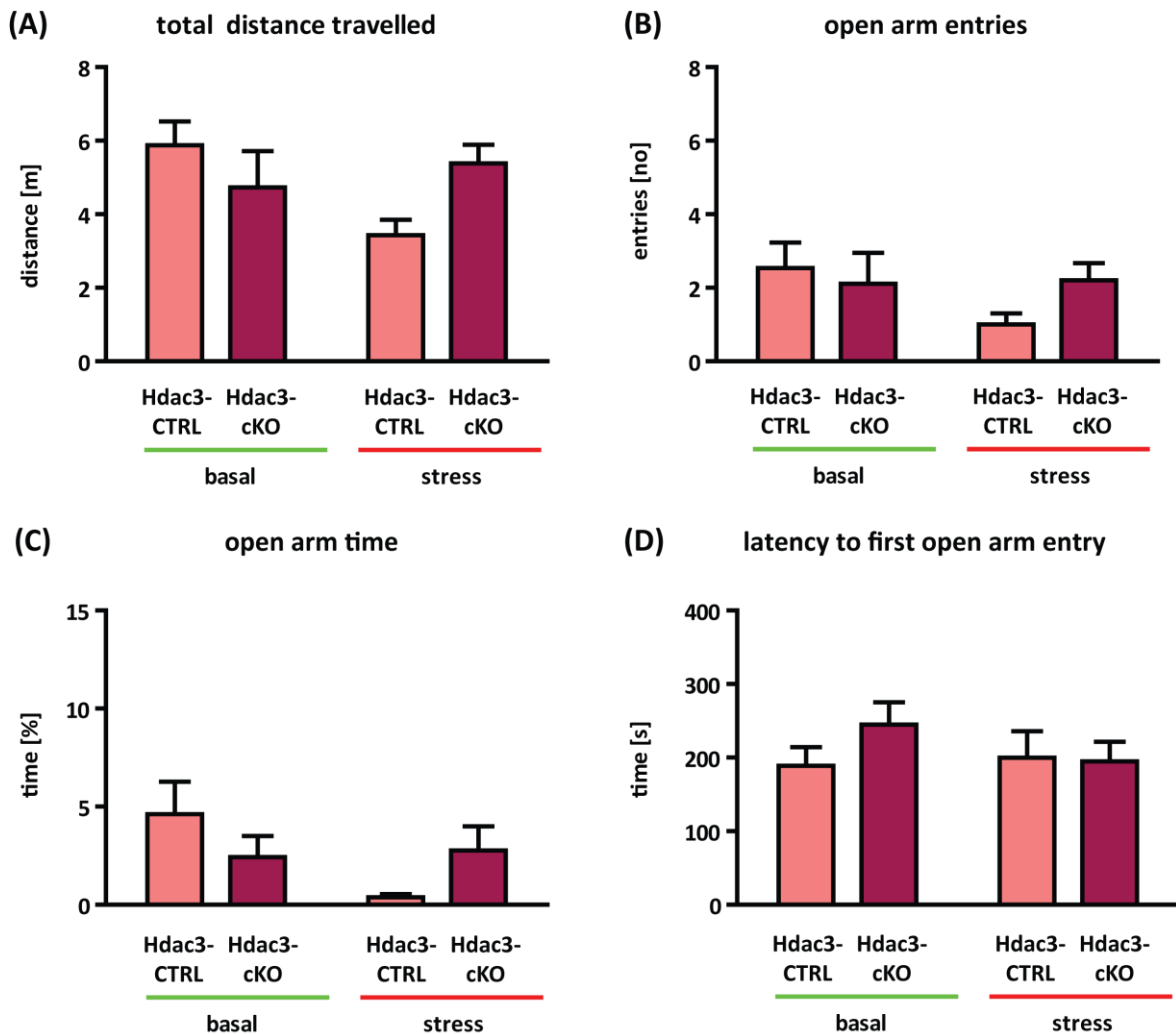


Figure 56. Analysis of conditional Hdac3 knockout mice in the elevated plus maze (EPM) test during the chronic social defeat stress (CSDS) paradigm (analysis of first five minutes). (A) No effect was observed in locomotion, (B) open arm entries, (C) open arm time or (D) the latency to the first open arm entry when analyzing the first five minutes of the test. | Test duration analyzed: 5 minutes; Data are presented as means \pm SEM; $n = 12$; EPM = elevated plus maze; CSDS = chronic social defeat stress; Hdac3-CTRL = control littermate; Hdac3-cKO = conditional Hdac3 knockout mouse.

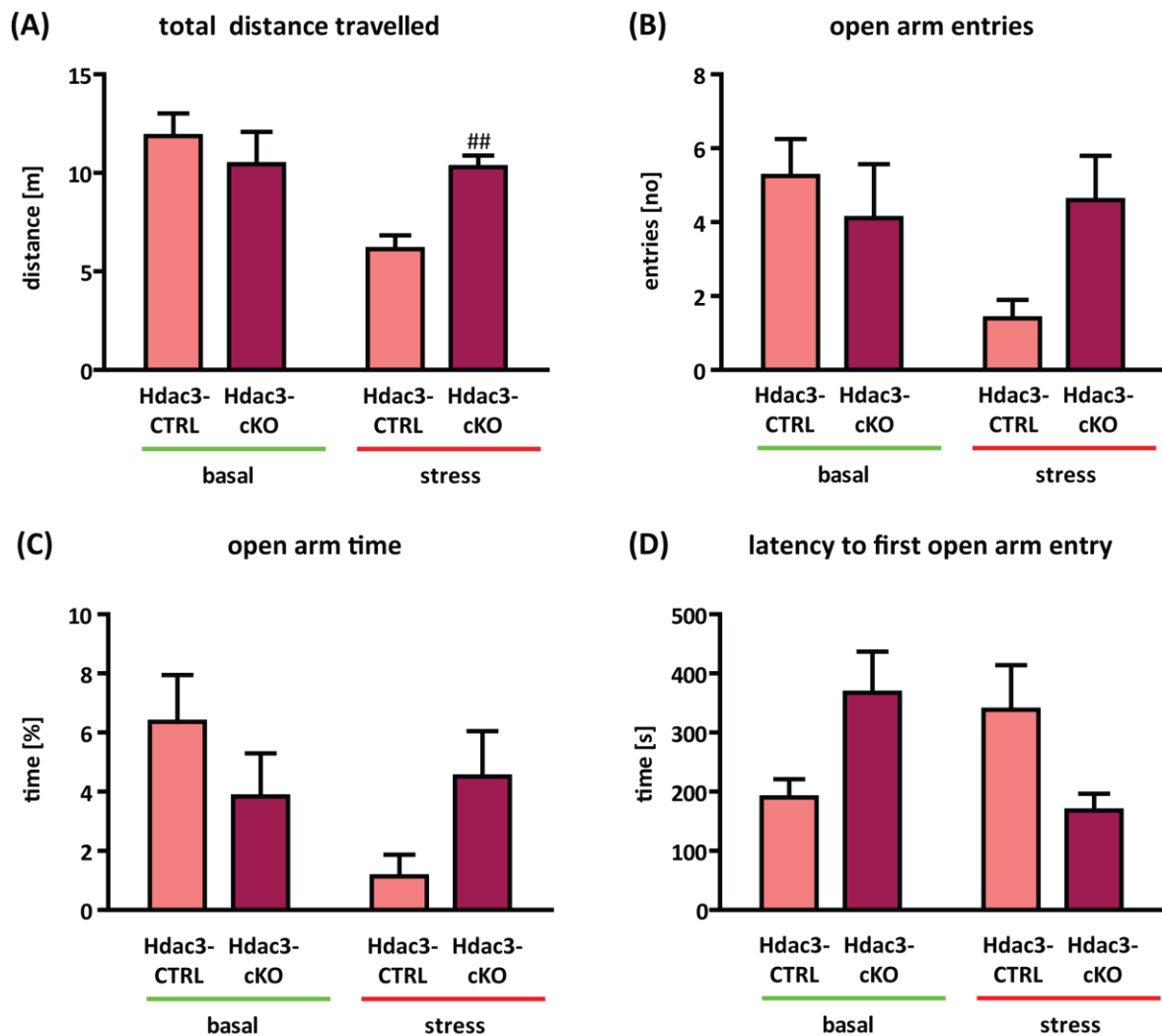


Figure 57. Analysis of conditional Hdac3 knockout mice in the elevated plus maze (EPM) during the chronic social defeat stress (CSDS) paradigm (analysis of first ten minutes). (A) When analyzing 10 minutes of the EPM test, we could observe for the total distance travelled a significantly increased genotype effect for the Hdac3-cKO mice. (B) But still no effects were observed for open arm entries, (C) open arm time or (D) the latency to the first open arm entry. | Test duration analyzed: 10 minutes; Data are presented as means \pm SEM; $n = 12$; # significantly different from control genotype of same condition, ## $p < 0.01$, Two-Way ANOVA, post-hoc test; EPM = elevated plus maze; CSDS = chronic social defeat stress; Hdac3-CTRL = control littermate; Hdac3-cKO = conditional Hdac3 knockout mouse.

To get an idea of depression-related or stress-coping behavior of defeated and undefeated conditional Hdac3 knockout mice, we performed the forced swim test (FST). Analysis of the two active stress-coping behavior types (struggling and swimming) and the passive stress-coping behavior (floating) revealed no differences between genotypes or conditions (Figure 58) which was also shown in the first basal screen of emotionality (Figure 49).

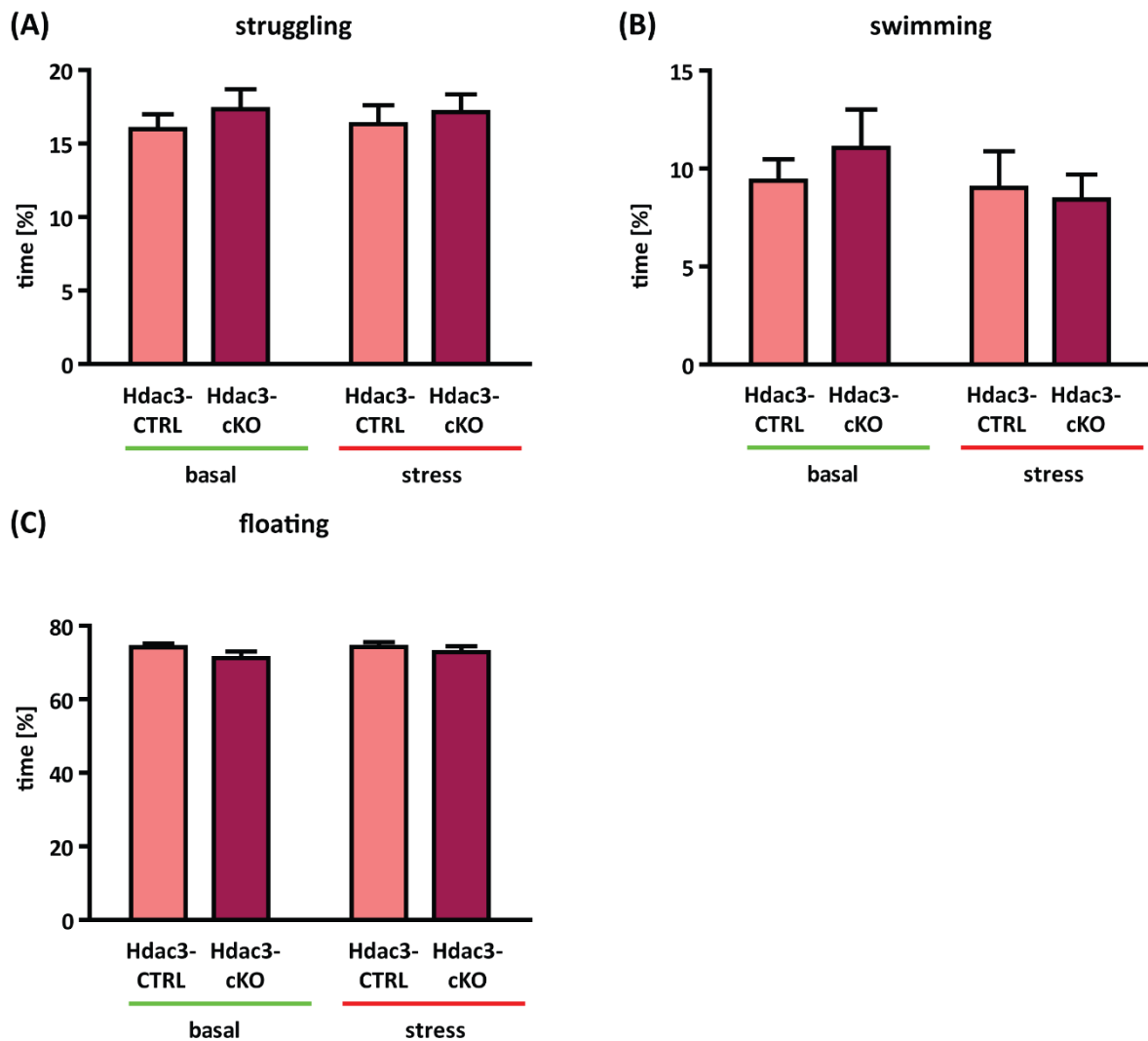


Figure 58: Analysis of conditional Hdac3 knockout mice in the forced swim test (FST) during the chronic social defeat stress (CSDS) paradigm. (A) For the active stress-coping behavior struggling no effect was detected as well as for (B) the parameter swimming and (C) the passive stress-coping behavior parameter floating. | Test duration analyzed: 6 minutes; Data are presented as means \pm SEM; $n = 12$; FST = forced swim test; CSDS = chronic social defeat stress; Hdac3-CTRL = control littermate; Hdac3-cKO = conditional Hdac3 knockout mouse.

To sum up: Conditional Hdac3 knockout mice were exposed to chronic stress by using the CSDS paradigm and we observed in stressed mice with no regard to genotypes a decrease in locomotor activity and an increase in anxiety-related behavior. The social approach/avoidance test showed a disruption of social behavior of stressed animals indicated by an increased amount of time the animals spent immobile. Furthermore, the female urine sniffing test revealed that stressed

conditional Hdac3 knockout mice were decreased in their anhedonic behavior due to the stress condition and thus, Hdac3-cKO animals sniffed more at the urine soaked tips compared to stressed control mice.

4.4.2.3 Cognitive performance of Hdac3 conditional knockout mice

In chapter 4.3.2.3 we already mentioned when describing the cognitive performance of conditional Hdac1 knockout mice, the importance and involvement of epigenetic mechanisms and especially of HDACs in the regulation and maintenance of memory consolidation and learning behavior. Most studies concerning learning and memory formation in regard to HDACs involve HDAC inhibitors. Furthermore, HDACs have been implicated in the pathogenesis of neurodegenerative diseases like Alzheimer's disease (Agis-Balboa et al., 2013; Broide et al., 2007; Covington et al., 2009; Fass et al., 2013). However, different HDACs appear to have specific roles in different types of learning and memory. HDAC3 could be shown to act as negative regulator of long-term memory formation as the inhibition of HDAC3 enhances long-term object recognition memory in mice and this is linked to an increase in H4K8 acetylation (Malvaez et al., 2010; McQuown et al., 2011). To get a first glance at the impact of HDAC3 loss in the murine forebrain in adulthood on memory and learning processes, we analyzed conditional Hdac3 knockout mice in the water cross maze (WCM) applying a protocol to assess hippocampus-dependent spatial learning.

The analysis of the performance of Hdac3-cKO mice in the WCM is indicated by the percent of accuracy (Figure 59.A). Given the natural tendency of mice to explore, one error within six trials per training day is permitted, which then manifests in an accuracy of 83.3% as the bottom threshold for a mouse to be considered as accurate. This threshold value was exceeded at training day five only for Hdac3-CTRL mice, but not for Hdac3-cKO mice. These mice showed a strong impairment in learning as they reached only 60% of accuracy at day three and could not further improve their performance by additional training days (Figure 59.A) (day 4: Repeated-measures ANOVA, post-hoc test, # $p < 0.05$; day5: Repeated-measures ANOVA, post-hoc test, ### $p < 0.001$) indicating that the deficit of Hdac3 in the principal forebrain neurons negatively influences the learning ability. A second parameter to assess the cognitive behavior in the WCM was provided by the number of accurate learners of each group displaying a high learning performance again for Hdac3-CTRL mice, but not for Hdac3-cKO mice, which did not reach values above 40% (Figure 59.B) (day 3: Repeated-measures ANOVA, post-hoc test, # $p < 0.05$; day 4: Repeated-measures ANOVA, post-hoc test, ### $p < 0.001$; day5: Repeated-measures ANOVA, post-hoc test, ### $p < 0.001$).

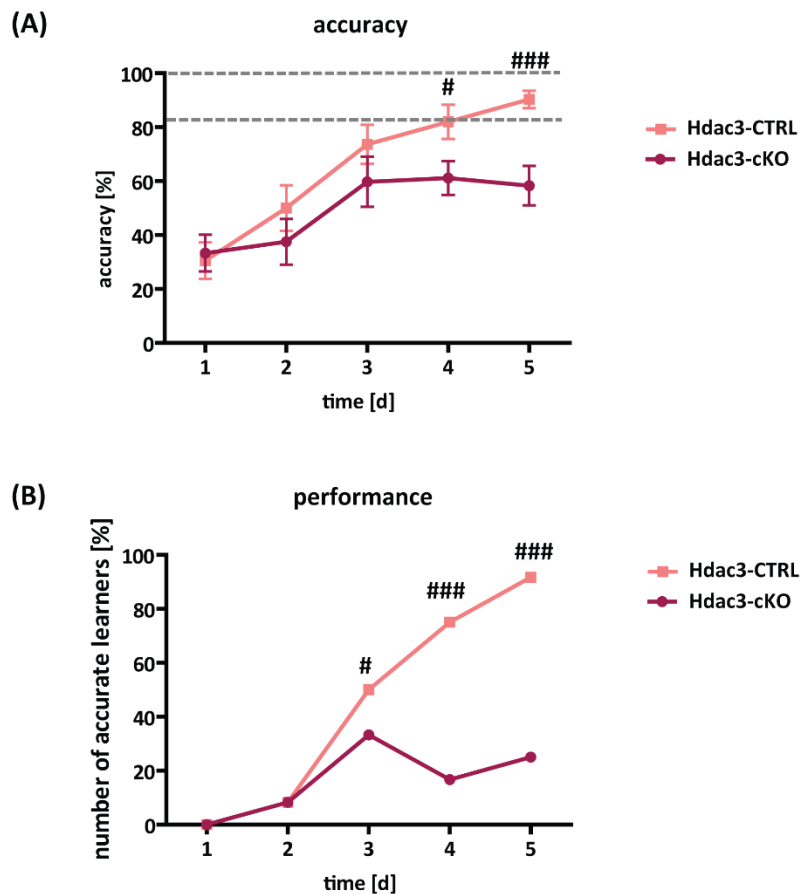


Figure 59: Analysis of conditional Hdac3 knockout mice in the water cross maze (WCM). (A) Spatial memory was evaluated by the accuracy indicating the success or failure of the mouse to swim the correct path to the platform. (B) A second parameter to interpret mice performance in the WCM is given by the number of accurate learners per group per day. | Data are presented as means \pm SEM; $n = 12$; # $p < 0.05$, ### $p < 0.001$, Repeated-measures ANOVA, post-hoc test; area between grey dashed lines = accuracy; WCM = water cross maze; Hdac3-CTRL = control; Hdac3-cKO = conditional Hdac3 knockout mouse.

In summary, it emerges in a first cognitive task, that the HDAC3 enzyme missing in the murine forebrain in adulthood caused severe deficits and impairment in memory and learning processes indicating that HDAC3 plays a crucial role in spatial learning.

5 DISCUSSION

5.1 Distribution of the classical HDACs throughout the adult murine brain

So far, the role of epigenetic mechanisms has been well investigated in many cellular and organismal processes as well as in pathologies like cancer, while the field of neuroepigenetics is just beginning to evolve (Agis-Balboa et al., 2013; Bartl et al., 1997; Broide et al., 2007; Covington et al., 2009; Fass et al., 2013; Glaser et al., 2003; Gwack et al., 2001; Lagger et al., 2002; Mal et al., 2001; Puri et al., 2001). Epigenetic mechanisms are important for chromatin remodeling to change gene expression profiles of not only dividing or differentiating cells, but also cells of non-dividing nature like mature neurons. A search for ‘*epigenetic*’ in the pubmed database revealed at the beginning of 2016 more than 45957 papers, but only about 4427 are linked to brain-related studies. Nevertheless, it is obvious and clear from the few studies, that epigenetic mechanisms are implicated to be important mediators in numerous brain processes such as development, the brain-regulated maintenance of body homeostasis, sensorimotor ability, adult neurogenesis, modulation of neural plasticity, higher brain functions like cognition, memory and learning, and development of neurologic and psychiatric disorders (Bird, 2007; Farah & Hook, 2008; Ravi & Kannan, 2013; Sweatt et al., 2013; Volmar & Wahlestedt, 2014). Major players of the epigenetic machinery are the histone deacetylases (HDACs) which are able to modify chromatin structure due to deacetylation of histone proteins or of non-histone proteins such as transcription factors (Delcuve et al., 2012; Gregoretti et al., 2004; H.-J. Kim & Bae, 2011; Sweatt et al., 2013). In fact, it has been suggested that regulatory acetylation/deacetylation is considerably more widespread than presently appreciated, acting in a manner similar to phosphorylation/dephosphorylation (Gregoretti et al., 2004; Kouzarides, 2000). Taken together the importance of regulatory acetylation/deacetylation and the relatively small number of studies addressing neuroepigenetics, we were strongly interested in gaining more knowledge about the expression level and spatial distribution of classical HDACs throughout the adult murine brain. For rodents, the expression profile of *Hdacs* within the CNS was only described in rats so far, however a detailed description for the expression in mice is missing (Broide et al., 2007). But as we, and many other research groups, are working mainly with the mouse (*Mus musculus*) as model organism, we were keen on revealing the neural *Hdac* expression profile within the main organism of interest. Key research questions were: How does the spatial *Hdac* expression profile for the eleven classical HDAC members appear in the mouse? Are all *Hdacs* expressed and if they are, do they have distinct or overlapping

expression patterns? And even further, can we obtain any useful information about involvement of HDACs in diseases when we identify distinct brain regions of *Hdac* expression which are known to be involved in pathologies?

With these questions in mind, we started to establish an atlas to comprehensively describe the mRNA expression pattern of all classical HDACs (HDAC1-11) throughout the adult murine brain. The analysis was conducted by using radioactive *in situ* hybridization (ISH) and assessment of silver grains following exposure of radiolabeled brain sections to photoemulsion. When designing highly specific antisense riboprobes for each single *Hdac*, we were facing the first difficulties as it turned out that all eleven classical HDACs are highly homologous to each other reflecting their close relationship. Indeed, the literature describes that HDAC1 and HDCA2 most probably arose from a recent gene duplication event of a common ancestor. This is strongly supported by our data showing that *Hdac1* and *Hdac2* cDNAs share highest homology with 68% similarity (de Ruijter et al., 2003; Gregoretto et al., 2004; Grozinger et al., 2001, 1999; Leipe & Landsman, 1997; Marmorstein, 2001; Shore, 2000). The lowest homology (*Hdac6* and *Hdac7*) still reaches 51% of identity which means that they are closely related to each other. But having a homology does not imply that the proteins fulfill similar functions. We could show that every single conventional HDAC is expressed within the adult murine brain suggesting that they all seem to serve a specific role within neural processes and normal brain function. However, we could not only prove the presence of all classical HDACs within the brain, but we could also show that each enzyme exhibits its unique and distinct expression pattern. The spectrum of expression profiles is difficult to describe as some *Hdacs* like *Hdac1* and *Hdac10* are expressed more globally all over the brain, albeit at low level with exception of some brain regions like the dentate gyrus of the hippocampal formation and the cerebellum, which show higher intensities. Thus, these HDACs might be involved in more common and general functions which are important for the maintenance of many cells or systems within the brain. *Hdac11* for example has in common with *Hdac1* and *Hdac10* that it is globally expressed as well, but it shows a very strong expression throughout the brain suggesting an important role in fundamental neural processes related to brain physiology. Although there is only little known about HDAC11 in general, the expression suggests that it is probably important in the brain. Other patterns were revealed for example for *Hdac4*. It is only expressed in very distinct brain regions and there it shows a relatively high expression whereas it is almost non-detectable in other brain regions.

To summarize the first and general impression of *Hdac* expression throughout the adult murine brain, similar results were observed as previously described for other organs and tissues besides the brain: class I HDACs are broadly expressed, whereas most class II HDACs show a more restricted

expression, but at least one member of class II HDACs is expressed in all analyzed brain regions suggesting again that acetylation/deacetylation is an important posttranslational modification relevant for brain physiology (Grozinger et al., 1999; H. Y. Kao et al., 2001, 2000; Wade, 2001).

In comparison with the atlas for *Hdac* mRNA expression in rat, we could show equal results for both, the highest and lowest expressed HDAC member (Broide et al., 2007). Thus, in rats and in mice, the only class IV member *Hdac11* scores as the highest expressed HDAC, whereas a class II HDAC (*Hdac10*) is the lowest expressed one. The second and third in expression intensity change their places when comparing rat and mouse. In the murine brain *Hdac5* shows a higher expression and is followed by *Hdac3*. Rather strong differences were found for two class I HDACs (*Hdac4* and *Hdac8*) and one class II member (*Hdac9*). Whereas, *Hdac8* and *Hdac9* are rather low expressed in the rat, these isoforms are highly expressed throughout the murine brain. In the case of *Hdac4* it is the other way round (*Hdac4* shows a rather low expression in mice). These results may suggest that distinct HDACs serve different functions in different organisms.

Furthermore, we can see that overlapping expression exists comparing the individual expression profiles. HDACs often act in concert with other HDAC members, either by forming directly a heterodimer or by interacting with each other as being part of the same complexes. Therefore, it is clear, that they require co-localization. Thus, for example HDAC1 is well known to form dimers with HDAC2 and they are members of the same (co-)repressor complexes, whereas HDAC3 interacts with the class II member HDAC4 (Bertos et al., 2001; de Ruijter et al., 2003; Fischle et al., 2002; Fischle, Dequiedt, et al., 2001; Grozinger et al., 1999; Johnstone, 2002; H.-Y. Kao et al., 2002; Taplick et al., 2001; Tong et al., 2002; W.-M. Yang et al., 2002; Zhou et al., 2000). It is also known that some HDAC proteins cannot only influence their own gene expression via a negative feedback loop in dependence of acetylation states, but also the expression of other HDAC members. Hence, HDAC1 is a good example which regulates the HDAC2 expression and *vice versa* (de Ruijter et al., 2003; Hauser et al., 2002; Johnstone, 2002; Schuettengruber et al., 2003; Taplick et al., 2001). Little is known about specific roles of each individual HDAC member in the body, and even less is known for the brain. But it would be important and very interesting to know, if some HDACs can compensate for each other in regions where they show an overlap in expression. Probably the overlap means for some HDACs to interact with each other or to have the same or even a synergistic role in this area. But which HDACs are these? This question goes in line with the problems we have in many pathologies of neuropsychiatric diseases. Often the prescribed drugs act in a broad spectrum against HDACs and therefore, it is difficult to obtain any information about individual roles of individual HDAC members. The problem is even bigger: these drugs not only inhibit the

harmful HDACs in these pathologies, but the *good* HDACs as well, which may have detrimental consequences.

Nevertheless, with our atlas of murine HDAC expression throughout the brain, we are able to provide an idea, in which brain regions which HDACs might play a pivotal role based on their expression. It might be possible to support studies from other research groups which are interested in distinct pathologies: being interested in a special neurological disease or pathology where it is known, that epigenetic modulation through acetylation states plays a crucial role; having then a closer look at the brain regions which are known to be involved in these diseases; extracting from the atlas which HDACs are expressed in these regions and investigating the potential role of this individual HDAC in the disease of interest. Of course, this description is oversimplified, but it illustrates our intention to establish this atlas.

Epigenetic markers have also emerged as important regulators for consolidation and maintenance of memory and learning behavior. Numerous studies could prove that epigenetic marks are actively and transiently regulated in post-mitotic neurons of adult rodents, honeybees, aplysia and drosophila during learning processes (Chwang et al., 2006; Gupta et al., 2010; Kilgore et al., 2010; Levenson & Sweatt, 2005; Levenson et al., 2004; Lockett et al., 2010; Lubin & Sweatt, 2007; Maddox & Schafe, 2011; L. Miller et al., 2011). Furthermore, it has been shown that chromatin remodeling mechanisms like acetylation induce lasting changes in behavior due to stimulus-specific cellular and molecular changes and will consolidate a memory into a permanent trace. With the use of HDAC inhibitors various studies could link histone acetylation/deacetylation to learning processes and memory. They showed that an increase in histone acetylation is associated with enhanced cognition (Korzus et al., 2004; Levenson & Sweatt, 2005; Swank & Sweatt, 2001; Volmar & Wahlestedt, 2014). These findings go in line with studies showing that HDACs are overexpressed in AD mouse models and that treatment with the pan-HDAC inhibitor sodium butyrate could restore a broad histone acetylation pattern which is usually found in mice with enhanced cognitive behavior due to environmental enrichment (Andre Fischer et al., 2007; Frick et al., 2003; F. L. Huang et al., 2006; Peleg et al., 2010; Pereira et al., 2007). As the hippocampus is the part of the brain primarily responsible for short-term memory which is affected or even destroyed early in AD's development, it is interesting to see which HDAC members are expressed. We could show with our expression analysis that in the pyramidal cell layer of the hippocampal formation all HDACs show a distinct expression with differences in their levels (high expression: *Hdac11*; medium expression: *Hdac2*, *Hdac3*, *Hdac4*, *Hdac5*, *Hdac9*; low expression: *Hdac1*; *Hdac6*, *Hdac7*, *Hdac8*, *Hdac10*), however only few *Hdacs* are expressed in the radiatum cell layer (*Hdac5*, *Hdac7*, *Hdac8*, *Hdac9*), the lacunosum moleculare (*Hdac5*, *Hdac7*, *Hdac8*, *Hdac9*) and the molecular layer of the dentate gyrus (*Hdac5*,

Hdac7, Hdac8). The hippocampus as a complex brain structure embedded deep into the temporal lobe plays a major role in learning and memory and is a plastic and vulnerable structure that gets damaged by a variety of stimuli. It is often affected in numerous neurological and psychiatric disorders (i.e. AD, PTSD, stress/depression, bipolar disorders, MS, Chorea Huntington) and therefore it might be useful to have the *Hdac* expression profile in mind, which might be illuminating for a lot of studies and investigations (Anand & Dhikav, 2012).

Further involvements of HDACs in pathological processes are described through comprehensive studies and reports, which show a strong correlation between histone acetylation patterns and the expression of distinct HDACs in response to commonly prescribed drugs for antidepressant treatment and mood stabilizer in specific brain regions such as the nucleus accumbens, striatum, cingulate cortex, amygdala and hippocampus (Benes et al., 2007; Hobara et al., 2010; Ookubo et al., 2013; Rudenko & Tsai, 2014; Volmar & Wahlestedt, 2014). Having a look in our atlas makes clear, that not all *Hdacs* are expressed within the nucleus accumbens (no expression: *Hdac2, Hdac6, Hdac10, Hdac11*) and that *Hdac8* is the highest expressed one. In contrast all *Hdacs* are present in the striatum except *Hdac10* while *Hdac5* shows the strongest expression.

There are many more studies which demonstrate or even prove the involvement of HDACs within neurological and psychiatric diseases and these strongly underline the importance of our established atlas of *Hdac* expression patterns within the murine brain. In the following I would like to highlight some of these studies: The *Hdac1* expression in the nucleus accumbens scores a value of 1.0 and this might be important for the study that MS-275, a HDAC1 specific inhibitor, was shown to restore a normal acetylation state of histone H3K14 when applied to the nucleus accumbens of mice subjected to the chronic social defeat stress paradigm and elicited a significant antidepressant effect (Covington et al., 2009). The *Hdac1* expression in the nucleus accumbens might further correlate with the down-regulation of CAMK2, CREB, ERK, REST and NAChR expression, which is associated with stress, and could be reversed by HDAC1 inhibition via MS-275 treatment (Covington et al., 2009). The expression of HDAC1 has been shown to be elevated in neurons under hypoxia conditions in post-mortem brain samples of schizophrenia patients and in a mouse model for Huntington's disease suggesting a specific role for HDAC1 in the pathogenesis of various brain disorders (Benes et al., 2007; André Fischer et al., 2010; Haberland et al., 2009; Sharma et al., 2008; Z. Wang et al., 2011). Therefore it is interesting to know how the physiological *Hdac1* expression pattern looks like in these affected brain regions under pathophysiological conditions (i.e. *Hdac1* expression: cingulate cortex (1.0); piriform cortex (1.0); striatum (1.0); amygdala (1.0); hippocampus CA1, CA2, CA3 (1.5); medial habenula (2.5); paraventricular nucleus (1.0); central

medial thalamic nucleus (1.0); ventral tegmental area (1.0); substantia nigra pars compacta (1.0)). In contrast, other studies implicated the loss of HDAC1 to be involved in neurodegeneration suggesting rather a neuroprotective than a neurotoxic function for HDAC1 (Bates et al., 2006; Cruz et al., 2003; André Fischer et al., 2010; D. Kim et al., 2008). Another class I HDAC member, HDAC3, has been shown to act as negative regulator of long-term memory formation as the inhibition of HDAC3 enhances long-term object recognition memory in mice and this is linked to an increase in H4K8 acetylation (*Hdac3* expression hippocampus: CA1, CA2 and CA3 (2.5); radiatum cell layer (0); lacunosum moleculare (0); DG granular cell layer (3.0); DG molecular cell layer (0)) (Malvaez et al., 2010; McQuown et al., 2011). The most recent finding of the role of class I HDACs in fear memory is that the phosphorylated form of a well-approved drug for treatment of multiple sclerosis, namely fingolimod (FTY720), inhibits members of class I HDACs and facilitates fear memories (Hait et al., 2014). For fear and anxiety disorders several brain regions are in the focus and it is interesting to have a closer look at the Hdac expression patterns in regions like the amygdala (*Hdac1*: 1.0; *Hdac2*: 2.0; *Hdac3*: 1.5; *Hdac4*: 0.5; *Hdac5*: 2.0; *Hdac6*: 1.5; *Hdac7*: 0.5; *Hdac8*: 1.5; *Hdac9*: 0.5; *Hdac10*: 0; *Hdac11*: 3.0). In 2013 a novel HDAC inhibitor, crebinostat, was identified and inhibits the class I HDACs HDAC1, HDAC2 and HDAC3 as well as the class II HDAC HDAC6. Wild-type mice treated with this inhibitor showed enhanced fear learning. Cultured primary neurons of these mice revealed on the molecular level an increase in BDNF and granulin expression and the density of dentritic synapsin 1 punctae was up-regulated (Fass et al., 2013); HDAC3 was shown to be neurotoxic in Huntington's disease (i.e. *Hdac3* expression in: cortex (2.0-2.5); caudate putamen (2.0); globus pallidus (2.0)) and the expression of *Hdac8* is significantly correlated with the occurrence of neuroblastoma (Bates et al., 2006; André Fischer et al., 2010; Oehme, Deubzer, Lodrini, et al., 2009; Oehme, Deubzer, Wegener, et al., 2009); For class II HDACs, the role of HDAC4 has been described to be important for synaptic plasticity and thus, for memory formation. Studies where HDAC4 was silenced or truncated showed impairments in spatial learning and memory in mice (*Hdac4* expression in hippocampus: CA1 and CA2 (2.0); CA3 (2.5); radiatum cell layer (0); lacunosum moleculare (0); DG granular cell layer (2.0); DG molecular cell layer (0)) (M.-S. Kim et al., 2012; Sando et al., 2012); Furthermore, HDAC4 seems to exert neurotoxic effects under certain conditions. Thus, the specific overexpression of HDAC4 in cerebellar granular neurons (physiological expression of *Hdac4*: 1.0) promoted neuronal cell death and recent studies revealed for HDAC4 a role in regulating muscle gene transcription in response to neural activity at the neuromuscular junction and therefore implicated HDAC4 in the etiology of neuromuscular diseases such as ALS (amyotrophic lateral sclerosis) (Cohen et al., 2007). In addition, a genetic association study found an HDAC4 single nucleotide polymorphism (SNP) to be associated with schizophrenia in a Korean

population (Bolger & Yao, 2005; Cohen et al., 2007, 2009; André Fischer et al., 2010; T. Kim et al., 2010; Williams et al., 2009). Another class II HDAC member, HDAC5 was shown not to be involved in spatial learning, but to be crucial for context- and tone-dependent fear memory formation (i.e. *Hdac5* expression in amygdala: 2.0) (Agis-Balboa et al., 2013; M.-S. Kim et al., 2012); HDAC5 also appears to be a critical regulator of adaptive responses to chronic stress and cocaine consumption (i.e. *Hdac5* expression in: ventral tegmental area (2.0); nucleus accumbens (2.0)), whereas HDAC6 is described to be both, neuroprotective and neurotoxic depending on the disorder it is implicated with (Ding et al., 2008; Fiesel et al., 2010; André Fischer et al., 2010; Kwiatkowski et al., 2009; J. Y. Lee et al., 2010; Ling et al., 2010; Pandey et al., 2007; Perez et al., 2009; Renthal et al., 2007; Tsankova et al., 2006).

However, HDACs are not only involved in pathological processes, but of course also in normal brain function and development. Some examples are: Global loss of HDAC1 leads to early embryonic lethality (E10.5), but studies could show that HDAC1 has no individual role in neuronal development although it is brain-wide expressed. Mice lacking HDAC1 or HDAC2 individually in neuronal precursor cells showed no overt histoarchitectural phenotype and the immature neurons could differentiate normally into mature neurons. *Hdac1* and *Hdac2* show a strong overlapping expression profile in our atlas and therefore seem to substitute for each other. Only the deletion of both, HDAC1 and HDAC2, caused abnormal development as differentiation of progenitors into mature neurons was not possible anymore. The severe effects of the neuronal double knockout (KO) of HDAC1 and HDAC2 leads to early embryonic death at E7.5 (Lagger et al., 2002; Montgomery et al., 2009). HDACs also appear to be involved in synapse development. Studies with differentiated murine hippocampal cells showed a pronounced increase in the maturation of synaptic function as well as a modest increase in synapse number when treated with HDAC inhibitors. Mice with conditional null alleles for HDAC1 and HDAC2 could prove that these two enzymes form a developmental switch that controls excitatory synapse maturation and function. In addition, also the knock-down of HDAC2 alone decreased the synaptic activity, but the loss of HDAC1 had no apparent effect in synapse development (*Hdac1 / Hdac2* expression in hippocampus: CA1, CA2 and CA3 (1.5 / 3.5); radiatum cell layer (0 / 0); lacunosum moleculare (0 / 0); DG granular cell layer (2.5 / 3.5); DG molecular cell layer (0 / 0)) (Akhtar et al., 2009). Furthermore, analysis of cell type-specific and developmental stage-specific expression of HDAC1 and HDAC2 in the mouse cerebellum suggests a potential role for HDAC1 in cell proliferation and for HDAC2 in cell migration and differentiation within the developing cerebellum (*Hdac1 / Hdac2* expression in cerebellum: granular cell layer (2.0 / 2.5); molecular cell layer (0 / 0); purkinje cell layer (0 / 2)) (Yoo et al., 2013). However, different HDACs appear to have specific roles in different types of learning and memory. Guan and

colleagues for instance identified HDAC2, but not HDAC1, to be a negative regulator of associative and spatial memory via overexpression and knockout studies (Guan et al., 2009); The class II HDAC members HDAC5 and HDAC6 seem also to be involved in the development of the CNS. Hence, HDAC5 has been implicated in the proliferation of NSC via its co-recruitment with LSD1 to the promoter of target genes downstream of the orphan nuclear receptor TLX, an essential regulator of the maintenance and self-renewal of neural stem cells in embryonic and adult brains (André Fischer et al., 2010; W. Li et al., 2008; Yanhong Shi et al., 2004; Sun et al., 2010). HDAC6 was demonstrated to be important for cellular processes such as neuronal transport and the cytoskeletal network during brain development (André Fischer et al., 2010; Y. Gao et al., 2007).

Concluding, it emerges that we were successful in establishing an atlas to comprehensively describe the mRNA expression of all classical HDACs (HDAC1-11) throughout the adult murine brain. All eleven HDAC members show high sequence similarities, but nevertheless, all are expressed within the adult murine brain, each with a distinct expression pattern. Comparing the results with studies of the rat brain, we could show equal results for the highest (*Hdac11*) and lowest (*Hdac10*) expressed HDAC member. However, differences were especially revealed for *Hdac4*, *Hdac8* and *Hdac9*. Furthermore, many neurological and psychiatric diseases as well as normal brain processes involve HDACs and therefore it is highly important to have an expression atlas revealing the spatial distribution, expression level and patterns of co-expression of *Hdacs* in the main mammalian model organism in biomedical research.

5.2 Establishing the oral application of tamoxifen via chow to activate the Cre/loxP system in conditional transgenic mouse models

Mouse models of transgenic overexpression or knockout mouse models are frequently used in many research laboratories since decades. The increase of gene activity (overexpression) or in contrast the loss of gene activity (knockout) often provide valuable insights into the physiological role of a gene of interest. The mouse as mammalian model organism shares approximately 70% of the protein-coding sequence with humans. Thus, the change in the mouse's phenotype (appearance, behavior and other observable physical and biochemical characteristics) due to a gain or loss of gene activity can largely be translated to the human system.

Especially in neurobiology mouse mutants with targeted inactivation of a desired gene or overexpression of a distinct gene in specific brain regions or cell types are used as powerful tools to analyze a gene's role in complex brain function such as learning, memory, emotional behavior, synaptic plasticity as well as neurogenesis and neuronal cell death (Anagnostopoulos et al., 2001; Bolivar et al., 2000; C. Chen & Tonegawa, 1997; Erdmann et al., 2007). However, often the early inactivation of a gene is detrimental and causes embryonic or developmental abnormalities leading to embryonic or postnatal lethality. Therefore, overexpression and knockout of genes often needs to be under spatial and/or temporal control. An elegant and most frequently used tool to bypass severe side effects of overexpression or knockout studies is the spatio-temporal control via the Cre/loxP system. The conditional overexpression or ablation of a gene is achieved by the cell-type-specific expression of the bacteriophage P1-derived Cre recombinase under the control of a distinct promoter. Thus, in the Cre expressing cells, the recombinase mediates excision of an essential part of the targeted gene/DNA sequence that has been flanked by two loxP recognition sequences in the same orientation (Branda & Dymecki, 2004; Deussing, 2013; Erdmann et al., 2007; Gu, Marth, Orban, Mossmann, & Rajewsky, 1994; Lewandoski, Wassarman, & Martin, 1997). To drive the spatial control of Cre expression in the brain, in most cases short promoter fragments of genes with the desired expression pattern have been cloned upstream of the Cre cassette. In order to target neurons in the adult brain that participate in important brain functions like learning, memory and long term potentiation, the Camk2a gene regulatory elements were chosen to drive Cre expression in the forebrain including limbic structures like hippocampus and amygdala (Erdmann et al., 2007; Tsien et al., 1996). In order to achieve a tight temporal control, the Cre recombinase was fused to a mutated estrogen receptor (ER) ligand-binding domain which results in binding to the heat-shock

protein 90 (HSP90) complex (Feil et al., 1997). Upon tamoxifen binding to the ER ligand binding domain, the fusion protein is released from the complex and translocates due to a nuclear localization signal (NLS) of Cre into the nucleus, where Cre-mediated recombination/deletion occurs (Feil et al., 1997; Hayashi et al., 2000; Indra et al., 1999; Metzger & Chambon, 2001).

At the beginning of this thesis, there is no stress-free method for tamoxifen administration in mice existed. In rodents, the most frequently used chemical form of tamoxifen is 4-hydroxytamoxifen (4-OHT), dissolved in alcohol and/or oil, administered usually by repeated intraperitoneal (i.p.) injections, supplied by gavaging or via the drinking water. However, i.p. injections and gavaging impose considerable stress on mice, whereas administration via drinking water is hampered by poor solubility (0.5 mg/ml at 37°C). Thus, feeding the animals with tamoxifen enriched chow would be an elegant way to reduce handling distress on mice, effort and costs. There are studies which describe the use of tamoxifen enriched chow, but high 4-OHT doses (2.5 mg/g) are needed meaning that mice consume up to 20% of the acute lethal dose. Even though there are no severe side-effects described so far, the administration via 4-OHT chow is limited by poor acceptance by mice due to the bitter taste of the food pellets (Agger et al., 2005; Brocard et al., 1997; Casanova et al., 2002; Forde et al., 2002; Indra et al., 2005; Kostetskii et al., 2005; Leone et al., 2003; M. Li et al., 2000; Metzger & Chambon, 2001; Mijimolle et al., 2005; Moosmang et al., 2003; Petrich et al., 2003; Sohal et al., 2001; Xiao et al., 2001; Yu et al., 2005). Kiermayer and colleagues described the use of soy-free chow containing another chemical form of tamoxifen, tamoxifen citrate salt (TCS), produced by LASvendi (Soest, Germany) (Kiermayer et al., 2007). In this chow, the tamoxifen dose can be kept at a minimum level of 400 mg/kg due to the use of TCS and the absence of the tamoxifen antagonist soy genistein which can be found in high concentrations in conventional chow. Thus, the total tamoxifen uptake can be minimized and the chow is more accepted by the rodents as the bitter taste is kept within a limit compared to high concentration 4-OHT soy-rich chow. The TCS enriched soy-free chow was shown to be effective in a heart-specific inactivation of thioredoxin reductase 2 (Kiermayer et al., 2007). To extend the use of the described TCS chow to brain-specific gene overexpression or disruption, we addressed the question, if the tamoxifen administered via the described TCS food pellets will result in efficient Cre-mediated recombination within the central nervous system (CNS). For this establishment of the tamoxifen chow, we chose to use an overexpressing mouse model providing a positive readout to assess the efficacy of tamoxifen treatment. Therefore, mice of the line CRH-COE^{IFB} were fed with tamoxifen chow (LASvendi, Soest, Germany). These mice express the Cre recombinase spatially and temporally controlled by the Camk2a promoter which is active in principal neurons of the forebrain from postnatal day 9. However, the fusion to the ER ligand binding domain presents Cre recombinase activity providing

another level of temporal control by the timing of tamoxifen administration. Mice were only fed with tamoxifen chow in adulthood resulting not only in an overexpression of *Crh* within the forebrain, but also in expression of the reporter gene *lacZ*. *LacZ* mRNA was easily and sensitively detected by *ISH* analysis.

In summary, various short-term (minimum 2 days) and long-term (maximum 5 weeks) tamoxifen administration periods with and without a wash-out phase (7 days) were carried out and analyzed. Both, the shortest and the longest administration showed high DNA recombination levels visible by *lacZ* expression. However, it seems that we can address the hippocampus already with short-term tamoxifen administration, whereas recombination in other structures like the cortex require longer phases of tamoxifen supply. This effect might also to some extent be explained by the higher cell density within the hippocampal pyramidal cell layer which might lead to an overestimation of the signal. The wash-out phase of seven days with standard diet even increased the number of recombined neurons and in addition allows to turn-over the tamoxifen before phenotypical analysis.

As TCS chow is known to be bitter in taste, the feeding and drinking behavior of mice during tamoxifen treatment was observed. However, although the mice accepted the tamoxifen chow, the mean food consumption is slightly lower compared to normal food. When mice were transferred from TCS chow back to standard diet for the wash-out phase, we could observe a distinct peak in food intake within the first 24 hours after the transfer (no genotype effect was observed). When analyzing the water consumption, we could detect the same effects observed for food intake. Mice seem to detect the differences in taste between the two kinds of pellets and they seem to prefer the standard diet which might explain the strong increase in food intake after the change of the chow. As the food pellets are low in liquid content, the mice probably need to increase their water consumption as well.

Taking these experiments and their results into account, we thus, suggest as the best compromise between recombination efficacy and aversive effects of tamoxifen food (i.e. on body weight) for the spatio-temporal control of either overexpression or knockout studies in principal forebrain neurons by the use of the *Camk2a-CreER^{T2}* mouse line the following treatment scheme: mice are fed seven days with tamoxifen chow followed by a seven day wash-out phase with standard diet prior phenotypical analysis or behavioral testing.

5.3 Genetically dissecting brain-specific functions of histone deacetylase 1 (HDAC1) and histone deacetylase 3 (HDAC3)

Genetically modified animal models such as knockout mice play a prominent role in the study of biological systems and pathways in many fields of biomedical research. The loss of gene activity often provides valuable clues about what a gene of interest is involved in and the knockout often causes changes in a mouse's phenotype including appearance, behavior and observable physical and biochemical characteristics. With the use of conditional mouse mutants, a target gene of interest can even be specifically inactivated in distinct tissues and/or at a given time point to bypass the limitations of traditional knockouts like embryonic lethality. With our two knockout mouse models concerning HDAC1 and HDAC3, we focused on addressing brain-specific functions of either HDAC1 or HDAC3. HDAC1 is the first protein found to possess histone deacetylase activity and belongs to the large protein family of histone deacetylases. HDAC3 as the third member out of four belonging also to class I HDACs was discovered after HDAC1 and HDAC2 and shares also a high sequence homology with yeast RPD3 yet distinct from HDAC1 and HDAC2. HDACs are known to act as epigenetic modifiers and therefore, regulate the acetylation/deacetylation state of histone proteins which in turn change chromatin formation and structure to regulate gene expression (de Ruijter et al., 2003; Gregoret et al., 2004; Kouzarides, 2000). Epigenetic mechanisms seem to serve a potential role in many biological processes and pathologies and also have fostered the emerging field of neuroepigenetics. Thus, epigenetic mechanisms in the central nervous system are just beginning to be understood and this is one of the most exciting areas of contemporary molecular and behavioral neuroscience. Furthermore, histone deacetylases do not only have histones as substrates, but also non-histone proteins and therefore serve multiple functions. HDAC1 and HDAC3 belong to class I HDACs which are usually found in the nucleus to fulfill their main function in epigenetic regulation by deacetylating histone molecules. The rather small proteins show a high sequence similarity between the human and mouse homologs. Thus, only three amino acids of HDAC1 are different within the whole sequence of 482 amino acids, whereas the HDAC3 enzyme in humans and mice comprise exactly the same amino acid sequence. Therefore, the results from the genetic mouse models targeting either *Hdac1* or *Hdac3* can be translated to potential functions of human HDAC1 or HDAC3, respectively.

In a first step, we used *Hdac1-lacZ* reporter mice and *Hdac3-lacZ* reporter mice which both express the reporter gene *lacZ* as a fusion transcript consisting of the first two *Hdac1* or *Hdac3* exons and the IRES-driven *lacZ* sequence regulated by either the *Hdac1* or *Hdac3* promoter. Mice of this line

were sacrificed and more than 20 organs and tissues were stained for *lacZ* expression, which demonstrates the expression pattern of HDAC1 or HDAC3 throughout the mouse body. From literature it is known that *Hdac1* and *Hdac3* are, like the other class I HDACs, ubiquitously expressed in almost all organs and tissues which we could confirm with our *lacZ* expression analysis as well (Montgomery et al., 2007). In addition, the *lacZ* staining of whole brain as well as brain sections showed that HDAC1 and HDAC3 are both specifically expressed within the murine brain revealing a unique expression pattern. Comparing the results of the *lacZ* staining of *Hdac1-lacZ* reporter mice with the *Hdac1* mRNA expression (chapter 4.1), both revealed a weak *Hdac1* expression throughout the brain in general and showed distinct and strong expression only in a few regions like the dentate gyrus. For *Hdac3*, both, the *lacZ* staining of *Hdac3-lacZ* reporter mice and the mRNA expression analysis (chapter 4.1) revealed a strong *Hdac3* expression throughout the whole brain. The mRNA expression patterns of all eleven HDACs showed that *Hdac3* ranks as the HDAC member with the third highest expression level when considering the overall expression in the brain. The *lacZ* staining also indicated a high expression level for *Hdac3*. Furthermore, both analyses, showed particularly intense expression in the granular cell layer of the olfactory bulb, cortical structures, the caudate putamen, the nucleus accumbens, the globus pallidus, the septum, the hippocampal formation, parts of the pons (dorsal raphe nucleus, interpenduncular nucleus, pendunculopontine tegmental nucleus), the cerebellum and all parts of the medulla except the facial nucleus. To specifically address HDAC1 or HDAC3 functions in the brain and to overcome the embryonic lethality of *Hdac1* or *Hdac3* total knockout mice, first described for HDAC1 by Lagger and colleagues (Lagger et al., 2002) and for HDAC3 by Dangond and colleagues (Dangond et al., 1998, 1999; Glaser et al., 2003; Robyr et al., 2002), but also shown by the viability of only heterozygous *Hdac1-lacZ* or *Hdac3-lacZ* reporter mice, we generated mouse models with a spatio-temporal control of the HDAC1 or HDAC3 inactivation, respectively. Therefore, we used for both mouse models the elegant tool of the Cre/loxP system. For the spatial control, we chose an expression of the Cre driven by regulatory elements of the *Camk2a* gene in order to target specifically principal neurons in the adult forebrain. Thus, we can inactivate the *Hdac1* or *Hdac3* gene specifically in principal neurons of limbic structures such as hippocampus and amygdala (Erdmann et al., 2007; Tsien et al., 1996).

In the literature, it is often described that the two class I HDAC members HDAC1 and HDAC2 are highly homologous. Indeed, they are known to share a DNA sequence similarity of more than 82%, which is the highest one among the HDACs (de Ruijter et al., 2003; Khier et al., 1999; W M Yang et al., 1996; Wen Ming Yang et al., 1997). There is also strong evidence that HDAC1 and HDAC2 most probably originate from a recent gene duplication event (Gregoretto et al., 2004). Furthermore, HDAC1 and HDAC2 often function together as heterodimers and they are found in the same co-

repressor complexes which are known as SIN3, NuRD and CoREST (Ayer, 1999; de Ruijter et al., 2003; Grozinger et al., 2001; Hui Ng & Bird, 2000). Both enzymes are exclusively found in the nucleus to fulfill their function. However, although they are often redundant in function and can substitute for each other, it is clear that they inhabit also distinct and unique roles. This is also indicated by the differences in their expression patterns shown in chapter 4.1. *Hdac2* is especially expressed at a higher level throughout the whole brain when compared to *Hdac1* expression. Furthermore, the knockout of *Hdac1* is described to lead to embryonic lethality at E10.5 meaning that HDAC2 cannot fully substitute the HDAC1 during development. Here we intended to specifically investigate HDAC1 functions in brain regulation and dysregulation through the above described spatio-temporal *Hdac1* knockout animals.

Moreover, HDAC3 lacks a small segment corresponding to the extreme N terminus of HDAC1 and HDAC2 and also regions that correspond to the C terminus of HDAC1 and HDAC2 are absent (HDAC1: 399-482; HDAC2: 400-488) suggesting that both HDAC3 ends possess unique functions that are distinct from other class I HDACs. In addition to the nuclear localization signal (NLS) which is present in all class I HDACs, a functional nuclear export signal (NES) resides in HDAC3 between residues 180-313, allowing the HDAC3 protein to shuttle in and out of the nucleus in almost all cell types to fulfill its function (de Ruijter et al., 2003; Takami & Nakayama, 2000; W.-M. Yang et al., 2002). HDAC3 mainly self-associates in dimers and trimers to be active, but also hetero-oligomerization with other HDACs is possible, although this has only been detected to a small extent. Endogenous HDAC3 only associates with HDAC4, whereas the oligomerization with other class II HDACs, namely HDAC5, HDAC7, HDAC9 and HDAC10 is only detected when HDAC3 is bound within one of the multi-protein complexes. Comparing the expression patterns of *Hdac3* and these five class II HDACs, it is clear that they show substantial overlap of signal (except *Hdac10*), especially in regions where *Hdac3* is highly expressed (see above). Similar to the overlapping expression patterns, HDAC3 shares with HDAC5 to inhabit not only a NLS, but also a NES (Lemercier et al., 2000; Sparrow et al., 1999). The co-repressor multi-protein complexes relying on HDAC3 activity are NCoR (nuclear receptor corepressor) and SMRT (silencing mediator for retinoid and thyroid hormone receptors) (Bertos et al., 2001; Fischle et al., 2002; Fischle, Dequiedt, et al., 2001; Grozinger et al., 1999; H. Y. Kao et al., 2000; Tong et al., 2002; W.-M. Yang et al., 2002; Zhou et al., 2000). However, NCoR and SMRT do not only bind HDAC3, but can also stimulate its activity via a conserved deacetylase-activating domain (DAD) (Guenther et al., 2000; Wen et al., 2000; J. Zhang et al., 2002). After the discovery of HDAC3, often its biological function has been extrapolated from the functions ascribed to HDAC1 and HDAC2. However, HDAC3 possesses many unique biological functions. With its repressive action on transcription it is not only involved in cell cycle control, but also critically

regulates ribosome biogenesis. Embryonic lethality of knockout mice at E10.5 emphasizes its unique function in development (Dangond et al., 1998, 1999; Glaser et al., 2003; Robyr et al., 2002). With our genetic *Hdac3* mouse model we focused on addressing brain-specific functions of the enzyme.

The temporal control of the gene inactivation of either *Hdac1* or *Hdac3* was induced by tamoxifen treatment in adulthood at an age of 8-12 weeks. We chose this time point because we did not want to obtain any disturbances in adult behavior due to a lack of either HDAC1 or HDAC3 in specific developmental stages. Previous studies on mice lacking HDAC1 or HDAC2 individually in neuronal precursor cells showed no overt histoarchitectural phenotype and the immature neurons could differentiate normally into mature neurons. Only the deletion of both, HDAC1 and HDAC2, caused abnormal development as differentiation of progenitors into mature neurons was not possible anymore. The severe effects of the neuronal double knockout of *Hdac1* and *Hdac2* lead to early embryonic death at E7.5 (Lagger et al., 2002; Montgomery et al., 2009). In addition, HDACs appear also to be involved in synapse development. Studies with differentiated murine hippocampal cells showed a pronounced increase in the maturation of synaptic function as well as a modest increase in synapse number when treated with HDAC inhibitors. Mice with conditional null alleles for *Hdac1* and *Hdac2* could prove that these two enzymes form a developmental switch that controls excitatory synapse maturation and function. In addition, also the knockdown of *Hdac2* alone decreased the synaptic activity, but the individual loss of HDAC1 had no apparent effect on synapse development (Akhtar et al., 2009). However, less is known about the potential role of HDAC3 in such processes of brain development or brain maintenance.

The quality of prenatal and early postnatal environment and experiences has consequences on adult behavior. Thus, persisting epigenetic marks are acquired through early-life experiences via epigenetic mechanisms and these marks cause lasting cellular effects which are responsible for the basis of adult behavior including positive aspects like greater courage and better learning as well as negative aspects like vulnerability to stress, susceptibility to diseases and cognitive deficits. HDACs have been demonstrated to be involved in these epigenetic processes. Hence, the positive effects of high-grooming maternal care on offspring brain development was linked to histone acetylation (André Fischer et al., 2010; Skinner, 2011; Weaver et al., 2004, 2005). Moreover, fundamental questions regarding animal behavior can be explained by putative factors such as early life stress, adversity, abuse and social interactions, and these behavioral patterns are not essentially ingrained, immutable and only determined by the genetic make-up. Genes and experience are mechanistically intertwined and epigenetic mechanisms contribute to this intertwining (Farah & Hook, 2008; Ravi &

Kannan, 2013; Sweatt et al., 2013). With the conditional knockout of either *Hdac1* or *Hdac3* specifically in principal forebrain neurons, we can address HDAC1 and HDAC3 functions in processes such as memory, learning and cognition or in emotional behavior. Of course, in regard to *Hdac1* and *Hdac3* expression in the brain, it makes not only sense to investigate the role of HDAC1 and HDAC3 in these forebrain regions, but also in other neuronal or glial cell types throughout the brain, e.g. in the cerebellum based on the high expressions of both HDACs in this brain structure. Both, the expression analysis of *Hdac1* on mRNA level (chapter 4.1) and the lacZ staining proved a high and distinct expression of *Hdac1* in the Purkinje cell layer of the cerebellum. Furthermore, analysis of cell type-specific and developmental stage-specific expression of *Hdac1* and *Hdac2* in the mouse cerebellum suggests a potential role for HDAC1 in cell proliferation and for HDAC2 in cell migration and differentiation within the developing cerebellum (Yoo et al., 2013). The cerebellum plays especially an important role in balance and motor control. However, for our studies it was more important to generate a forebrain-specific knockout to study the HDAC1- and HDAC3-specific function in memory and cognitive processes, as well as emotional behavior as little is known about the particular role of HDAC1 and HDAC3.

Human anxiety disorders are broadly grouped according to symptomology and responsiveness to pharmacological and psychological treatment with the use of the classification and diagnostic tool DSM-5 (diagnostic and statistical manual of mental disorders, fifth edition) (Bailey & Crawley, 2001; Nutt, 1990; Weiss, 2007). Generalized anxiety disorders and panic disorders are the two primary classifications of pathological anxiety in humans. In an attempt to assess anxiety in rodents, a wide range of behavioral testing paradigms has been developed (Bailey & Crawley, 2001; Borsini, Lecci, Volterra, & Meli, 1989; J. Crawley & Goodwin, 1980; File, 1980; Hall, 1934; Slotnick & Jarvik, 1966; Vogel, Beer, & Clody, 1971). Many of these tests induce a fearful response through an aversive event or anticipated aversive event. Others integrate an approach–avoidance conflict designed to inhibit an ongoing behavior that is characteristic for the animal, such as contrasting the tendency of mice to engage in exploratory activity or social investigation against the aversive properties of an open, brightly lit, or elevated space. The premise that basic physiological mechanisms underlying fear in rodents can be equated to similar mechanisms operating in humans provides a high degree of face validity for the paradigms (Cryan & Holmes, 2005; Ohl, 2005; R. J. Rodgers & Dalvi, 1997).

Comprehensive studies show a strong correlation between histone acetylation patterns and the expression of distinct HDACs in response to commonly prescribed drugs for antidepressant treatment and mood stabilizer in specific brain regions such as the nucleus accumbens, striatum, cingulate cortex, amygdala and hippocampus (Benes et al., 2007; Hobara et al., 2010; Ookubo et

al., 2013; Rudenko & Tsai, 2014; Volmar & Wahlestedt, 2014). All these brain structures show a high expression level of *Hdac3* and are addressed with both of our *Hdac1* and *Hdac3* knockout models. Up to date, most of the HDAC-related findings have been obtained through inhibitor studies. Therefore, we intended with our *Hdac1* and *Hdac3* knockout mice to specifically address the role of HDAC1 and HDAC3 in emotional behaviors such as anxiety.

In a basic emotionality screening, we assessed the behavior of the conditional *Hdac1* and *Hdac3* knockout animals in comparison to the control littermates using a battery of well-known and established tests. The first test was the OF test, which revealed for both, the conditional *Hdac1* knockout mice as well as the conditional *Hdac3* knockout mice no deficits in locomotion. This was very important ensuring, that all effects, we obtained in these behavioral testings were independent of locomotor alterations. There might have been a potential role of either HDAC1 or HDAC3 in balance and motor control due to their high expression in the cerebellum (Yoo et al., 2013), but in our conditional knockout mice, HDAC1 and HDAC3 are still expressed in the cerebellum as we specifically deleted *Hdac1* or *Hdac3*, respectively, in the forebrain. Moreover, the OF test as initial screen for anxiety-related behavior did not show any significant difference comparing *Hdac1* or *Hdac3* conditional knockout animals with control littermates. Other well established tests screening for anxiety-related behavior are the EPM test and the DaLi test. The former is one of the most validated tests of anxiety in rodents. The natural explorative tendency of mice is in opposition to the innate fear of illuminated, elevated and unprotected areas. This approach–avoidance conflict results in behaviors that have been correlated with increases in physiological stress indicators. In contrast, administration of benzodiazepines and other anxiolytic treatments results in increased exploration of the open arms, without affecting general motivation or locomotion (Bailey & Crawley, 2001; Bailey, Rustay, & Crawley, 2006; Gonzalez & File, 1997; Handley & Mithani, 1984; R J Rodgers, Johnson, Carr, & Hodgson, 1997; R. J. Rodgers & Dalvi, 1997). Parameters of interest included ‘open arm time versus closed arm time’, ‘latency until first open arm entry’, ‘number of open arm entries’, and ‘total distance travelled’. We observe in the EPM test that the conditional *Hdac1* knockout mice showed reduced anxiety-related behavior indicated by all analyzed parameters. Thus, HDAC1 seems to be a negative regulator of anxiety-related behavior as the conditional *Hdac1* knockout mice exhibit decreased anxiety. In contrast, we could not show any effects or changes in anxiety-related behavior of conditional *Hdac3* knockout mice in the EPM when compared to control littermates. In addition, the DaLi test, a precursor to the EPM test, developed by Crawley and Goodwin provides another means of examining anxiety-related behavior in rodents. Here the mice are also exposed to a novel environment with both, protected (dark compartment) and unprotected (light compartment) areas. The conflict between the innate

aversion of rodents to brightly illuminated areas and the spontaneous exploratory behavior of rodents in response to mild stressors, that is, novel environment and light is thought to inhibit exploration. Most mice naturally demonstrate a preference for the dark, protected area. To assess anxiety-related behavior in this design a change in willingness to explore the illuminated, unprotected compartment is indispensable and reflected in an increase or decrease in analyzed parameters such as 'number of transitions' and 'time spent in each compartment' (Blumstein & Crawley, 1983; J. Crawley & Goodwin, 1980; J. N. Crawley, 1981). However, the DaLi test could not strengthen or support the findings of the EPM test for conditional Hdac1 knockout mice as these showed no overt phenotype when compared to control animals. Thus, it seems that conditional Hdac1 knockout mice lose the aversion against an unprotected area faster if this is an elevated open arm of the EPM test than a highly illuminated area. As a limitation of the DaLi test, it has been reported that dark/light transitions are likely to be confounded by alterations in general activity, and it was suggested that the behavioral expression of decreased anxiety in the dark/light box may be determined by genetically based spontaneous exploration (Bourin & Hascoët, 2009; Ohl, 2005). For conditional Hdac3 knockout mice, the DaLi test did not show any change in anxiety-related behavior and therefore supports the results of the EPM test, but conditional Hdac3 knockout animals entered the lit compartment more often and traveled there a longer distance, whereas the total time the knockout animals spent in the lit compartment was not changed compared to control littermates. Thus, HDAC3 seems not to be involved in the regulation of anxiety-related behavior as the conditional Hdac3 knockout mice showed no overt phenotype.

For further studies, we analyzed both mouse models, the conditional Hdac1 and Hdac3 knockout animals within the chronic social defeat stress (CSDS) paradigm (Berton et al., 2006; Wagner et al., 2011). The decision to use this paradigm was based on two factors: The first one is the fact that HDACs are epigenetic modifiers which regulate gene x environment interactions. Therefore, it is interesting to learn more about the HDAC1- and HDAC3-specific roles when the subjects are exposed to chronic stress before behavioral phenotyping and thus to assess the importance of gene x environment interactions for the etiology of psychiatric disorders. The other factor is mainly valid for conditional Hdac1 knockout animal, since the HDAC1-specific inhibitor MS-275 was shown to restore a normal acetylation state of histone H3K14 when applied to the nucleus accumbens of mice subjected to the chronic social defeat stress paradigm which elicited a significant antidepressant effect. Thus, we were interested, if also the anxiety-related behavior is changed. Therefore, the animals were analyzed in the OF test and the EPM test analogous to the basal screen before. However, the OF test showed no significant effect between conditional Hdac1 knockout animals and control animals. We could only observe a condition effect revealing that chronically

stressed animals traveled less, were longer immobile and stayed less time in the inner zone. These condition effects reflect the efficacy of the chronic social defeat stress paradigm. When analyzing the EPM test data for conditional Hdac1 knockout mice, we found a significant genotype by condition interaction suggesting that the anxiety-related behavior in conditional Hdac1 knockout mice observed under basal conditions is reverted when mice are exposed to chronic stress. Here, HDAC1 as epigenetic regulator potentially modifies chromatin structure and gene expression in response to the environmental stimuli (chronic stress) in a way which reverts the phenotypical outcome. The basal effect was confirmed in the non-stressed group of the CSDS paradigm when analyzing parameters such as the 'latency to first open arm entry' of the two genotypes. The other parameters did not reach statistical significance (only trends were observed), but that might be due to handling of mice every day during the three weeks of chronic stress. In case of conditional Hdac3 knockout animals, we were interested, if the anxiety-related behavior which is not changed under normal conditions is subjected to changes by chronic stress. Therefore, the animals were analyzed in the OF test and the EPM test analogous to the basic screening before. However, neither the OF test, nor the EPM test showed any differences, analogous to the previous basic screen suggesting again no specific role for HDAC3 in the expression of emotional behavior, i.e. anxiety-related behavior.

Besides anxiety-related readouts, we were also interested in stress-coping and depression-related behavior in the conditional Hdac1 and Hdac3 knockout mice as some studies in the literature describe the inhibition of HDAC isoforms to be beneficial to treat symptoms of depression (Benes et al., 2007; Covington et al., 2009; Hobara et al., 2010; Kurita et al., 2012). Furthermore, the down-regulation of CAMK2, CREB, ERK, REST and nAChR expression, which is associated with stress, could be reversed by MS-275 treatment (Covington et al., 2009). To get an idea if HDAC1 or HDAC3 play a role in maladaptive or pathological responses leading to depression-related behavior, we analyzed the conditional Hdac1 and Hdac3 knockout mice in the FST. This test was first introduced by Porsolt in 1977 and is one of the most frequently used models to assess stress-coping/depression-related behavior in rodents. We assessed depression-related behavior in the basic emotionality screening as well as in the CSDS paradigm. In the former, the amount of struggling was decreased in the conditional Hdac1 knockout animals and this could be confirmed in the CSDS paradigm under basal conditions and was also visible following chronic stress. As a decrease in struggling means a decrease in despair, we might hypothesize that the conditional knockout of Hdac1 leads to an antidepressant-like effect. In contrast, under neither of the conditions any disturbances in stress-coping behavior caused by the ablation of HDAC3 was observed.

Furthermore, it is widely known that stress enhances plasma corticosterone levels. Therefore, basal levels of corticosterone were assessed for both mouse models (conditional Hdac1 and Hdac3 knockout) in all animal groups tested in the CSDS paradigm during the circadian nadir in the morning. For conditional Hdac1 knockout animals no effects were observed, whereas a genotype effect was obtained for the stressed conditional Hdac3 knockout animals meaning that conditional Hdac3 knockout mice responded stronger to the chronic stress than the control animals did. To gain more insight in the behavioral alterations caused by the interaction of the missing HDAC1 or HDAC3 enzyme and chronic stress, we assessed deficits in social behavior by the use of the SA test, which was established by Berton and colleagues (Berton et al., 2006) and represents social avoidance or fear of an unfamiliar interaction partner. When subjected to stress, some individuals develop maladaptive symptoms whereas others retain normal behavior (E. Lee et al., 2015). A variety of neurological and psychiatric disorders are characterized by deficits in social behavior. However, we could not observe any condition by genotype interaction in these tests, neither for conditional Hdac1 knockout mice nor for conditional Hdac3 knockout mice. Both, HDAC1 and HDAC3 do not seem to be dominantly involved in regulation of social interaction as mice seem to retain normal behavior although they are often made socially avoidant by the chronic social defeat procedure (E. Lee et al., 2015). As anhedonia is one of the core symptoms of depression, the behavior of the conditional knockout mice was also observed by the use of the FUST, which is a test designed for reward-seeking behavior and was adopted from Malkesman and colleagues (Malkesman et al., 2010). However, we could not observe any changes in anhedonic behavior for conditional Hdac1 knockout animals, but we saw, that HDAC3 seems to play an important role in hedonic behavior as the knockout mice were more interested in the tips soaked with female urine compared to control littermates.

Finally, we were interested in the cognitive performance of the conditional Hdac1 and Hdac3 knockout mice as previous studies have shown an involvement of HDACs in cognition compared to anxiety-related behavior (D. Kim et al., 2007; Korzus et al., 2004; Levenson & Sweatt, 2005; Malvaez et al., 2010; McQuown & Wood, 2011; Swank & Sweatt, 2001; Volmar & Wahlestedt, 2014). Chromatin remodeling mechanisms like acetylation have the potential to induce lasting changes in behavior due to stimulus-specific cellular and molecular changes and will consolidate a memory into an everlasting trace. However, most studies linking histone acetylation to learning processes and memory were conducted using HDAC inhibitors. These studies could show that increased histone acetylation is associated with enhanced cognition. Histone acetylation was especially shown to be involved in critical steps of stabilizing short-term memory into long-term memory in wild-type mice (Korzus et al., 2004; Levenson & Sweatt, 2005; Swank & Sweatt, 2001; Volmar &

Wahlestedt, 2014). In aged mice or neurodegenerative mouse models linked to Alzheimer's disease the treatment with the pan-HDAC inhibitor sodium butyrate could restore a broad histone acetylation pattern which is usually found in mice with enhanced cognitive behavior due to environmental enrichment (Andre Fischer et al., 2007; Frick et al., 2003; F. L. Huang et al., 2006; Peleg et al., 2010; Pereira et al., 2007). However, different HDACs appear to have specific roles in different types of learning and memory. Guan and colleagues for instance identified HDAC2, but not HDAC1, to be a negative regulator of associative and spatial memory via overexpression and knockout studies (Guan et al., 2009). Furthermore, with the use of MS-275, a HDAC1-specific inhibitor, and virus-induced overexpression of *Hdac1* within the hippocampal formation of adult mice, HDAC1 was proven to enhance the extinction of contextual fear memories (Bahari-Javan et al., 2012). Moreover, HDAC3 was shown to act as negative regulator of long-term memory formation as the inhibition of HDAC3 enhances long-term object recognition memory in mice and this is linked to an increase in H4K8 acetylation (Malvaez et al., 2010; McQuown et al., 2011).

With the conditional *Hdac1* knockout and conditional *Hdac3* knockout, both restricted to principal neurons of the forebrain we specifically addressed brain structures which are involved in memory processes. We used the water cross maze (WCM) to assess spatial learning via allocentric navigation of mice. As expected and before described by Guan and colleagues with the use of *Hdac1* overexpressing mice, our results support the idea that HDAC1 seems not to be involved in the regulation of spatial memory (Guan et al., 2009). In contrast, conditional *Hdac3* knockout mice showed in comparison with control littermates a strong impairment in spatial learning. These were rather unexpected results having the above mentioned study in mind in which HDAC3 was described as a negative regulator of long-term memory formation (McQuown et al., 2011). However, this study used another cognition test, the object recognition test. Furthermore, the knockout was induced by viruses specifically injected only in the hippocampus. In our conditional knockout animals, *Hdac3* is ablated in all principal neurons of the adult forebrain meaning that these neurons show all a change in histone acetylation patterns which might affect learning procedures.

To sum up, our experiments with both, conditional *Hdac1* and conditional *Hdac3* knockout mice, showed that both enzymes, HDAC1 and HDAC3, are ubiquitously expressed in various murine tissues including the central nervous system. In addition, both enzymes seem to play a pivotal role in embryonic development as in both cases two null alleles cause embryonic lethality. With a spatio-temporal knockout restricted to principal forebrain neurons in adult animals we could specifically address brain structures and systems which are involved in anxiety as well as in memory formation

processes. The conditional Hdac1 knockout leads under basal conditions to a decrease in anxiety-related behavior suggesting HDAC1 to be important in the regulation of emotional behavior and perhaps involved in pathological processes leading to anxiety. However, under conditions of chronic stress, the decreased anxiety-related behavior in conditional Hdac1 knockout mice is abolished. Furthermore, the ablation of HDAC1 leads under basal and stressed conditions to a decrease in passive stress-coping/depression-related behavior. In the formation of spatial memory, we could not observe any involvement of HDAC1. On the other hand, the conditional Hdac3 knockout animals did not show changes in anxiety-related, nor in stress-coping/depression-related behavior under basal housing conditions, nor as a consequence of chronic stress, but the HDAC3 ablation lead to a severe impairment in learning and spatial memory formation.

6 GENERAL CONCLUSION AND OUTLOOK

To shortly summarize all findings, it emerges that all classical HDACs are expressed throughout the adult murine brain, each member having a unique and distinct expression pattern. To induce a conditional knockout or overexpression within genetic mouse models via the Cre/loxP system, we established a stress-free tamoxifen application via food pellets. To handle aversive effects of tamoxifen food (i.e. on feeding and drinking behavior), but to ensure at the same time a high recombination efficacy, we established the following strategy to induce the knockout/overexpression of desired genes in principal forebrain neurons by the use of the Camk2a-CreER^{T2} mouse line: mice are fed seven days with tamoxifen chow followed by a seven day wash-out phase with standard diet prior phenotypical analysis or behavioral testing. To investigate the brain-specific functions of HDAC1 and HDAC3 we used respective conditional mouse models and induced the knockout in principal forebrain neurons in adulthood via the previously described tamoxifen food strategy. Both enzymes are as expected for class I HDAC members ubiquitously expressed in various murine tissues including the central nervous system (CNS). The detailed analysis of mRNA expression throughout the adult murine brain, revealed for *Hdac1* mRNA a ubiquitous, but at the same time a weak expression, except for distinct brain regions, where stronger expression is present (i.e. the dentate gyrus (DG) of the hippocampus). *Hdac3* is much higher expressed and emerges as the HDAC with the third highest brain-wide expression in the mouse. Comprehensive phenotypical analysis of both conditional mouse models under basal and chronically stressed conditions, revealed that conditional *Hdac1* knockout mice showed no cognitive phenotype, but a decrease in anxiety-related behavior under basal conditions, which is lost under conditions of chronic stress suggesting a role for HDAC1 in the management of anxiety-related behavior. In contrast, conditional *Hdac3* knockout mice showed no overt phenotype in regard to emotional behaviors, but were strongly impaired in memory formation indicating that HDAC3 is important for learning and memory formation processes.

With the established atlas of comprehensive gene expression mapping of all classical HDACs within the adult murine brain, we obtained knowledge about the HDACs' mRNA distribution. However, in a next step it would be interesting to confirm these results on protein level and further to determine via immunohistochemical analysis the cell types (neurons, astrocytes, oligodendrocytes and endothelial cells in the CNS) which express HDACs. It would also be of great interest to obtain more information about the epigenetic targets of classical HDACs addressing the question whether acetylation state of distinct histone proteins, even of distinct lysine residues within histone molecules are deacetylated through different HDACs.

The conditional Hdac1 or Hdac3 knockout animals should also be subjected to further investigations. For instance, it would be interesting to gain more information about the expression of other HDACs in the knockout animals, especially in those regions, where HDAC1 or HDAC3 are physiologically higher expressed and deleted in the knockout mice, i.e. the DG for HDAC1 or the whole hippocampal formation and cortical structures for HDAC3. Especially the expression of HDAC2 should be investigated in the conditional Hdac1 knockout animals, whereas HDAC4 expression is more useful for the conditional Hdac3 knockout animals as these two HDAC members are direct binding partners and heterodimerize with HDAC1 or HDAC3, respectively. Therefore, *ISH* analysis of the mRNA expression and immunohistochemistry (staining of brain slices) for the protein and cell-specific expression, both methods followed by imaging, would be useful as well as immunohistochemistry (Western Blotting) applied on extracted brain tissues. With the immunohistochemistry on brain sections as well as extracted brain tissues, not only the HDAC2 and HDAC4 expression should be analyzed, but also if there are any changes in the acetylation states of specific lysine residues in distinct histones when comparing Hdac1 or Hdac3 knockout animals to control littermates. For a more detailed description of the phenotypes revealed for conditional Hdac1 or Hdac3 knockout animals in regard to anxiety-related behavior or memory performances, the mice should be subjected to further behavioral tests. Especially tests like a posttraumatic stress disorder (PTSD) model should be employed as this reflects anxiety-related behavior as well as memory performances. Furthermore, our conditional knockout models are perfect tools to investigate the relevance of the HDAC1 or HDAC3 ablation, respectively, before or after the traumatic event for development of a PTSD. It would also be worth, generating an Hdac1 and Hdac3 double knockout mouse model which should be especially subjected to tests combining the two knockout phenotypes (deficits in anxiety-related behavior and memory performance) like the PTSD model. Of course the establishment of other knockouts of classical HDAC members are reasonable as well as double knockouts of Hdac1 and Hdac2 or Hdac3 and Hdac4 as these directly heterodimerize and seem to complement in many functions for each other. In our studies we only generated conditional Hdac1 or Hdac3 knockout mice which lack Hdac1 or Hdac3 expression in principal forebrain neurons in adulthood. But indeed, it would also be interesting to establish other specific knockouts, i.e. in other cell-types of the CNS besides neurons which might show *Hdac* expression or even to ablate HDACs in other brain regions like the cerebellum. Another reasonable study might involve developmental roles of HDACs and therefore, the knockouts could be induced early in postnatal stages. Further interesting investigations would be to subject cells of extracted tissues (i.e. hippocampus) of either Hdac1 or Hdac3 knockout animals before and after behavioral analysis to the next generation sequencing. With the use of this powerful tool we might be

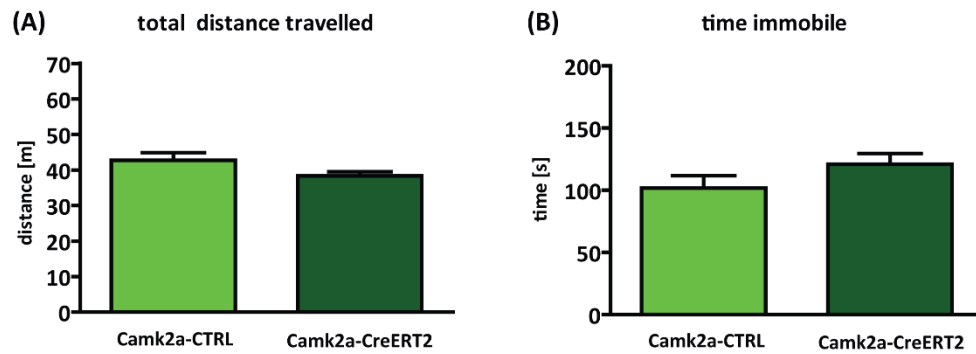
successful in finding target genes which are directly changed in their transcription rate due to the knockout and/or due to the experiences from the behavioral testing. Also the direct targets of the HDACs, the lysine residues of histone molecules, should be analyzed for a change in acetylation state.

Of course there are many investigations which can be done in this broad and highly interesting research field. We only described the epigenetic aspect of HDACs, but, the change in the acetylation state of signaling molecules as direct targets of HDACs as key mediators of signal transduction is also a promising research field.

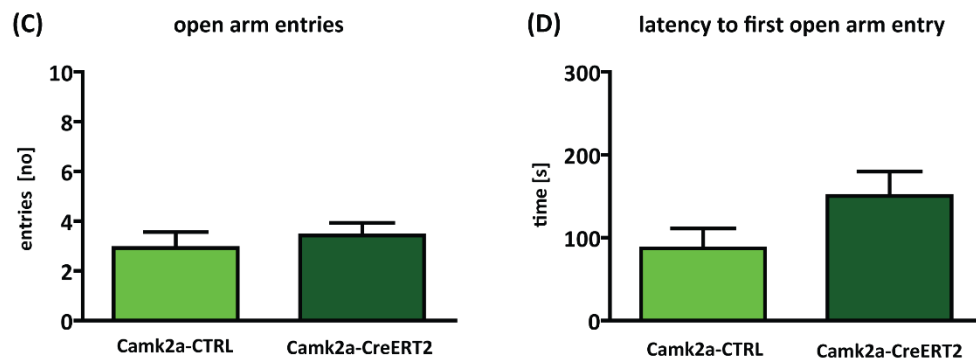
7 SUPPLEMENTS

7.1 Control experiment to rule out influences of Cre recombinase on mice behavior

Open Field Test



Elevated Plus Maze Test



Dark/Light Box Test

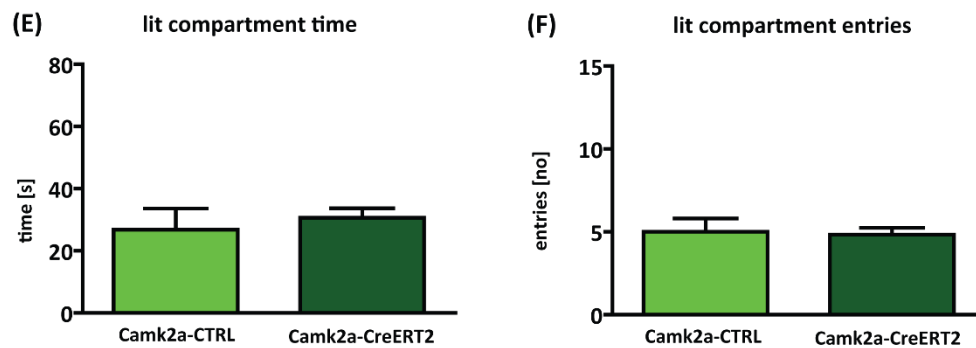


Figure 60. Analysis of transgenic mice of the line Camk2a-CreERT2. No significant differences were observed in the Open Field Test: total distance travelled (A), time spent immobile (B); in the Elevated Plus Maze Test: open arm entries (C), latency to first open arm entry (D); in the Dark/Light Box Test: lit compartment time (E), lit compartment entries (F). | Test duration analyzed: Open Field Test: 15 minutes; Elevated Plus Maze Test: 5 minutes; Dark/Light Box Test: 5 minutes; Data are presented as means \pm SEM; n = 10-12; Camk2a-CTRL = control littermate; Camk2a-CreERT2 = transgenic Cre mouse.

8 REFERENCES

- Agger, K., Santoni-Rugiu, E., Holmberg, C., Karlström, O., & Helin, K. (2005). Conditional E2F1 activation in transgenic mice causes testicular atrophy and dysplasia mimicking human CIS. *Oncogene*, *24*, 780–789. doi:10.1038/sj.onc.1208248
- Agis-Balboa, R. C., Pavelka, Z., Kerimoglu, C., & Fischer, A. (2013). Loss of HDAC5 impairs memory function: implications for Alzheimer's disease. *Journal of Alzheimer's Disease : JAD*, *33*, 35–44. doi:10.3233/JAD-2012-121009
- Akhtar, M. W., Raingo, J., Nelson, E. D., Montgomery, R. L., Olson, E. N., Kavalali, E. T., & Monteggia, L. M. (2009). Histone deacetylases 1 and 2 form a developmental switch that controls excitatory synapse maturation and function. *The Journal of Neuroscience : The Official Journal of the Society for Neuroscience*, *29*(25), 8288–97. doi:10.1523/JNEUROSCI.0097-09.2009
- Alarcón, J. M., Malleret, G., Touzani, K., Vronskaya, S., Ishii, S., Kandel, E. R., & Barco, A. (2004). Chromatin acetylation, memory, and LTP are impaired in CBP+/- mice: A model for the cognitive deficit in Rubinstein-Taybi syndrome and its amelioration. *Neuron*, *42*, 947–959. doi:10.1016/j.neuron.2004.05.021
- Alberts, B., Johnson, A., Lewis, J., Raff, M., Roberts, K., & Walter, P. (2002). *Molecular Biology of the Cell. Molecular Biology of the Cell*.
- Anagnostopoulos, A. V., Mobraaten, L. E., Sharp, J. J., & Davisson, M. T. (2001). Transgenic and knockout databases: Behavioral profiles of mouse mutants. *Physiology and Behavior*. doi:10.1016/S0031-9384(01)00525-X
- Anand, K. S., & Dhikav, V. (2012). Hippocampus in health and disease: An overview. *Annals of Indian Academy of Neurology*, *15*(4), 239–46. doi:10.4103/0972-2327.104323
- Arents, G., Burlingame, R. W., Wang, B. C., Love, W. E., & Moudrianakis, E. N. (1991). The nucleosomal core histone octamer at 3.1 Å resolution: a tripartite protein assembly and a left-handed superhelix. *Proceedings of the National Academy of Sciences of the United States of America*, *88*, 10148–10152. doi:10.1073/pnas.88.22.10148
- Arney, K. L., & Fisher, A. G. (2004). Epigenetic aspects of differentiation. *Journal of Cell Science*, *117*, 4355–4363. doi:10.1242/jcs.01390
- Ashburner, B. P., Westerheide, S. D., & Baldwin, A. S. (2001). The p65 (RelA) subunit of NF-kappaB interacts with the histone deacetylase (HDAC) corepressors HDAC1 and HDAC2 to negatively regulate gene expression. *Molecular and Cellular Biology*, *21*, 7065–7077. doi:10.1128/MCB.21.20.7065-7077.2001
- Austin, C. A., & Marsh, K. L. (1998). Eukaryotic DNA topoisomerase II beta. *BioEssays : News and Reviews in Molecular, Cellular and Developmental Biology*, *20*, 215–26. doi:10.1002/(SICI)1521-1878(199803)20:3<215::AID-BIES5>3.0.CO;2-Q

- Ayer, D. E. (1999). Histone deacetylases: Transcriptional repression with SINers and NuRDs. *Trends in Cell Biology*. doi:10.1016/S0962-8924(99)01536-6
- Bahari-Javan, S., Maddalena, A., Kerimoglu, C., Wittnam, J., Held, T., Bähr, M., ... Sananbenesi, F. (2012). HDAC1 regulates fear extinction in mice. *The Journal of Neuroscience : The Official Journal of the Society for Neuroscience*, 32(15), 5062–73. doi:10.1523/JNEUROSCI.0079-12.2012
- Bailey, K. R., & Crawley, J. N. (2001). *Methods of BEHAVIOR ANALYSIS in NEUROSCIENCE*. New York (Vol. 3). doi:10.1016/0005-7916(93)90032-R
- Bailey, K. R., Rustay, N. R., & Crawley, J. N. (2006). Behavioral phenotyping of transgenic and knockout mice: practical concerns and potential pitfalls. *ILAR Journal / National Research Council, Institute of Laboratory Animal Resources*, 47(2), 124–131. doi:za2963e q8zab q8zbe q8zc8 q8zdf q8zed q8zf8 q8zg1
- Bartl, S., Taplick, J., Lagger, G., Khier, H., Kuchler, K., & Seiser, C. (1997). Identification of mouse histone deacetylase 1 as a growth factor-inducible gene. *Molecular and Cellular Biology*, 17, 5033–5043.
- Bates, E. A., Victor, M., Jones, A. K., Shi, Y., & Hart, A. C. (2006). Differential contributions of *Caenorhabditis elegans* histone deacetylases to huntingtin polyglutamine toxicity. *The Journal of Neuroscience : The Official Journal of the Society for Neuroscience*, 26, 2830–2838. doi:10.1523/JNEUROSCI.3344-05.2006
- Baulcome, D. (2005). RNA silencing. *Trends Biochem Sci.*, 30, 290–3.
- Baylin, S. B. (2008). Epigenetics and Cancer. In *The Molecular Basis of Cancer* (pp. 57–65). doi:10.1016/B978-141603703-3.10005-6
- Benes, F. M., Lim, B., Matzilevich, D., Walsh, J. P., Subburaju, S., & Minns, M. (2007). Regulation of the GABA cell phenotype in hippocampus of schizophrenics and bipolars. *Proceedings of the National Academy of Sciences of the United States of America*, 104, 10164–10169. doi:10.1073/pnas.0703806104
- Berton, O., Mcclung, C. A., Dileone, R. J., Krishnan, V., Renthal, W., Russo, S. J., ... Nestler, E. J. (2006). Essential Role of BDNF in the in Social Defeat Stress. *Science*, 311, 864–868. doi:10.1126/science.1120972
- Bertos, N. R., Wang, A. H., & Yang, X. J. (2001). Class II histone deacetylases: structure, function, and regulation. *Biochem Cell Biol*. Retrieved from http://www.ncbi.nlm.nih.gov/entrez/query.fcgi?db=pubmed&cmd=Retrieve&dopt=AbstractPlus&list_uids=11467738 \nhttp://www.ncbi.nlm.nih.gov/entrez/query.fcgi?cmd=Retrieve&db=PubMed&dopt=Citation&list_uids=11467738
- Bird, A. (2007). Perceptions of epigenetics. *Nature*, 447(7143), 396–8. doi:10.1038/nature05913

- Bjerling, P., Silverstein, R. A., Thon, G., Caudy, A., Grewal, S., & Ekwall, K. (2002). Functional divergence between histone deacetylases in fission yeast by distinct cellular localization and in vivo specificity. *Molecular and Cellular Biology*, *22*, 2170–2181. doi:10.1128/MCB.22.7.2170-2181.2002
- Blumstein, L. K., & Crawley, J. N. (1983). Further characterization of a simple, automated exploratory model for the anxiolytic effects of benzodiazepines. *Pharmacology, Biochemistry, and Behavior*, *18*, 37–40. doi:10.1016/0091-3057(83)90247-2
- Bolger, T. A., & Yao, T.-P. (2005). Intracellular trafficking of histone deacetylase 4 regulates neuronal cell death. *The Journal of Neuroscience : The Official Journal of the Society for Neuroscience*, *25*, 9544–9553. doi:10.1523/JNEUROSCI.1826-05.2005
- Bolivar, V., Cook, M., & Flaherty, L. (2000). List of transgenic and knockout mice: Behavioral profiles. *Mammalian Genome*, *11*(4), 260–274. doi:10.1007/s003350010051
- Bonasio, R., Tu, S., & Reinberg, D. (2010). Molecular signals of epigenetic states. *Science (New York, N.Y.)*, *330*, 612–616. doi:10.1126/science.1191078
- Borsini, F., Lecci, A., Volterra, G., & Meli, A. (1989). A model to measure anticipatory anxiety in mice? *Psychopharmacology*, *98*(2), 207–211. doi:10.1007/BF00444693
- Bourin, M., & Hascoët, M. (2009). The mouse light-dark box test. *Neuromethods*, *42*, 197–223. doi:10.1007/978-1-60761-303-9-11
- Branda, C. S., & Dymecki, S. M. (2004). Talking about a revolution: The impact of site-specific recombinases on genetic analyses in mice. *Developmental Cell*. doi:10.1016/S1534-5807(03)00399-X
- Brehm, A., Miska, E. A., McCance, D. J., Reid, J. L., Bannister, A. J., & Kouzarides, T. (1998). Retinoblastoma protein recruits histone deacetylase to repress transcription. *Nature*, *391*, 597–601. doi:10.1038/35404
- Brennecke, J., Aravin, A. A., Stark, A., Dus, M., Kellis, M., Sachidanandam, R., & Hannon, G. J. (2007). Discrete Small RNA-Generating Loci as Master Regulators of Transposon Activity in *Drosophila*. *Cell*, *128*, 1089–1103. doi:10.1016/j.cell.2007.01.043
- Brocard, J., Warot, X., Wendling, O., Messaddeq, N., Vonesch, J. L., Chambon, P., & Metzger, D. (1997). Spatio-temporally controlled site-specific somatic mutagenesis in the mouse. *Proceedings of the National Academy of Sciences of the United States of America*, *94*, 14559–14563. doi:10.1073/pnas.94.26.14559
- Broide, R. S., Redwine, J. M., Aftahi, N., Young, W., Bloom, F. E., & Winrow, C. J. (2007). Distribution of histone deacetylases 1-11 in the rat brain. *Journal of Molecular Neuroscience : MN*, *31*, 47–58. doi:10.1007/BF02686117
- Buggy, J. J., Sideris, M. L., Mak, P., Lorimer, D. D., McIntosh, B., & Clark, J. M. (2000). Cloning and

- characterization of a novel human histone deacetylase, HDAC8. *The Biochemical Journal*, 350 Pt 1, 199–205.
- Cai, R., Kwon, P., Yan-Neale, Y., Sambucetti, L., Fischer, D., & Cohen, D. (2001). Mammalian histone deacetylase 1 protein is posttranslationally modified by phosphorylation. *Biochemical and Biophysical Research Communications*, 283, 445–453. doi:10.1006/bbrc.2001.4786
- Cai, R. L., Yan-Neale, Y., Cueto, M. A., Xu, H., & Cohen, D. (2000). HDAC1, a histone deacetylase, forms a complex with Hus1 and Rad9, two G2/M checkpoint rad proteins. *Journal of Biological Chemistry*, 275, 27909–27916. doi:10.1074/jbc.M000168200
- Candido, E. P. M., & Davie, J. R. (1978). Sodium Butyrate Cultured Cells Inhibits Histone Deacetylation in. *Cell*, 14, 105–113.
- Carthew, R. W., & Sontheimer, E. J. (2009). Origins and Mechanisms of miRNAs and siRNAs. *Cell*. doi:10.1016/j.cell.2009.01.035
- Casanova, E., Fehsenfeld, S., Lemberger, T., Shimshek, D. R., Sprengel, R., & Mantamadiotis, T. (2002). ER-based double iCre fusion protein allows partial recombination in forebrain. *Genesis*, 34, 208–214. doi:10.1002/gene.10153
- Casey, D. E., Daniel, D. G., Wassef, A. A., Tracy, K. A., Wozniak, P., & Sommerville, K. W. (2003). *Effect of divalproex combined with olanzapine or risperidone in patients with an acute exacerbation of schizophrenia. Neuropsychopharmacology: official publication of the American College of Neuropsychopharmacology* (Vol. 28). doi:10.1038/sj.npp.1300369
- Chang, S., Young, B. D., Li, S., Qi, X., Richardson, J. a, & Olson, E. N. (2006). Histone deacetylase 7 maintains vascular integrity by repressing matrix metalloproteinase 10. *Cell*, 126(2), 321–34. doi:10.1016/j.cell.2006.05.040
- Chatterjee, T. K., Basford, J. E., Knoll, E., Tong, W. S., Blanco, V., Blomkalns, A. L., ... Weintraub, N. L. (2014). HDAC9 knockout mice are protected from adipose tissue dysfunction and systemic metabolic disease during high-fat feeding. *Diabetes*, 63(January), 176–187. doi:10.2337/db13-1148
- Chen, C., & Tonegawa, S. (1997). Molecular genetic analysis of synaptic plasticity, activity-dependent neural development, learning, and memory in the mammalian brain. *Annu Rev Neurosci*, 20, 157–184. doi:10.1146/annurev.neuro.20.1.157
- Chen, Z. F., Paquette, A. J., & Anderson, D. J. (1998). NRSF/REST is required in vivo for repression of multiple neuronal target genes during embryogenesis. *Nature Genetics*, 20, 136–142. doi:10.1038/2431
- Chong, J. A., Tapia-Ramírez, J., Kim, S., Toledo-Aral, J. J., Zheng, Y., Boutros, M. C., ... Mandel, G. (1995). REST: A mammalian silencer protein that restricts sodium channel gene expression to neurons. *Cell*, 80, 949–957. doi:10.1016/0092-8674(95)90298-8

- Choy, M.-K., Movassagh, M., Goh, H.-G., Bennett, M. R., Down, T. A., & Foo, R. S. Y. (2010). Genome-wide conserved consensus transcription factor binding motifs are hyper-methylated. *BMC Genomics*, *11*, 519. doi:10.1186/1471-2164-11-519
- Christmas, A., & Maxwell, D. (1970). A comparison of the effects of some benzodiazepines and other drugs on aggressive and exploratory behaviour in mice and rats. *Neuropharmacology*, *9*(1), 17–29. doi:10.1016/0028-3908(70)90044-4
- Chwang, W. B., O’Riordan, K. J., Levenson, J. M., & Sweatt, J. D. (2006). ERK/MAPK regulates hippocampal histone phosphorylation following contextual fear conditioning. *Learning & Memory*, *13*, 322–328. doi:10.1101/lm.152906
- Cohen, T. J., Barrientos, T., Hartman, Z. C., Garvey, S. M., Cox, G. A., & Yao, T.-P. (2009). The deacetylase HDAC4 controls myocyte enhancing factor-2-dependent structural gene expression in response to neural activity. *The FASEB Journal: Official Publication of the Federation of American Societies for Experimental Biology*, *23*, 99–106. doi:10.1096/fj.08-115931
- Cohen, T. J., Waddell, D. S., Barrientos, T., Lu, Z., Feng, G., Cox, G. A., ... Yao, T. P. (2007). The histone deacetylase HDAC4 connects neural activity to muscle transcriptional reprogramming. *Journal of Biological Chemistry*, *282*, 33752–33759. doi:10.1074/jbc.M706268200
- Collins, L. J., Schönfeld, B., & Chen, X. S. (2011). The epigenetics of non-coding RNA. In *Handbook of Epigenetics* (pp. 49–61). doi:10.1016/B978-0-12-375709-8.00004-6
- Cosgrove, M. S., & Wolberger, C. (2005). How does the histone code work? *1*, 476, 468–476. doi:10.1139/O05-137
- Covington, H. E., Maze, I., LaPlant, Q. C., Vialou, V. F., Ohnishi, Y. N., Berton, O., ... Nestler, E. J. (2009). Antidepressant actions of histone deacetylase inhibitors. *The Journal of Neuroscience: The Official Journal of the Society for Neuroscience*, *29*(37), 11451–60. doi:10.1523/JNEUROSCI.1758-09.2009
- Crawley, J., & Goodwin, F. K. (1980). Preliminary report of a simple animal behavior model for the anxiolytic effects of benzodiazepines. *Pharmacology, Biochemistry, and Behavior*, *13*, 167–170. doi:10.1016/0091-3057(80)90067-2
- Crawley, J. N. (1981). Neuropharmacologic specificity of a simple animal model for the behavioral actions of benzodiazepines. *Pharmacology, Biochemistry, and Behavior*, *15*(5), 695–699. doi:10.1016/0091-3057(81)90007-1
- Cress, W. D., & Seto, E. (2000). Histone deacetylases, transcriptional control, and cancer. *J. Cell. Physiol.*, *184*, 1–16. doi:10.1002/(SICI)1097-4652(200007)184:1<1::AID-JCP1>3.0.CO;2-7
- Cruz, J. C., Tseng, H. C., Goldman, J. A., Shih, H., & Tsai, L. H. (2003). Aberrant Cdk5 activation by p25 triggers pathological events leading to neurodegeneration and neurofibrillary tangles. *Neuron*, *40*, 471–483. doi:10.1016/S0896-6273(03)00627-5

- Cryan, J. F., & Holmes, A. (2005). The ascent of mouse: advances in modelling human depression and anxiety. *Nature Reviews. Drug Discovery*, 4(9), 775–790. doi:10.1038/nrd1825
- Cryan, J. F., & Mombereau, C. (2004). In search of a depressed mouse: utility of models for studying depression-related behavior in genetically modified mice. *Molecular Psychiatry*, 9, 326–357. doi:10.1038/sj.mp.4001457
- Cui, X. S., Zhang, D. X., Ko, Y. G., & Kim, N. H. (2009). Aberrant epigenetic reprogramming of imprinted microRNA-127 and Rtl1 in cloned mouse embryos. *Biochemical and Biophysical Research Communications*, 379, 390–394. doi:10.1016/j.bbrc.2008.12.148
- Dagerlind, Å., Friberg, K., Bean, A. J., & Hökfelt, T. (1992). Sensitive mRNA detection using unfixed tissue: combined radioactive and non-radioactive in situ hybridization histochemistry. *Histochemistry*, 98, 39–49. doi:10.1007/BF00716936
- Dangond, F., Foerznlner, D., Weremowicz, S., Morton, C. C., Beier, D. R., & Gullans, S. R. (1999). Cloning and expression of a murine histone deacetylase 3 (mHdac3) cDNA and mapping to a region of conserved synteny between murine chromosome 18 and human chromosome 5. *Molecular Cell Biology Research Communications: MCBRC*, 2, 91–96. doi:10.1006/mcbr.1999.0156
- Dangond, F., Hafler, D. A., Tong, J. K., Randall, J., Kojima, R., Utku, N., & Gullans, S. R. (1998). Differential display cloning of a novel human histone deacetylase (HDAC3) cDNA from PHA-activated immune cells. *Biochemical and Biophysical Research Communications*, 242, 648–652. doi:10.1006/bbrc.1997.8033
- David, G., Neptune, M. A., & Depinho, R. A. (2002). SUMO-1 modification of histone deacetylase 1 (HDAC1) modulates its biological activities. *Journal of Biological Chemistry*, 277, 23658–23663. doi:10.1074/jbc.M203690200
- David, G., Turner, G. M., Yao, Y., Protopopov, A., & DePinho, R. A. (2003). mSin3-associated protein, mSds3, is essential for pericentric heterochromatin formation and chromosome segregation in mammalian cells. *Genes and Development*, 17, 2396–2405. doi:10.1101/gad.1109403
- Davie, J. R., He, S., Li, L., Sekhvat, A., Espino, P., Drobic, B., ... Wang, X. (2008). Nuclear organization and chromatin dynamics - Sp1, Sp3 and histone deacetylases. *Advances in Enzyme Regulation*, 48, 189–208. doi:10.1016/j.advenzreg.2007.11.016
- de Ruijter, A. J. M., van Gennip, A. H., Caron, H. N., Kemp, S., & van Kuilenburg, A. B. P. (2003). Histone deacetylases (HDACs): characterization of the classical HDAC family. *The Biochemical Journal*, 370(Pt 3), 737–49. doi:10.1042/BJ20021321
- Delcuve, G. P., Khan, D. H., & Davie, J. R. (2012). Roles of histone deacetylases in epigenetic regulation: emerging paradigms from studies with inhibitors. *Clinical Epigenetics*, 4(1), 5. doi:10.1186/1868-7083-4-5
- Dequiedt, F., Kasler, H., Fischle, W., Kiermer, V., Weinstein, M., Herndier, B. G., & Verdin, E. (2003).

- HDAC7, a thymus-specific class II histone deacetylase, regulates Nur77 transcription and TCR-mediated apoptosis. *Immunity*, *18*, 687–698. doi:10.1016/S1074-7613(03)00109-2
- Deussing, J. M. (2013). Targeted mutagenesis tools for modelling psychiatric disorders. *Cell and Tissue Research*. doi:10.1007/s00441-013-1708-5
- Dietrich, M. R. (2003). Richard Goldschmidt: hopeful monsters and other “heresies”. *Nature Reviews. Genetics*, *4*, 68–74. doi:10.1038/nrg979
- Ding, H., Dolan, P. J., & Johnson, G. V. W. (2008). Histone deacetylase 6 interacts with the microtubule-associated protein tau. *Journal of Neurochemistry*, *106*, 2119–2130. doi:10.1111/j.1471-4159.2008.05564.x
- Dogini, D. B., Pascoal, V. D. B., Avansini, S. H., Vieira, A. S., Pereira, T. C., & Lopes-Cendes, I. (2014). The new world of RNAs. *Genetics and Molecular Biology*, *37*, 285–293. doi:10.1590/S1415-47572014000200014
- Dokmanovic, M., Clarke, C., & Marks, P. A. (2007). Histone deacetylase inhibitors: overview and perspectives. *Molecular Cancer Research : MCR*, *5*, 981–989. doi:10.1158/1541-7786.MCR-07-0324
- Dressel, U., Bailey, P. J., Wang, S. C., Downes, M., Evans, R. M., & Muscat, G. E. (2001). A dynamic role for HDAC7 in MEF2-mediated muscle differentiation. *The Journal of Biological Chemistry*, *276*, 17007–17013. doi:10.1074/jbc.M101508200
- Dupont, C., Armant, D. R., & Brenner, C. A. (2009). Epigenetics: Definition, mechanisms and clinical perspective. *Seminars in Reproductive Medicine*. doi:10.1055/s-0029-1237423
- Duvic, M., Talpur, R., Ni, X., Zhang, C., Hazarika, P., Kelly, C., ... Frankel, S. R. (2007). Phase 2 trial of oral vorinostat (suberoylanilide hydroxamic acid, SAHA) for refractory cutaneous T-cell lymphoma (CTCL). *Blood*, *109*, 31–39. doi:10.1182/blood-2006-06-025999
- Egger, G., Liang, G., Aparicio, A., & Jones, P. A. (2004). Epigenetics in human disease and prospects for epigenetic therapy. *Nature*, *429*, 457–463. doi:10.1038/nature02625
- Emiliani, S., Fischle, W., Van Lint, C., Al-Abed, Y., & Verdin, E. (1998). Characterization of a human RPD3 ortholog, HDAC3. *Proceedings of the National Academy of Sciences of the United States of America*, *95*, 2795–2800. doi:10.1073/pnas.95.6.2795
- Erdmann, G., Schütz, G., & Berger, S. (2007). Inducible gene inactivation in neurons of the adult mouse forebrain. *BMC Neuroscience*, *8*, 63. doi:10.1186/1471-2202-8-63
- Eriksson, P. S., Perfilieva, E., Björk-Eriksson, T., Alborn, A. M., Nordborg, C., Peterson, D. A., & Gage, F. H. (1998). Neurogenesis in the adult human hippocampus. *Nature Medicine*, *4*, 1313–1317. doi:10.1038/3305
- Farah, M. J., & Hook, C. J. (2008). The seductive allure of “seductive allure.” *Cognition*, *107*, 343–352. doi:10.1177/1745691612469035

- Fass, D. M., Reis, S. A., Ghosh, B., Hennig, K. M., Joseph, N. F., Zhao, W. N., ... Haggarty, S. J. (2013). Crebinostat: A novel cognitive enhancer that inhibits histone deacetylase activity and modulates chromatin-mediated neuroplasticity. *Neuropharmacology*. doi:10.1016/j.neuropharm.2012.06.043
- Featherstone, M. (2002). Coactivators in transcription initiation: Here are your orders. *Current Opinion in Genetics and Development*. doi:10.1016/S0959-437X(02)00280-0
- Feil, R., Wagner, J., Metzger, D., & Chambon, P. (1997). Regulation of Cre recombinase activity by mutated estrogen receptor ligand-binding domains. *Biochemical and Biophysical Research Communications*, 237(3), 752–757. doi:10.1006/bbrc.1997.7124
- Ferreira, R., Magnaghi-Jaulin, L., Robin, P., Harel-Bellan, A., & Trouche, D. (1998). The three members of the pocket proteins family share the ability to repress E2F activity through recruitment of a histone deacetylase. *Proceedings of the National Academy of Sciences of the United States of America*, 95, 10493–10498. doi:10.1073/pnas.95.18.10493
- Fiesel, F. C., Voigt, A., Weber, S. S., Van den Haute, C., Waldenmaier, A., Görner, K., ... Kahle, P. J. (2010). Knockdown of transactive response DNA-binding protein (TDP-43) downregulates histone deacetylase 6. *The EMBO Journal*, 29, 209–221. doi:10.1038/emboj.2009.324
- File, S. E. (1980). The use of social interaction as a method for detecting anxiolytic activity of chlordiazepoxide-like drugs. *Journal of Neuroscience Methods*, 2(3), 219–238. doi:10.1016/0165-0270(80)90012-6
- Filipowicz, W. (2005). RNAi: The nuts and bolts of the RISC machine. *Cell*. doi:10.1016/j.cell.2005.06.023
- Finnin, M. S., Donigian, J. R., Cohen, A., Richon, V. M., Rifkind, R. A., Marks, P. A., ... Pavletich, N. P. (1999). Structures of a histone deacetylase homologue bound to the TSA and SAHA inhibitors. *Nature*, 401, 188–193. doi:10.1038/43710
- Fischer, A., Sananbenesi, F., Mungenast, A., & Tsai, L. H. (2010). Targeting the correct HDAC(s) to treat cognitive disorders. *Trends in Pharmacological Sciences*. doi:10.1016/j.tips.2010.09.003
- Fischer, A., Sananbenesi, F., Schrick, C., Spiess, J., & Radulovic, J. (2004). Distinct roles of hippocampal de novo protein synthesis and actin rearrangement in extinction of contextual fear. *The Journal of Neuroscience : The Official Journal of the Society for Neuroscience*, 24, 1962–1966. doi:10.1523/JNEUROSCI.5112-03.2004
- Fischer, A., Sananbenesi, F., Wang, X., Dobbin, M., & Tsai, L.-H. (2007). Recovery of learning and memory is associated with chromatin remodelling. *Nature*, 447, 178–182. doi:10.1038/nature05772
- Fischer, D. D., Cai, R., Bhatia, U., Asselbergs, F. A., Song, C., Terry, R., ... Cohen, D. (2002). Isolation and characterization of a novel class II histone deacetylase, HDAC10. *J Biol Chem*, 277, 6656–6666. doi:10.1074/jbc.M108055200

- Fischle, W., Dequiedt, F., Fillion, M., Hendzel, M. J., Voelter, W., & Verdin, E. (2001). Human HDAC7 histone deacetylase activity is associated with HDAC3 in vivo. *The Journal of Biological Chemistry*, *276*, 35826–35835. doi:10.1074/jbc.M104935200
- Fischle, W., Dequiedt, F., Hendzel, M. J., Guenther, M. G., Lazar, M. A., Voelter, W., & Verdin, E. (2002). Enzymatic activity associated with class II HDACs is dependent on a multiprotein complex containing HDAC3 and SMRT/N-CoR. *Molecular Cell*, *9*, 45–57. doi:10.1016/S1097-2765(01)00429-4
- Fischle, W., Emiliani, S., Hendzel, M. J., Nagase, T., Nomura, N., Voelter, W., & Verdin, E. (1999). A new family of human histone deacetylases related to *Saccharomyces cerevisiae* HDA1p. *Journal of Biological Chemistry*, *274*, 11713–11720. doi:10.1074/jbc.274.17.11713
- Fischle, W., Kiermer, V., Dequiedt, F., & Verdin, E. (2001). The emerging role of class II histone deacetylases. *Biochemistry and Cell Biology*, *79*(3), 337–348. doi:10.1139/bcb-79-3-337
- Fischle, W., Wang, Y., & Allis, C. D. (2003). Histone and chromatin cross-talk. *Current Opinion in Cell Biology*, *15*, 172–183. doi:10.1016/S0955-0674(03)00013-9
- Flood, D. G., Choinski, M., Marino, M. J., & Gasior, M. (2009). Mood stabilizers increase prepulse inhibition in DBA/2NCRl mice. *Psychopharmacology*, *205*, 369–377. doi:10.1007/s00213-009-1547-y
- Forde, A., Constien, R., Gröne, H. J., Hämmerling, G., & Arnold, B. (2002). Temporal Cre-mediated recombination exclusively in endothelial cells using Tie2 regulatory elements. *Genesis*, *33*, 191–197. doi:10.1002/gene.10117
- Forsberg, E. C., & Bresnick, E. H. (2001). Histone acetylation beyond promoters: Long-range acetylation patterns in the chromatin world. *BioEssays*, *23*, 820–830. doi:10.1002/bies.1117
- Frick, K. M., Stearns, N. A., Pan, J.-Y., & Berger-Sweeney, J. (2003). Effects of Environmental Enrichment on Spatial Memory and Neurochemistry in Middle-Aged Mice. *Learning & Memory*, *10*, 187–198. doi:10.1101/lm.50703
- Fujita, N., Watanabe, S., Ichimura, T., Tsuruzoe, S., Shinkai, Y., Tachibana, M., ... Nakao, M. (2003). Methyl-CpG binding domain 1 (MBD1) interacts with the Suv39h1-HP1 heterochromatic complex for DNA methylation-based transcriptional repression. *The Journal of Biological Chemistry*, *278*, 24132–24138. doi:10.1074/jbc.M302283200
- Fuks, F., Hurd, P. J., Wolf, D., Nan, X., Bird, A. P., & Kouzarides, T. (2003). The methyl-CpG-binding protein MeCP2 links DNA methylation to histone methylation. *The Journal of Biological Chemistry*, *278*, 4035–4040. doi:10.1074/jbc.M210256200
- Furukawa, Y., Kawakami, T., Sudo, K., Inazawa, J., Matsumine, A., Akiyama, T., & Nakamura, Y. (1996). Isolation and mapping of a human gene (RPD3L1) that is homologous to RPD3, a transcription factor in *Saccharomyces cerevisiae*. *Cytogenetics and Cell Genetics*, *73*, 130–133.

- Galasinski, S. C., Resing, K. A., Goodrich, J. A., & Ahn, N. G. (2002). Phosphatase inhibition leads to histone deacetylases 1 and 2 phosphorylation and disruption of corepressor interactions. *The Journal of Biological Chemistry*, *277*, 19618–19626. doi:10.1074/jbc.M201174200
- Gao, L., Cueto, M. A., Asselbergs, F., & Atadja, P. (2002). Cloning and functional characterization of HDAC11, a novel member of the human histone deacetylase family. *The Journal of Biological Chemistry*, *277*, 25748–25755. doi:10.1074/jbc.M111871200
- Gao, Y., Hubbert, C. C., Lu, J., Lee, Y.-S., Lee, J.-Y., & Yao, T.-P. (2007). Histone deacetylase 6 regulates growth factor-induced actin remodeling and endocytosis. *Molecular and Cellular Biology*, *27*, 8637–8647. doi:10.1128/MCB.00393-07
- Gavazzo, P., Vassalli, M., Costa, D., & Pagano, A. (2013). Novel ncRNAs transcribed by Pol III and elucidation of their functional relevance by biophysical approaches. *Frontiers in Cellular Neuroscience*, *7*, 203. doi:10.3389/fncel.2013.00203
- Glaser, K. B., Li, J. L., Staver, M. J., Wei, R. Q., Albert, D. H., & Davidsen, S. K. (2003). Role of Class I and Class II histone deacetylases in carcinoma cells using siRNA. *Biochemical and Biophysical Research Communications*, *310*, 529–536. doi:DOI 10.1016/j.bbrc.2003.09.043
- Goldberg, A. D., Allis, C. D., & Bernstein, E. (2007). Epigenetics: A Landscape Takes Shape. *Cell*. doi:10.1016/j.cell.2007.02.006
- Goldschmidt, R. (1940). *The Material Basis of Evolution*.
- Gonzalez, L. E., & File, S. E. (1997). A five minute experience in the elevated plus-maze alters the state of the benzodiazepine receptor in the dorsal raphe nucleus. *The Journal of Neuroscience : The Official Journal of the Society for Neuroscience*, *17*(4), 1505–1511.
- Gregoret, I. V., Lee, Y. M., & Goodson, H. V. (2004). Molecular evolution of the histone deacetylase family: Functional implications of phylogenetic analysis. *Journal of Molecular Biology*, *338*, 17–31. doi:10.1016/j.jmb.2004.02.006
- Griffith, J. S., & Mahler, H. R. (1969). No TitleDNA ticketing theory of memory. *Nature*, *223*(5206), 580–2.
- Grimes, J. A., Nielsen, S. J., Battaglioli, E., Miska, E. A., Speh, J. C., Berry, D. L., ... Kouzarides, T. (2000). The co-repressor mSin3A is a functional component of the REST-CoREST repressor complex. *Journal of Biological Chemistry*, *275*, 9461–9467. doi:10.1074/jbc.275.13.9461
- Groth, A., Rocha, W., Verreault, A., & Almouzni, G. (2007). Chromatin Challenges during DNA Replication and Repair. *Cell*. doi:10.1016/j.cell.2007.01.030
- Grozinger, C. M., Chao, E. D., Blackwell, H. E., Moazed, D., & Schreiber, S. L. (2001). Identification of a class of small molecule inhibitors of the sirtuin family of NAD-dependent deacetylases by phenotypic screening. *The Journal of Biological Chemistry*, *276*, 38837–38843. doi:10.1074/jbc.M106779200

- Grozinger, C. M., Hassig, C. A., & Schreiber, S. L. (1999). Three proteins define a class of human histone deacetylases related to yeast Hda1p. *Proceedings of the National Academy of Sciences of the United States of America*, *96*, 4868–4873. doi:10.1073/pnas.96.9.4868
- Gu, H., Marth, J., Orban, P., Mossmann, H., & Rajewsky, K. (1994). Deletion of a DNA polymerase beta gene segment in T cells using cell type-specific gene targeting. *Science*. doi:10.1126/science.8016642
- Guan, J.-S., Haggarty, S. J., Giacometti, E., Dannenberg, J.-H., Joseph, N., Gao, J., ... Tsai, L.-H. (2009). HDAC2 negatively regulates memory formation and synaptic plasticity. *Nature*, *459*(7243), 55–60. doi:10.1038/nature07925
- Guardiola, A. R., & Yao, T.-P. (2002). Molecular cloning and characterization of a novel histone deacetylase HDAC10. *The Journal of Biological Chemistry*, *277*(5), 3350–6. doi:10.1074/jbc.M109861200
- Guenther, M. G., Lane, W. S., Fischle, W., Verdin, E., Lazar, M. A., & Shiekhatar, R. (2000). A core SMRT corepressor complex containing HDAC3 and TBL1, a WD40-repeat protein linked to deafness. *Genes & Development*, *14*, 1048–1057. doi:10.1101/gad.14.9.1048
- Gupta, S., Kim, S. Y., Artis, S., Molfese, D. L., Schumacher, A., Sweatt, J. D., ... Lubin, F. D. (2010). Histone methylation regulates memory formation. *The Journal of Neuroscience : The Official Journal of the Society for Neuroscience*, *30*, 3589–3599. doi:10.1523/JNEUROSCI.3732-09.2010
- Gwack, Y., Byun, H., Hwang, S., Lim, C., & Choe, J. (2001). CREB-binding protein and histone deacetylase regulate the transcriptional activity of Kaposi's sarcoma-associated herpesvirus open reading frame 50. *Journal of Virology*, *75*, 1909–1917. doi:10.1128/JVI.75.4.1909-1917.2001
- Haberland, M., Montgomery, R. L., & Olson, E. N. (2009). The many roles of histone deacetylases in development and physiology: implications for disease and therapy. *Nature Reviews. Genetics*, *10*, 32–42. doi:10.1038/nrg2485
- Haddad, P. M., Das, A., Ashfaq, M., & Wieck, A. (2009). A review of valproate in psychiatric practice. *Expert Opinion on Drug Metabolism & Toxicology*, *5*, 539–551. doi:10.1517/17425250902911455
- Haig, D. (2004). The (dual) origin of epigenetics. *Cold Spring Harbor Symposia on Quantitative Biology*, *69*, 67–70. doi:10.1101/sqb.2004.69.67
- Hait, N. C., Wise, L. E., Allegood, J. C., O'Brien, M., Avni, D., Reeves, T. M., ... Spiegel, S. (2014). Active, phosphorylated fingolimod inhibits histone deacetylases and facilitates fear extinction memory. *Nature Neuroscience*, *17*, 971–80. doi:10.1038/nn.3728
- Hall, C. S. (1934). Emotional behavior in the rat. I. Defecation and urination as measures of individual differences in emotionality. *Journal of Comparative Psychology*, *18*(3), 385–403.

doi:10.1037/h0071444

- Handley, S. L., & Mithani, S. (1984). Effects of alpha-adrenoceptor agonists and antagonists in a maze-exploration model of "fear"-motivated behaviour. *Naunyn-Schmiedeberg's Archives of Pharmacology*, *327*(1), 1–5. doi:10.1007/BF00504983
- Hauser, C., Schuettengruber, B., Bartl, S., Lagger, G., & Seiser, C. (2002). Activation of the mouse histone deacetylase 1 gene by cooperative histone phosphorylation and acetylation. *Molecular and Cellular Biology*, *22*, 7820–7830. doi:10.1128/MCB.22.22.7820-7830.2002
- Hayashi, T., Sakai, K., Sasaki, C., Zhang, W. R., Warita, H., & Abe, K. (2000). c-Jun N-terminal kinase (JNK) and JNK interacting protein response in rat brain after transient middle cerebral artery occlusion. *Neuroscience Letters*, *284*, 195–199. doi:10.1016/S0304-3940(00)01024-7
- Heerboth, S., Lapinska, K., Snyder, N., Leary, M., Rollinson, S., & Sarkar, S. (2014). Use of epigenetic drugs in disease: An overview. *Genetics and Epigenetics*, *1*, 9–19. doi:10.4137/GeG.s12270
- Heinzel, T., Lavinsky, R. M., Mullen, T. M., Söderstrom, M., Laherty, C. D., Torchia, J., ... Rosenfeld, M. G. (1997). A complex containing N-CoR, mSin3 and histone deacetylase mediates transcriptional repression. *Nature*, *387*, 43–48. doi:10.1038/387043a0
- Herring, S. W. (1993). Formation of the vertebrate face epigenetic and functional influences. *Integrative and Comparative Biology*, *33*, 472–483. doi:10.1093/icb/33.4.472
- Hobara, T., Uchida, S., Otsuki, K., Matsubara, T., Funato, H., Matsuo, K., ... Watanabe, Y. (2010). Altered gene expression of histone deacetylases in mood disorder patients. *Journal of Psychiatric Research*, *44*, 263–270. doi:10.1016/j.jpsychires.2009.08.015
- Holliday, R. (1990). Mechanisms for the control of gene activity during development. *Biol Rev Camb Philos Soc.*, *65*(4), 431–71.
- Holliday, R. (2002). Epigenetics comes of age in the twentyfirst century. *Journal of Genetics*, *81*(1), 1–4. Retrieved from <http://www.ncbi.nlm.nih.gov/pubmed/12357072>
- Holliday, R. (2006). Epigenetics: a historical overview, *1*(2), 76–80.
- Holliday, R., & Pugh, J. E. (1975). DNA modification mechanisms and gene activity during development. *Science (New York, N.Y.)*, *187*, 226–232. doi:10.1126/science.1111098
- Hook, S. S., Orian, A., Cowley, S. M., & Eisenman, R. N. (2002). Histone deacetylase 6 binds polyubiquitin through its zinc finger (PAZ domain) and copurifies with deubiquitinating enzymes. *Proceedings of the National Academy of Sciences of the United States of America*, *99*, 13425–13430. doi:10.1073/pnas.172511699
- Hsieh, J., & Gage, F. H. (2004). Epigenetic control of neural stem cell fate. *Current Opinion in Genetics & Development*, *14*, 461–469. doi:10.1016/j.gde.2004.07.006
- Hu, E., Chen, Z., Fredrickson, T., Zhu, Y., Kirkpatrick, R., Zhang, G. F., ... Winkler, J. (2000). Cloning

- and characterization of a novel human class I histone deacetylase that functions as a transcription repressor. *The Journal of Biological Chemistry*, *275*, 15254–15264. doi:10.1074/jbc.M908988199
- Huang, F. L., Huang, K.-P., Wu, J., & Boucheron, C. (2006). Environmental enrichment enhances neurogranin expression and hippocampal learning and memory but fails to rescue the impairments of neurogranin null mutant mice. *The Journal of Neuroscience: The Official Journal of the Society for Neuroscience*, *26*, 6230–6237. doi:10.1523/JNEUROSCI.1182-06.2006
- Huang, Y., Myers, S. J., & Dingledine, R. (1999). Transcriptional repression by REST: recruitment of Sin3A and histone deacetylase to neuronal genes. *Nature Neuroscience*, *2*, 867–872. doi:10.1038/13165
- Hubbert, C., Guardiola, A., Shao, R., Kawaguchi, Y., Ito, A., Nixon, A., ... Yao, T.-P. (2002). HDAC6 is a microtubule-associated deacetylase. *Nature*, *417*, 455–458. doi:10.1038/417455a
- Hui Ng, H., & Bird, A. (2000). Histone deacetylases: Silencers for hire. *Trends in Biochemical Sciences*. doi:10.1016/S0968-0004(00)01551-6
- Hurd, P. J. (2010). The era of epigenetics. *Briefings in Functional Genomics*, *9*(5-6), 425–8. doi:10.1093/bfpg/elq039
- Hüttenhofer, A., Schattner, P., & Polacek, N. (2005). Non-coding RNAs: Hope or hype? *Trends in Genetics*. doi:10.1016/j.tig.2005.03.007
- Huxley, J. (1956). Epigenetics. *Nature*, *177*, 806–8.
- Indra, A. K., Dupé, V., Bornert, J.-M., Messaddeq, N., Yaniv, M., Mark, M., ... Metzger, D. (2005). Temporally controlled targeted somatic mutagenesis in embryonic surface ectoderm and fetal epidermal keratinocytes unveils two distinct developmental functions of BRG1 in limb morphogenesis and skin barrier formation. *Development (Cambridge, England)*, *132*, 4533–4544. doi:10.1242/dev.02019
- Indra, A. K., Warot, X., Brocard, J., Bornert, J. M., Xiao, J. H., Chambon, P., & Metzger, D. (1999). Temporally-controlled site-specific mutagenesis in the basal layer of the epidermis: Comparison of the recombinase activity of the tamoxifen-inducible Cre-ER(T) and Cre-ER(T2) recombinases. *Nucleic Acids Research*, *27*(22), 4324–4327. doi:10.1093/nar/27.22.4324
- Ito, K., Barnes, P. J., & Adcock, I. M. (2000). Glucocorticoid receptor recruitment of histone deacetylase 2 inhibits interleukin-1beta-induced histone H4 acetylation on lysines 8 and 12. *Molecular and Cellular Biology*, *20*, 6891–6903. doi:10.1128/MCB.20.18.6891-6903.2000
- Jenuwein, T., & Allis, C. D. (2001). Translating the histone code. *Science (New York, N.Y.)*, *293*(5532), 1074–80. doi:10.1126/science.1063127
- Johnson, C. A., Padget, K., Austin, C. A., & Turner, B. M. (2001). Deacetylase Activity Associates with

- Topoisomerase II and I α Necessary for Etoposide-induced Apoptosis. *Journal of Biological Chemistry*, 276, 4539–4542. doi:10.1074/jbc.C000824200
- Johnstone, R. W. (2002). Histone-deacetylase inhibitors: novel drugs for the treatment of cancer. *Nature Reviews. Drug Discovery*, 1, 287–299. doi:10.1038/nrd772
- Kaikkonen, M. U., Lam, M. T. Y., & Glass, C. K. (2011). Non-coding RNAs as regulators of gene expression and epigenetics. *Cardiovascular Research*. doi:10.1093/cvr/cvr097
- Kalueff, A. V., & Murphy, D. L. (2007). The importance of cognitive phenotypes in experimental modeling of animal anxiety and depression. *Neural Plasticity*. doi:10.1155/2007/52087
- Kao, H. Y., Downes, M., Ordentlich, P., & Evans, R. M. (2000). Isolation of a novel histone deacetylase reveals that class I and class II deacetylases promote SMRT-mediated repression. *Genes & Development*, 14, 55–66. doi:10.1101/gad.14.1.55
- Kao, H. Y., Verdel, A., Tsai, C. C., Simon, C., Juguilon, H., & Khochbin, S. (2001). Mechanism for nucleocytoplasmic shuttling of histone deacetylase 7. *The Journal of Biological Chemistry*, 276, 47496–47507. doi:10.1074/jbc.M107631200
- Kao, H.-Y., Lee, C.-H., Komarov, A., Han, C. C., & Evans, R. M. (2002). Isolation and characterization of mammalian HDAC10, a novel histone deacetylase. *The Journal of Biological Chemistry*, 277, 187–193. doi:10.1074/jbc.M108931200
- Khier, H., Bartl, S., Schuettengruber, B., & Seiser, C. (1999). Molecular cloning and characterization of the mouse histone deacetylase 1 gene: Integration of a retrovirus in 129SV mice. *Biochimica et Biophysica Acta - Gene Structure and Expression*, 1489, 365–373. doi:10.1016/S0167-4781(99)00203-1
- Kiefer, J. C. (2007). Epigenetics in development. *Developmental Dynamics : An Official Publication of the American Association of Anatomists*, 236(4), 1144–56. doi:10.1002/dvdy.21094
- Kiermayer, C., Conrad, M., Schneider, M., Schmidt, J., & Brielmeier, M. (2007). Optimization of spatiotemporal gene inactivation in mouse heart by oral application of tamoxifen citrate. *Genesis*, 45, 11–16. doi:10.1002/dvg.20244
- Kijima, M., Yoshida, M., Sugita, K., Horinouchi, S., & Beppu, T. (1993). Trapoxin, an antitumor cyclic tetrapeptide, is an irreversible inhibitor of mammalian histone deacetylase. *Journal of Biological Chemistry*, 268, 22429–22435.
- Kilgore, M., Miller, C. a, Fass, D. M., Hennig, K. M., Haggarty, S. J., Sweatt, J. D., & Rumbaugh, G. (2010). Inhibitors of class 1 histone deacetylases reverse contextual memory deficits in a mouse model of Alzheimer's disease. *Neuropsychopharmacology : Official Publication of the American College of Neuropsychopharmacology*, 35(4), 870–80. doi:10.1038/npp.2009.197
- Kim, D., Frank, C. L., Dobbin, M. M., Tsunemoto, R. K., Tu, W., Peng, P. L., ... Tsai, L. H. (2008). Deregulation of HDAC1 by p25/Cdk5 in Neurotoxicity. *Neuron*, 60, 803–817.

doi:10.1016/j.neuron.2008.10.015

- Kim, D., Nguyen, M. D., Dobbin, M. M., Fischer, A., Sananbenesi, F., Rodgers, J. T., ... Tsai, L.-H. (2007). SIRT1 deacetylase protects against neurodegeneration in models for Alzheimer's disease and amyotrophic lateral sclerosis. *The EMBO Journal*, *26*, 3169–3179. doi:10.1038/sj.emboj.7601758
- Kim, H.-J., & Bae, S.-C. (2011). Histone deacetylase inhibitors: molecular mechanisms of action and clinical trials as anti-cancer drugs. *American Journal of Translational Research*, *3*(2), 166–79. Retrieved from <http://www.pubmedcentral.nih.gov/articlerender.fcgi?artid=3056563&tool=pmcentrez&rendertype=abstract>
- Kim, M.-S., Akhtar, M. W., Adachi, M., Mahgoub, M., Bassel-Duby, R., Kavalali, E. T., ... Monteggia, L. M. (2012). An essential role for histone deacetylase 4 in synaptic plasticity and memory formation. *The Journal of Neuroscience : The Official Journal of the Society for Neuroscience*, *32*, 10879–86. doi:10.1523/JNEUROSCI.2089-12.2012
- Kim, T., Park, J. K., Kim, H. J., Chung, J. H., & Kim, J. W. (2010). Association of histone deacetylase genes with schizophrenia in Korean population. *Psychiatry Research*, *178*, 266–269. doi:10.1016/j.psychres.2009.05.007
- Kirsh, O., Seeler, J. S., Pichler, A., Gast, A., Müller, S., Miska, E., ... Dejean, A. (2002). The SUMO E3 ligase RanBP2 promotes modification of the HDAC4 deacetylase. *EMBO Journal*, *21*, 2682–2691. doi:10.1093/emboj/21.11.2682
- Kleinknecht, K. R., Bedenk, B. T., Kaltwasser, S. F., Grünecker, B., Yen, Y.-C., Czisch, M., & Wotjak, C. T. (2012). Hippocampus-dependent place learning enables spatial flexibility in C57BL6/N mice. *Frontiers in Behavioral Neuroscience*, *6*, 87. doi:10.3389/fnbeh.2012.00087
- Kornberg, R. D. (1974). Chromatin structure: a repeating unit of histones and DNA. *Science*, *184*, 868–871.
- Kornberg, R. D., & Lorch, Y. (1999). Twenty-five years of the nucleosome, fundamental particle of the eukaryote chromosome. *Cell*, *98*(3), 285–94. Retrieved from <http://www.ncbi.nlm.nih.gov/pubmed/10458604>
- Korzus, E., Rosenfeld, M. G., & Mayford, M. (2004). CBP histone acetyltransferase activity is a critical component of memory consolidation. *Neuron*, *42*, 961–972. doi:10.1016/j.neuron.2004.06.002
- Kosak, S. T., & Groudine, M. (2004). Form follows function: The genomic organization of cellular differentiation. *Genes & Development*, *18*, 1371–1384. doi:10.1101/gad.1209304
- Kostetskii, I., Li, J., Xiong, Y., Zhou, R., Ferrari, V. A., Patel, V. V., ... Radice, G. L. (2005). Induced deletion of the N-cadherin gene in the heart leads to dissolution of the intercalated disc structure. *Circulation Research*, *96*, 346–354. doi:10.1161/01.RES.0000156274.72390.2c

- Kouzarides, T. (2000). Acetylation: a regulatory modification to rival phosphorylation? *The EMBO Journal*, *19*, 1176–1179. doi:10.1093/emboj/19.6.1176
- Kovacs, J. J., Murphy, P. J. M., Gaillard, S., Zhao, X., Wu, J. T., Nicchitta, C. V., ... Yao, T. P. (2005). HDAC6 regulates Hsp90 acetylation and chaperone-dependent activation of glucocorticoid receptor. *Molecular Cell*, *18*, 601–607. doi:10.1016/j.molcel.2005.04.021
- Kumar, A., Choi, K. H., Renthal, W., Tsankova, N. M., Theobald, D. E. H., Truong, H. T., ... Nestler, E. J. (2005). Chromatin remodeling is a key mechanism underlying cocaine-induced plasticity in striatum. *Neuron*, *48*, 303–314. doi:10.1016/j.neuron.2005.09.023
- Kurdistani, S. K., & Grunstein, M. (2003). Histone acetylation and deacetylation in yeast. *Nature Reviews. Molecular Cell Biology*, *4*, 276–284. doi:10.1038/nrm1075
- Kurita, M., Holloway, T., García-Bea, A., Kozlenkov, A., Friedman, A. K., Moreno, J. L., ... González-Maeso, J. (2012). HDAC2 regulates atypical antipsychotic responses through the modulation of mGlu2 promoter activity. *Nature Neuroscience*. doi:10.1038/nn.3181
- Kwiatkowski, T. J., Bosco, D. A., Leclerc, A. L., Tamrazian, E., Vanderburg, C. R., Russ, C., ... Brown, R. H. (2009). Mutations in the FUS/TLS gene on chromosome 16 cause familial amyotrophic lateral sclerosis. *Science (New York, N.Y.)*, *323*, 1205–1208. doi:10.1126/science.1166066
- Kwon, S., Zhang, Y., & Matthias, P. (2007). The deacetylase HDAC6 is a novel critical component of stress granules involved in the stress response. *Genes & Development*, *21*(24), 3381–94. doi:10.1101/gad.461107
- Lagger, G., O'Carroll, D., Rembold, M., Khier, H., Tischler, J., Weitzer, G., ... Seiser, C. (2002). Essential function of histone deacetylase 1 in proliferation control and CDK inhibitor repression. *EMBO Journal*, *21*, 2672–2681. doi:10.1093/emboj/21.11.2672
- Lau, O. D., Courtney, A. D., Vassilev, A., Marzilli, L. A., Cotter, R. J., Nakatani, Y., & Cole, P. A. (2000). p300/CBP-associated factor histone acetyltransferase processing of a peptide substrate: Kinetic analysis of the catalytic mechanism. *Journal of Biological Chemistry*, *275*, 21953–21959. doi:10.1074/jbc.M003219200
- Lee, E., Hong, J., Park, Y.-G., Chae, S., Kim, Y., & Kim, D. (2015). Left brain cortical activity modulates stress effects on social behavior. *Scientific Reports*, *5*, 13342. doi:10.1038/srep13342
- Lee, H., Rezai-Zadeh, N., & Seto, E. (2004). Negative Regulation of Histone Deacetylase 8 Activity by Cyclic AMP-Dependent Protein Kinase A. *Molecular and Cellular Biology*. doi:10.1128/MCB.24.2.765-773.2004
- Lee, J. Y., Nagano, Y., Taylor, J. P., Lim, K. L., & Yao, T. P. (2010). Disease-causing mutations in Parkin impair mitochondrial ubiquitination, aggregation, and HDAC6-dependent mitophagy. *Journal of Cell Biology*, *189*, 671–679. doi:10.1083/jcb.201001039
- Leipe, D. D., & Landsman, D. (1997). Histone deacetylases, acetoin utilization proteins and

- acetylpolyamine amidohydrolases are members of an ancient protein superfamily. *Nucleic Acids Research*, 25, 3693–3697. doi:10.1093/nar/25.18.3693
- Lemercier, C., Verdel, A., Galloo, B., Curtet, S., Brocard, M. P., & Khochbin, S. (2000). mHDA1/HDAC5 histone deacetylase interacts with and represses MEF2A transcriptional activity. *Journal of Biological Chemistry*, 275, 15594–15599. doi:10.1074/jbc.M908437199
- Leone, D. P., Genoud, S., Atanasoski, S., Grausenburger, R., Berger, P., Metzger, D., ... Suter, U. (2003). Tamoxifen-inducible glia-specific Cre mice for somatic mutagenesis in oligodendrocytes and Schwann cells. *Molecular and Cellular Neuroscience*, 22, 430–440. doi:10.1016/S1044-7431(03)00029-0
- Levenson, J. M., O’Riordan, K. J., Brown, K. D., Trinh, M. A., Molfese, D. L., & Sweatt, J. D. (2004). Regulation of histone acetylation during memory formation in the hippocampus. *The Journal of Biological Chemistry*, 279, 40545–40559. doi:10.1074/jbc.M402229200
- Levenson, J. M., & Sweatt, J. D. (2005). Epigenetic mechanisms in memory formation. *Nature Reviews. Neuroscience*, 6, 108–118. doi:10.1038/nrn1604
- Lewandoski, M., Wassarman, K. M., & Martin, G. R. (1997). Zp3-cre, a transgenic mouse line for the activation or inactivation of loxP-flanked target genes specifically in the female germ line. *Current Biology*, 7(2), 148–151. doi:10.1016/S0960-9822(06)00059-5
- Li, J., Wang, J., Nawaz, Z., Liu, J. M., Qin, J., & Wong, J. (2000). Both corepressor proteins SMRT and N-CoR exist in large protein complexes containing HDAC3. *The EMBO Journal*, 19, 4342–4350. doi:10.1093/emboj/19.16.4342
- Li, L., Suzuki, T., Mori, N., & Greengard, P. (1993). Identification of a functional silencer element involved in neuron-specific expression of the synapsin I gene. *Proceedings of the National Academy of Sciences of the United States of America*, 90, 1460–1464. doi:10.1073/pnas.90.4.1460
- Li, M., Indra, A. K., Warot, X., Brocard, J., Messaddeq, N., Kato, S., ... Chambon, P. (2000). Skin abnormalities generated by temporally controlled RXRalpha mutations in mouse epidermis. *Nature*, 407, 633–636. doi:10.1038/35036595
- Li, W., Sun, G., Yang, S., Qu, Q., Nakashima, K., & Shi, Y. (2008). Nuclear receptor TLX regulates cell cycle progression in neural stem cells of the developing brain. *Molecular Endocrinology (Baltimore, Md.)*, 22, 56–64. doi:10.1210/me.2007-0290
- Lightman, S. L., Wiles, C. C., Atkinson, H. C., Henley, D. E., Russell, G. M., Leendertz, J. A., ... Conway-Campbell, B. L. (2008). The significance of glucocorticoid pulsatility. *European Journal of Pharmacology*. doi:10.1016/j.ejphar.2007.11.073
- Ling, S.-C., Albuquerque, C. P., Han, J. S., Lagier-Tourenne, C., Tokunaga, S., Zhou, H., & Cleveland, D. W. (2010). ALS-associated mutations in TDP-43 increase its stability and promote TDP-43 complexes with FUS/TLS. *Proceedings of the National Academy of Sciences of the United States*

- of America*, 107, 13318–13323. doi:10.1073/pnas.1008227107
- Liu, H., Hu, Q., D'ercole, A. J., & Ye, P. (2009). Histone deacetylase 11 regulates oligodendrocyte-specific gene expression and cell development in OL-1 oligodendroglia cells. *Glia*, 57, 1–12. doi:10.1002/glia.20729
- Lockett, G. A., Helliwell, P., & Maleszka, R. (2010). Involvement of DNA methylation in memory processing in the honey bee. *Neuroreport*, 21, 812–816. doi:10.1097/WNR.0b013e32833ce5be
- Lu, A., Steiner, M. A., Whittle, N., Vogl, A. M., Walser, S. M., Ableitner, M., ... Deussing, J. M. (2008). Conditional mouse mutants highlight mechanisms of corticotropin-releasing hormone effects on stress-coping behavior. *Molecular Psychiatry*, 13, 1028–1042. doi:10.1038/mp.2008.51
- Lu, F., Zhou, J., Wiedmer, A., Madden, K., Yuan, Y., & Lieberman, P. M. (2003). Chromatin remodeling of the Kaposi's sarcoma-associated herpesvirus ORF50 promoter correlates with reactivation from latency. *Journal of Virology*, 77, 11425–11435. doi:10.1128/JVI.77.21.11425-11435.2003
- Lubin, F. D., & Sweatt, J. D. (2007). The I κ B Kinase Regulates Chromatin Structure during Reconsolidation of Conditioned Fear Memories. *Neuron*, 55, 942–957. doi:10.1016/j.neuron.2007.07.039
- Luger, K., Mäder, A. W., Richmond, R. K., Sargent, D. F., & Richmond, T. J. (1997). Crystal structure of the nucleosome core particle at 2.8Å resolution. *Nature*, 389.
- Maddox, S. A., & Schafe, G. E. (2011). Epigenetic alterations in the lateral amygdala are required for reconsolidation of a Pavlovian fear memory. *Learning & Memory (Cold Spring Harbor, N.Y.)*, 18, 579–593. doi:10.1101/lm.2243411
- Magnaghi-Jaulin, L., Groisman, R., Naguibneva, I., Robin, P., Lorain, S., Le Villain, J. P., ... Harel-Bellan, A. (1998). Retinoblastoma protein represses transcription by recruiting a histone deacetylase. *Nature*, 391, 601–605. doi:10.1038/35410
- Mahlknecht, U., Bucala, R., Hoelzer, D., & Verdin, E. (1999). High resolution physical mapping of human HDAC3, a potential tumor suppressor gene in the 5q31 region. *Cytogenetics and Cell Genetics*, 86, 237–239.
- Mahlknecht, U., Emiliani, S., Najfeld, V., Young, S., & Verdin, E. (1999). Genomic organization and chromosomal localization of the human histone deacetylase 3 gene. *Genomics*, 56, 197–202.
- Mahlknecht, U., & Hoelzer, D. (2000). Histone acetylation modifiers in the pathogenesis of malignant disease. *Molecular Medicine (Cambridge, Mass.)*, 6, 623–644.
- Mal, A., Sturniolo, M., Schiltz, R. L., Ghosh, M. K., & Harter, M. L. (2001). A role for histone deacetylase HDAC1 in modulating the transcriptional activity of MyoD: Inhibition of the myogenic program. *EMBO Journal*, 20, 1739–1753. doi:10.1093/emboj/20.7.1739

- Malkesman, O., Scattoni, M. L., Paredes, D., Tragon, T., Pearson, B., Shaltiel, G., ... Manji, H. K. (2010). The Female Urine Sniffing Test: A Novel Approach for Assessing Reward-Seeking Behavior in Rodents. *Biological Psychiatry*, *67*, 864–871. doi:10.1016/j.biopsych.2009.10.018
- Malvaez, M., Sanchis-Segura, C., Vo, D., Lattal, K. M., & Wood, M. A. (2010). Modulation of Chromatin Modification Facilitates Extinction of Cocaine-Induced Conditioned Place Preference. *Biological Psychiatry*, *67*, 36–43. doi:10.1016/j.biopsych.2009.07.032
- Marks, P. A., & Breslow, R. (2007). Dimethyl sulfoxide to vorinostat: development of this histone deacetylase inhibitor as an anticancer drug. *Nature Biotechnology*, *25*, 84–90. doi:10.1038/nbt1272
- Marks, P., Rifkind, R. A., Richon, V. M., Breslow, R., Miller, T., & Kelly, W. K. (2001). Histone deacetylases and cancer: causes and therapies. *Nature Reviews. Cancer*, *1*, 194–202. doi:10.1038/35106079
- Marmorstein, R. (2001). Structure of histone deacetylases: Insights into substrate recognition and catalysis. *Structure*. doi:10.1016/S0969-2126(01)00690-6
- Maue, R. A., Kraner, S. D., Goodman, R. H., & Mandel, G. (1990). Neuron-specific expression of the rat brain type II sodium channel gene is directed by upstream regulatory elements. *Neuron*, *4*, 223–231. doi:10.1016/0896-6273(90)90097-Y
- McGhee, J. D., Felsenfeld, G., & Eisenberg, H. (1980). Nucleosome structure and conformational changes. *Biophysical Journal*, *32*, 261–270. doi:10.1146/annurev.bi.49.070180.005343
- McKinsey, T. A., Zhang, C. L., Lu, J., & Olson, E. N. (2000). Signal-dependent nuclear export of a histone deacetylase regulates muscle differentiation. *Nature*, *408*, 106–111. doi:10.1038/35040593
- McNairn, A. J., & Gilbert, D. M. (2003). Epigenomic replication: Linking epigenetics to DNA replication. *BioEssays*. doi:10.1002/bies.10305
- McQuown, S. C., Barrett, R. M., Matheos, D. P., Post, R. J., Rogge, G. a, Alenghat, T., ... Wood, M. a. (2011). HDAC3 is a critical negative regulator of long-term memory formation. *The Journal of Neuroscience: The Official Journal of the Society for Neuroscience*, *31*(2), 764–74. doi:10.1523/JNEUROSCI.5052-10.2011
- McQuown, S. C., & Wood, M. A. (2011). NIH Public Access. *Neurobiol Learn Mem.*, *96*(1), 27–34. doi:10.1016/j.nlm.2011.04.005.HDAC3
- Mercer, T. R., & Mattick, J. S. (2013). Structure and function of long noncoding RNAs in epigenetic regulation. *Nature Structural & Molecular Biology*, *20*, 300–7. doi:10.1038/nsmb.2480
- Metzger, D., & Chambon, P. (2001). Site- and time-specific gene targeting in the mouse. *Methods (San Diego, Calif.)*, *24*, 71–80. doi:10.1006/meth.2001.1159
- Mijimolle, N., Velasco, J., Dubus, P., Guerra, C., Weinbaum, C. A., Casey, P. J., ... Barbacid, M. (2005).

- Protein farnesyltransferase in embryogenesis, adult homeostasis, and tumor development. *Cancer Cell*, 7, 313–324. doi:10.1016/j.ccr.2005.03.004
- Miller, C. A., Campbell, S. L., & Sweatt, J. D. (2008). DNA methylation and histone acetylation work in concert to regulate memory formation and synaptic plasticity. *Neurobiology of Learning and Memory*, 89, 599–603. doi:10.1016/j.nlm.2007.07.016
- Miller, L., Foradori, C. D., Lalmansingh, A. S., Sharma, D., Handa, R. J., & Uht, R. M. (2011). Histone deacetylase 1 (HDAC1) participates in the down-regulation of corticotropin releasing hormone gene (crh) expression. *Physiology & Behavior*, 104(2), 312–20. doi:10.1016/j.physbeh.2011.03.026
- Mineur, Y. S., Prasol, D. J., Belzung, C., & Crusio, W. E. (2003). Agonistic behavior and unpredictable chronic mild stress in mice. In *Behavior Genetics* (Vol. 33, pp. 513–519). doi:10.1023/A:1025770616068
- Miska, E. A., Langley, E., Wolf, D., Karlsson, C., Pines, J., & Kouzarides, T. (2001). Differential localization of HDAC4 orchestrates muscle differentiation. *Nucleic Acids Research*, 29, 3439–3447. doi:10.1093/nar/29.16.3439
- Montgomery, R. L., Davis, C. A., Potthoff, M. J., Haberland, M., Fielitz, J., Qi, X., ... Olson, E. N. (2007). Histone deacetylases 1 and 2 redundantly regulate cardiac morphogenesis, growth, and contractility. *Genes & Development*, 21, 1790–1802. doi:10.1101/gad.1563807
- Montgomery, R. L., Hsieh, J., Barbosa, A. C., Richardson, J. a, & Olson, E. N. (2009). Histone deacetylases 1 and 2 control the progression of neural precursors to neurons during brain development. *Proceedings of the National Academy of Sciences of the United States of America*, 106(19), 7876–81. doi:10.1073/pnas.0902750106
- Moosmang, S., Schulla, V., Welling, A., Feil, R., Feil, S., Wegener, J. W., ... Klugbauer, N. (2003). Dominant role of smooth muscle L-type calcium channel Cav1.2 for blood pressure regulation. *The EMBO Journal*, 22, 6027–6034. doi:10.1093/emboj/cdg583
- Morgan, T. H. (1910). SEX LIMITED INHERITANCE IN DROSOPHILA. *Science (New York, N.Y.)*, 32, 120–122. doi:10.1126/science.32.812.120
- Mori, N., Schoenherr, C., Vandenberg, D. J., & Anderson, D. J. (1992). A common silencer element in the SCG10 and type II Na⁺ channel genes binds a factor present in nonneuronal cells but not in neuronal cells. *Neuron*, 9, 45–54. doi:10.1016/0896-6273(92)90219-4
- Nanney, D. (1958). Epigenetic control systems. *Proc Nat Acad Sci USA*, (44), 712–717.
- Naruse, Y., Oh-hashii, K., Iijima, N., Naruse, M., Yoshioka, H., & Tanaka, M. (2004). Circadian and light-induced transcription of clock gene Per1 depends on histone acetylation and deacetylation. *Molecular and Cellular Biology*, 24, 6278–6287. doi:10.1128/MCB.24.14.6278-6287.2004

- Nöthiger, R. (2002). Ernst Hadorn, a pioneer of developmental genetics. *The International Journal of Developmental Biology*, 46(1), 23–7. Retrieved from <http://www.ncbi.nlm.nih.gov/pubmed/11902684>
- Nutt, D. J. (1990). The pharmacology of human anxiety. *Pharmacology & Therapeutics*, 47(2), 233–266. doi:[http://dx.doi.org/10.1016/0163-7258\(90\)90089-K](http://dx.doi.org/10.1016/0163-7258(90)90089-K)
- Oehme, I., Deubzer, H. E., Lodrini, M., Milde, T., & Witt, O. (2009). Targeting of HDAC8 and investigational inhibitors in neuroblastoma. *Expert Opinion on Investigational Drugs*, 18, 1605–1617. doi:10.1517/14728220903241658
- Oehme, I., Deubzer, H. E., Wegener, D., Pickert, D., Linke, J. P., Hero, B., ... Witt, O. (2009). Histone deacetylase 8 in neuroblastoma tumorigenesis. *Clinical Cancer Research*, 15, 91–99. doi:10.1158/1078-0432.CCR-08-0684
- Ohl, F. (2005). Animal models of anxiety. *Handbook of Experimental Pharmacology*, 169, 35–69. doi:10.1007/3-540-28082-0-2
- Ookubo, M., Kanai, H., Aoki, H., & Yamada, N. (2013). Antidepressants and mood stabilizers effects on histone deacetylase expression in C57BL/6 mice: Brain region specific changes. *Journal of Psychiatric Research*, 47(9), 1204–14. doi:10.1016/j.jpsychires.2013.05.028
- Owen-Hughes, T., & Bruno, M. (2004). Molecular biology. Breaking the silence. *Science*, 303(5656), 324–5.
- Pandey, U. B., Nie, Z., Batlevi, Y., McCray, B. A., Ritson, G. P., Nedelsky, N. B., ... Taylor, J. P. (2007). HDAC6 rescues neurodegeneration and provides an essential link between autophagy and the UPS. *Nature*, 447, 859–863. doi:10.1038/nature05853
- Paquette, A. J., Perez, S. E., & Anderson, D. J. (2000). Constitutive expression of the neuron-restrictive silencer factor (NRSF)/REST in differentiating neurons disrupts neuronal gene expression and causes axon pathfinding errors in vivo. *Proceedings of the National Academy of Sciences of the United States of America*, 97, 12318–12323. doi:10.1073/pnas.97.22.12318
- Paroni, G., Mizzau, M., Henderson, C., Del Sal, G., Schneider, C., & Brancolini, C. (2004). Caspase-dependent regulation of histone deacetylase 4 nuclear-cytoplasmic shuttling promotes apoptosis. *Molecular Biology of the Cell*, 15, 2804–2818. doi:10.1091/mbc.E03-08-0624
- Peleg, S., Sananbenesi, F., Zovoilis, A., Burkhardt, S., Bahari-Javan, S., Agis-Balboa, R. C., ... Fischer, A. (2010). Altered histone acetylation is associated with age-dependent memory impairment in mice. *Science (New York, N.Y.)*, 328, 753–756. doi:10.1126/science.1186088
- Pereira, L. O., Arteni, N. S., Petersen, R. C., da Rocha, A. P., Achaval, M., & Netto, C. A. (2007). Effects of daily environmental enrichment on memory deficits and brain injury following neonatal hypoxia-ischemia in the rat. *Neurobiology of Learning and Memory*, 87, 101–108. doi:10.1016/j.nlm.2006.07.003

- Perez, M., Santa-Maria, I., De Barreda, E. G., Zhu, X., Cuadros, R., Cabrero, J. R., ... Avila, J. (2009). Tau - An inhibitor of deacetylase HDAC6 function. *Journal of Neurochemistry*, *109*, 1756–1766. doi:10.1111/j.1471-4159.2009.06102.x
- Petrich, B. G., Molkenin, J. D., & Wang, Y. (2003). Temporal activation of c-Jun N-terminal kinase in adult transgenic heart via cre-loxP-mediated DNA recombination. *The FASEB Journal : Official Publication of the Federation of American Societies for Experimental Biology*, *17*, 749–751. doi:10.1096/fj.02-0438fje
- Pflum, M. K., Tong, J. K., Lane, W. S., & Schreiber, S. L. (2001). Histone deacetylase 1 phosphorylation promotes enzymatic activity and complex formation. *The Journal of Biological Chemistry*, *276*, 47733–47741. doi:10.1074/jbc.M105590200
- Porsolt, R. D., Bertin, A., & Jalfre, M. (1977). Behavioral despair in mice: a primary screening test for antidepressants. *Archives Internationales de Pharmacodynamie et de Therapie*, *229*, 327–336. doi:10.1196/annals.1317.038
- Prut, L., & Belzung, C. (2003). The open field as a paradigm to measure the effects of drugs on anxiety-like behaviors: A review. *European Journal of Pharmacology*. doi:10.1016/S0014-2999(03)01272-X
- Puri, P. L., Iezzi, S., Stiegler, P., Chen, T. T., Schiltz, R. L., Muscat, G. E. O., ... Sartorelli, V. (2001). Class I histone deacetylases sequentially interact with MyoD and pRb during skeletal myogenesis. *Molecular Cell*, *8*, 885–897. doi:10.1016/S1097-2765(01)00373-2
- Quina, a S., Buschbeck, M., & Di Croce, L. (2006). Chromatin structure and epigenetics. *Biochemical Pharmacology*, *72*(11), 1563–9. doi:10.1016/j.bcp.2006.06.016
- Rall, J. E. (1997). This is Biology, The Science of the Living World. *The Journal of Nervous & Mental Disease*. doi:10.1097/00005053-199711000-00011
- Ravi, B., & Kannan, M. (2013). Epigenetics in the nervous system: An overview of its essential role. *Indian Journal of Human Genetics*, *19*, 384–391. doi:10.4103/0971-6866.124357
- Refojo, D., Schweizer, M., Kuehne, C., Ehrenberg, S., Thoeringer, C., Vogl, a. M., ... Deussing, J. M. (2011). Glutamatergic and Dopaminergic Neurons Mediate Anxiogenic and Anxiolytic Effects of CRHR1. *Science*, *333*(6051), 1903–1907. doi:10.1126/science.1202107
- Renthal, W., Maze, I., Krishnan, V., Covington, H. E., Xiao, G., Kumar, A., ... Nestler, E. J. (2007). Histone Deacetylase 5 Epigenetically Controls Behavioral Adaptations to Chronic Emotional Stimuli. *Neuron*, *56*, 517–529. doi:10.1016/j.neuron.2007.09.032
- Richman, R., Chicoine, L. G., Collini, M. P., & Cook R.G. Allis, C. D. (1988). Micronuclei and the Cytoplasm of Growing Tetrahymena Contain a Histone Acetylase Activity Which Is Highly Specific for Free Histone H4, *106*(April), 1017–1026.
- Richon, V. M. (2006). Cancer biology: mechanism of antitumour action of vorinostat

- (suberoylanilide hydroxamic acid), a novel histone deacetylase inhibitor. *British Journal of Cancer*, 95, S2–S6. doi:10.1038/sj.bjc.6603463
- Richon, V. M., Emiliani, S., Verdin, E., Webb, Y., Breslow, R., Rifkind, R. A., & Marks, P. A. (1998). A class of hybrid polar inducers of transformed cell differentiation inhibits histone deacetylases. *Proceedings of the National Academy of Sciences of the United States of America*, 95, 3003–3007. doi:10.1073/pnas.95.6.3003
- Riggs, A. D. (1975). X inactivation, differentiation, and DNA methylation. *Cytogenetics and Cell Genetics*, 14, 9–25. doi:10.1159/000130315
- Riggs, A. D. (1996). Introduction. In Epigenetic mechanisms of gene regulation. *Cold Spring Harbor Laboratory Press, Cold Spring Harbor, New York*.
- Robyr, D., Suka, Y., Xenarios, I., Kurdistani, S. K., Wang, A., Suka, N., & Grunstein, M. (2002). Microarray deacetylation maps determine genome-wide functions for yeast histone deacetylases. *Cell*, 109, 437–446. doi:10.1016/S0092-8674(02)00746-8
- Rodgers, R. J., & Dalvi, A. (1997). Anxiety, defence and the elevated plus-maze. In *Neuroscience and Biobehavioral Reviews* (Vol. 21, pp. 801–810). doi:10.1016/S0149-7634(96)00058-9
- Rodgers, R. J., Johnson, N. J., Carr, J., & Hodgson, T. P. (1997). Resistance of experientially-induced changes in murine plus-maze behaviour to altered retest conditions. *Behavioural Brain Research*, 86(1), 71–7. doi:http://dx.doi.org/10.1016/S0166-4328(96)02248-6
- Rodriguez, C., Bucholz, F., Galloway, J., Sequerra, R., Kasper, J., Avala, R., ... Dymecki, S. (2000). High-efficiency deleter mice show that FLPe is an alternative to Cre-loxP. *Nature Genetics*, 2, 139–40.
- Rudenko, A., & Tsai, L.-H. (2014). Epigenetic modifications in the nervous system and their impact upon cognitive impairments. *Neuropharmacology*, 80, 70–82. doi:10.1016/j.neuropharm.2014.01.043
- Rundlett, S. E., Carmen, A. A., Kobayashi, R., Bavykin, S., Turner, B. M., & Grunstein, M. (1996). HDA1 and RPD3 are members of distinct yeast histone deacetylase complexes that regulate silencing and transcription. *Proceedings of the National Academy of Sciences of the United States of America*, 93, 14503–14508. doi:10.1073/pnas.93.25.14503
- Sahakian, E., Powers, J. J., Chen, J., Deng, S. L., Cheng, F., Distler, A., ... Pinilla-Ibarz, J. (2015). Histone deacetylase 11: A novel epigenetic regulator of myeloid derived suppressor cell expansion and function. *Molecular Immunology*, 63(2), 579–85. doi:10.1016/j.molimm.2014.08.002
- Sandler, I., & Sandler, L. (1985). A conceptual ambiguity that contributed to the neglect of Mendel's paper. *History Phil Life Sciences*, 7, 3–70.
- Sando, R., Gounko, N., Pieraut, S., Liao, L., Yates, J., & Maximov, A. (2012). HDAC4 governs a transcriptional program essential for synaptic plasticity and memory. *Cell*, 151, 821–834.

doi:10.1016/j.cell.2012.09.037

- Schuettengruber, B., Simboeck, E., Khier, H., & Seiser, C. (2003). Autoregulation of mouse histone deacetylase 1 expression. *Molecular and Cellular Biology*, *23*, 6993–7004. doi:10.1128/MCB.23.19.6993-7004.2003
- Shahbazian, M. D., & Grunstein, M. (2007). Functions of site-specific histone acetylation and deacetylation. *Annual Review of Biochemistry*, *76*, 75–100. doi:10.1146/annurev.biochem.76.052705.162114
- Sharma, R. P., Grayson, D. R., & Gavin, D. P. (2008). Histone deacetylase 1 expression is increased in the prefrontal cortex of schizophrenia subjects: analysis of the National Brain Databank microarray collection. *Schizophrenia Research*, *98*(1-3), 111–7. doi:10.1016/j.schres.2007.09.020
- Shi, Y., Chichung Lie, D., Taupin, P., Nakashima, K., Ray, J., Yu, R. T., ... Evans, R. M. (2004). Expression and function of orphan nuclear receptor TLX in adult neural stem cells. *Nature*, *427*, 78–83. doi:10.1038/nature02211
- Shi, Y., Lan, F., Matson, C., Mulligan, P., Whetstine, J. R., Cole, P. A., ... Shi, Y. (2004). Histone demethylation mediated by the nuclear amine oxidase homolog LSD1. *Cell*, *119*, 941–953. doi:10.1016/j.cell.2004.12.012
- Shogren-Knaak, M., Ishii, H., Sun, J.-M., Pazin, M. J., Davie, J. R., & Peterson, C. L. (2006). Histone H4-K16 acetylation controls chromatin structure and protein interactions. *Science (New York, N.Y.)*, *311*, 844–847. doi:10.1126/science.1124000
- Shore, D. (2000). The Sir2 protein family: A novel deacetylase for gene silencing and more. *Proceedings of the National Academy of Sciences of the United States of America*, *97*(26), 14030–2. doi:10.1073/pnas.011506198
- Skinner, M. K. (2011). Environmental epigenomics and disease susceptibility. *EMBO Reports*, *12*, 620–622. doi:10.1038/embor.2011.125
- Slotnick, B. M., & Jarvik, M. E. (1966). Deficits in Passive Avoidance and Fear Conditioning in Mice with Septal Lesions. *Science*, *154*, 1207–1208.
- Sohal, D. S., Nghiem, M., Crackower, M. A., Witt, S. A., Kimball, T. R., Tymitz, K. M., ... Molkenin, J. D. (2001). Temporally regulated and tissue-specific gene manipulations in the adult and embryonic heart using a tamoxifen-inducible Cre protein. *Circulation Research*, *89*, 20–25. doi:10.1161/hh1301.092687
- Somoza, J. R., Skene, R. J., Katz, B. A., Mol, C., Ho, J. D., Jennings, A. J., ... Tari, L. W. (2004). Structural snapshots of human HDAC8 provide insights into the class I histone deacetylases. *Structure*, *12*, 1325–1334. doi:10.1016/j.str.2004.04.012
- Sontheimer, E. J., & Carthew, R. W. (2005). Silence from within: Endogenous siRNAs and miRNAs.

Cell. doi:10.1016/j.cell.2005.06.030

- Sparrow, D. B., Miska, E. A., Langley, E., Reynaud-Deonauth, S., Kotecha, S., Towers, N., ... Mohun, T. J. (1999). MEF-2 function is modified by a novel co-repressor, MITR. *EMBO Journal*, *18*, 5085–5098. doi:10.1093/emboj/18.18.5085
- Strahl, B. D., & Allis, C. D. (2000). The language of covalent histone modifications, *403*(January), 41–45.
- Sun, G., Alzayady, K., Stewart, R., Ye, P., Yang, S., Li, W., & Shi, Y. (2010). Histone demethylase LSD1 regulates neural stem cell proliferation. *Molecular and Cellular Biology*, *30*, 1997–2005. doi:10.1128/MCB.01116-09
- Swank, M. W., & Sweatt, J. D. (2001). Increased histone acetyltransferase and lysine acetyltransferase activity and biphasic activation of the ERK/RSK cascade in insular cortex during novel taste learning. *The Journal of Neuroscience : The Official Journal of the Society for Neuroscience*, *21*, 3383–3391. doi:21/10/3383 [pii]
- Sweatt, J. D., Nestler, E. J., & Michael, J. (2013). *An Overview of the Molecular Basis of Epigenetics. Epigenetic Regulation in the Nervous System* (First Edit.). Elsevier Inc. doi:10.1016/B978-0-12-391494-1.00001-X
- Takami, Y., & Nakayama, T. (2000). N-terminal region, C-terminal region, nuclear export signal, and deacetylation activity of histone deacetylase-3 are essential for the viability of the DT40 chicken B cell line. *Journal of Biological Chemistry*, *275*, 16191–16201. doi:10.1074/jbc.M908066199
- Tan, J., Cang, S., Ma, Y., Petrillo, R. L., & Liu, D. (2010). Novel histone deacetylase inhibitors in clinical trials as anti-cancer agents. *Journal of Hematology & Oncology*, *3*, 5. doi:10.1186/1756-8722-3-5
- Tanner, K. G., Langer, M. R., & Denu, J. M. (2000). Kinetic mechanism of human histone acetyltransferase P/CAF. *Biochemistry*, *39*, 11961–11969. doi:10.1021/bi001272h
- Taplick, J., Kurtev, V., Kroboth, K., Posch, M., Lechner, T., & Seiser, C. (2001). Homo-oligomerisation and nuclear localisation of mouse histone deacetylase 1. *Journal of Molecular Biology*, *308*, 27–38. doi:10.1006/jmbi.2001.4569
- Taunton, J., Hassig, C. A., & Schreiber, S. L. (1996). A mammalian histone deacetylase related to the yeast transcriptional regulator Rpd3p. *Science (New York, N.Y.)*, *272*, 408–411. doi:10.1126/science.272.5260.408
- Tolman, E. C., Ritchie, B. F., & Kalish, D. (1946). Studies in spatial learning: Orientation and the short-cut. *J Exp Psychol.*, *Feb*(36), 13–24.
- Tong, J. J., Liu, J., Bertos, N. R., & Yang, X.-J. (2002). Identification of HDAC10, a novel class II human histone deacetylase containing a leucine-rich domain. *Nucleic Acids Research*, *30*, 1114–1123.

doi:10.1093/nar/30.5.1114

- Tremolizzo, L., Doueiri, M. S., Dong, E., Grayson, D. R., Davis, J., Pinna, G., ... Guidotti, A. (2005). Valproate corrects the schizophrenia-like epigenetic behavioral modifications induced by methionine in mice. *Biological Psychiatry*, *57*, 500–509. doi:10.1016/j.biopsych.2004.11.046
- Tsai, S. C., Valkov, N., Yang, W. M., Gump, J., Sullivan, D., & Seto, E. (2000). Histone deacetylase interacts directly with DNA topoisomerase II. *Nature Genetics*, *26*, 349–353. doi:10.1038/81671
- Tsankova, N. M., Berton, O., Renthal, W., Kumar, A., Neve, R. L., & Nestler, E. J. (2006). Sustained hippocampal chromatin regulation in a mouse model of depression and antidepressant action. *Nature Neuroscience*, *9*, 519–525. doi:10.1038/nn1659
- Tse, C., Sera, T., Wolffe, A. P., & Hansen, J. C. (1998). Disruption of higher-order folding by core histone acetylation dramatically enhances transcription of nucleosomal arrays by RNA polymerase III. *Molecular and Cellular Biology*, *18*, 4629–4638.
- Tsien, J. Z., Chen, D. F., Gerber, D., Tom, C., Mercer, E. H., Anderson, D. J., ... Tonegawa, S. (1996). Subregion- and cell type-restricted gene knockout in mouse brain. *Cell*, *87*(7), 1317–1326. doi:10.1016/S0092-8674(00)81826-7
- Turner, B. M. (2000). Histone acetylation and an epigenetic code. *BioEssays*, *22*, 836–845. doi:10.1002/1521-1878(200009)22:9<836::AID-BIES9>3.0.CO;2-X
- Van den Wyngaert, I., de Vries, W., Kremer, A., Neefs, J., Verhasselt, P., Luyten, W. H., & Kass, S. U. (2000). Cloning and characterization of human histone deacetylase 8. *FEBS Letters*, *478*, 77–83. doi:10.1016/S0014-5793(00)01813-5
- Vaute, O., Nicolas, E., Vandiel, L., & Trouche, D. (2002). Functional and physical interaction between the histone methyl transferase Suv39H1 and histone deacetylases. *Nucleic Acids Research*, *30*, 475–481. doi:10.1093/nar/30.2.475
- Verdel, A., & Khochbin, S. (1999). Identification of a new family of higher eukaryotic histone deacetylases: Coordinate expression of differentiation-dependent chromatin modifiers. *Journal of Biological Chemistry*, *274*, 2440–2445. doi:10.1074/jbc.274.4.2440
- Vidal, M., & Gaber, R. F. (1991). RPD3 encodes a second factor required to achieve maximum positive and negative transcriptional states in *Saccharomyces cerevisiae*. *Molecular and Cellular Biology*, *11*, 6317–6327. doi:10.1128/MCB.11.12.6317.Updated
- Vogel, J. R., Beer, B., & Clody, D. E. (1971). A simple and reliable conflict procedure for testing anti-anxiety agents. *Psychopharmacologia*, *21*(1), 1–7. doi:10.1007/BF00403989
- Volmar, C.-H., & Wahlestedt, C. (2014). Histone deacetylases (HDACs) and brain function. *Neuroepigenetics*. doi:10.1016/j.nepig.2014.10.002
- Waddington, C. H. (1939). Introduction to Modern Genetics. *London: Allen and Unwin*.

- Waddington, C. H. (1942). The epigenotype. *Endeavour*, *1*, 18–20.
- Waddington, C. H. (1957). *The Strategy of the Genes; a Discussion of Some Aspects of Theoretical Biology*. London: Allen and Unwin.
- Waddington, C. H. (1968). *Towards a Theoretical Biology*. Edinburgh, Scotland: Edinburgh University Press; (The Basic Ideas of Biology), 1–32.
- Wade, P. A. (2001). Transcriptional control at regulatory checkpoints by histone deacetylases: molecular connections between cancer and chromatin. *Human Molecular Genetics*, *10*, 693–698. doi:10.1093/hmg/10.7.693
- Wagner, K. V., Wang, X. D., Liebl, C., Scharf, S. H., Müller, M. B., & Schmidt, M. V. (2011). Pituitary glucocorticoid receptor deletion reduces vulnerability to chronic stress. *Psychoneuroendocrinology*, *36*, 579–587. doi:10.1016/j.psyneuen.2010.09.007
- Waltregny, D., De Leval, L., Glénisson, W., Ly Tran, S., North, B. J., Bellahcène, A., ... Castronovo, V. (2004). Expression of histone deacetylase 8, a class I histone deacetylase, is restricted to cells showing smooth muscle differentiation in normal human tissues. *The American Journal of Pathology*, *165*, 553–564. doi:10.1016/S0002-9440(10)63320-2
- Waltregny, D., Glénisson, W., Tran, S. L., North, B. J., Verdin, E., Colige, A., & Castronovo, V. (2005). Histone deacetylase HDAC8 associates with smooth muscle alpha-actin and is essential for smooth muscle cell contractility. *The FASEB Journal : Official Publication of the Federation of American Societies for Experimental Biology*, *19*, 966–968. doi:10.1096/fj.04-2303fje
- Wang, A. H., Bertos, N. R., Vezmar, M., Pelletier, N., Crosato, M., Heng, H. H., ... Yang, X. J. (1999). HDAC4, a human histone deacetylase related to yeast HDA1, is a transcriptional corepressor. *Molecular and Cellular Biology*, *19*, 7816–7827.
- Wang, A. H., Kruhlak, M. J., Wu, J., Bertos, N. R., Vezmar, M., Posner, B. I., ... Yang, X. J. (2000). Regulation of histone deacetylase 4 by binding of 14-3-3 proteins. *Molecular and Cellular Biology*, *20*, 6904–6912. doi:10.1128/MCB.20.18.6904-6912.2000
- Wang, X., He, C., Moore, S. C., & Ausio, J. (2001). Effects of histone acetylation on the solubility and folding of the chromatin fiber. *The Journal of Biological Chemistry*, *276*, 12764–12768. doi:10.1074/jbc.M100501200
- Wang, Z., Yang, D., Zhang, X., Li, T., Li, J., Tang, Y., & Le, W. (2011). Hypoxia-induced Down-regulation of Neprilysin by histone modification in mouse primary cortical and Hippocampal neurons. *PLoS ONE*, *6*. doi:10.1371/journal.pone.0019229
- Weaver, I. C. G., Cervoni, N., Champagne, F. A., D'Alessio, A. C., Sharma, S., Seckl, J. R., ... Meaney, M. J. (2004). Epigenetic programming by maternal behavior. *Nature Neuroscience*, *7*, 847–854. doi:10.1038/nn1276
- Weaver, I. C. G., Champagne, F. A., Brown, S. E., Dymov, S., Sharma, S., Meaney, M. J., & Szyf, M.

- (2005). Reversal of maternal programming of stress responses in adult offspring through methyl supplementation: altering epigenetic marking later in life. *The Journal of Neuroscience: The Official Journal of the Society for Neuroscience*, 25, 11045–11054. doi:10.1523/JNEUROSCI.3652-05.2005
- Weiss, S. J. (2007). Neurobiological alterations associated with traumatic stress. *Perspectives in Psychiatric Care*, 43(3), 114–22. doi:10.1111/j.1744-6163.2007.00120.x
- Wen, Y. D., Perissi, V., Staszewski, L. M., Yang, W. M., Krones, A., Glass, C. K., ... Seto, E. (2000). The histone deacetylase-3 complex contains nuclear receptor corepressors. *Proceedings of the National Academy of Sciences of the United States of America*, 97, 7202–7207. doi:10.1073/pnas.97.13.7202
- Williams, A. H., Valdez, G., Moresi, V., Qi, X., McAnally, J., Elliott, J. L., ... Olson, E. N. (2009). MicroRNA-206 delays ALS progression and promotes regeneration of neuromuscular synapses in mice. *Science (New York, N.Y.)*, 326, 1549–1554. doi:10.1126/science.1181046
- Wolffe, A. P., & Hayes, J. J. (1999). Chromatin disruption and modification. *Nucleic Acids Research*. doi:10.1093/nar/27.3.711
- Wu, X., Li, H., Park, E. J., & Chen, J. D. (2001). SMRTE inhibits MEF2C transcriptional activation by targeting HDAC4 and 5 to nuclear domains. *The Journal of Biological Chemistry*, 276, 24177–24185. doi:10.1074/jbc.M100412200
- Xiao, G., Mao, S., Baumgarten, G., Serrano, J., Jordan, M. C., Roos, K. P., ... MacLellan, W. R. (2001). Inducible activation of c-Myc in adult myocardium in vivo provokes cardiac myocyte hypertrophy and reactivation of DNA synthesis. *Circulation Research*, 89, 1122–1129. doi:10.1161/hh2401.100742
- Yang, W. M., Inouye, C., Zeng, Y., Bearss, D., & Seto, E. (1996). Transcriptional repression by YY1 is mediated by interaction with a mammalian homolog of the yeast global regulator RPD3. *Proceedings of the National Academy of Sciences of the United States of America*, 93, 12845–12850. doi:10.1073/pnas.93.23.12845
- Yang, W. M., Yao, Y. L., Sun, J. M., Davie, J. R., & Seto, E. (1997). Isolation and characterization of cDNAs corresponding to an additional member of the human histone deacetylase gene family. *Journal of Biological Chemistry*, 272, 28001–28007. doi:10.1074/jbc.272.44.28001
- Yang, W.-M., Tsai, S.-C., Wen, Y.-D., Fejer, G., & Seto, E. (2002). Functional domains of histone deacetylase-3. *The Journal of Biological Chemistry*, 277, 9447–9454. doi:10.1074/jbc.M105993200
- Yoo, J. Y. J., Larouche, M., & Goldowitz, D. (2013). The expression of HDAC1 and HDAC2 during cerebellar cortical development. *Cerebellum (London, England)*, 12(4), 534–46. doi:10.1007/s12311-013-0459-x
- Yoshida, M., Furumai, R., Nishiyama, M., Komatsu, Y., Nishino, N., & Horinouchi, S. (2001). Histone

- deacetylase as a new target for cancer chemotherapy. *Cancer Chemotherapy and Pharmacology*, 48 Suppl 1, S20–S26. doi:10.1007/s002800100300
- Yoshida, M., Horinouchi, S., & Beppu, T. (1995). Trichostatin A and trapoxin: novel chemical probes for the role of histone acetylation in chromatin structure and function. *BioEssays : News and Reviews in Molecular, Cellular and Developmental Biology*, 17, 423–430. doi:10.1002/bies.950170510
- Yoshida, M., Kijima, M., Akita, M., & Beppu, T. (1990). Potent and specific inhibition of mammalian histone deacetylase both in vivo and in vitro by trichostatin A. *The Journal of Biological Chemistry*, 265, 17174–17179.
- Yu, D., Dews, M., Park, A., Tobias, J. W., & Thomas-Tikhonenko, A. (2005). Inactivation of Myc in murine two-hit B lymphomas causes dormancy with elevated levels of interleukin 10 receptor and CD20: Implications for adjuvant therapies. *Cancer Research*, 65, 5454–5461. doi:10.1158/0008-5472.CAN-04-4197
- Zhang, J., Kalkum, M., Chait, B. T., & Roeder, R. G. (2002). The N-CoR-HDAC3 nuclear receptor corepressor complex inhibits the JNK pathway through the integral subunit GPS2. *Molecular Cell*, 9, 611–623. doi:10.1016/S1097-2765(02)00468-9
- Zhang, Y., Li, N., Caron, C., Matthias, G., Hess, D., Khochbin, S., & Matthias, P. (2003). HDAC-6 interacts with and deacetylates tubulin and microtubules in vivo. *EMBO Journal*, 22, 1168–1179. doi:10.1093/emboj/cdg115
- Zhang, Y., Ng, H. H., Erdjument-Bromage, H., Tempst, P., Bird, A., & Reinberg, D. (1999). Analysis of the NuRD subunits reveals a histone deacetylase core complex and a connection with DNA methylation. *Genes & Development*, 13, 1924–1935. doi:10.1101/gad.13.15.1924
- Zhou, X., Marks, P. A., Rifkind, R. A., & Richon, V. M. (2001). Cloning and characterization of a histone deacetylase, HDAC9. *Proceedings of the National Academy of Sciences of the United States of America*, 98, 10572–10577. doi:10.1073/pnas.191375098
- Zhou, X., Richon, V. M., Rifkind, R. A., & Marks, P. A. (2000). Identification of a transcriptional repressor related to the noncatalytic domain of histone deacetylases 4 and 5. *Proceedings of the National Academy of Sciences of the United States of America*, 97, 1056–1061. doi:10.1073/pnas.97.3.1056

9 CURRICULUM VITAE

Personal details

Name: Michaela Katja Stangl (maiden name: Möllmann)

Date of birth: November 18th, 1981

Place of birth: Heilbronn, Germany

Citizenship: German

Education

- 10/2009 – 02/2013** PhD thesis in the laboratory of "Molecular Neurogenetics" of Dr. Jan Deussing at the Max Planck Institute of Psychiatry, Munich and the IDG at the Technische Universität München, Prof. Dr. Wolfgang Wurst.
Title: "Dissecting brain-specific functions of histone deacetylases 1 and 3 by using genetic mouse models"
- 11/2008 – 07/2009** Diploma thesis in the laboratory of "ROS and oxidative stress" of Dr. Marcus Conrad at the Institute of Clinical Molecular Biology and Tumor Genetics at the Helmholtz Center Munich and the IDG at the Technische Universität München, Prof. Dr. Wolfgang Wurst.
Title: "Investigations on two main redox-regulating systems: The glutathione (GSH)-dependent system and the Thioredoxin (Txn)-dependent system"
- 10/2006 – 07/2009** Master Studies in Biochemistry, Technische Universität München,
Final grade: 1.1
- 10/2002 – 09/2005** Bachelor Studies in Biochemistry, Technische Universität München,
Final grade: 1.9
- 1988 – 2001** Primary and Secondary Education
June 2001: University-entrance diploma
(Abitur; finale grade: 1.9)

Scientific Work Experience

- 10/2009 – 02/2013** PhD thesis in the laboratory of "Molecular Neurogenetics" of Dr. Jan Deussing at the Max Planck Institute of Psychiatry, Munich and the IDG at the Technische Universität München, Prof. Dr. Wolfgang Wurst.
Title: "Dissecting brain-specific functions of histone deacetylases 1 and 3 by using genetic mouse models"
- 11/2008 – 07/2009** Diploma thesis in the laboratory of "ROS and oxidative stress" of Dr. Marcus Conrad at the Institute of Clinical Molecular Biology and Tumor Genetics at the Helmholtz Center Munich and the IDG at the Technische Universität München, Prof. Dr. Wolfgang Wurst.
Title: "Investigations on two main redox-regulating systems: The glutathione (GSH)-dependent system and the Thioredoxin (Txn)-dependent system"
- 04/2007 – 05/2007** Internship in the laboratory of Prof. Dr. Justus Duyster, III. Medical Clinic at the Klinikum Rechts der Isar, Technische Universität München.
Title: "Learning mouse-techniques in an oncological research laboratory"
- 02/2007 – 03/2007** Internship in the laboratory of Prof. Dr. Peter Köhler, Chair of Food Chemistry, Chemistry Department, Technische Universität München.
Title: "Investigations on Xylanases for the food industry"
- 04/2006 – 10/2006** Internship in the laboratory of Dr. Eric Quéméneur at the CEA Life Science Division, Marcoule, France.
Title: "Purification and characterization of saxiphilin from *R. catesbeiana*"
- 08/2005 – 01/2006** Internship in the laboratory of Prof. Jeremy Thorner, Molecular Cell Biology Department, University of California, Berkeley, USA.
Title: "Effects of *cdc10Δ/shs1Δ* and interaction mapping of *cdc10* in *S. cerevisiae*"
- 05/2005 – 07/2005** Bachelor thesis in the laboratory of Prof. Dr. Johannes Buchner, Chair of Biotechnology, Chemistry Department, Technische Universität München.
Title: "Purification of Hsp25 from *C. elegans*"

- 10/2004 – 04/2005** Auxiliary-Student's-Job in the laboratory of Prof. Dr. Johannes Buchner, Chair of Biotechnology, Chemistry Department, Technische Universität München.
Title: "Purification of Hsp25 from *C. elegans*"
- 09/2004 – 10/2004** Internship in the laboratory of Prof. Dr. Johannes Buchner, Chair of Biotechnology, Chemistry Department, Technische Universität München.
Title: "Purification and Characterization of Hsp26 from *S. cerevisiae*"
- 08/2003 – 10/2003** Internship in the laboratory of Prof. Dr. Nils Walter, Chemistry Department, University of Michigan, Ann Arbor, USA:
Title: "Investigation of RNA and proteins of the small ribosomal subunit of *E. coli*"
- 03/2002 – 05/2002** Internship in the laboratory of Dr. Thomas Langenickel, Molecular Medicine, Max-Delbrück Center, Berlin, Germany.
Title: "Learning of basic techniques in a research lab"

Publications

Stangl KM, Deussing JM. Distribution of the classical HDACs throughout the adult murine brain (working title) - manuscript in preparation

Conferences, memberships and stipends

- 12/2012** 2. Epigenetics meeting at the Max Planck Institute of Immunology and Epigenetics, Freiburg, Germany.
(Poster presentation; Title: "Dissecting brain-specific functions of histone deacetylases 1 and 3")
- 07/2012** Institute symposium, Max Planck Institute of Psychiatry, Munich, Germany.
(Talk; Title: "Dissecting brain-specific functions of histone deacetylases 1 and 3")
- 10/2011** 27. AGNP Symposium, Ludwig-Maximilians-University, Munich, Germany.
(Poster presentation; Title: "Dissecting brain-specific functions of histone deacetylases 1 and 3")

- 05/2011** 31. Blankenese Conference, Hamburg, Germany.
(Poster presentation; Title: "Dissecting brain-specific functions of histone deacetylases 1 and 3")
- 02/2007 - 12/2011** Stipend and membership at e-fellows
(e-fellows.net/online Stipendium)
- 12/2002 - 12/2013** Membership at the German Association of Biochemists and Molecular Biologists (GBM)
- 04/2006 - 10/2006** Erasmus Stipend at Unîmes, Nîmes, Frankreich
- 04/2006** Joint Advanced Student's School (JASS) stipend of the Technische Universität München and Siemens
- 08/2005 - 01/2006** Stipend of the University of California, Berkeley, USA
- 08/2005** DAAD (Deutscher Akademischer Auslandsdienst) travel stipend
- 03/2004** Stipend of the Klinikum Rechts der Isar, Technische Universität München for the Biosensor-Symposium in Regensburg
- 12/2003 - 12/2004** Membership at the biotechnologische Studenteninitiative (btS)
- 08/2003 - 10/2003** Stipendium of the University of Michigan, Ann Arbor, USA
- 07/2000** Stipendium of the Martin Luther Universität Halle-Wittenberg for a technical workshop

Additional Skills

Languages: German (native); English (excellent command); French (working knowledge); Latin ("Großes Latinum"); Spanish (basics);

10 ACKNOWLEDGMENTS

I am very grateful to Prof. Dr. Wolfgang Wurst for his support and supervision of my PhD thesis at the IDG at the Helmholtz-Zentrum München.

Moreover, I wish to express my gratitude for the time and effort of the examination board, Prof. Dr. Wolfgang Wurst, Prof. Dr. Kay Schneitz and Prof. Dr. Ramon Torres Ruiz, for evaluation and examination of my thesis.

I am grateful to Prof. Dr. Dr. Dr. h.c. Florian Holsboer for providing an excellent scientific environment at the Max Planck Institute of Psychiatry.

I am deeply grateful to Dr. Jan Deussing as my direct supervisor for permanent guidance, constant support and thorough proofreading of my thesis.

Furthermore, I would like to thank my colleagues of the Max Planck Institute of Psychiatry for successful collaboration and support: Dr. Nina Dedic, Dr. Sandra Walser, Marcel Schieven and Dr. Mira Jacovcevski (RG Deussing); Dr. Damian Refojo, Dr. Annette Vogl, Dr. Sebastián Giusti and Anna Möbus (RG Refojo); Dr. Klaus Wagner and Dr. Mathias Schmidt (RG Schmidt).

My gratitude also goes to our technical assistants, our animal care takers and to all colleagues who feel concerned for their help and support over all the years at the MPI.

My special thanks goes to Dr. Annette Vogl, Dr. Nina Dedic and Dr. Sebastián Giusti for their true friendship, support in all situations, great scientific input and advice.

My deep gratitude finally goes to my husband, my son, my parents and my sister for their continuous patience, never ending encouragement and faith in me.

11 ERKLÄRUNG

Ehrenwörtliche Versicherung:

Ich versichere hiermit ehrenwörtlich, dass ich die Dissertation mit dem Titel "Dissecting brain-specific functions of histone deacetylases 1 and 3 by using genetic mouse models" selbständig und ohne unerlaubte Hilfe angefertigt habe. Ich habe mich dabei keiner anderen als der von mir ausdrücklich bezeichneten Hilfen und Quellen bedient.

Erklärung:

Hiermit erkläre ich, dass ich mich nicht anderweitig einer Doktorprüfung ohne Erfolg unterzogen habe. Die Dissertation wurde in ihrer jetzigen oder ähnlichen Form bei keiner anderen Hochschule eingereicht und hat noch keinen sonstigen Prüfungszwecken gedient.

München, Mai 2016

Michaela Katja Stangl